DEUQUA EXCURSIONS

Edited by Hanns Kerschner, Karl Krainer and Christoph Spötl

From the foreland to the Central Alps

Field trips to selected sites of Quaternary research in the Tyrolean and Bavarian Alps

GEOZON

From the foreland to the Central Alps

Preface

The Tyrolean and Bavarian Alps offer a fascinating plethora of Quaternary issues ranging from outcrops of Pleistocene sediment successions to modern glacial and periglacial environments. Twelve such areas were selected and are part of this field guidebook, the first of its kind for the Quaternary in this part of the Alps.

Produced for the 2014 convention of the German Quaternary Association (DEUQUA) this book was published in English to allow also the non-German speaking colleagues, students and interested lay people to visit these field areas and to access this information. Many sites including the Hötting Breccia and its well-known flora, the banded clays of Baumkirchen and the Gschnitz and Egesen glacier advances, to name just a few, are key to the understanding of the Quaternary history and dynamics of the entire Alps including their foreland. We express our hopes that this guidebook will foster further international collaboration in and across this fascinating mountain range, its multifaceted Quaternary evolution and landscape evolution.

We extend our gratitude to all authors who contributed to this book, to Andrew Moran for carefully checking and improving English style and grammar, to Sascha Fricke for his professional support and collaboration, and to the sponsors who made it possible to publish this as a full-colour and open-access book.

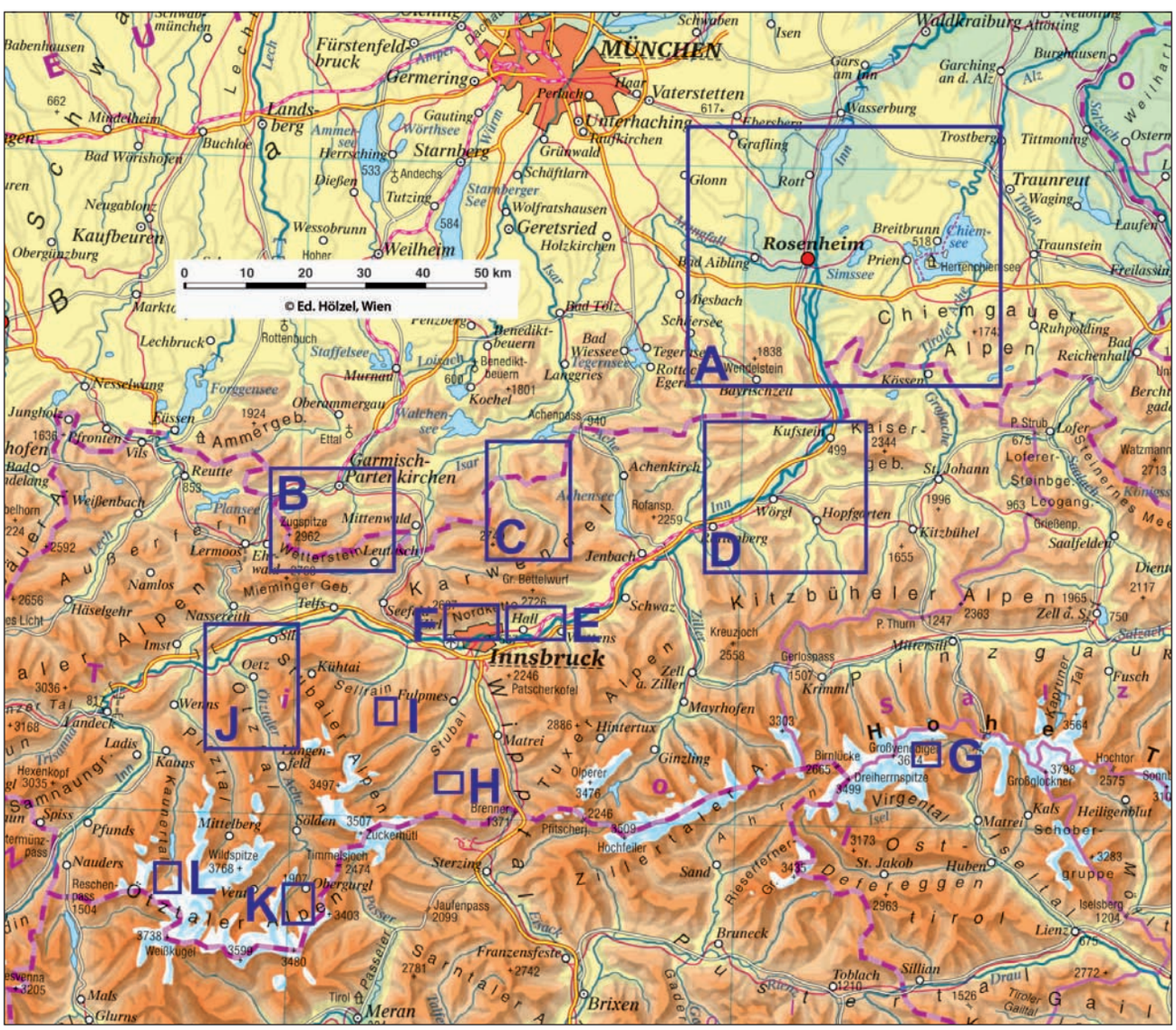

A

The Rosenheim Basin: Würmian and Pre-Würmian deposits and the Höhenmoos interglacial (MIS 7)

Das Rosenheimer Becken: Würm- und Präwürmzeitliche Ablagerungen und das Höhenmoos Interglazial (MIS 7)

Martin Herz, Maria Knipping, Ernst Kroemer

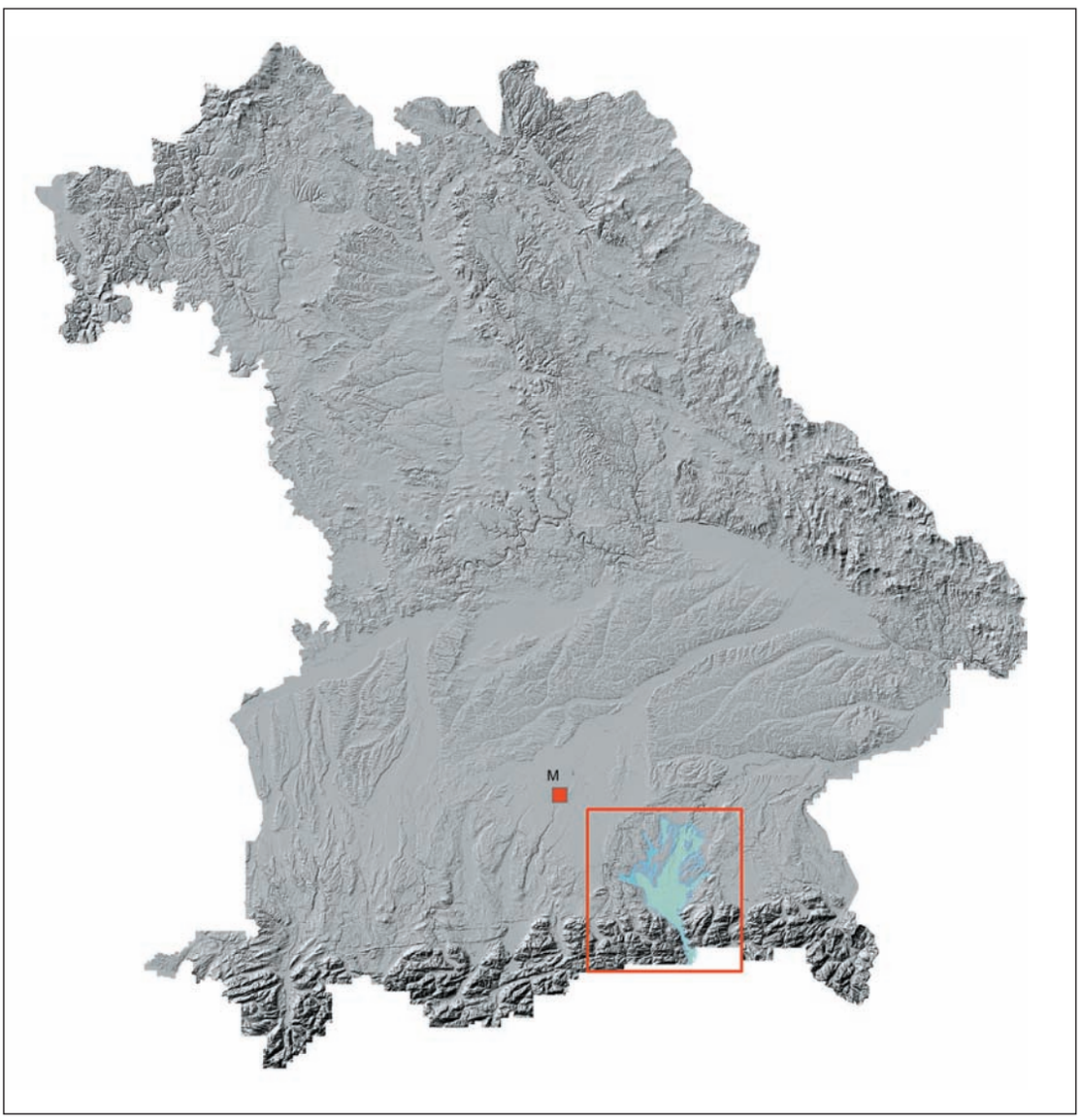

Fig. 1: Map of Bavaria showing the excursion area (red rectangle). M. Munich.
Abb. 1: Karte von Bayern mit Exkursionsgebiet (rot umrandet). M. München.

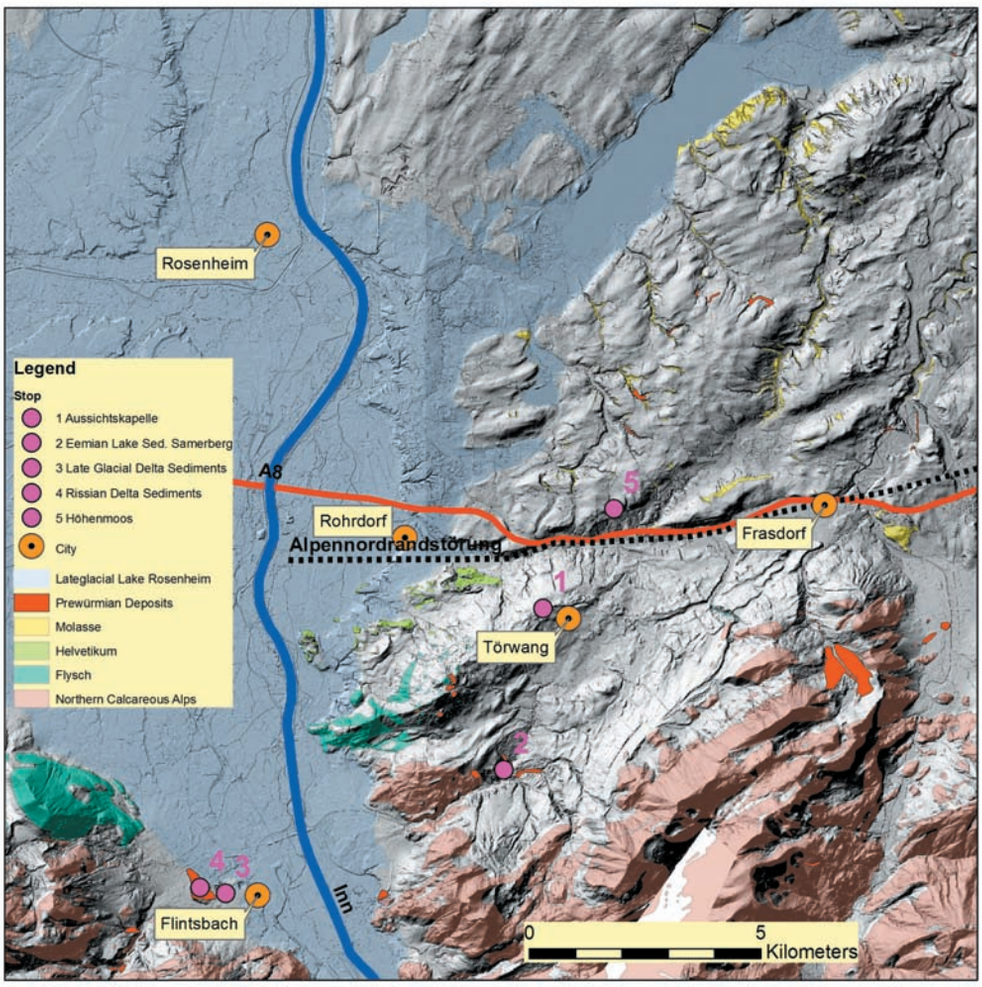

Fig. 2: Simplified geological map with listed stops. 1 = view point Törwang – Aussichtskapelle - Overview of the Rosenheim Basin and the Inn Valley. 2 = The Eemian lake sediments of Samerberg. 3 = Lateglacial delta sediments of the late Würmian Lake Rosenheim – Gravel pit Grad Nagelfluhwerk, Brannenburg. 4 = Delta conglomerates of the Rissian Lake Rosenheim at quarry Grad Nagelfluhwerk, Brannenburg and foresets of the Delta conglomerates at quarry Anton Huber, Brannenburg. 5 = The interglacial of Höhenmoos (MIS 7).

Abb. 2: Vereinfachte geologische Karte mit den Exkursionshalten. 1 = Aussichtspunkt Törwang – Aussichtskapelle – Übersicht über das Rosenheimer Becken und das Inntal. 2 = Eemzeitliche Seeablagerungen des Samerberg. 3 = Spätglaziale Deltaablagerungen des spätwürmzeitlichen Rosenheimer Sees, Kiesgrube Nagelfluhwerk Brannenburg. 4 = Deltakonglomerate des rißzeitlichen Rosenheimer Sees im Steinbruch Grad Nagelfluhwerk, Brannenburg und „foresets" der Deltakonglomerate im Steinbruch Anton Huber, Brannenburg. 5 = Das Interglazial von Höhenmoos (MIS 7).

1 Introduction

On this field trip new results of the extensive mapping program (IOGI) performed by the Bavarian Geological Survey of the Bavarian Environmental Agency are presented. Figure 1 shows the excursion area in southern Bavaria southeast of Munich. Fig. 2 shows a simplified geological map of the field trip area based on the work of Wolf (1973), Ganss (1980), Kunz et al. (2013) and Kroemer et al. (in press).

The light blue color, mostly on the western part of the map, shows the extent of the former Lateglacial lake, which filled the Rosenheim Basin after the retreat of the Inn Glacier. In the northern part the remains of this big lake (todays Simssee) can be identified in a SW–NE trending sub-basin. Today this area is dominated by fine-grained lake sediments, in wide parts covered with peat, and along the Inn, by coarse grained river gravels. These deposits were formed after the basin was drained at the end of the Lateglacial and during the Holocene.

The eastern part of the map is mostly covered by a light grey colour, which represents glacial and fluvioglacial sediments of Würmian age. Only limited parts in the small valleys and depressions are covered by Holocene sediments and peats. In the central part of this area a depression between Rohrdorf in the West and Frasdorf in the East is developed. This depression, in which the Autobahn A8 was built, follows the main fault, which divides the folded part of the Alps in the South from the unfolded part in the north. The yellow colour in the North represents sediments of the Molasse basin, which are mainly found in areas of steep river and creek slopes. Due to the location in the upturned part of the Molasse, the wide range of sediments from the Lower Freshwater Molasse to the Upper Marine- and finally to the Upper Freshwater Molasse can be seen in the outcrops from South to North. South of the fault and underneath the Quaternary, nappes of the Helvetic (light green), the Flysch (darker green) and the Northern Calcareous Alps (light brown) are present.

Between these sedimentary basement rocks and the Würmian and Holocene deposits, which cover most of the area, there are – marked by red areas and dots – Quaternary glacial and interglacial deposits. It looks as though in some parts, the pre-Würmian landscape with its hills and valleys is buried beneath the younger sediments and is therefore somehow preserved. But to our current knowledge, the relationship between these individual deposits is not clear, especially because unambiguous stratigraphical data is not yet available.

2 Excursion

Stop 1: Törwang – Aussichtskapelle – Overview of the Inn Valley

The first stop of the field trip is the view point from a little chapel (Aussichtskapelle) outside of Törwang. The stop will permit a short geological and geomorphological introduction to the Rosenheim basin and its eastern surroundings.

Fig. 3: Panorama of the Rosenheim Basin; View to the West and North.

Abb. 3: Panorama des Rosenheimer Beckens, Blick nach Westen und Norden.

First we will take a look to the West and North into the glacially over-deepened basin of Rosenheim and the Inn Valley. The continuous line of the horizon represents more or less the Würmian outer moraines of the Inn Glacier, which encircle the basin. The city of Rosenheim is located at the center of the basin. At the end of the Würmian Pleniglacial and during the Lateglacial, the depression was occupied by former Lake Rosenheim. The lake level once reached up to the plane of the delta of Rohrdorf and the Samerberg rest area located along Autobahn A8. To the North, the former shore can be followed along the fir woods up to the basin of Simssee, which was once also part of a much bigger water shed. Due to erosion, the lake level today is about 10 m deeper. According to the new mapping results and the evaluation of the digital terrain model, the former lake level rises from the north (delta of Edling ca. 480 m a.s.l.) to the south (beach terraces of Kiefersfelden ca. 490 m a.s.l.) by about 10 m. The reasons for this are not completely understood at the moment, but isostatic or tectonic processes or a combination of both likely play a role.

As mentioned earlier, the basement of the hills is built up by Molasses deposits. The outcrops of these Tertiary sediments and sedimentary rocks are more or less restricted to the steep embankments of the creeks and small rivers. Most of the surface, however, is covered by Würmian till, glaciofluvial meltwater sediments and glacial lake deposits, which themselves often contain, especially in surface depressions, peat sediments. During geological mapping we found sediments, mostly in the form of buried valley fills of pre-Würmian age. These outcrops are commonly small, some only 10 to 100 m in length and a few metres in height. Some of the sediments might also be regarded as glacial in origin, but others contain a reasonable amount of organic matter and fossils. Later we will see an example of this (Stop 5), in a creek east of the little village of Höhenmoos.

To the South, the peaks and tops of the Northern Calcareous Alps form an impressive panorama with Hochries (1588 m a.s.l.) and Heuberg (1338 m a.s.l.) constituting the highest elevations. In the foreground in front of the mountains another depression in the terrain developed. The so-called basin of Törwang – Gernmühl was formed by a branch of the Inn Glacier. It is filled by a sequence of diamicts and lake sediments. In the 1950s to the 1970s Proebstl recognized the interglacial and interstadial character of parts of these fine grained sediments.

Fig. 4: Panorama to the Northeast: The hills between Simssee and the depression of Rohrdorf Frasdorf north of the Alpine front.

Abb. 4: Panorama Blick nach Nordosten: Die Hügel zwischen dem Simssee und der Furche Rohrdorf Frasdorf nördlich der Alpenfront.

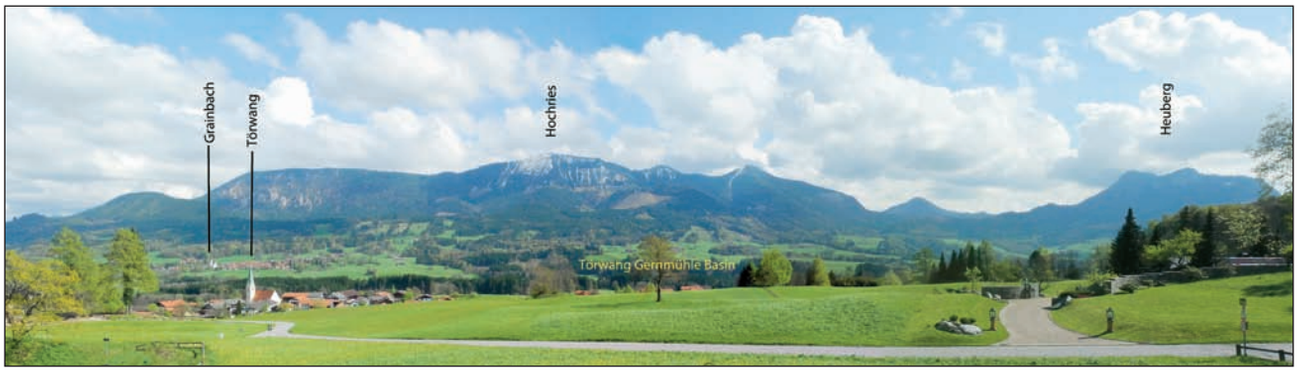

Fig. 5: Panorama to the South: The Northern Calcareous Alps and the depression of Törwang – Gernmühl.

Abb. 5: Panorama Blick nach Süden: Die Nördlichen Kalkalpen und die Eintiefung von Törwang – Gernmühl.

Stop 2 : Eemian lake sediments of Samerberg

After decades of research Proebstl described in detail the geological setting of the Eemian Interglacial, as well as the early Würmian Interstadial and late Würmian sediments (Proebstl 1982). Besides a sedimentological description of the outcrops, the author also listed the faunal and herbal inventory. In 1973 the Samerberg 1 core (SAM1) was drilled by the Bavarian Geological Survey (Jerz 1980). It was followed (1974/1975) by geophysical research (Jerz et al. 1979, Baader 1983), which found that the NE-SW extended Törwang – Gernmühl basin has a length of about 4 km, is up to 1 km wide and up to 100 m deep. The nose of the Moosen divides the basin in two parts: The Törwang subbasin in the North and the Gernmühl subbasin in the South. The main drainage occurs via the Achen stream. In the South, the Gernmühl Basin is fed by three inlets: Hundsgraben, Weißen- and Fluderbach. In 1981 a second drilling, "Samerberg 2" (SAM2), was performed (Jerz 1983). The palynological work was carried out by Grüger (1979 and 1983), who identified two interglacials. He considered the lower warm period as equivalent of the Holsteinian (MIS 9 or 11) and the upper one as Eemian (MIS 5).

The goal of the stop at the Samerberg is to gain a view of the outcrop(s) of the Eemian interglacial lake sediments, especially with respect to the second outcrop of interglacial sediments at Höhenmoos.

Stop 3: Lateglacial delta sediments of the late Würmian Lake Rosenheim at the gravel pit Grad Nagelfluhwerk, Brannenburg.

Lake Rosenheim has a long and ongoing history of investigations with Penck & Brückner (1901–1909) and Troll (1924) as the most prominent regional workers. Regional mapping on different map sheets (scale 1 : 25 000) was conducted by

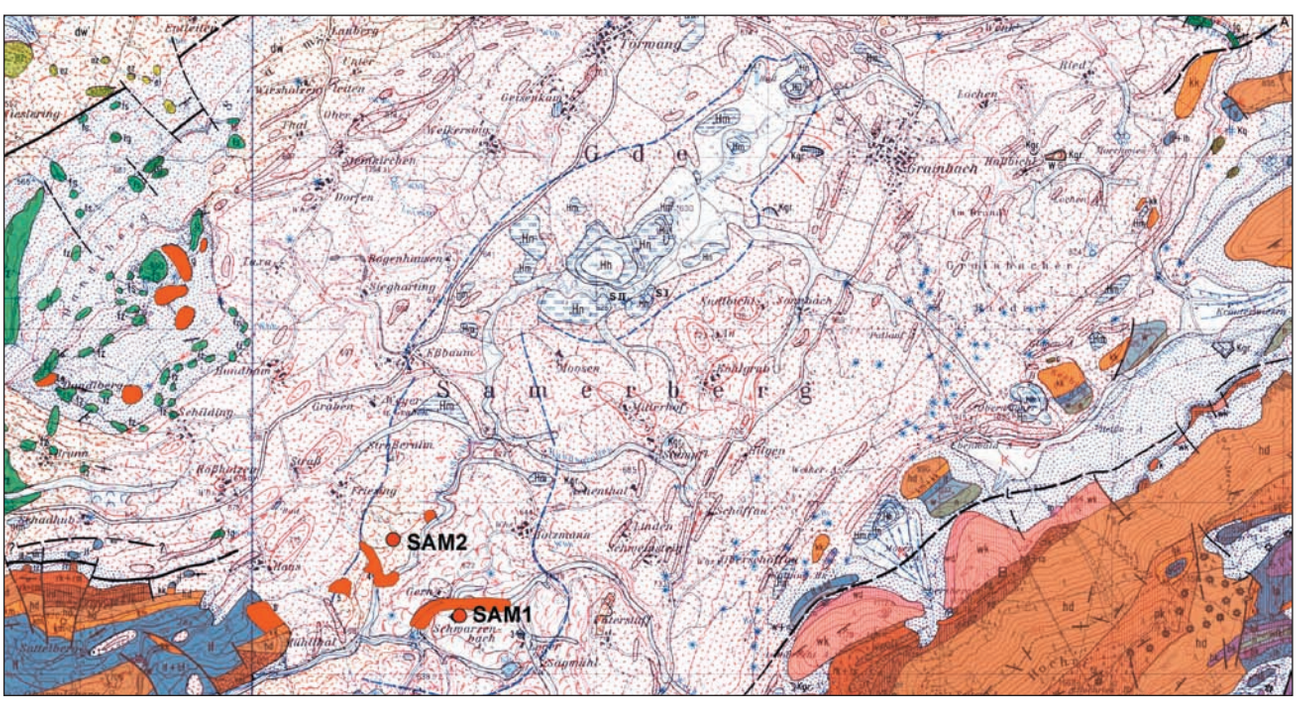

Fig. 6: In this slightly modified part of the geological map sheet 8239 Aschau (Gans 1980) the extent of the Törwang – Gernmühl basin is indicated by the dashed blue line. The red points SAM1 und SAM2 mark the locations of the scientific drilling sites and the outcrops of fine grained lake sediments are represented in orange.

Abb. 6: In dem gering veränderten Ausschnitt der Geologischen Karte Blatt 8239 Aschau (Gans 1980) ist die Ausdehnung des Törwang – Gernmühler Beckens durch die gestrichelte blaue Line angezeigt. Die roten Punkte SAM1 und SAM 2 markieren die Bohransatzpunkte der Forschungsbohrungen. Die Aufschlüsse der feinkörnigen Seesedimente sind in orange eingetragen.

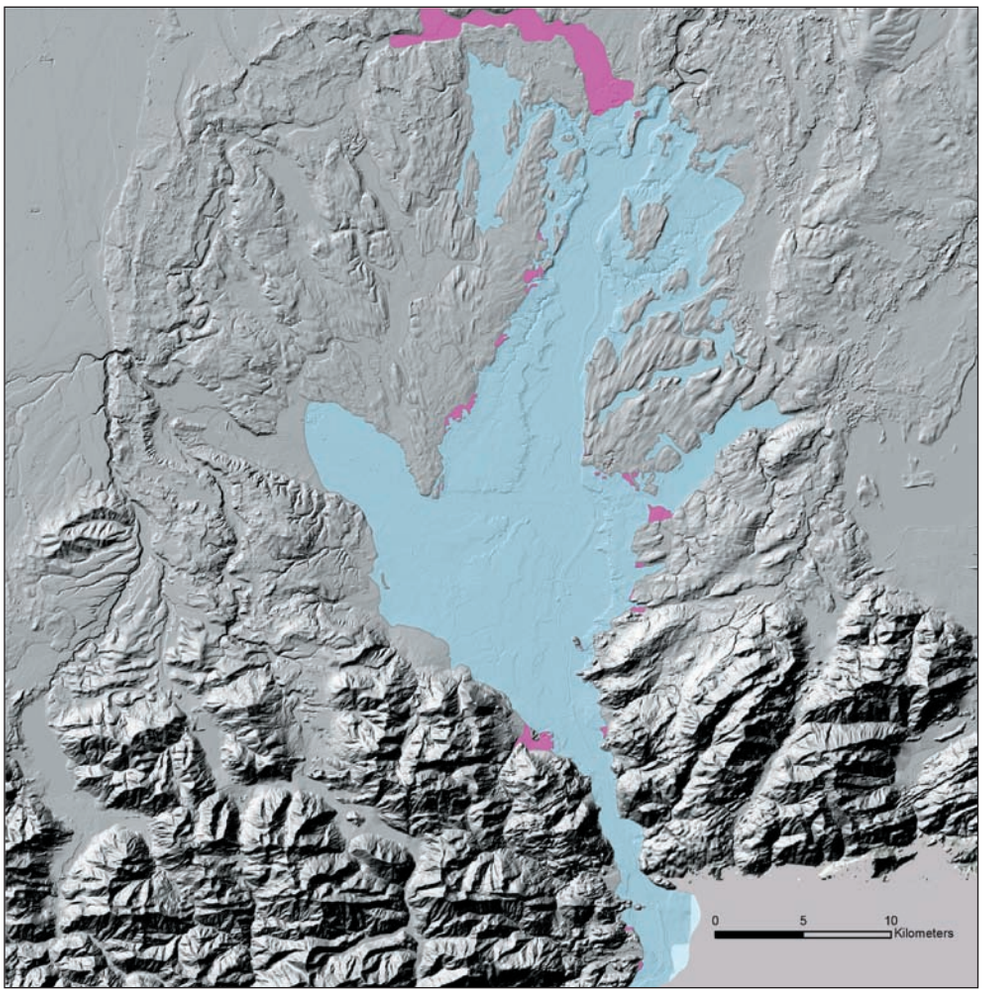

Fig. 7: Extent of Lateglacial Lake Rosenheim (blue) and shoreline features (magenta).

Abb. 7: Ausdehnung des spätglazialen Rosenheimer Sees (blau) und Uferbildungen (magenta).

Fig. 8: The gravel pit Grad exposes delta sediments deposited by local mountain creeks (Grießenbach and others) into former Lake Rosenheim.

Abb. 8: In der Kiesgrube Grad sind Deltaablagerungen aufgeschlossen, die durch lokale Gebirgsbäche (Grießenbach und andere) in den ehemaligen Rosenheimer See geschüttet wurden.

Wolff (1973, the Quaternary research was partly done by H. Jerz), Kunz et al. (2013a, 2013b), Kroemer et al. (in press), and Wallner (2011a, 2011b, 2011c, 2011d). Veit (in Wolff 1973, p. 283) presented a map showing the thickness of the late Würmian lake sediments. Kroemer (2011) estimated the extent of Lake Rosenheim to about 450 km² and pointed out implications of isostatic movement by using Lidar data.

During the geological mapping of the central area of the Rosenheim basin (Kunz et al. 2013a, 2013b, Kroemer et al., in press) the question about the extent of the Lateglacial Lake Rosenheim was raised. The existing map and interpretation of the lake and surrounding sediments (Troll 1924,

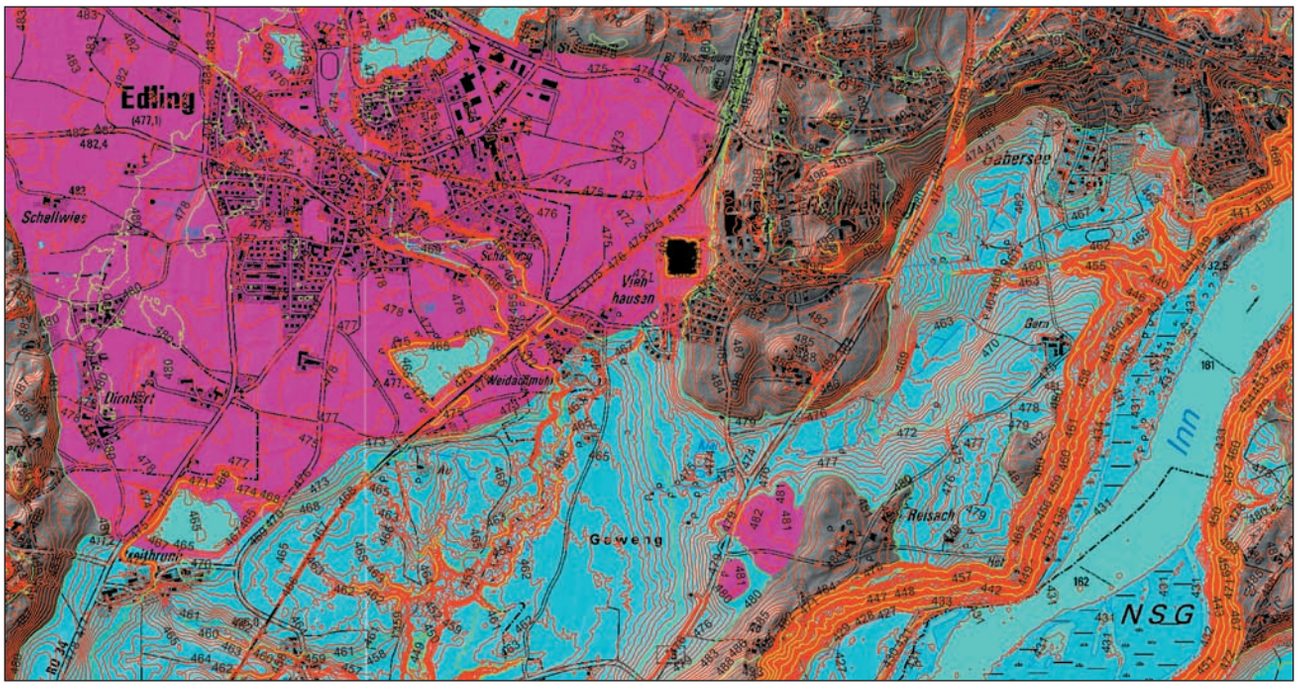

Fig. 9: Edling: Delta sediments (magenta) on the northern end of the palaeolake (blue) were deposited shortly after the Last Glacial Maximum by meltwater runoff between morainic ridges and delineate the highest lake level (478–480 m a.s.l.).

Abb. 9: Die Deltaablagerungen von Edling (magenta) am nördlichen Ende des ehemaligen Sees (blue) wurden kurz nach dem Maximalstand der letzten Eiszeit durch zwischen Moränenrücken fließenden Schmelzwasserabflüsse geschüttet und weisen den höchsten Seespiegel (478–480 m ü. NN) aus.

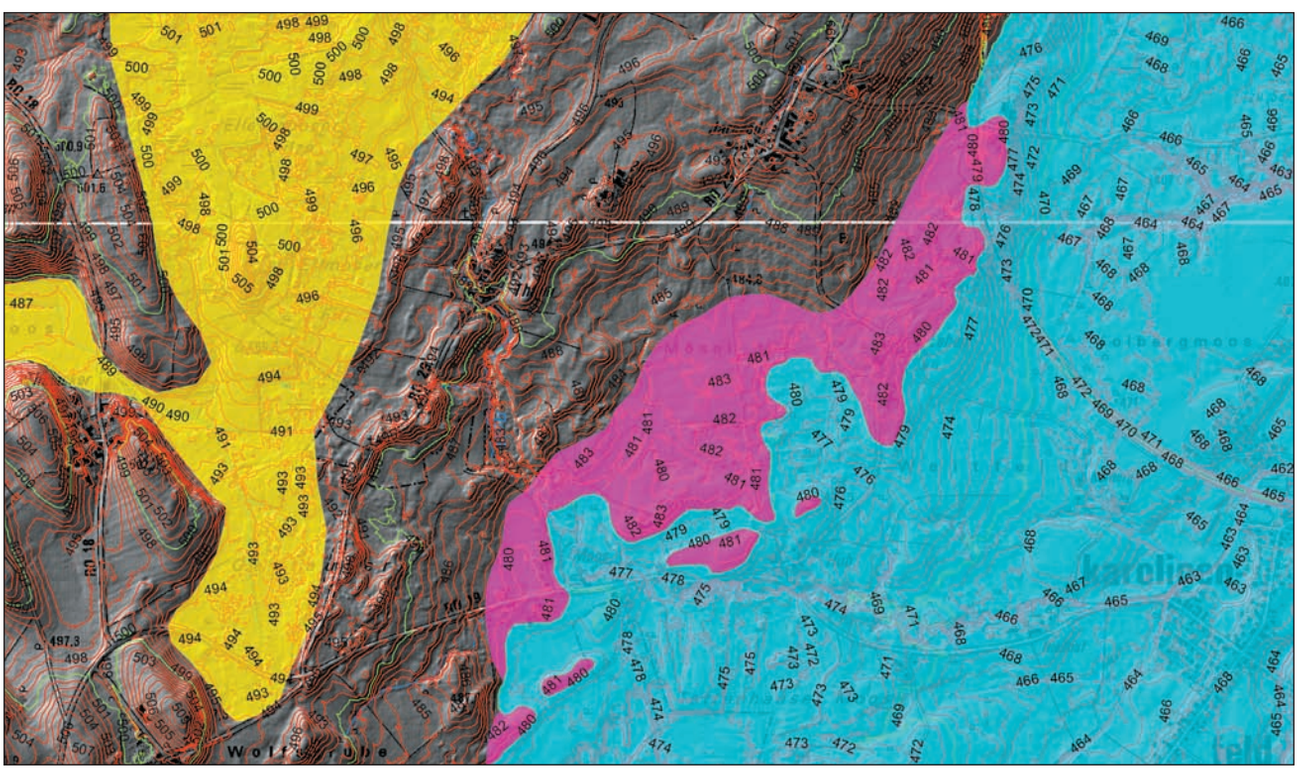

Fig. 10: Großkarolinenfeld: Beach terrace (magenta) of Lake Rosenheim (blue) at ~482 m a.s.l. Area of a former ice-dammed lake, which was not part of Lake Rosenhein in yellow, contour lines in red with labels in metres a.s.l.

Abb. 10: Großkarolinenfeld: Strandterrasse (magenta) des Rosenheimer Sees (blau) bei ~482 m ü. NN. Fläche eines ehemaligen Eisrandstausees, der nicht Teil des Rosenheimer Sees war in gelb, rot beschriftete Höhenlinien in Meter ü. NN.

p. 92–97, plate IV) were useful, but were only based on a scale of 1 : 100,000. Using Lidar data a hitherto unrecognized shoreline could be identified. Interestingly, the lake level of around 480 m a.s.l. at the Edling delta seems to correspond to a slight incline cumulating around 490 m a.s.l. at Kiefersfelden, some 40 km south of Edling.

Fig. 8: Here we present deltaic sediments of Lake Rosenheim at an elevation between 484 and 486 m a.s.l. Foresets

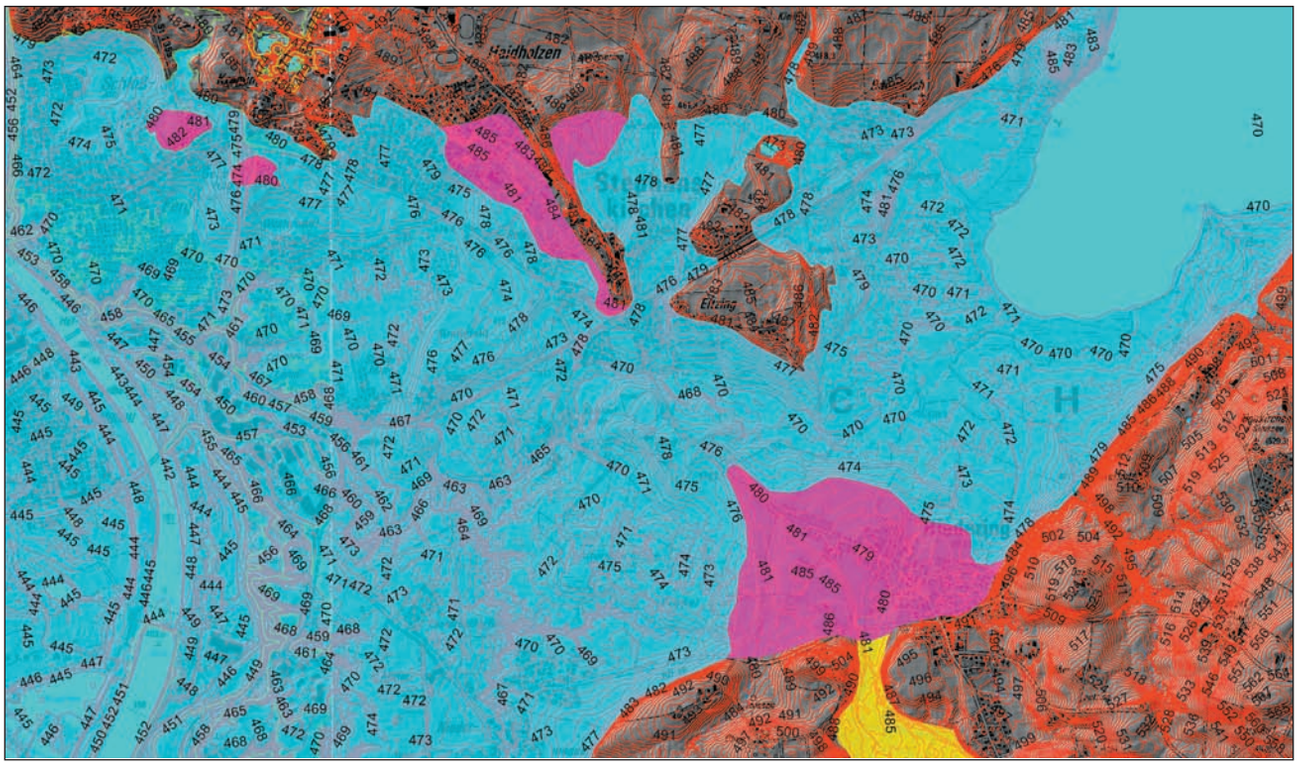

Fig. 11: Stephanskirchen: Delta deposits, beach terraces and abrasional platforms (magenta) at ~483 m a.s.l. Area of a former ice-dammed lake, which was not part of the Lake Rosenhein in yellow, contour lines in red with labels in m a.s.l.

Abb. 11: Stephanskirchen: Deltaablagerungen, Strandterrassen und Abrasionsplatformen (magenta) bei ~483 m ü. NN. Fläche eines ehemaligen Eisrandstausees, der nicht Teil des Rosenheimer Sees war, in gelb, rot beschriftete Höhenlinien in Meter ü. NN.

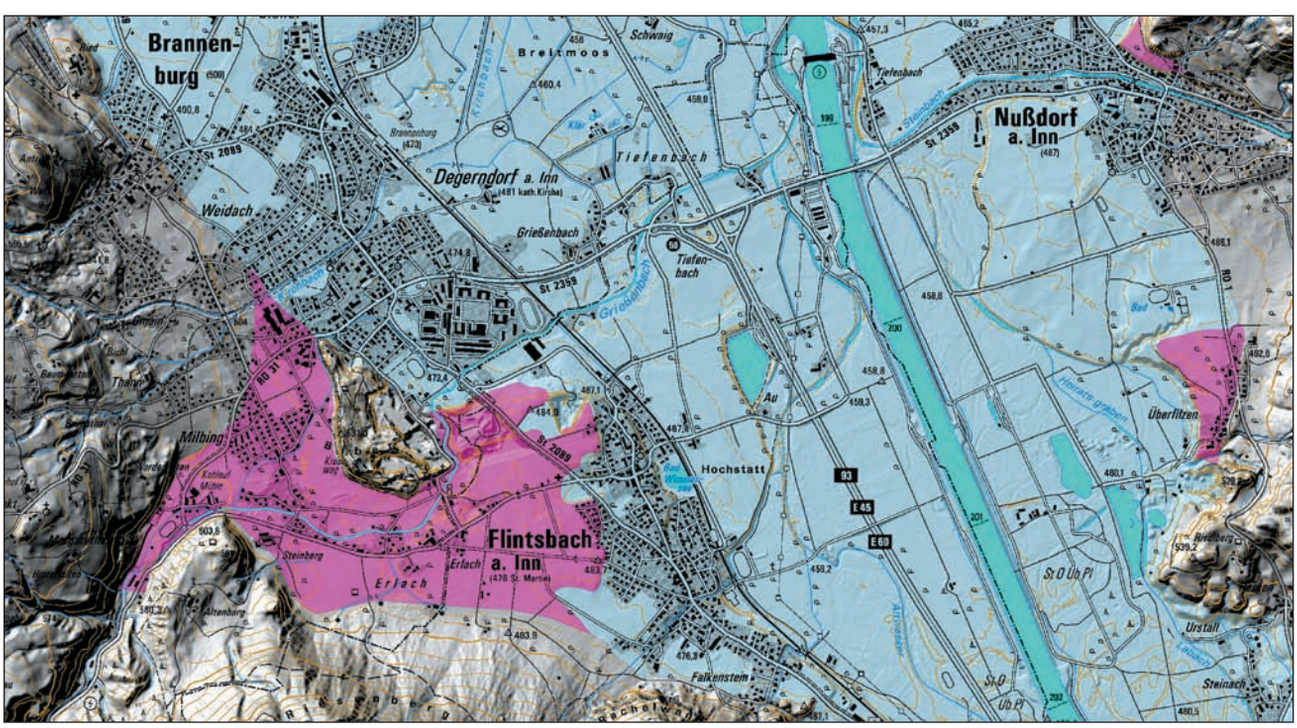

Fig. 12: Delta sediments on the western shore (magenta) south of Brannenburg and beach terraces on the eastern shore (magenta) near Nußdorf and Überfilzen of Lake Rosenheim (blue) at 484–486 m a.s.l.

Abb. 12: Deltaablagerungen des Westufer südlich von Brannenburg (magenta) und Strandterrassen des Ostufers (magenta) bei Nußdorf und Überfilzen des Rosenheimer Sees (blau) um 484–486 m ü. NN.

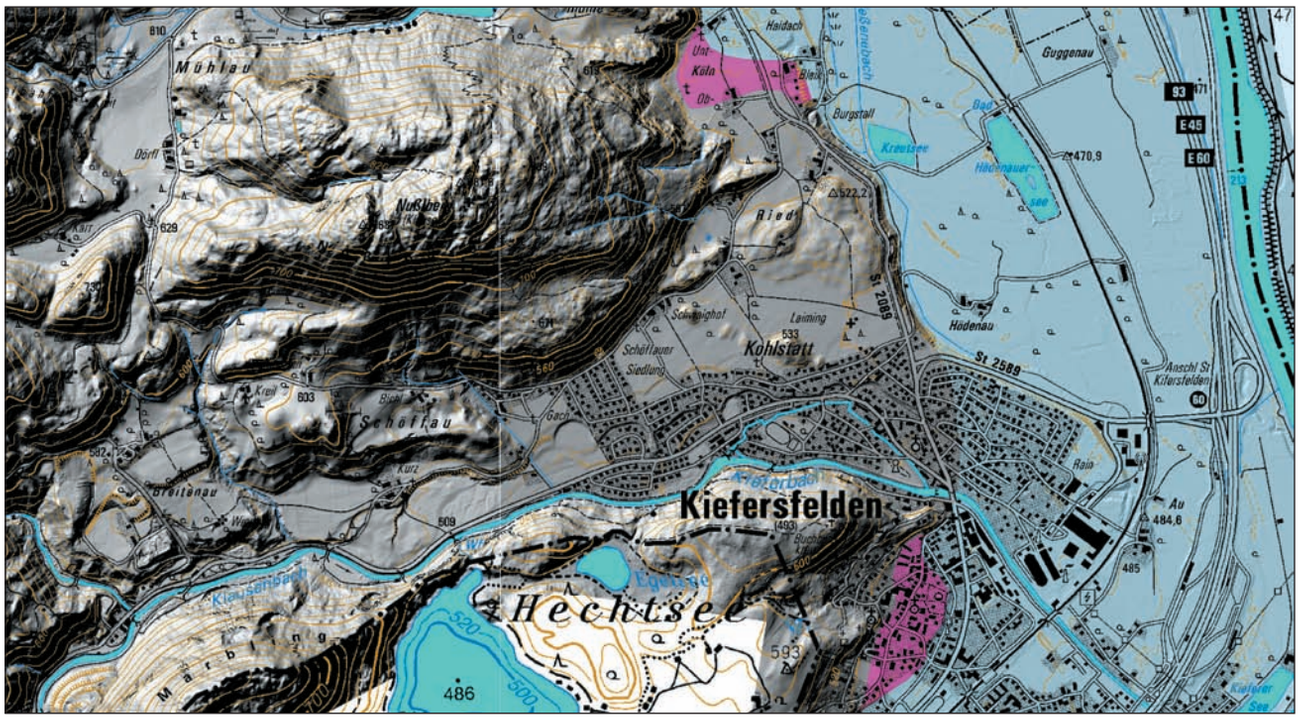

Fig. 13: Kiefersfelden: Beach terraces at ~490 m a.s.l.

Abb. 13: Kiefersfelden: Strandterrasse um ~490 m u. NN.

and topsets are well developed. This is an example of the different deltas. Some additional examples of deltas and shorelines are shown in the figures 9 to 12.

Stop 4a: Delta conglomerates of the Rissian Lake Rosenheim at the quarry Grad Nagelfluhwerk, Brannenburg

Stop 4b: Foresets of the delta conglomerates at quarry Anton Huber, Brannenburg

The Late Würmian Lake Rosenheim was not the first lake in this area. At this site conglomerated deltaic sediments of Rissian or older age (Wolff 1973) can be seen, which point to a lake level of around 520 m a.s.l.. and about 30 m higher than the lake level estimated for the Late Würmian successor. It is possible that the extension of this older lake reached almost to the city of Erding 55 km in the North, where fine grained Rissian lake sediments at an elevation lower than 510 m a.s.l. occur.

Stop 5: The interglacial of Höhenmoos (MIS 7)

In November 2009 the graben east of the village of Höhenmoos was examined in the course of the geological mapping (IOGI project of the Bavarian Geological Survey, Kunz

Fig. 14: Foreset conglomerates of Rissian age ("Biber-Nagelfluh") at the quarry Grad Nagelfluhwerk, Brannenburg.

Abb. 14: Rißzeitliche konglomerierte „Foresets" (Biber-Nagelfluh) im Steinbruch Grad Nagelfluhwerke, Brannenburg.

Fig. 15: Topsets of the Rissian delta deposits ("Biber-Nagelfluh"), quarry Anton Huber, Brannenburg.

Abb. 15. Konglomerierte „Topsets" der rißzeitlichen Deltaablagerungen (Biber-Nagelfluh) im Steinbruch Anton Huber, Brannenburg.

et al. 2013) of the area. The north-south trending creek is a tributary of the Rohrdorfer Achen which flows westward to the Inn River. Along an approximately 250 m-long stretch of the stream bed and in some undercuts up to 5 m thick grey lake sediments crop out. Due to the presence of gastropods, bivalves and plant remains a warm-stage environment was proposed and the overlying till outside the trench indicated an age older than the Würmian Pleniglacal.

Tertiary "Chatt" sands crop out at the southern tip of the lake sediments forming the pre-Quaternary substrate. The sediment layers strike NW-SE and dip 70° towards the North.

The Upper Würmian till and the pre-Würmian lake sediments in the graben are covered by Holocene fluvial deposits, slope debris and loam. Stream erosion caused local slumping of the cohesive sediments which renders a correlation of the sedimentary sections along the outcrop impossible and the stratigraphy below and above the fine grained sediments is still unclear. Especially the expansion and dimensions of the former lake basin are not known.

The exposed pre-Würmian lake deposits are silts with few and thin clay and sand layers with the exception of a single 15 to 30 cm-thick sand layer which is present in the upper third of the sequence and forms a possible marker bed. The lake deposits are characterised by decimetre to metre-thick bedding. Locally, millimetre-thin lamination can be seen. The sediments are over-consolidated due to ice loading. Macroscopic fossil remains include a few millimetre large shells of gastropods and bivalves. Also common are plant remains such as twigs, leaves, needles and rarely seeds.

The next paragraphs provide a short summary of the pollen analysis commissioned by the Bavarian Geological Survey (Bavarian Environmental Agency) and carried out by M. Knipping from the University of Hohenheim.

By correlating the four analyzed profiles, the development of vegetation at Höhenmoos can be described as follows (Fig. 17). In the oldest part of the profile (local pollen zone 1- LPZ 1) the pollen spectra show high amounts of light-demanding taxa and reworked palynomorphs suggesting open vegetation. In LPZ 2 nonarboreal pollen (NAP) decrease sharply while pollen of *Pinus* dominate the arboreal pollen (AP) beside *Picea* and *Betula*. First thermophilous taxa (*Quercus, Ulmus*) show the onset of interglacial/interstadial conditions. In LPZ 3 the *Pinus* pollen values decrease while pollen of *Picea, Quercus, Ulmus* and *Tilia* increase. *Abies* is present at low values. In LPZ 4 *Abies* increases up to 65 % and *Corylus* is frequent while *Picea* declines. *Carpinus* is absent throughout this entire warm phase. Increasing values of *Picea* and decreasing values of *Abies* show less favourable conditions in LPZ 5. After a short peak of *Pinus* pollen in LPZ 6, high values of *Picea* characterise LPZ 7. In this zone four intervals with high values of NAP, indeterminables and reworked taxa indicate erosion processes and an opening of the vegetation. Subsequent high values of *Juniperus* indicate reforestation phases. No interuptions or mechanical doubling are visible in the non-faulted sediment which could indicate a disruption of sedimentation. Dominance of *Pinus* with subdominance of *Betula* and *Picea* and frequent pollen of *Juniperus, Larix* and *Pinus cembra* types are typical of LPZ 8. Decreasing values of *Betula* pollen, with simultaneously increasing values of *Pinus, Ulmus* and *Quercus* indicate the beginning of a second warm phase in LPZ 9. In the following LPZ 10 *Quercus, Ulmus* and *Fraxinus* reach high values. Of special interest is the presence of *Celtis* pollen around LPZ 10. *Carpinus*, which was found only as a few grains in the previous zones, reach nearly 10 % in LPZ 11. Very high values of *Abies* pollen (up to 90 %) and the occurrence of pollen of *Fagus* and *Buxus* characterise LPZ 12. The end of this warm phase is indicated in LPZ 13 by declining values of *Abies* und increasing values of *Picea* and *Pinus*. Rising NAP values, especially of Poaceae and *Artemisia* in LPZ 14, point to climatic deterioration and an opening of the former woodland.

The development of vegetation in the Höhenmoos profiles is unique for southern Germany. Two different warm phases could be confirmed, separated by a cool-moist phase (LPZ 7) and a following cool-dry phase (LPZ 8). Below and above cool/cold phases exist with open vegetation.

No autochthonous Tertiary relicts were found, which

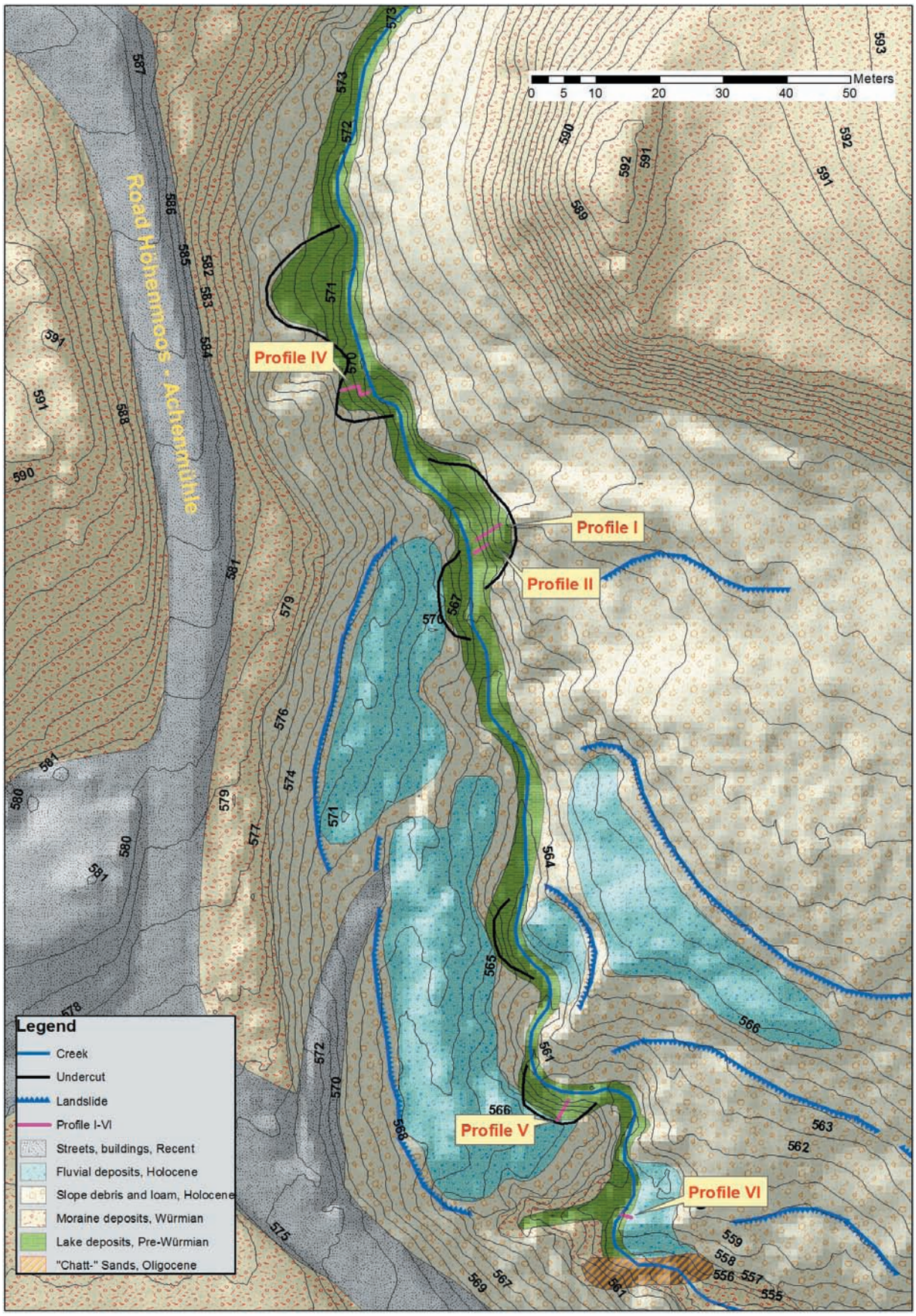

Fig. 16: Geological sketch map of the graben east of Höhenmoos showing the locations of the sections used for the palynological study.
Abb. 16: Geologische Kartenskizze des Grabens östlich von Höhenmoos mit den Lokalitäten der palynologisch bearbeiteten Profile.

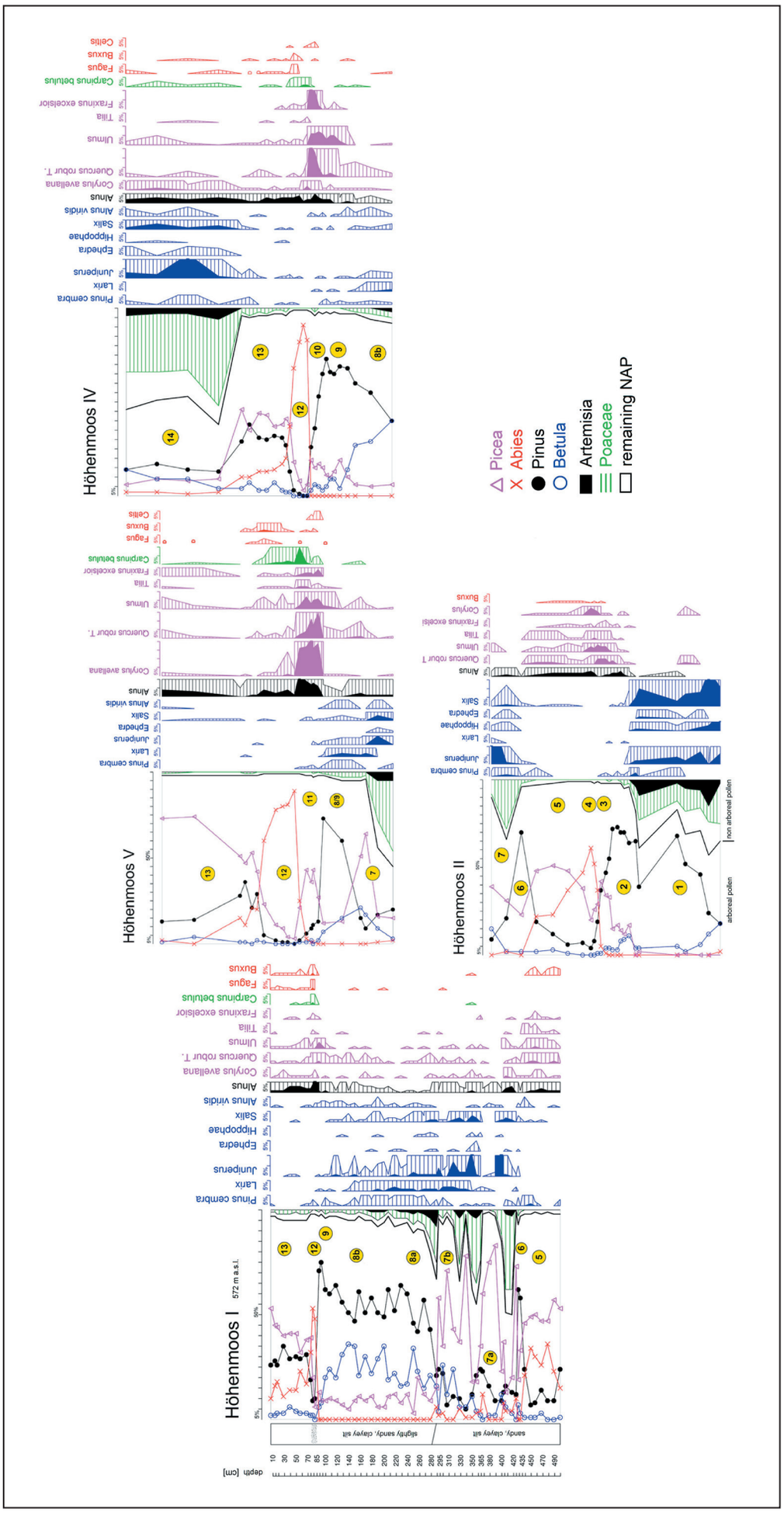

Fig. 17: Pollen profiles from Höhenmoos.
Abb. 17: Pollenprofile von Höhenmoos.

would indicate an Early Pleistocene age. *Pterocarya* is absent as well. This suggests that the Höhenmoos succession can neither be correlated with the Eemian, the Holsteinian/"Pterocarya-Interglacial", nor with the Early Weichselian (Drescher-Schneider 2000, Grüger 1979, 1983, Müller 2000, 2001). Due to the occurrence of *Fagus* in the youngest warm phase in Meikirch II (Preusser et al. 2005) a correlation with the upper warm phase in Höhenmoos seems possible, but the middle warm phase in Meikirch is absent in the Höhenmoos sequence until now. A further possible correlation with the „Mannheim-Interglacial" (Knipping 2008) appears possible which shows *Fagus* and *Celtis* during a warm phase in the Upper Rhine Graben and which is younger than 440 ka based on new datings (Lauer et al. 2011). This sequence, however, shows different pollen spectra due to the greater distance and lower altitude. First luminescence datings of three samples from the Höhenmoos sequence revealed ages of 190, 210 and 215 ka as well as a younger one of 120 ka for a stadial sample (Starnberger & Spötl, unpublished data). Therefore a Middle Pleistocene age of the Höhenmoos sequence and a correlation with MIS 7 seems most likely.

References

Bader, K. (1983): Das Seetonbecken von Samerberg. Übertiefung und Füllung nach geophysikalischen Untersuchungen. – Geologica Bavarica, 84: 17–20.

Drescher-Schneider, R. (2000): 2. Halt: Kiesgrube Thalgut: Pollen- und großrestanalytische Untersuchungen. – In: Kelly, M., Linden, U. & Schlüchter, Ch. (ed.) – Exkursionsführer DEUQUA 2000, Eiszeitalter und Alltag, Bern 6–8 September 2000: 128-136.

Ganss, O. (1980): Geologische Karte von Bayern 1 : 25 000, Blatt Nr. 8239 Aschau i. Chiemgau. – München (Bayerisches Geologisches Landesamt).

Ganss, O. (1980): Geologische Karte von Bayern 1 : 25 000, Erläuterungen zum Blatt Nr. 8239 Aschau i. Chiemgau. – München (Bayerisches Geologisches Landesamt).

Grüger, E. (1979): Spätriß, Riß/Würm und Frühwürm am Samerberg in Oberbayern – ein vegetationsgeschichtlicher Beitrag zur Gliederung des Jungpleistozäns. – Geologica Bavarica, 80: 5–64.

Grüger, E. (1983): Untersuchungen zur Gliederung und Vegetationsgeschichte des Mittelpleistozäns am Samerberg in Oberbayern. – Geologica Bavarica, 84: 21–45.

Jerz, H. (1980): Die Forschungsbohrung Samerberg 1. – In Ganss, O. (1980): Geologische Karte von Bayern 1 : 25 000, Erläuterungen zum Blatt Nr. 8239 Aschau i. Chiemgau. – München (Bayerisches Geologisches Landesamt).

Jerz, H. (1983): Die Bohrung Samerberg 2 östlich Nußdorf am Inn. – Geologica Bavarica, 84, 5–16.

Jerz, H., Bader, K. & Pröbst, M. (1979): Zum Interglazialvorkommen von Samerberg bei Nußdorf am Inn. – Geologica Bavarica, 80, 65–71.

Knipping, M. (2008): Early and Middle Pleistocene pollen assemblages of deep core drillings in the northern Upper Rhine Graben, Germany. – Netherlands Journal of Geosciences — Geologie en Mijnbouw, 87: 51–65.

Kroemer, E. (2011): Extent of the Late Glacial Lake Rosenheim and implications of isostatic movements (Southern Germany, Upper Bavaria). – XVIII. INQUA BERN 2011, Poster Abstracts ID 2491, Bern.

Kroemer, E., Wallner, J., Herz, M. & Kunz, R. (in press): Geologische Karte von Bayern 1 : 25 000, Blatt Nr. 8138 Rosenheim. – Augsburg (Bayerisches Landesamt für Umwelt).

Kunz, R., Herz, M.,Grottenthaler, W. & Kroemer, E. (2013a): Geologische Karte von Bayern 1 : 25 000, Blatt Nr. 8139 Stephanskirchen. – Augsburg (Bayerisches Landesamt für Umwelt).

Kunz, R., Herz, M. & Pippèr, M. (2013b): Geologische Karte von Bayern 1 : 25 000, Blatt Nr. 8139 Stephanskirchen. – Augsburg (Bayerisches Landesamt für Umwelt).

Lauer, T., Krebschek, M., Frechen, M., Tsukamoto, S., Hoselmann, Ch. & Weidenfeller, M. (2011): Infrared radiofluorescence (IR-RF) dating of Middle Pleistocene fluvial archives of the Heidelberg Basin (Southwest Germany). – Geochronometria, 38: 23–33.

Müller, U. (2000): A Late-Pleistocene pollen sequence from the Jammertal, south-western Germany with particular reference to location and altitude as factors determining Eemian forest composition. – Vegetation History and Archaeobotany, 9: 125–131.

Müller, U. (2001): Die Vegetations- und Klimaentwicklung im jüngeren Quartär anhand ausgewählter Profile aus dem südwestdeutschen Alpenvorland. – Tübinger Geowissenschaftliche Arbeiten, D7: 1–118.

Penck, A. & Brückner, F. (1901/09): Die Alpen im Eiszeitalter. – 3 vol., 1199 p., Leipzig (Tauchnitz).

Preusser, F., Drescher-Schneider, R., Fiebig, M. & Schlüchter, Ch. (2005): Re-interpretation of the Meikirch pollen record, Swiss Alpine Foreland, and implications for Middle Pleistocene chronostratigraphy. – Journal of Quaternary Science, 20: 607–620.

Pröbstl, M. (1982): Der Samerberg im Eiszeitalter. Hunderttausend Jahre auf einen Blick. – 224 p., Rosenheim (Verlag Historischer Verein Rosenheim).

Troll, K. (1924): Der diluviale Inn-Chiemsee-Gletscher. Das geographische Bild eines typischen Alpenvorlandgletschers. – Forschungen zur Deutschen Landes- und Volkskunde, 23: 121 p., Stuttgart.

Wallner, J. (2011a): Vorläufige geologische Karte von Bayern 1 : 25 000, Blatt Nr. 8037 Glonn (Teilblatt), digitaler Vektordatensatz. – Augsburg (Bayerisches Landesamt für Umwelt).

Wallner, J. (2011b): Vorläufige geologische Karte von Bayern 1 : 25 000, Blatt Nr. 8038 Rott am Inn (Teilblatt), digitaler Vektordatensatz. – Augsburg (Bayerisches Landesamt für Umwelt).

Wallner, J. (2011c): Vorläufige geologische Karte von Bayern 1 : 25 000, Blatt Nr. 7938 Steinhöring (Teilblatt), digitaler Vektordatensatz. – Augsburg (Bayerisches Landesamt für Umwelt).

Wallner, J. (2011d): Vorläufige geologische Karte von Bayern 1 : 25 000, Blatt Nr. 7939 Wasserburg, digitaler Vektordatensatz. – Augsburg (Bayerisches Landesamt für Umwelt).

Wolf, H. (1973): Geologische Karte von Bayern 1 : 25 000, Blatt Nr. 8238 Neubeuern. – München (Bayerisches Geologisches Landesamt).

Quaternary sediments in the Werdenfels region (Bavaria, southern Germany)

Quartäre Ablagerungen im Werdenfelserland (Bayern, Süddeutschland)

Ulrich Haas, Marc Ostermann, Diethard Sanders, Thomas Hornung

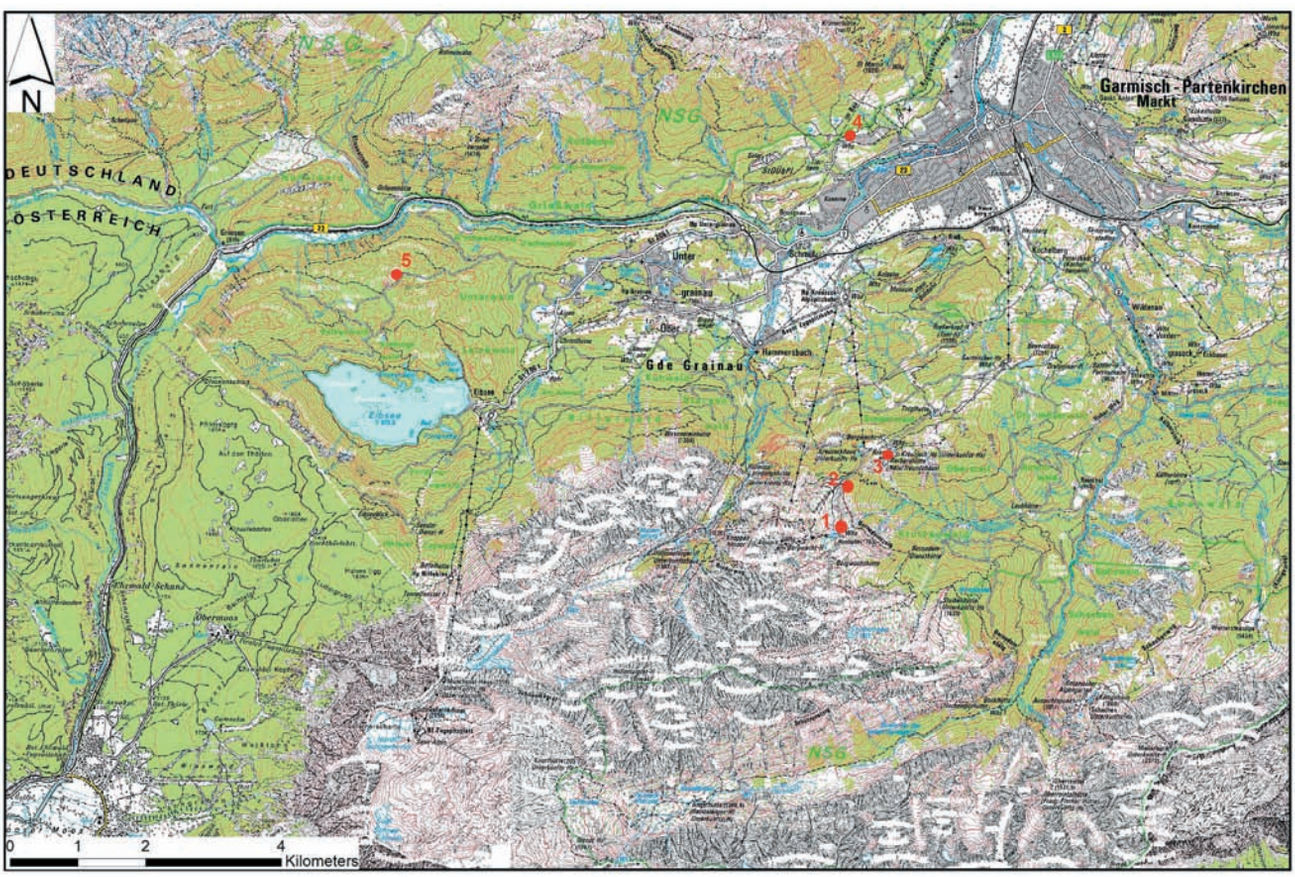

Fig. 1: Excursion route and stops 1–5. Stop 1: Road north of Hochalm hut: overview of the Quaternary sediments in the Wetterstein mountains including the Schachen/Teufelsgsäss breccias and the conglomerates and conglobreccias at Meilerhütte/Törl; Stop 2: Road north of the Kreuzeck house: outcrops in the Längenfeld conglomerate and Pleistocene lake beds; Stop 3: Outcrops south of Kreuzalm in the Kreuzeck conglomerate; Stop 4: Breitenau north of Garmisch-Partenkirchen: overview of the Eibsee landslide area; Stop 5: Vordermoos north of the village Eibsee, location of the 1993 drilling site. Map source: TK50 © Bayerische Vermessungsverwaltung 2014.

***Abb. 1**: Exkursionsroute und Halte 1–5. Halt 1: Straße nördlich der Hochalm Hütte: Überblick über die quartären Sedimente in der Wettersteingruppe einschließlich der Schachen/Teufelsgsäss Brekzien und der Konglomerate und Konglobrekzien bei der Meilerhütte / Törl; Halt 2: Straße nördlich des Kreuzeckhauses: Aufschlüsse im Längenfeld Konglomerat und pleistozäne Seeablagerungen; Halt 3: Aufschlüsse im Kreuzeck-Konglomerat südlich der Kreuzalm; Halt 4: Breitenau nördlich Garmisch-Partenkirchen: Überblick über das Eibsee - Bergsturzgebiet; Halt 5: Vordermoos nördlich von Eibsee, Bohrstelle von 1993. Karte: TK50 © Bayerische Vermessungsverwaltung 2014.*

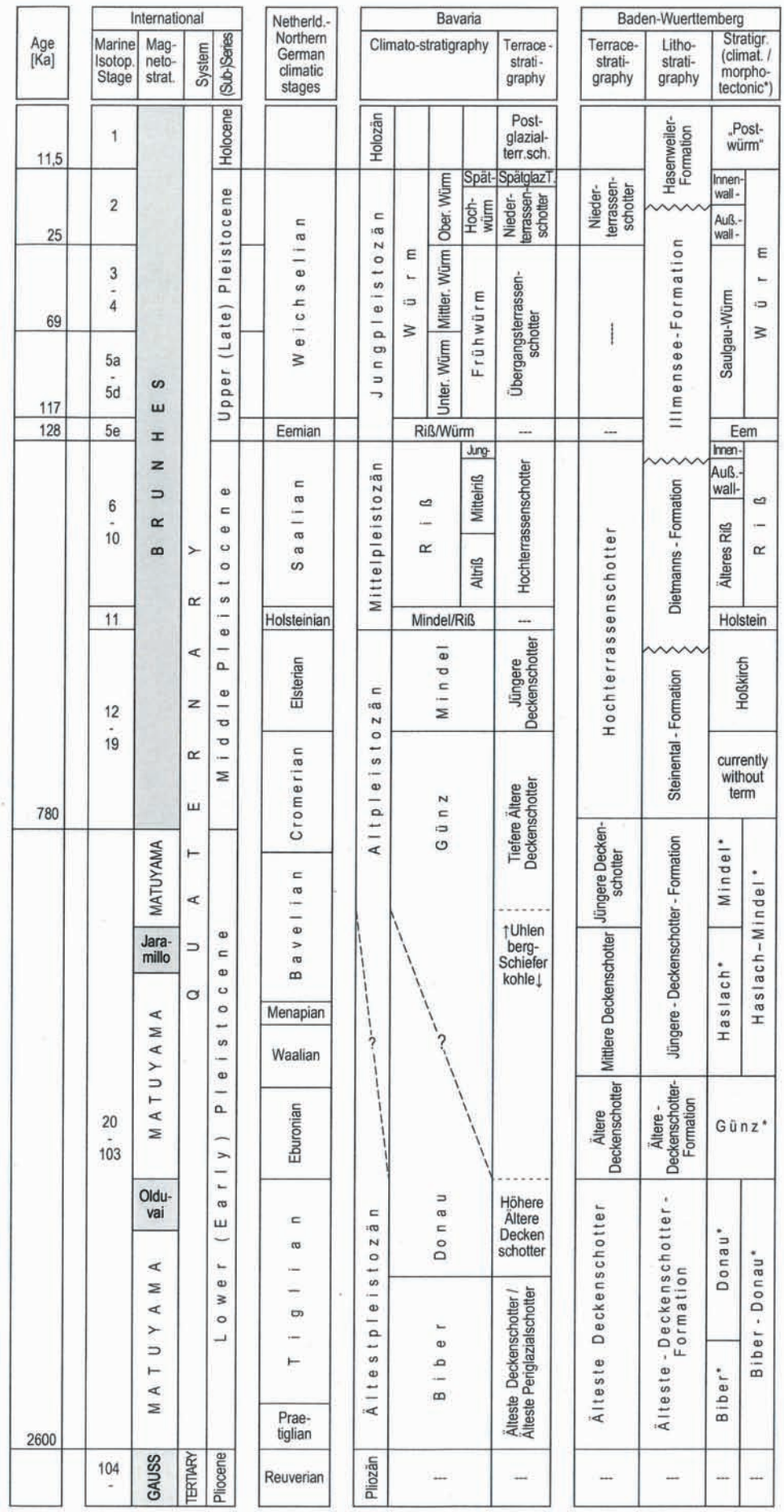

Fig. 2: Stratigraphic systems for the Quaternary of southrn Bavaria according to the "Stratigraphische Kommission" (2002), Ogg & Smith (2004), Ellwanger et al. (2003). Source: Doppler et al. (2011).

***Abb. 2:** Stratigraphische Gliederung für das Quartär von Südbayern entsprechend der „Stratigraphischen Kommission" (2002), Ogg & Smith (2004), Ellwanger et al. (2003). Quelle: Doppler et al. (2011).*

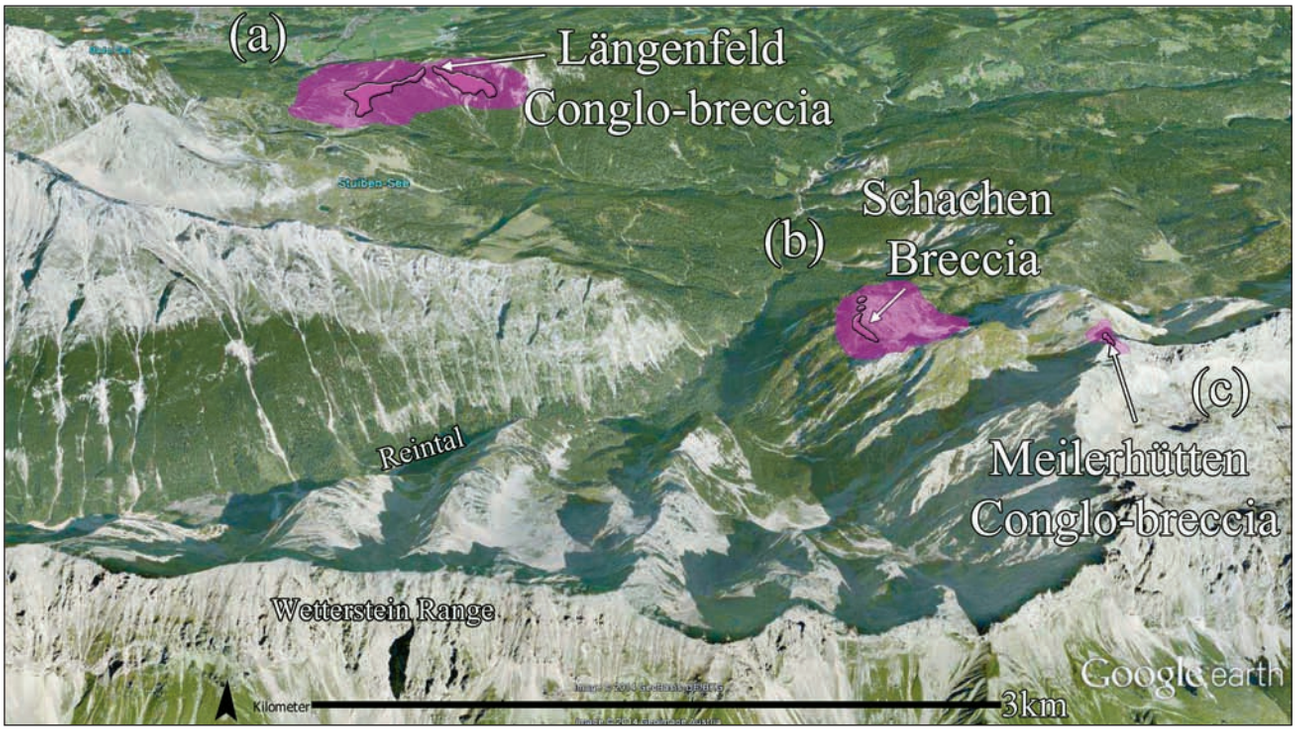

Fig. 3: Overview image (Google Earth) of the central part of the Wetterstein Range (foreground), view towards the Garmisch basin (background). The relicts (pink) and the assumed former extent (shaded pink) of fossil **(a)** glacio-fluvial (Längenfeld), **(b)** talus (Schachen) and **(c)** fluvial deposits (Meilerhütte) are denoted. Each of them represents an isolated geomorphological setting so that the deposits could neither be produced by the present processes and/or pathways of downslope transport at the respective sites, nor could accumulate at their respective locations within the recent setting.

Abb. 3: *Überblicksbild (Google Earth) des zentralen Teils der Wettersteingruppe (Vordergrund), Blick Richtung des Beckens von Garmisch (Hintergrund). Die Reste (lila) und die angenommene frühere Ausdehnung (helleres lila) von fossilen* ***(a)*** *glaziofluvialen,* ***(b)*** *Halden und* ***(c)*** *fluvialen Ablagerungen (Meilerhütte) sind vermerkt. Jede von ihnen repräsentiert eine isolierte geomorphologische Situation, die Ablagerungen konnten weder durch gegenwärtige Prozesse oder hangabwärts gerichtete Transportwege entstehen noch könnten sie an ihren jeweiligen Stellen in der gegenwärtigen Situation akkumuliert werden.*

1 Introduction

In the Werdenfels egion region in the South of Germany some very interesting Quaternary sediments can be found. Erosional remnants of lithified deposits (Fig. 3), mainly of subaerial talus slopes and alluvial fans perched high up in intramontane settings, have attracted the attention of earth scientists for more than a century. A most startling aspect of these erosional relicts ('Hochgebirgsbrekzien') is that in many cases they hint at former landscape configurations that have vanished since then (e.g. Ampferer 1907, Penck 1925). This holds in particular for remnants of lithified pebbly alluvium preserved at altitudes and in settings that seemed to suggest even a Pliocene age (Penck 1925, Winkler-Hermaden 1957). Wehrli (1928) perhaps made the most ambitious approach to reconstruct their former geomorphological contexts. Yet, for decades, interest in these erosional relicts was limited mainly because it was not possible to assign absolute ages beyond mere speculation.

At present, however, recent progress in radiometric dating methods allows to absolutely date, either the deposit or a diagenetic precipitate within. For the first time it is possible to define physically-based age constraints. In this paper, relicts of 'Hochgebirgsbrekzien' are described that are obviously isolated from their present geomorphological setting. Late Pleistocene U/Th cementation ages for two of the relicts suggest that they accumulated during the Quaternary rather than having been deposited during the Pliocene.

2 Definitions

In the following descriptions, the formal rank of lithostratigraphic units is given according to Piller et al. (2004). "Conglobreccias" are designated as sedimentary facies or successions that consist of subequal amounts of lithoclasts of angular and rounded shape and that typically show a wide range of rounding per stratum. Earlier authors often designated erosional relicts of coarse-grained deposits as 'breccias' even if their components may explicitly be described as 'well rounded'. As a result, the ruditic deposits of Kreuzeck-Längenfeld entered the literature as 'breccias', although, as described below, they are designated as conglobreccias to conglomerates.

3 Geological setting

The main morphological feature of the excursion area is the Wetterstein range with Zugspitze (2962 m a.s.l.), being the highest summit of Bavaria. In the environs of Garmisch-Partenkirchen within the Northern Calcareous Alps, the scenery is characterised by thick stacks of carbonate rocks. There, the sedimentary succession starts with Middle Triassic (Anisian and Ladinian pro parte) limestones and dolostones of the Gutenstein-, Steinalm- and Reifling Formations (Rüffer 1995), locally with intercalated marls and volcanic tuffites (pietra verde). During the Ladinian and early Carnian, the Wetterstein Limestone accumulated from banktop to reefal to slope environments of carbonate platforms; this succession also comprises most of the major peaks of the

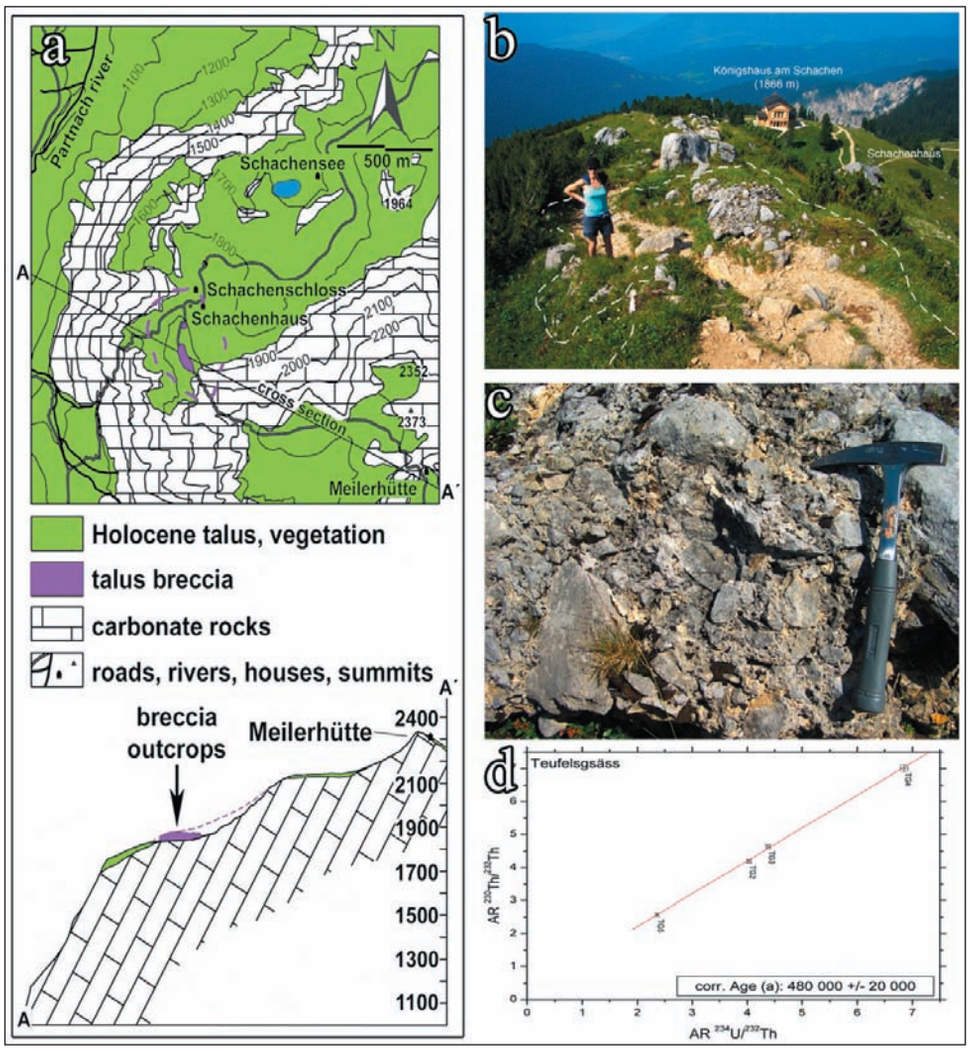

Fig. 4: (a) Sketch map and cross section of the fossil talus deposits at Schachen (Teufelsgsäss). The recent remnants are coloured pink and the assumed minimum former extent of the talus sediments is marked by a pink dashed line. **(b)** Outcrop photo of the Schachen breccia, view towards the North. The deposits are preserved in an isolated geomorphic setting along a ridge. The largest part of the deposits has already been eroded and the cliffs, as source of the talus, are far away from the deposits now. **(c)** Outcrop photo of the deposits at Schachen. The typical rock fall dominated talus breccia shows angular clasts of Wettersteinkalk in predominant chaotic texture. **(d)** Isochron-plot of the U/Th-ages of the calcite precipitations found at Schachen (Teufelsgsäss) showing a perfect regression line.

Abb. 4: (a) *Lageskizze und Querprofil der fossilen Halden bei Schachen (Teufelsgsäss). Die derzeitigen Reste sind in lila angegeben und die angenommene frühere Ausdehnung ist mit einer lila gestrichelten Linie eingezeichnet.* ***(b)*** *Aufschlussfoto der Schachen Brekzie, Blick Richtung Norden. Die Ablagerungen sind in einer isolierten geomorphologischen Situation erhalten. Der größte Teil der Ablagerungen wurde bereits erodiert und die Felswände als Quelle für die Halden sind heute weit von den Ablagerungen entfernt.* ***(c)*** *Aufschlussfoto der Ablagerungen beim Schachen. Die typische steinschlagdominierte Talusbrekzie zeigt eckige Stücke von Wettersteinkalk mit vorherrschend chaotischer Textur.* ***(d)*** *Isochronen-Diagramm der U/Th-Alter der Kalzite bei Schachen/Teufelsgsäss mit einer perfekten Regressionsgeraden.*

Wetterstein range, such as Zugspitze, Alpspitze and Dreitorspitze. The correlative basin succession (Partnach Formation) prevails east of Risserkopf and into the gorge of the river Partnach. A large carbonate platform was established (Hauptdolomit-Dachsteinkalk megabank), following repeated phases of siliciclastic deposition during the middle Carnian. From latest Carnian to Norian times, as a result of continued subsidence kept up by carbonate deposition, a succession of platform dolostones and limestones accumulated (Hauptdolomit and Plattenkalk unit, respectively) up to more than 2000 m in thickness. In the excursion area, these latter units comprise the area between Kreuzeck, Hochalm and Elmau. The Triassic series is topped by the Rhaetian shallow basin succession of the Kössen Formation.

With the beginning of the Jurassic, the Hauptdolomit platform subsided and disintegrated by rifting into deepmarine basins and intercalated swells. In the basins, thick successions of cherty deep-water marls and limestones were deposited (Allgäu-, Ruhpolding and Ammergau Formations). In the excursion area these formations prevail south of Gatterl and in the region of Eibsee. Alpine shortening and consequent formation of thrust nappes started during the terminal Jurassic and continued into the Early Cretaceous (Eo-Alpine phase). Deep-water sedimentation continued until the late Early Cretaceous, with increasing terrigenous input from emergent areas of the orogenic wedge (Schrambach Formation). In Albian times, basanitic dykes (local name is "Ehrwaldite") cross-cut the thrust nappe stack of the future Northern Calcareous Alps (Trommsdorff et al. 1990). During subsequent orogenic deformations (Meso- and Neo-Alpine phase), the nappes were subject to transverse thrusting and folding, and to strike-slip disintegration (Eisbacher & Brandner 1996).

4 Breccia at Schachen/Teufelsgsäss

Location: about 6 km south of Garmisch-Partenkirchen, Germany, on the northern flanks of the Wetterstein mountain range, coordinates [UTM, WGS 84, zone 32N]: E 659268 N 5253700, 1940 m a.s.l.

Schachen Alp is located at the north facing slope of the Wetterstein mountain chain. It is very famous, because King Ludwig II's mountain refuge is situated there, built from plans by Georg Dollmann in 1869 to 1872.

The mountain ridge south of Schachen is called Teufelsgsäss. At an altitude of about 1850–1950 m a.s.l., directly beside the footpath to Meilerhütte, breccia deposits are cropping out (Figs. 4a & 4b). The sediments are preserved as small erosional remnants along the Teufelsgsäss. Today they cover an area of about 5000 m^2. The former extent is not assessable because the whole accumulation area has been intensely transformed and reshaped through time.

The Schachen breccia is characterised by angular clasts of all sizes that are extremely poorly sorted (Fig. 4d). The breccia is clast supported and contains little matrix, and there is no recognizable bedding. All clasts belong to the Middle Triassic limestones of the Wettersteinkalk Formation. The Schachen breccia is a typically rock fall dominated talus breccia. The breccia deposits have already been mentioned by Penck (1925) and Jerz (1966). Jerz (1966) assigned a Lower Pleistocene age to the Schachen breccia. Fortunately calcite cements suitable for U/Th-dating were found within the lithified talus sediments. The closed system check indicated a homogenous behaviour of the sub-samples, resulting in a very well-defined isochron line (Fig. 4d). The calculated cementation age of 480,000 ± 20,000 yr BP reaches the upper limit of the method of about 500 ka (Ivanovich & Harmon 1992). The well-defined regression line, the outcrop situation and the geomorphological context underline the accuracy of the calculations.

The breccias at Schachen are an example for a fossil talus relict in an isolated geomorphic setting. They are preserved along a crestline and isolated from a cliff.

5 Kreuzeck–Längenfeld conglomerate

Location: about 3 km south of Garmisch-Partenkirchen on the north facing flanks of the Zugspitz Mountains, coordinates [UTM, WGS 84, zone 32 N]: E 655089 N 5256555,1600-1750 m a.s.l.

The term Kreuzeck–Längenfeld conglomerate designates two erosional relicts, closely adjacent to each other, consisting of a succession of lithified pebbly to cobbly alluvium. Previous investigators of these deposits all suggested that both relicts pertain to the same sedimentary succession (Penck 1925, Vaché 1961), a view that we concur with. The alluvial succession onlaps a truncation surface incised into the Northalpine Raibl (NAR) beds) that here consist mainly of dolostones and cellular dolostones. The truncation surface rises from ~1500 m a.s.l. near Kreuzeck at the northeastern limit of preservation to ~1750 m a.s.l. at Längenfeld at the southwestern end (Fig. 5a). Overall, the truncation surface onlapped by the alluvial deposits dips towards the northeast.

Basal part of succession near Kreuzeck: On the valley flank to the North and downslope of Kreuzeck, the basal part of the northeastern end of the preserved succession is exposed. Here, the upper part of the NAR succession consists of clast-supported, monomictic, poorly lithified breccias a few tens of metres thick. These breccias do not show sedimentary stratification, and opposite clast boundaries commonly fit with each other; between the clasts, a scarce cataclastic matrix is present; only locally, small patches and lenses are present wherein the clasts obviously are rotated relative to each other. The breccia interval is interlayered with and cross-cut by levels and lenses up to a few centimetres in thickness characterised by cataclastic gouges. In the topmost few metres of this succession, the monomictic NAR breccia is intercalated with (i) scattered rounded lithoclasts up to 50 cm in size (Fig. 5e), and (ii) diffusely delimited patches and lenses with rounded lithoclasts derived from the Wetterstein Formation (Fig. 6a). Up-section, a succession of conglomerates and conglobreccias of clear-cut sedimentary origin, i. e. the Kreuzeck ruditic deposits, are exposed (Fig. 6b).

Kreuzeck-Längenfeld outcrops: The main part of the succession is best exposed in outcrops along and above a road from Kreuzeck to Längenfeld. Here, the succession at first glance appears to consist of strata that dip with a few degrees towards NE-E (Fig. 5c). Bed sets with subhorizontal-parallel stratification are intercalated with cross-stratified intervals (Fig. 5d). Typical facies include: (a) lenses of clast-supported, coarse-pebbly to cobbly conglobreccias to conglomerates with a matrix of carbonate-lithic arenite (Fig. 6c); (b) lenses with disordered clast fabrics supported by, either, the lithoclasts, and/or by a matrix of carbonate-lithic arenite; (c) intervals up to ~1 m in thickness of poorly to moderately sorted, fine pebbly to cobbly, clast-supported conglobreccias; these intervals may show indistinct upward-fining; in bedsets of this facies, stratification is mainly evident by vertical changes in sorting and mean clast size; this facies is typically intercalated with finer-grained lithologies (Fig. 6d) (d) intervals similar to the former, up to a few decimetres in thickness, but with the clasts supported by a matrix of winnowed carbonate-lithic sand, (e) lenses up to a few metres in length and ~1 m in thickness of well-sorted carbonate-lithic arenite, locally displaying parallel-horizontal lamination; and (f) levels up to 10 cm thick of parallel-horizontally laminated carbonate siltstone to lime mudstone. A sample of this latter facies consisted mainly of calcite and a few percent each, of dolomite, quartz and muscovite (X-ray diffraction analysis). The Kreuzeck-Längenfeld deposits lithified mainly by micritic cement precipitated in interstitial pores of the arenitic matrix. In relatively rare pebbly layers with openwork clast fabrics, however, fringes of isopachous calcite spar are present. In a sample of this facies, a calcite cement was dated with the U/Th disequilibrium method (see section 'Age'). The Kreuzeck succession was deformed while the sediment was still unlithified. Features of deformation include (i) 'sag-like' synclinal structures (Fig. 6e), (ii) recumbent folds (Fig. 6f), and (iii) loss of sedimentary stratification to impart a 'massive', homogenized aspect to the sediment; this latter feature is associated with the other deformation structure.

5.1 Interpretation and discussion

The succession of Kreuzeck-Längenfeld accumulated within an alluvial system with characteristics reminiscent of a stream-dominated alluvial fan and/or the proximal part of a braided stream. With respect to facies, the succession is not peculiar, as numerous comparable depositional systems exist

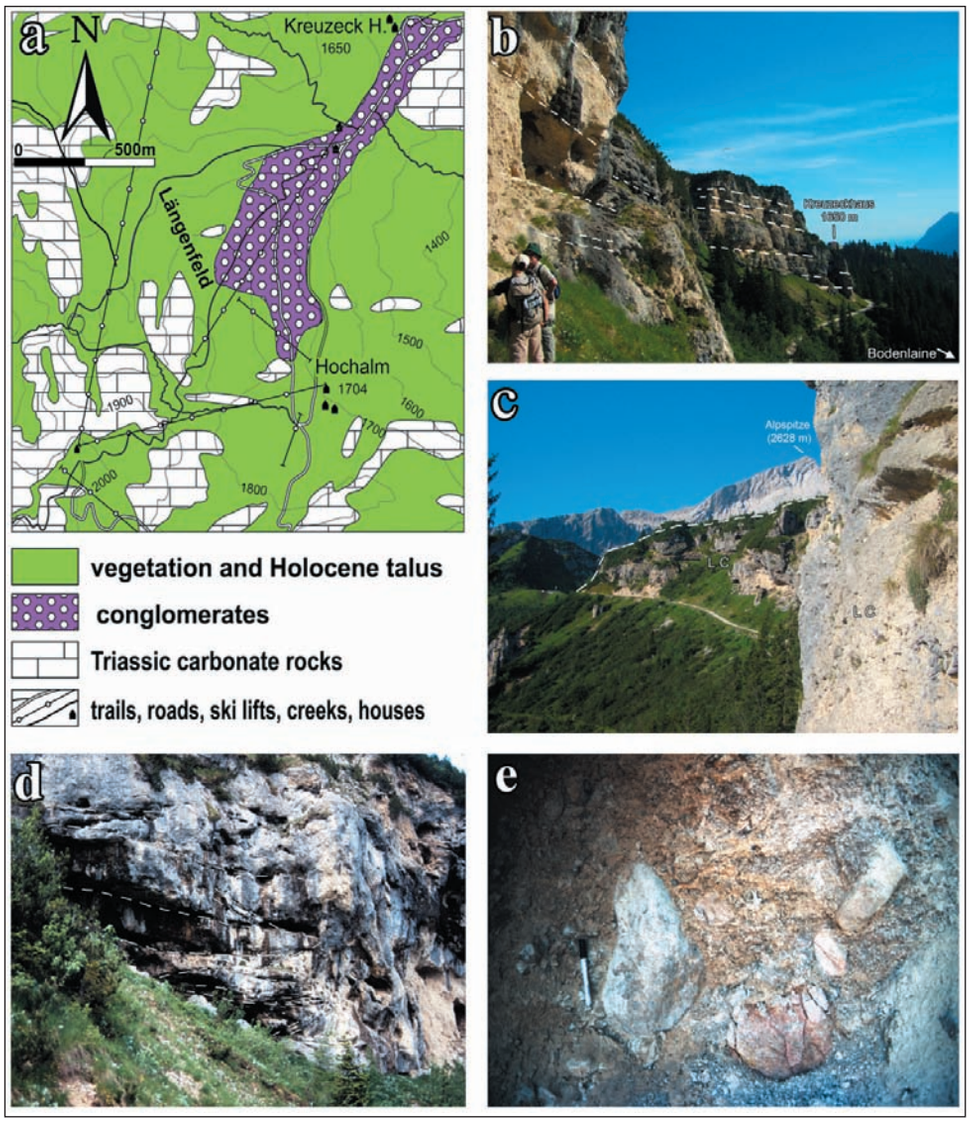

Fig. 5: (a) Sketch map of the deposits at Längenfeld/Kreuzeck. **(b)** Outcrop photo of the middle part of the Längenfeld conglobreccia, view towards the North. The succession forms a rock wall with a maximum height of about 70 m. The major bedding planes mainly dipping towards the Bodenlaine are denoted. **(c)** Outcrop photo of the Längenfeld conglobreccia (LC), view towards the South. Note the difference in inclination of the bedding planes. In the foreground the alternating sequences of coarse grained angular material (lower part) with fine grained sub-rounded material (upper part) can be seen. **(d)** Bedsets in the middle part of the Längenfeld conglobreccia show subhorizontal to parallel stratification intercalated with cross-stratified intervals. Outcrop height is about 20 m. **(e)** Topmost metres of the basal part of the succession near Kreuzeck shows scattered rounded lithoclasts up to 50 cm in size in a clast-supported, monomictic, poorly lithified breccia matrix.

Abb. 5: (a) *Lageskizze der Ablagerungen bei Längenfeld/Kreuzeck.* ***(b)*** *Aufschlussfoto des mittleren Teils der Längenfeld Konglobrekzie, Blick Richtung Norden. Die Sukzession bildet eine Felswand mit einer größten Höhe von 70 m. Die hauptsächlichen Schichtflächen die vor allem zur Bodenlaine einfallen, sind bezeichnet. Im Vordergrund kann man die alternierenden Folgen von grobem, eckigen Material (unterer Teil) mit feinkörnigem angerundeten Material (oberer Teil) sehen.* **(c)** *Aufschlussbild der Längenfeld Konglobrekzie (LC), Blick nach Süden. Man bemerke den Unterschied in der Neigung der Schichtflächen. Im Vordergund sieht man die alternierende Folge von grobem, eckigem Material (unterer Teil) und feinkörnigem, schlecht gerundeten Material (oberer Teil).* **(d)** *Schichtfolgen im mittleren Teil der Längenfeld Konglobrekzie zeigt subhorizontale bis parallele Schichtung mit eingeschalteten kreuzgeschichteten Intervallen. Aufschlusshöhe ist etwa 20 m.* ***(e)*** *Die obersten Meter des untersten Teiles der Abfolge unweit Kreuzeck zeigen geundete Lithoklasten bis zu einer Größe von 50 cm in einer grobmaterialgestützten, monomiktischen und schlecht verfestigten brekziösen Matrix.*

in the present Northern Calcareous Alps. Surface runoff can be recognized as the dominant process in the formation of the final facies due to (i) transport, resulting in rounding of clasts up to small boulder size, (ii) the typical matrix of winnowed carbonate-lithic sand, and (iii) cross-stratified bedsets of conglomerates. The overall composition of the succession of subangular to well-rounded pebbles to small boulders combined with the extremely-poor to moderate sorting of most lithologies, indicates that the depositional system was characterised by fluctuations of watershed; it also seems possible that runoff intermittently ceased, which is often typical for stream-dominated fans and proximal braided-stream systems. The intervals of parallel-laminated arenite and of siltstone to lime mudstone with accessory dolomite, quartz and muscovite, probably both accumulated from waning sheet flows in areas laterally adjacent to channels (e.g., on top of braid bars, lateral bars, or terraces). The quartz grains were not investigated separately; they may be suited for optically-stimulated luminescence dating. The muscovite grain fraction suggests that erosion of glacigenic material contributed to this type of sediment. The rise of local base-level that led to the accumulation of the Kreuzeck-Längenfeld succession can only be speculated on because of both the limited preservation of the succession, and its isolation from

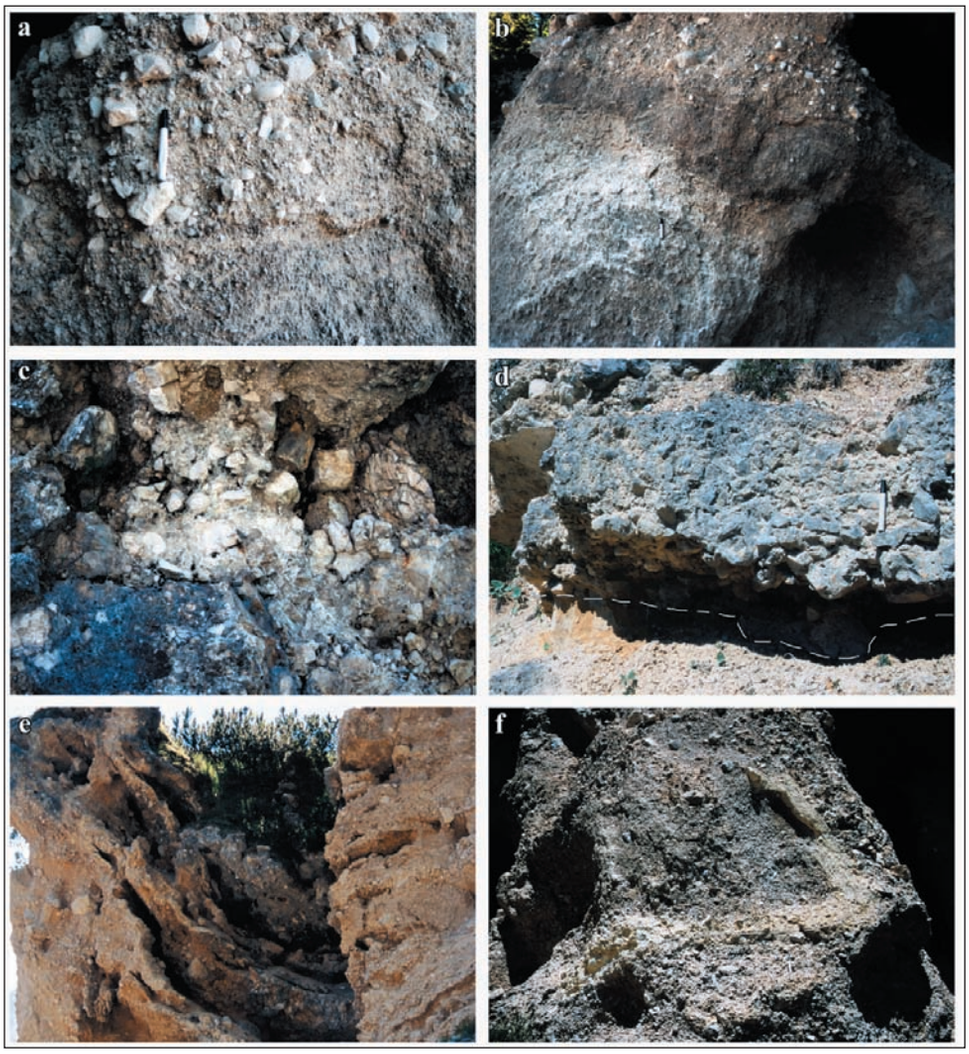

Fig. 6: (a) The basal part of the succession near Kreuzeck is characterised by unsharply-delimited patches and lenses of rounded lithoclasts derived from the Wetterstein Formation. **(b)** Succession of conglomerates and conglobreccias at the basal part of the succession near Kreuzeck. **(c)** At the Kreuzeck-Längenfeld outcrops lenses of clast-supported, coarse-pebbly to cobbly conglobreccias to conglomerates in a matrix of carbonate-lithic arenite are common. Image size is about 1.5 m in height. **(d)** At the Kreuzeck-Längenfeld outcrops, intervals of poorly to moderately sorted, fine pebbly to cobbly, clast-supported conglobreccias (upper part of image) are intercalated with bedsets of fine-grained sand to silt (lower part of image). **(e)** 'Sag-like' synclinal deformation structures at the Kreuzeck succession. Outcrop height is about 5 m. **(f)** Recumbent fold of fine-grained material at the Längenfeld succession. Outcrop height is about 1.5 m.

Abb. 6: (a) *Der basale Teil der Abfolge unweit Kreuzeck ist durch unscharf begrenzte Flecken und Linsen von gerundeten Lithoklasten aus der Wetterstein Formation gekennzeichnet.* ***(b)*** *Abfolge von Konglomeraten und Konglobrekzien im basalen Teil der Abfolge unweit Kreuzeck.* ***(c)*** *Bei den Kreuzeck-Längenfeld Aufschlüssen sind Linsen von klastengestützten, grobkiesig bis blockigen Konglobrekzien bis Konglomeraten in einer Matrix von karbonatisch-verfestigten Arenit verbreitet.* ***(d)*** *Bei den Kreuzeck-Längenfeld Aufschlüssen sind Abschnitte von schlecht bis mäßig sortierten, feinkiesigen bis blockigen klastengestützten Konglobrekzien (oberer Teil des Bildes) wechselgelagert mit feinkörnigem Sand bis Schluff (unterer Teil des Bildes).* ***(e)*** *Durchhängende synklinale Verformungsstrukturen der Kreuzeck-Abfolge. Aufschlusshöhe ist 5 m.* ***(f)*** *liegende Falte aus feinkörnigem Material der Längenfeld-Abfolge. Aufschlusshöhe ist etwa 1,5 m.*

the present geomorphic setting. In an intramontane setting such as that of the Quaternary of the Northern Calcareous Alps, probable causes for local base-level rises are (i) deposition shortly after the last major glaciation, i.e., accumulation related to readjustment of longitudinal valley profile, (ii) deposition caused by an advancing ice stream that blocked an unpreserved valley ahead, (iii) accumulation related to mass-wasting, or (iv) a relative increase in bedload, perhaps combined with a transition to more ephemeral runoff.

We interpret the basal interval of monomictic, poorly lithified breccias to unlithified angular pebbly deposits on top of the NAR beds, located near Kreuzeck, as a deposit of mass-wasting. This facies resembles a rockslide deposit with because of its monomictic composition, the fabric of fitted angular clasts separated by a scarce matrix composed of fine-grained material of the same lithology (cataclastic gouge), and the intercalated levels and lenses of cataclastic gouge. A rockslide origin of this facies does not contradict the overall preservation of the stratigraphic succession above. In fact, a typical feature of rockslides is that the stratigraphic succession of the detachment area is roughly preserved, albeit with some mixing in the final rockslide deposit. The limited vertical mixing of Kreuzeck conglomerates with the cataclastic rockslide material thus would furthermore agree with a rockslide origin. The sag-like syncline and the recumbent fold in the outcrops along the road from Kreuzeck to Längenfeld indicate that this part of the succession was also affected by deformation before lithification. This deformation may have taken place on top or adjacent to a rockslide mass. Alternatively, the transitional interval from cataclastic

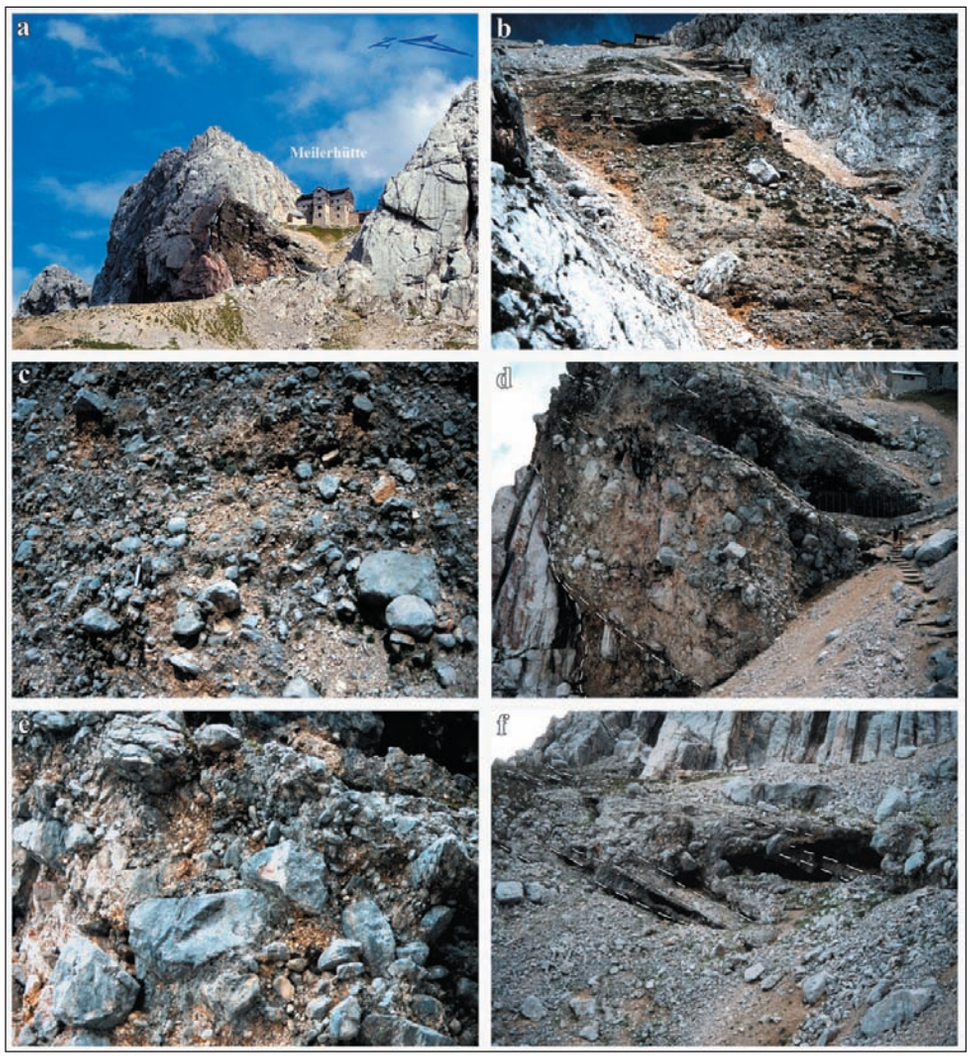

Fig. 7: (a) Conglomerates and conglobreccias at Meilerhütte/Törl. View towards the East. The Meilerhütte rests on a succession at least 90 m in thickness of pebbly to bouldery conglobreccias (bordered by dashed line). **(b)** On the southern side of the mountain crest the succession consists of amalgamated layers of extremely-poorly to very-poorly sorted, pebbly to cobbly deposits with a few intercalated, subangular to rounded boulders up to >1 m in size. The Meilerhütte can be seen on top of the sediments. **(c)** The conglobreccias at Meilerhütte/Törl show subangular to very well-rounded pebbles to cobbles of Wetterstein Formation and the Northern Alpine Raibl beds in a subhorizontal stratification. **(d)** On the northern side of the mountain crest the succession consists of extremely-poorly sorted bouldery conglobreccias with widely-spaced stratification surfaces that dip 20–25° to SSE. Boulders range up to 2.5-3 m in size. **(e)** Detail image of Fig. 5d. Most pebbles to boulders are subangular to subrounded in shape, with a minor fraction also moderately-well to well-rounded. **(f)** Toward the top of the succession at the Meilerhütte the deposits become overall more finer-grained and better-sorted, mainly because of a decrease in maximum size and percentage of boulders.

***Abb. 7: (a)** Konglomerate und Konglobrekzien bei der Meilerhütte / Törl. Blickrichtung Osten. Die Meilerhütte liegt auf einer mindestens 90 m mächtigen Abfolge von kiesigen bis blockigen Konglobrekzien (abgegrenzt mit gestrichelter Linie). **(b)** auf der Südseite des Bergrückens besteht die Abfolge aus amalgamierten Lagen von extrem schlecht bis sehr schlecht sortierten kiesigen bis blockigen Ablagerungen mit einigen wenigen eingeschalteten angerundeten bis gerundeten Blöcken bis zu einer Größe von >1 m. Die Meilerhütte liegt am Oberrand der Ablagerungen. **(c)** Die Konglobrekzien bei der Meilerhütte / Törl zeigen angerundete bis sehr gut gerundete Kiese und Blöcke aus der Wetterstein Formation und den Nordalpinen Raibler Schichten in einer subhorizontalen Lagerung. **(d)** Auf der Nordseite des Bergzuges besteht die Abfolge aus extrem schlecht sortierten Konglobrekzien mit weit auseinanderliegenden Schichtflächen, die 20–25° nach SSE einfallen. Die Blöcke sind bis zu 2,5 bis 3 m groß. **(e)** Detail von Abb. 5d. Die meisten Kiese bis Blöcke sind angerundet bis schlecht gerundet, ein geringer Anteil ist mäßig gut bis gut gerundet. **(f)** Gegen die Oberkante der Abfolge bei der Meilerhütte werden die Ablagerungen allgemein feinkörniger und besser sortiert, hauptsächlich wegen der Abnahme von Größe und Anteil der Blöcke.*

breccias to conglomerates at Kreuzeck and the deformation structures in the outcrops along the road are related to a collapse from evaporite dissolution in the NAR beds. However a collapse due to dissolution should hardly result in the type of rock cataclasis and low-dipping cataclasite levels as those described here. For this hypothesis to be upheld, an older origin of the cataclasites would be required, for instance due to intense deformation in old fault zones or fold hinges.

6 Conglomerates and conglobreccias at Meilerhütte/Törl

Meiler hut (Meilerhütte, 2374 m a.s.l.) is located on top of a natural pass called Törl, at the crest of the western Wetterstein range of Triassic rocks (mainly carbonate rocks of the Wetterstein Formation and NAR beds). This area is crossed by a segment of a former bedrock gorge, which is filled with a succession of pebbly to bouldery conglobreccias at least 90 m thick. (Fig. 7a). This gorge segment strikes NNW-SSE and is 230 m long. Upward from the lowest exposure of the sedimentary gorge-fill at 2285 m a.s.l., the gorge widens from a mere 15 m to 60 m directly at Meiler hut. From above it can be observed that particularly the northeastern bedrock wall of the gorge is notably straight. This suggests that incision took place along a zone of structural weakness (fault or joint planes). Bedrock exposures on both sides of the mountain

crest suggest that the base of the sediment-filled gorge segment sloped from 2335 m a.s.l. at the northern end of the outcrop to at least 2285 m a.s.l. at the southern end. This indicates a mean minimum dip of the rock surface at the bottom of the gorge of 12°, a value that is easily attained in gorges with steps, waterfalls and plunge pools.

Lithologies and succession: **(a)** On the southern side of the mountain crest, the exposed sedimentary gorge-filling starts at 2285 m a.s.l. There, the succession consists of amalgamated layers of extremely-poorly to very-poorly sorted, pebbly to cobbly deposits with a few intercalated, subangular to rounded boulders up to >1 m in size (Fig. 7b). Pebbles to cobbles range in rounding from subangular to very well-rounded, but most are subrounded to wellrounded (Fig. 7c). The stratification appears to be subhorizontal; however, because of the outcrop intersection, a potential southward dip could hardly be identified. All lithoclasts are derived from the Wetterstein Formation and the NAR beds. The primary matrix of the conglobreccia is winnowed carbonate-lithic sand. In addition, local small pockets of secondary matrix of geopetally-laminated lime mudstone are present in interstitial pores. Openwork clast fabrics are lithified by thin crusts of light-brown lime mudstone or, more rarely, by a very thin layer of isopachous calcite spar. On the southern side, the exposure ends approximately 25 m in altitude below Meiler hut (Fig. 7b). Near the top of the exposed succession, there is an interval a few metres in thickness that consists of relatively distinct strata 10 cm to a few decimetres thick. This interval consists of overall better-sorted, fine- to coarse-pebbly alluvium with a few intercalated, subrounded to well-rounded cobbles. The clasts of the pebble-size fraction range mainly from subangular to subrounded. **(b)** On the northern side of the mountain crest, exposure starts only at 2340 m a.s.l. There, the succession consists of extremely-poorly sorted bouldery conglobreccias with widely-spaced stratification surfaces that dip 20–25° to SSE. The boulders range up to 2.5–3 m in size (Fig. 7d). Most pebbles to boulders are subangular to subrounded in shape, with a minor fraction also moderately-well to well-rounded (Fig. 7e). The primary matrix is winnowed, carbonate-lithic sand; and again, small interstitial pockets may contain geopetally-laminated, light-brown lime mudstone. With respect to its origin, the clast spectrum is identical to that of the southern side of outcrop. Up-section, the deposits become overall more finer-grained and better-sorted, mainly because of a decrease in maximum size and amount of boulders. Near Meiler hut there is an interval of conglobreccia that consists of: (i) a lower bedset positioned with SSE/20–25, sharply topped by (ii) an upper bedset that shows a gentle dip of a few degrees towards the South (Fig. 7f).

6.1 Interpretation and discussion

We interpret the gorge-filling succession described above as lithified, pebbly to bouldery alluvium that was transported and accumulated during ephemeral runoff events. It seems highly probable that surface runoff ceased intermittently, i.e., the partly sediment-filled gorge fell dry between various events. This interpretation is based on a lack of both genuine channel-fills and pebbly-cobbly channel armours, which could be expected in case of permanent surface runoff. The poorly organized, bouldery deposits in the northern part of outcrop probably were topped with 'incipient' cascade channels and step-pool channels during brief episodes of surface runoff. The overall better-sorted and more distinctly stratified intervals, in contrast, are interpreted as sheet-flow deposits accumulated during the waning stage of floods. Inclined, parallel to divergent bedsets topped by more gently-dipping beds are typical of aggrading-prograding fronts of alluvial fans or talus fans. The sediment-filled gorge segment is obviously even isolated from its wider environs. The gorge-filling might represent a vestige of a pre-Quaternary land surface, but this is considered improbable. The incision of deep and narrow rock gorges, such as the 'Törl gorge' described herein, requires high-gradient streams. High-gradient streams or stream sections rich in bedload may relate to: (i) stream diversion and knickpoints, e.g., because of glacial-interglacial cycles or mass-wasting, or (ii) to subglacial runoff. Due to the limited preservation of the gorge segment, none of these settings can be ruled out. The stratal dips in the gorge-filling indicate a northerly transport; the extremely poorly-sorted deposits record proximity to a source area; and the clast spectrum stemming only from the Wetterstein Formation and NAR beds all fit with a source area a 'short' distance towards the North. To fill a gorge with sediment requires a rise of base-level downstream, and/or a relative increase in bedload exceeding the transport capacity within the watershed. The gorge-filling records the encroachment of a depositional system capable of carrying and depositing extremely-poorly sorted deposits consisting of clasts up to boulder size. Deposystems capable of this include alluvial fans or talus fans dominated by debris flows or snow flows, and/or with a local (cirque) glacier or rock glacier source. In the Northern Calcareous Alps, short and narrow bedrock gorges are locally present (i) along the toe of rock cliffs where surface runoff is concentrated, and (ii) in the central to distal part of glacial cirques. However, due to the incomplete preservation of the gorge, no discriminative interpretation of the former geomorphic setting and the depositional system supplying its filling can be put forward.

7 Age

Because of the geomorphic isolation of each of the described successions (Kreuzeck, Schachen, Törl), earlier authors assumed that these deposits may be of Pliocene age (Penck 1925, Wehrli 1928, Uhlig 1954, Winkler-Hermaden 1957). With no numerical ages and no information on uplift history at hand, these authors had to base their age estimates on a number of mere assumptions. Rudites such as those described in this paper are still difficult to date nowadays. In deposits such as the conglomerates of Kreuzeck or the talus breccia of Schachen, the calcite cements can be dated with the $^{234}U/^{230}Th$ disequilibrium method (Geyh 2005; see also Ostermann et al. 2006, 2007, for detailed description). With the methods available to us in 2005, the cements identified in the Törl conglobreccia were found to be too thin to be extracted. Although U/Th dating yields only a mean age of cement precipitation, it also constrains the minimum age of a succession. For the Kreuzeck-Längenfeld conglomerate, the age is 74 ± 3 ka (early Würmian). The fine-grained, quartz-bearing levels in the Kreuzeck succession, however, might be suited for optically-stimulated luminescence dating.

For the Schachen Breccia, a mean precipitation age of

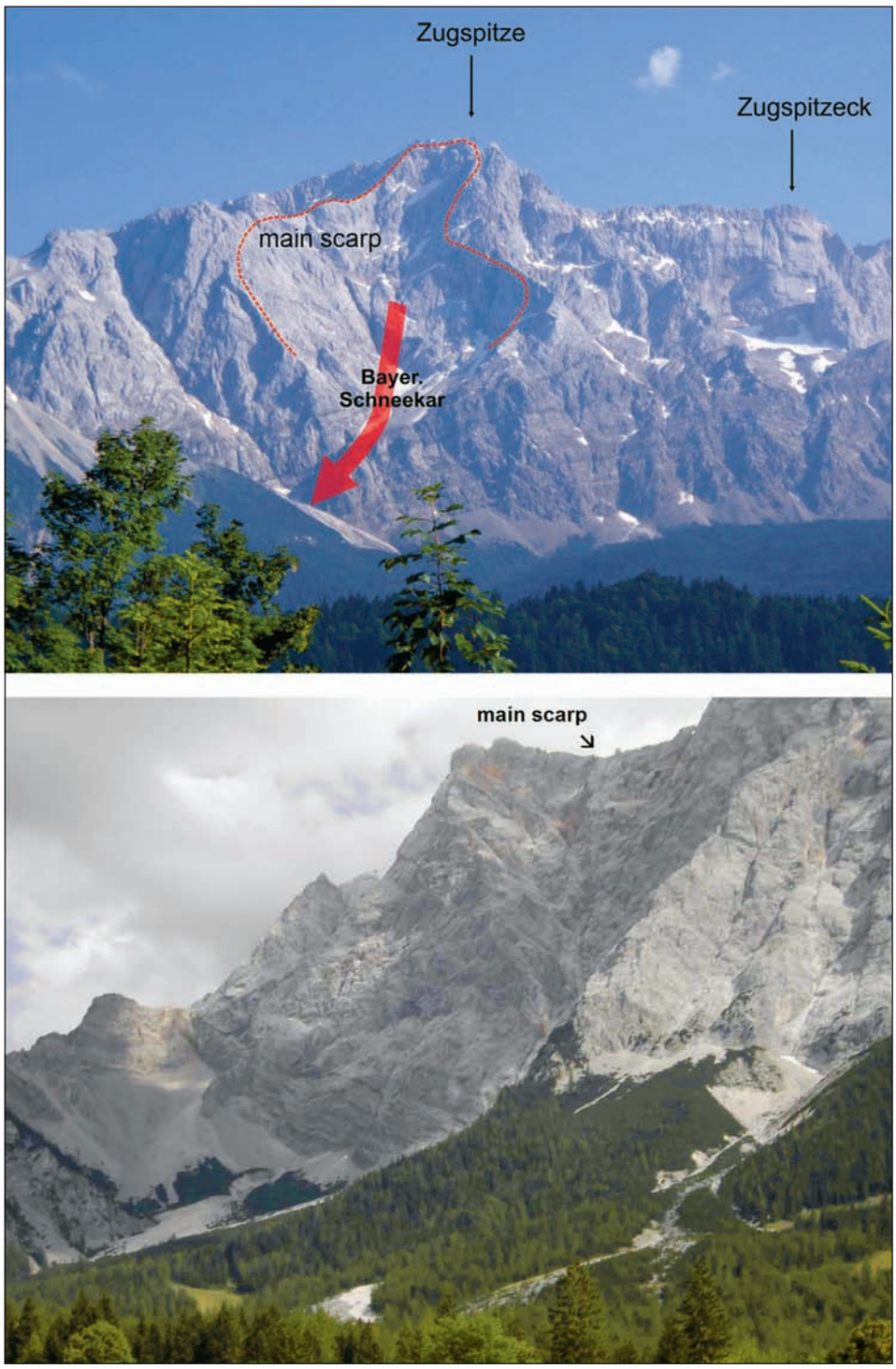

Fig. 8: (a) View to the central part of the Wetterstein Mountains. The main scarp of the Eibsee landslide is high-lighted by the red stippled line. The upper light grey part of Zugspitze is built up of limestone of the Wetterstein-Formation, the lower part consists of marlstones, limestones and marls of the Partnach-, Reifling-, Steinalm- and Gutenstein-Formation.
(b) Main scarp of the distal landslide from the Riffelwand northeast of Zugspitze. The rock wall consists of marlstones, limestones and marls of the Wetterstein-, Partnach-, Reifling-, Steinalm- and Gutenstein-Formation.

Abb. 8: (a) *Blick auf den zentralen Teil der Wettersteingruppe. Die Hauptabbruchsnische des Eibsee-Bergsturzes ist rot umrandet. Die obere hellgraue Zone der Zugspitze ist aus Wettersteinkalk aufgebaut, der untere Teil besteht aus mergeligen, Kalken und Mergeln der Partnach-, Reifling-, Steinalm- und Gutenstein Formation.* ***(b)*** *Hauptabbruchnische des distalen Bergsturzes an der Riffelwand nordöstlich der Zugspitze. Die Wand besteht aus (mergeligen) Kalken und Mergeln der Wetterstein-, Partnach-, Reifling-, Steinalm- und Gutenstein Formation.*

the sampled cements was dated to 480 ± 20 ka (late Günz-Mindel interglacial). In this case, the regression line connecting the sub-samples in the 'Rosholt errorchron' (Rosholt 1976) enables only a single mean age of cementation to be deduced (Ostermann 2006). Both cement precipitation ages (Kreuzeck, Schachen) seem inconsistent with a Pliocene age of the deposits. In mountain ranges undergoing uplift, erosional processes appear too intense and too widespread to allow an unlithified Pliocene ruditic deposit to be preserved until its cementation hundreds of thousands of years to more than a million years later. A check of U/Th cementation ages from talus- and fan successions of unequivocal pre-/post-LGM chronostratigraphic positions showed that the method can yield cementation ages that fit well with the stratigraphic position of the deposit. This underscores the overall applicability of the method to provide a minimum age of deposition (Ostermann 2006; see also Ostermann et al. 2007).

8 Eibsee rockslide area

An overview at Breitenau

Location: about 1.8 km east of the centre of Garmisch, coordinates [DHDN 3 Degree Gauss Zone 4]: E 4429442, N 5262029, 785 m a.s.l.

The Eibsee Landslide, with a volume of about 400 million m^3, is the largest landslide in Bavaria (Abele 1974) and

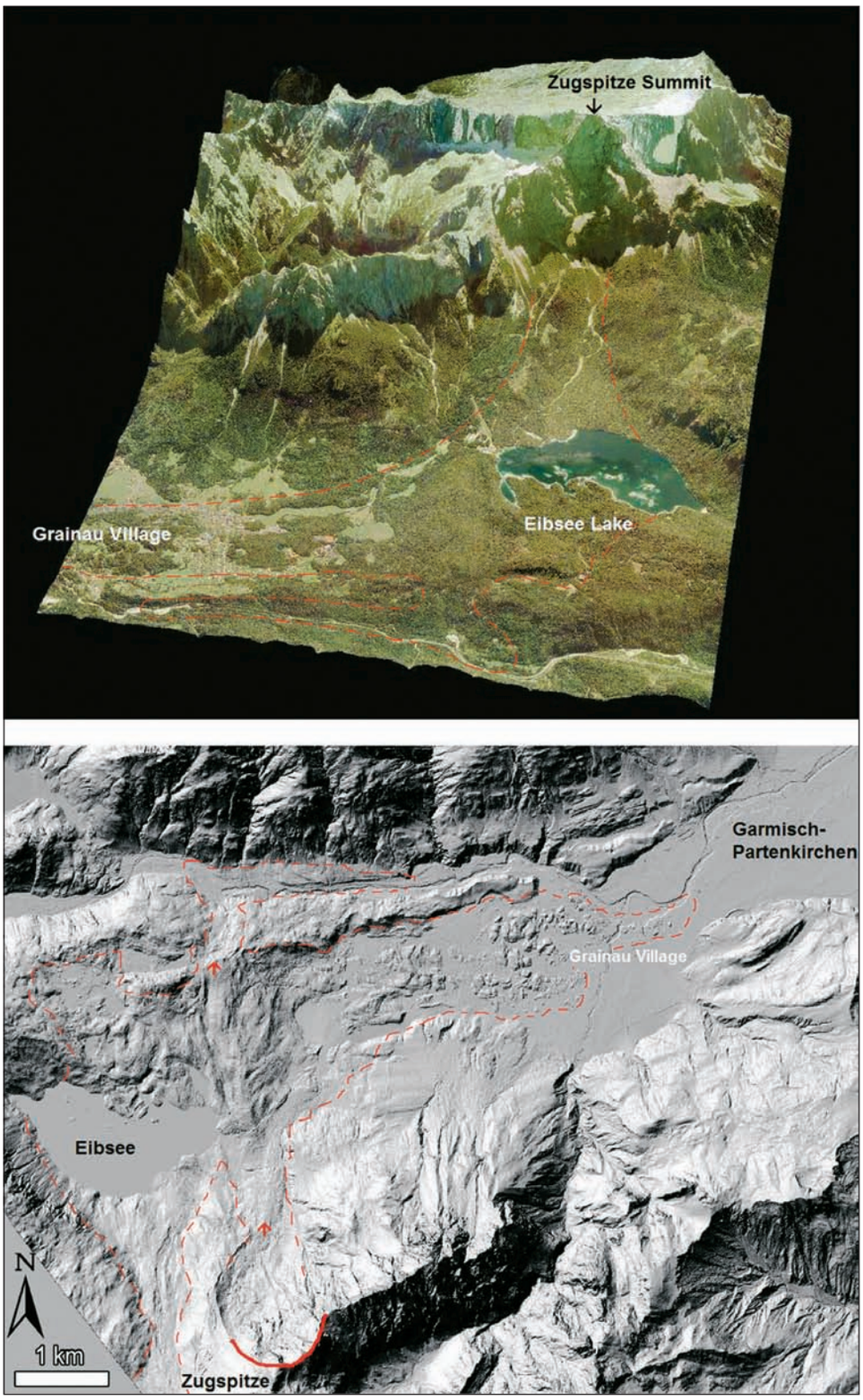

Fig. 9: (a) 3D-model of the landslide deposit area within the red-stippled line and the head of the landslide near Zugspitze summit. The deposition area of the landslide masses ranges from the village of Grainau to Eibsee lake. **(b)** Digital terrain model of the area between Zugspitze summit, Eibsee and the Loisach River near Garmisch-Partenkirchen. In the left part of the picture the landslide track of a second landslide event is visible. The red arrows show the main track of this rockslide event. (Source: Geobasisdaten © Bayerische Vermessungsverwaltung 2014).

***Abb. 9: (a)** 3D-Modell der Bergsturzablagerungen und der obere Abschnitt des Bergsturzes nahe des Zugspitzgipfels. Das Ablagerungsgebiet der Bergsturzmassen ist Rot umrandet und reicht von Grainau bis zum Eibsee. **(b)** Digitales Geländemodell des Raumes zwischen Zugspitzgipfel, Eibsee und Loisach nach Garmisch-Partenkirchen. Im linken Teil des Bildes sieht man die Sturzbahn des zweiten Bergsturzes (rote Pfeile). Quelle: Geobasisdaten © Bayerische Vermessungsverwaltung 2014.*

covers an area of about 15 km^2 (Fig. 9a). Its runout distance is about 9.5 km and it has a maximum vertical distance of 2300 m. The main scarp area is NNE of the Zugspitze summit (2.962 m a.s.l.) in the surroundings of the Riffelwand and Bayerisches Schneekar (Figs. 8a & b). The Zugspitze mountain is built up by rocks belonging to a thick carbonate platform, which predominantly consist of limestone (Wettersteinkalk Formation). In the lower part of the Zugspitze mountain outcrops of Triassic marlstones and dolomites can be found. These Middle Triassic Units are part of the Wamberg Anticline, which is dislocated and overthrusted to the north. North of this a syncline can be identified. South of the Eibsee lake, in the central part of this syncline, outcrops of marlstones, cherty marlstones, limestones and marls can be found.

Vordermoos, location of the 1993 drilling site

Location: about 2.15 km north-northeast of the village Eibsee, coordinates [DHDN 3 Degree Gauss Zone 4]: E 4422910, N 5260070, 1000 m.a.s.l.

Seismic investigations within the Eibsee rockslide accumulation area resulted in a bedrock surface depth between

50 to 70 metres. One of the intensions of a drilling project in 1993 was to check the real depth of the rock debris deposition. The drilling Grainau IV at Vordermoos hit the rock surface at a depth of 46 metres (Jerz & Poschinger 1995). The drilling Grainau V in Untergrainau as well as the drillings for the water supply of Grainau show that the landslide deposits are less thick than previously expected based on the seismic results. New analyses with digital terrain models (DGM) and geographic information systems (GIS) also lead to the conclusion that the landslide masses were less thick. Especially the main scarp allows the assumption that the initial volume of the landslide mass ranges around 150–200 million m^3. Nevertheless it is possible that the Zugspitz summit was higher than 3.000 metres prior to the Eibsee landslide. Up to now it is still under debate whether the landslide was one large event, or whether the landslide was a multiphase rockfall event like the Randa rockfall near Zermatt (Schindler et al. 1993). The runout distance of the Eibsee landslide masses and the dynamics of the landslide suggest a progression similar to the Val Pola rockslide (Erisman & Abele 2001). The DGM allows another landslide track besides the main track to be identified. The main scarp of this second event is between the Riffeltorkopf and the Riffelspitzen (Fig. 9b). Its track follows the Hammersbach southeast of the village Eibsee to the peak 1012 east of the Zirmerskopf summit.

The cores Grainau IV and V as well as the drillings for the water supply of Grainau yielded wood fragments and lacustrine sediments rich in organic remnants. ^{14}C-dating of the wood fragments yield an age of ca. 3,700 cal yr BP. This age concurs with the pollen analysis performed by Grüger (Jerz 1999). The laminated lake deposits were dislocated by the landslide. These deposits provide an indication of an older Eibsee lake at the same place. After the Eibsee landslide event the present Eibsee lake formed nearly at the same place. The idea of a great dead ice mass speeding up the landslide can now be excluded (Vidal 1953).

References

Abele, G. (1974): Bergstürze in den Alpen ihre Verbreitung, Morphologie und Folgeerscheinungen. – Wissenschaftliche Alpenvereinshefte, 25: 1–165.

Ampferer, O. (1907): Über Gehängebreccien in den nördlichen Kalkalpen. – Jahrbuch der Geologischen Reichsanstalt, 57: 727–752.

Doppler, G., Kroemer, E., Rögner, K., Wallner, J., Jerz, H. & Grottenthaler, W. (2011): Quaternary stratigraphy of southern Bavaria. – Eiszeitalter und Gegenwart/Quaternary Science Journal, 60: 329–365.

Eisbacher, G. & Brandner, R. (1996): Superposed fold-thrust structures and high-angle faults, Northwestern Calcareous Alps, Austria. – Eclogae geologicae Helvetiae, 89: 553–571.

Erisman, T.H. & Abele, G. (2001): Dynamics of Rockslides and Rockfalls. – 316 p., Berlin (Springer).

Geyh, M.A. (2005): Handbuch der physikalischen und chemischen Altersbestimmung. – 211 p., Darmstadt (Wissenschaftliche Buchgesellschaft).

Gümbel, C. W. (1861): Geognostische Beschreibung des bayrischen Alpengebirges und seines Vorlandes. – 950 p., Gotha (Perthes).

Hantke, R. (1983): Eiszeitalter 3: Die jüngste Erdgeschichte der Schweiz und ihrer Nachbargebiete. Westliche Ostalpen mit ihrem bayerischen Vorland bis zum Inn-Durchbruch und Südalpen zwischen Dolomiten und Mont-Blanc. – 730 p., Thun (Ott).

Jerz, H. (1966): Untersuchungen über Stoffbestand, Bildungsbedingungen und Paläogeographie der Raibler Schichten zwischen Lech und Inn (Nördliche Kalkalpen). – Geologica Bavarica, 56: 3–102.

Jerz, H. (1999): Nacheiszeitliche Bergstürze in den Bayerischen Alpen. – Relief Boden Paläoklima, 14: 31–40.

Jerz, H. & Poschinger, A. von (1995): Neuere Ergebnisse zum Bergsturz Eibsee-Grainau. – Geologica Bavarica, 99: 383–398.

Ivanovich, M. & Harmon, R.S. (1992): Uranium-series disequilibrium, applications to earth, marine, and environmental sciences. – 910 p., Oxford (Clarendon Press, 2nd ed.).

Ostermann, M. (2006): Uranium/Thorium age-dating of „impure" carbonate cements of selected Quaternary depositional systems of western Austria: results, implications, and problems. – Unpublished PhD thesis, University of Innsbruck.

Ostermann, M., Sanders, D. & Kramers, J. (2006): $^{230}Th/^{234}U$ ages of calcite cements of the proglacial valley fills of Gamperdona and Bürs (Riss ice age, Vorarlberg, Austria): geological implications. – Austrian Journal of Earth Sciences, 99: 31–41.

Ostermann, M., Sanders, D., Prager, C. & Kramers, J. (2007): Aragonite and calcite cementation in "boulder-controlled" meteoric environments on the Fern Pass rockslide (Austria): implications for radiometric age-dating of catastrophic mass movements. – Facies, 53: 189–208.

Penck, A. (1925a): Glazialgeologische Beobachtungen in den bayerischen Hochalpen. – Sitzungsberichte der preußischen Akademie der Wissenschaften, physikalisch-mathematische Klasse, 17: 301–329.

Penck, A. (1925b): Alte Breccien und junge Krustenbewegungen in den bayerischen Hochalpen. – Sitzungsberichte der preußischen Akademie der Wissenschaften, physikalisch-mathematische Klasse, 17: 330–348.

Penck, A. (1925c): Die Eiszeit in den bayerischen Hochalpen. – Sitzungsberichte der preußischen Akademie der Wissenschaften, physikalisch-mathematische Klasse, 17: 349–371.

Piller, W. E., Egger, H., Erhart, C.W., Gross, M., Harzhauser, M., Hubmann, B., van Husen, D., Krenmayr, H.-G., Krystyn, L., Lein, R., Lukeneder, A., Mandl, G., Rögl, F., Roetzel, R., Rupp, C., Schnabel, W., Schönlaub, H. P., Summesberger, H. ,Wagreich, M. & Wessely, G. (2004): Die stratigraphische Tabelle von Österreich 2004 (sedimentäre Schichtfolgen). – PANGEO Austria 2004, „Erdwissenschaften und Öffentlichkeit" vom 24.–26. September 2004 in Graz, Beitragskurzfassungen, 329–330, Graz.

Rüffer, T. (1995): Entwicklung einer Karbonat-Plattform: Fazies, Kontrollfaktoren und Sequenzstratigraphie in der Mitteltrias der westlichen Nördlichen Kalkalpen (Tirol, Bayern). – Gaea heidelbergensis, 1: 1–282.

Schindler, C., Cuenod, Y., Eisenlohr, T. & Joris, C.-L. (1993): Die Ereignisse vom 18. April und 9. Mai 1991

bei Randa (VS) – ein atypischer Bergsturz in Raten. – Eclogae geologicae Helvetiae, 86: 643–665.

Trommsdorff, V., Dietrich, V., Flisch, M., Stille, P. & Ulmer, P. (1990): Mid-Cretaceous, primitive alkaline magmatism in the Northern Calcareous Alps: significance for Austroalpinesgeodynamics. – Geologische Rundschau, 79: 85–97.

Uhlig, H. (1954): Die Altformen des Wettersteingebirges mit Vergleichen in den Allgäuer und Lechtaler Alpen. – Forschungen zur deutschen Landeskunde, 79: 1–103.

Vaché, R. (1961): Prädiluviale Hochgebirgsbrekzien im mittleren Wettersteingebirge. – Sitzungsberichte der Bayerischen Akademie der Wissenschaften, Mathematisch-naturwissenschaftliche Klasse, 170: 373–381.

Vidal, H. (1953): Neue Ergebnisse zur Stratigraphie und Tektonik des nordwestlichen Wettersteingebirges und seines nördlichen Vorlands. – Geologica Bavarica, 17: 56–88.

Wehrli, H. (1928): Monographie der interglazialen Ablagerungen im Bereich der nördlichen Ostalpen zwischen Rhein und Salzach. – Jahrbuch der Geologischen Bundesanstalt, 78: 357–498.

Winkler-Hermaden, A. (1957): Geologisches Kräftespiel und Landformung. – 822 p., Wien (Springer).

Notes

From Vorderriß to Großer Ahornboden: Quaternary geology of the Riss Valley (Karwendel Mountains)

Von Vorderriß bis zum Großen Ahornboden: Quartärgeologie des Risstales (Karwendelgebirge)

Christoph Spötl, David Mair, Reinhard Starnberger

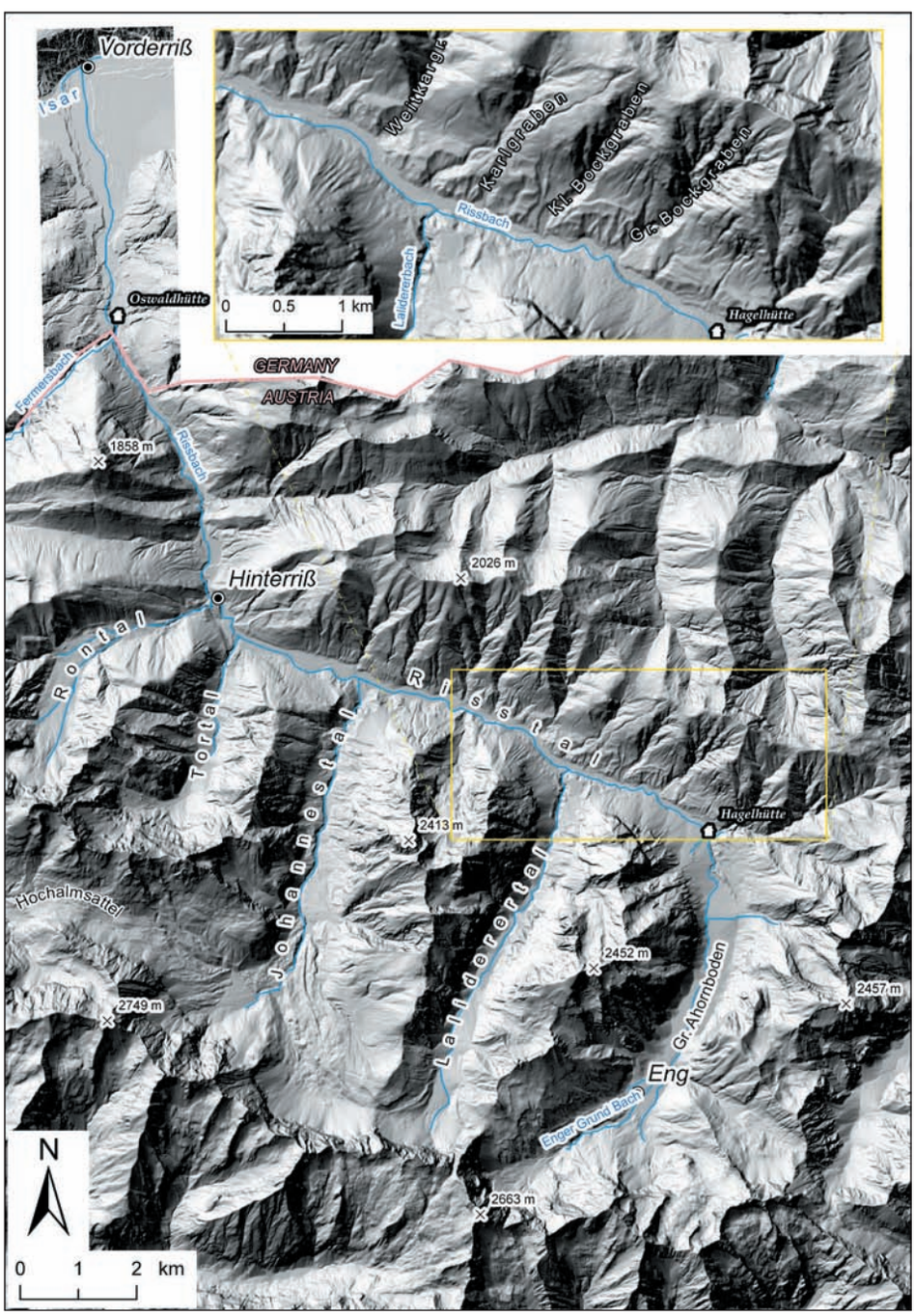

Fig. 1: Digital elevation map of the Riss Valley and key locations mentioned in the text. The yellow rectangle represents a close-up of the central Riss Valley (©Land Tirol, tiris, www.tirol.gv.at/tiris).

Abb. 1: Digitales Höhenmodell des Risstales mit den im Text erwähnten Lokalitäten. Das gelbe Rechteck zeigt den rechts oben vergrößerten Ausschnitt des zentralen Risstales (©Land Tirol, tiris, www.tirol.gv.at/tiris).

1 Introduction

This excursion will lead into a glacially carved valley with exceptionally well exposed Upper Pleistocene and Holocene sediments, interesting morphological features and scenic landscapes. The field trip will start in Vorderriß at the junction of Rissbach and Isar, follow the Rissbach upstream all the way to the valley head (Fig. 1), thereby crossing the border from Germany (Bavaria) to Austria (Tyrol), and will end at the southern tip of the Großer Ahornboden, famous for its population of old maple trees.

To make one point clear right at the beginning: When Penck and Brückner coined the name Riß for the penultimate glaciation reaching the foreland of the Alps they were thinking of another Riß, i.e. a small tributary of the Danube in Upper Swabia, Baden-Württemberg (type locality Biberach an der Riß). Penck had in fact also shortly visited the Riss Valley in the Karwendel Mountains (see below).

2 A brief history of research

The interior of the Karwendel Mountains in general and the Risstal[1] (Riss Valley) in particular have received rather little attention by Quaternary scientists in the last century which is reflected by a limited number of publications. This is surprising, though, given the abundance of Quaternary sediments and landscape features in this valley and the excellent exposure quality.

Ampferer (1903) was probably the first to obtain a good overview of the Quaternary inventory of this valley. He mapped the northern part of the Karwendel Mountains with a focus on bedrock stratigraphy and structural geology. He mentioned Quaternary features in short, including the presence of erratic blocks in the valley of the Fermersbach, the prominent terrace near Oswaldhütte, as well as striated pebbles in outcrops south of Hinterriß.

The Riss Valley joins the Isar Valley at Vorderriß and both show prominent terraces which attracted the attention of Levy (1920) and Penck (1922). Penck investigated fine-grained lacustrine sediments preserved along the Isar Valley between Seefeld and today's Sylvenstein reservoir and observed that the elevation of these sediments decreases with increasing distance from the interior of the mountain range. He also visited the Riss Valley and recognized moraine ridges in the inner valley, lacustrine sediments and delta gravel, but stated that he could not study them in more detail.

Wolf (1922) collected field evidence of Pleistocene glaciation in the area of Achensee to the east of the Riss Valley. A couple of years later he studied this valley in slightly more detail (1924) and mentioned two erratic blocks each over 3 m in size in the Rissbach downstream of Oswaldhütte and implied a transport via the Fermersbach Valley. He drew a map of the maximum ice elevation in the area of the Riss Valley which shows WNW-ESE-oriented contour lines decreasing from an elevation of 1850 m a.s.l. at Hinterriß to 1650 m a.s.l at Vorderriß. These values are about 100 m higher than those in the more recent compilation map by van Husen (1987). He conceded that he was unable to differentiate between terraces formed prior to the Last Glacial Maximum (which he considered interglacial at that time) and late- to postglacial terraces. In the prominent exposures of Quaternary sediments on the western side of the Rissbach opposite of Oswaldhütte he already identified a lower level characterised by cross-bedded gravel dipping northwards and a higher abundance of fines, overlain by a level of horizontally bedded gravel. Downstream he noticed "*beiderseits der Riß eine ungewöhnlich feine, wohlverarbeitete Moräne*" (p. 270), which is now identified as water-lain till (see Stop 2). He already mentioned that this and other large exposures along the stream are rapidly changing due to fast erosion along the river.

Sauer (1938) presented a detailed study of fine-grained, calcareous deposits in the upper Isar Valley, collectively known as "Seekreide" at that time. Her granulometric and petrographic work also included one sample from the area near Oswaldhütte and showed a high degree of similarity between these sediments and the matrix of (glacial) till.

Mutschlechner (1948) mapped the Karwendel Mountains and used the occurrence of erratic rocks (down to cm-size) in order to delineate the maximum elevation of the former ice surface. He confirmed the scarcity of such crystalline rock material in the Riss Valley, with the exception of a transfluence from the Isar Valley north of Mittenwald across the pass of the Vereiner Alm (1395 m a.s.l.), i.e. along Seinsbach and Fermersbach. He reported two erratic blocks composed of mica schist in the large outcrop at Neunerreisen (across the toll station in Riss Valley), but concluded that a transfluence of central-alpine ice via Scharnitz, Karwendel Valley, Hochalmsattel (1803 m a.s.l.) and Johannes Valley remains doubtful. He found a tiny piece of rounded crystalline rock on the Westliche Lamsenjoch (1940 m a.s.l.), which may imply some ice flow from the Southeast into the innermost Riss Valley.

1947 marked the start of the construction of the Rissbach-Stollen, diverting water from the Rissbach along a 7 km-long conduit to Walchensee to generate electricity. As part of this project and the planning for the Sylvenstein dam (which in its original version would have flooded the Isar Valley up to almost 10 km west of Vorderriß) the area of the Isar and Riss Valleys was studied by Schmidt-Thomé (1950). Drillings at Sylvenstein, Fall and Ochsensitz revealed that "Seekreide" is common in the basin-fill around Vorderriß.

Ampferer (1950) mapped the eastern Karwendel Mountains at a scale of 1:25,000 which includes the Riss Valley between Hagelhütte and Eng. He mapped right-lateral moraine ridges at the northern end of Großer Ahornboden.

As a consequence of destructive debris-flow events and the decline of the maple tree population a study of the Großer Ahornboden was initiated which also included soil-related investigations (Czell et al. 1966). This study documents the presence of loamy sediment buried by 1–2 m of alluvial gravel in the northern part of Großer Ahornboden (Fig. 13). The old maple trees root in this highly impermeable layer and have been progressively buried by gravel.

A detailed geomorphological study of the Riss Valley was conducted by Sommerhoff. His 1971 publication includes a geomorphological map of the Riss Valley south of Hagelhütte showing remnants of a quadripartite moraine ridge at the northern end of Großer Ahornboden. He attributed this advance to the Schlern stage, unfortunately without provid-

[1] With regard to geographic names we follow the spelling of the Austrian Map (Bundesamt für Eich- und Vermessungswesen; http://www.austrian-map.at)

ing arguments (the name of this Lateglacial advance stage is now obsolete). Sommerhoff also reported "Bändertone" which were deposited in a lake presumably dammed by these ridges. Debris-flow fans prograded across these lacustrine sediments, and apparently also interfingered with them locally, pointing towards synchronous deposition. Terminal moraines southwest of Eng Alm were attributed to the Gschnitz stadial (again without data supporting this). The author also examined a 5 m-high outcrop exposing debris flow layers near Eng Alm separated by paleosols, which were later radiocarbon-dated (Sommerhoff 1977; see Stop 6). His mapping suggested that the Johannesbach glacier did not reach the Riss Valley during the Lateglacial, whereas the Lalidererbach glacier left terminal moraines on the right side of the Riss Valley, i.e. it reached the main valley and expanded anvil-like. The author attributed the presence of lacustrine sediments and delta foresets to the ponding of water behind an ice dam created by the advancing tributary glaciers from the Ron, Tor and Laliderer Valleys and reconstructed a lake level at an elevation of ca. 1180 m.

Bader (1979) performed seismic measurements in glacially overdeepened valleys of southern Bavaria and commonly observed a bipartition between a glacially overconsolidated lower level (with high seismic velocities) and a non-glacial consolidated upper unit. In the Isar Valley near Vorderriß this subdivision was less clear and the author concluded that overconsolidated sediments reach up close to the surface. The Isar data, however, were consistent with those from other valleys in that most of the sediment-fill appeared overconsolidated, suggesting a rather insignificant glacial erosion during the Last Glacial Maximum. In a parallel study, Frank (1979) expanded on these observations and suggested that the Isar Valley was excavated during the Mindel and Riss Glaciations, whereas the Würm ice had a comparably minor erosional impact.

An important event was the deep drilling at Vorderriß, which took place between 1977 and 1978 and provided important information about the deep tectonic style of the Northern Calcareous Alps. Vorderriß 1, as this drilling was termed, penetrated 362 m of Quaternary sediments and hence provided final proof of significant glacial overdeepening at the confluence of Rissbach and Isar glaciers (Bachmann & Müller 1981).

Doben (1993) published sheet "Vorderriß" of the Geological Map of Bavaria at a scale of 1:25,000, which covers the Isar Valley around Vorderriß and the Riss Valley as far south as Weitgries Alm.

Our research in this area commenced about a decade ago and includes three unpublished Master theses (Brandstätter 2006, Büsel 2008, Mair 2014), a series of field courses and a number of other field activities, which will be partly presented during this excursion.

3 Setting

The Riss Valley is the longest valley in the Karwendel Mountains (24 km) and provides the most direct access into their interior from the North. Major tributaries drain to the Rissbach from the West and Southwest, i.e. the Ron, Tor, Johannes and Laliderer Valleys (Fig. 1). The Riss Valley also hosts the only permanent settlement inside the Karwendel Mountains, the village of Hinterriß (928 m a.s.l.). The Großer Ahornboden and the area of Eng Alm in the interior of the valley are top tourist attractions with several hundreds of thousands of visitors between early May and end of October each year. The Tyrolean part of the Riss Valley and all its tributaries are part of the "Alpenpark Karwendel" (www.karwendel.org), a nature reserve, which is also listed as a Natura 2000 area. Its information centre is located in Hinterriß.

The entrance to the Riss Valley near Vorderriß suggests a broad valley, but in fact most of the valley is deeply incised and the areal extent of flat valley floor is very limited. The only exception – apart from the wide alluvial corridor near the junction with the Isar Valley – is the Großer Ahornboden, pointing towards its unique geological history. Most tributary valleys terminate as hanging valleys, e.g. Johannes Valley with its impressive gorge. On the other hand, there is no elevation difference between the northernmost Riss and the Isar Valleys and both valleys show approximately the same widths.

Geologically speaking, the Riss Valley is incised into rocks of the Lechtal Nappe except for the southernmost parts where the Inntal Nappe is thrusted above the former giving rise to the spectacular scenery of the Karwendel-Hauptkamm (central ridge). The rocks of the Lechtal Nappe are dominated by Upper Triassic dolomites (Hauptdolomit) and form a prominent syncline just north of Hinterriß, known as Karwendel-Syncline (as the extension of the Thiersee-Syncline further east; Eisbacher & Brandner 1996, Ortner & Gruber 2011). Jurassic to Lower Cretaceous limestones, marls and siliceous rocks form the core of this syncline. 5 km ENE of Hinterriß the transition between the uppermost Triassic (Kössen Formation) and the lowermost Jurassic (Kendlbach Formation) at Kuhjoch has been selected as the Global Stratotype Section and Point (GSSP) for the Triassic-Jurassic boundary (Hillebrandt et al. 2013). South of Hagelhütte the Riss Valley transects the boundary to the Inntal Nappe which forms the adjacent summits (e.g. Falk, Gamsjoch, Sonnjoch) as well as the almost 1 km-high rock wall south of Eng Alm. The structural geology of this part of the Karwendel Mountains has puzzled generations of geologists and at this point no modern tectonic interpretation has been published.

The Quaternary geology of the Riss Valley is dominated by glacially carved troughs, hanging valleys, a few cirques in the South, and prominent fluvial terraces in the northern part passing over to similarly impressive ones in the Isar Valley. A characteristic element of the Riss Valley, however, is the abundance of large-scale sediment outcrops along the river as well as along steep gullies on the flanks of the valley. The high sediment yield from this valley is underpinned by the impressively wide and long alluvial corridor of the Rissbach south of Vorderriß, rivalling the equally impressive river plain of the Isar.

4 Excursion route

Stop 1: Vorderriß

The purpose of this first stop is to introduce the study area and to provide the regional context. Vorderriß is a very small village at the junction of Riss and Isar Valley and was the location of one of the few deep drillings penetrating the en-

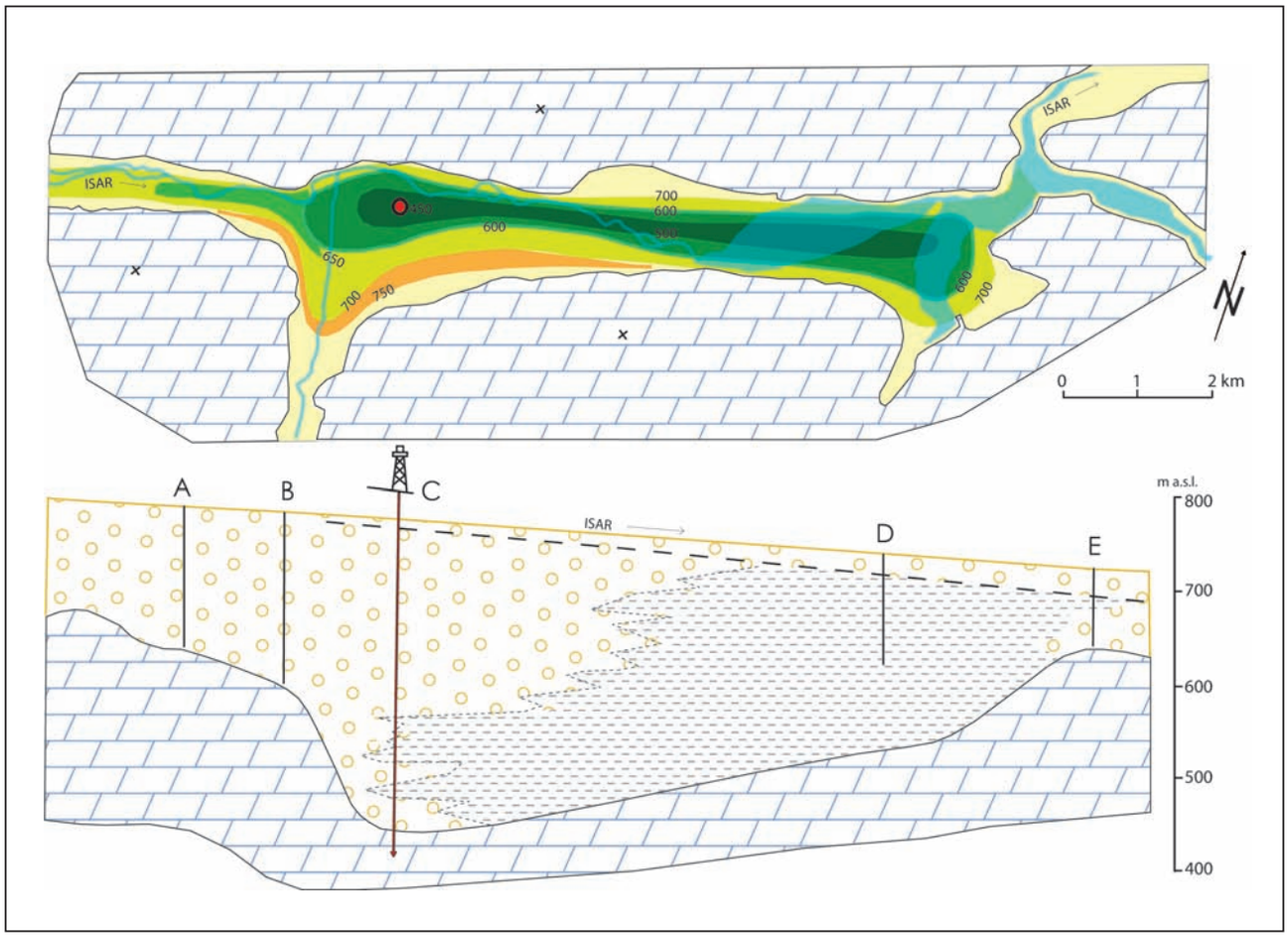

Fig. 2: Map showing the glacial overdeepening of the Isar Valley at the junction with the Riss Valley (upper panel). Values of the isolines are in metres a.s.l. The red dot marks the location of the deep drilling "Vorderriß 1". The lower panel is a vertically exaggerated W-E cross section of the Quaternary sediment fill of the Isar Valley showing an interfingering of gravel and silts. Letters indicate drillings including the deep drilling Vorderriß 1 (C). The erosion base of the ice during the Last Glacial Maximum is suggested by the implied dashed line. Modified after Frank (1979) and Bachmann & Müller (1981).

Abb. 2: Karte der glazialen Übertiefung des Isartales an der Einmündung des Risstales (obere Abbildung). Die Isolinien geben die Seehöhe der Felsoberkante in Meter an. Die Bohrung Vorderriß 1 ist durch den roten Punkt markiert. Die untere Abbildung gibt einen überhöhten W-E Schnitt durch die quartären Sedimentfüllung des Isartales mit der Verzahnung von Kies und Schluff wider. Bohrungen sind durch Buchstaben markiert (C ist Vorderriß 1). Die strichlierte Linie zeigt die vermutete Erosionsbasis des Eises während des letzten glazialen Maximums an. Modifiziert nach Frank (1979) und Bachmann & Müller (1981).

tire nappe stack of the Northern Calcareous Alps. The drill site was located at 812 m a.s.l. and first encountered 42 m of uncompacted gravel attributed to the Lateglacial and Holocene (no chronostratigraphic data available; Bachmann & Müller 1981, 1982). The Isar River has incised ca. 25 m into these sediments, forming prominent terraces. The basin-fill below -42 m is overconsolidated and consists of a series of fining-upward cycles dominated by gravel and capped by calcareous silt ("Kalkschluff"). These fine-grained sediments become more abundant below -236 m (576 m a.s.l.) and interfinger with gravel layers (Fig. 2). In total, 362 m of Quaternary sediments were encountered, validating the seismic survey and the pronounced glacial overdeepening at the confluence of the two Pleistocene glaciers (Fig. 2). According to the core descriptions no till was encountered in the entire succession.

The drilling eventually stopped at a depth of 6468 m reaching Helvetic rock units below the nappe stack of the Northern Calcareous Alps, hence demonstrating the allochthonous nature of the Northern Calcareous Alps. Although the drilling missed the primary goal of finding hydrocarbon reservoirs in this thrust complex it nevertheless represents an invaluable source of information for tectonic models (e.g. Ortner et al. 2006) and assessments of the degree of thermal maturity at great depth along the northern rim of the Northern Calcareous Alps.

Stop 2: Bridge 850 m N Oswaldhütte

The second stop introduces a key sedimentary unit of the Riss Valley, which is very well exposed on both sides of the Rissbach. The stream bed can be easily accessed from the bridge located 850 m north of Oswaldhütte. The outcrops show a massive, light-grey diamict with varying amounts of clasts (Fig. 3). The latter range in size from less than 1 cm to typically no larger than about 20 cm; rare out-sized blocks of slightly over 1 m in diameter were encountered as well. The matrix is fine carbonate silt with rare sandy intercalations (in the South) and shows a conspicuously high degree of compaction. The components are predominantly Hauptdolomit and less commonly Wettersteinkalk and red Jurassic rocks showing angular to subangular to locally rounded

Fig. 3: Diamictic lacustrine sediments exposed along the Rissbach and sharply overlain by Holocene fluvial sediments (in the background).

Abb. 3: Entlang des Rissbaches sind diamiktische Seesedimente scharf überlagert von holozänen Flusssedimenten aufgeschlossen (im Hintergrund).

shapes. Striated clasts (Fig. 4) and clasts showing a conspicuously smooth surface are present at small percentages. Clasts composed of crystalline rocks – typically well rounded – are present in small quantities and mainly include amphibolite and gneiss. They indicate ice flow via the Fermersbach Valley, i.e. a transfluence of the Inn Valley ice stream across the pass of the Vereiner Alm, as mentioned already by early researchers (e.g., Mutschlechner 1948).

The diamict in the Riss Valley has previously been described as "Kalkschluff" or "Beckenschluff" (e.g. Doben 1993). This lake extended all the way into the Isar Valley where similar sediments occur both on the surface (e.g. Staffelgraben 3.7 km E Vorderriß) and in the subsurface (Fig. 2). Whether the outcrops of this type of diamict in Milchgraben and Zellergraben 9.7 km upstream of Vorderriß formed in the same lake is currently not known. Mapping of these fine-grained basin sediments in the Riss and Isar Valleys showed that the massive, pebbly diamict facies laterally grades into well-bedded and commonly also laminated bottomset sediments showing either no larger clasts or discrete layers and heaps thereof. The pebbly diamict facies dominates in the outcrops near Stop 2 and suggests a close proximity to the source of the coarse grained fraction, whereas the matrix was likely deposited as background sediment throughout the lake. The striated clasts and erratics, together with the abundance of fine-grained matrix provide strong evidence that till was a significant source of the sediment dumped into this lake. We therefore regard the coarse grained fraction as a waterlain till deposited underneath and in front of glacier tongues calving into the lake from the South and Southeast. The high sedimentation rate and dynamics prevented the development of bedding and gave rise to the massive appearance of this diamict. We did not observe compelling evidence for the deposition of iceberg dump structures in the outcrops of Stop 2, i.e. flat-based mounds of coarse material which occurs in isolation (Benn & Evans, 2010). Such features, however, are not uncommon elsewhere in the Riss and Isar Valleys.

An aquatic origin of this spectacular diamict in the northernmost Riss Valley is also supported by the occurrence of diatoms. Although rare, small, ca 10 to 38 µm-long, thin shelled valves are present in these sediments, with signs of compaction (Fig. 5). Preliminary analyses showed the presence of the following benthic and planktonic genera and species: *Neidium*, *Eunotia*, *Nitzschea*, *Achnanthes marginulata*, *Meliosira* or *Aulacoseira*; in addition cysts probably of chrysophyceae are common (pers. comm. K. Koinig).

The diamict shows characteristic sets of horizontal and vertical extensional joints whose origin was tentatively attributed to relaxation of this overcompacted sediment in very recent time (Costantini & Ortner 2014).

Near the present-day river bed the diamict is commonly

Fig. 4: Striated dolomite clast embedded in the diamict north of Oswaldhütte.

Abb. 4: Gekritzter Dolomitklast im Diamikt nördlich der Oswaldhütte.

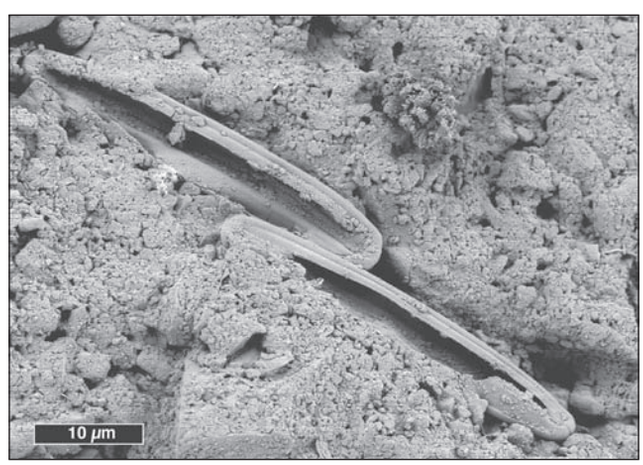

Fig. 5: Scanning electron photomicrograph of a freshly broken surface of diamict showing two diatom valves.

Abb. 5: Rasterelektronenmikroskopieaufnahme zweier Diatomeenschalen auf einer frischen Bruchfläche des Diamikts.

sharply overlain by unconsolidated, coarse-grained gravel containing well-rounded components up to ca. 1 m in diameter which were deposited by the Rissbach (Fig. 3) when its level was higher than today (note: Doben (1993) erroneously ascribed this fluvial sediment as till). The down-cutting resulted in a series of fluvial terraces which range from about 0.5 m to ca. 43 m above the present river bed. The chronology of this down-cutting is not known, but it likely commenced during the Lateglacial. An attempt was made to date the uppermost terrace at Stop 3 using organic remains found at the base of the soil, but the radiocarbon age (6563 ± 80 BP; 7318–7584 cal BP; INTCAL13, 2 sigma range) probably significantly underestimates the age of terrace formation. These Rißbach terraces likely correspond to the even larger ones in the Isar Valley, but again no detailed studies have been performed.

Stop 3: Oswaldhütte

This large outcrop on the western side of Rissbach opposite of Oswaldhütte offers insights into an exceptionally well preserved delta complex. The distinction of foreset and topset appears straightforward at first glance, but turns out to be more complex. Detailed inspection of the outcrop revealed that the horizontally bedded gravel shows no indication of overconsolidation, whereas the underlying foreset gravel is distinctly overconsolidated, suggesting ice loading. This is shown by both the strength of the sediment and the presence of cracked pebbles. As a consequence, the horizontally bedded gravel is not the topset of this delta, but most likely younger, i.e. of Lateglacial age, postdating deglaciation of the area (Fig. 6).

The foreset beds dip towards N, NE and E, suggesting that the sediment was largely if not exclusively derived from the Fermersbach Valley. This is supported by the accessory presence of crystalline rock fragments which document ice transfluence via the pass at Vereiner Alm (see above) and which are almost absent in the Riss Valley further south. The southern part of the delta is covered by talus and cannot be inspected, but we would expect also southeast-dipping foreset beds there.

Some of the foreset beds are clearly over-steepened, indicating rapid dumping of sediment, associated sediment relocation and differential compaction. This is supported by de-watering structures. The foreset gravels range from matrix-supported to less commonly clast-supported, the latter showing occasional cracked clasts.

An important detail was temporarily exposed on the eastern bank of the riverbed. Distal, north-dipping foreset beds were onlapped by diamict and later cut by an erosional surface (Fig. 7). This is/was the only outcrop showing the stratigraphic link between the delta and the diamict facies which is the dominant type of sediment further north. Rapid riverbank erosion has meanwhile deteriorated the outcrop which also showed that the foreset did not pass gradually into the bottomset, but interfingered with it. We favour a model of fluctuations of the lake level, whereby a rise in lake level caused the drowning of the delta and deposition of bottomset beds (diamict facies) on the foreset. This is consistent with the presence of reworked clasts of diamict

Fig. 6: S-N panoramic view of the delta complex at Oswaldhütte. Black lines delineate bedding planes in the foreset. The boundary between the overconsolidated foreset and the overlying topset is marked by the red line. Late Holocene fluvial gravel of the Rissbach forms a low-lying terrace in the North (yellow line). White arrows mark terrace surfaces.

Abb. 6: S-N Panorama des Deltakomplexes bei der Oswaldhütte. Schwarze Linien zeigen das Einfallen des Foresets an. Die rote Linie markiert die Grenze zwischen dem überkonsolidierten Foreset und dem hangenden Topset. Spätholozäne fluviatile Kiese des Rissbaches bilden eine niedere Terrasse im Norden (gelbe Linie) und die weißen Pfeile markieren diese und weitere Terrassen.

Fig. 7: Temporary outcrop (2009) on the eastern side of Rissbach exposing lacustrine diamict onlapping (black line) on the toe of the delta foreset. The light gray blocks beneath the soil belong to a thin veneer of Late Holocene fluvial gravel of the Rissbach (yellow line).

Abb. 7: Temporärer Aufschluss (2009) am orografisch rechten Ufer des Rissbaches, der den Onlap (schwarze Linie) von lakustrinem Diamikt auf dem Fuß der Deltaschrägschichtungen zeigt. Die hellgrauen Blöcke unter dem Bodenhorizont sind Teil einer geringmächtigen Sedimentlage des spätholozänen Rissbaches (gelbe Linie).

Fig. 8: Reworked diamictic blocks (yellow arrows) in the distal delta foreset. Width of image ca. 3 m.

Abb. 8: Aufgearbeitete Diamiktblöcke (gelbe Pfeile) im distalen Delta-Foreset. Bildbreite ca. 3 m.

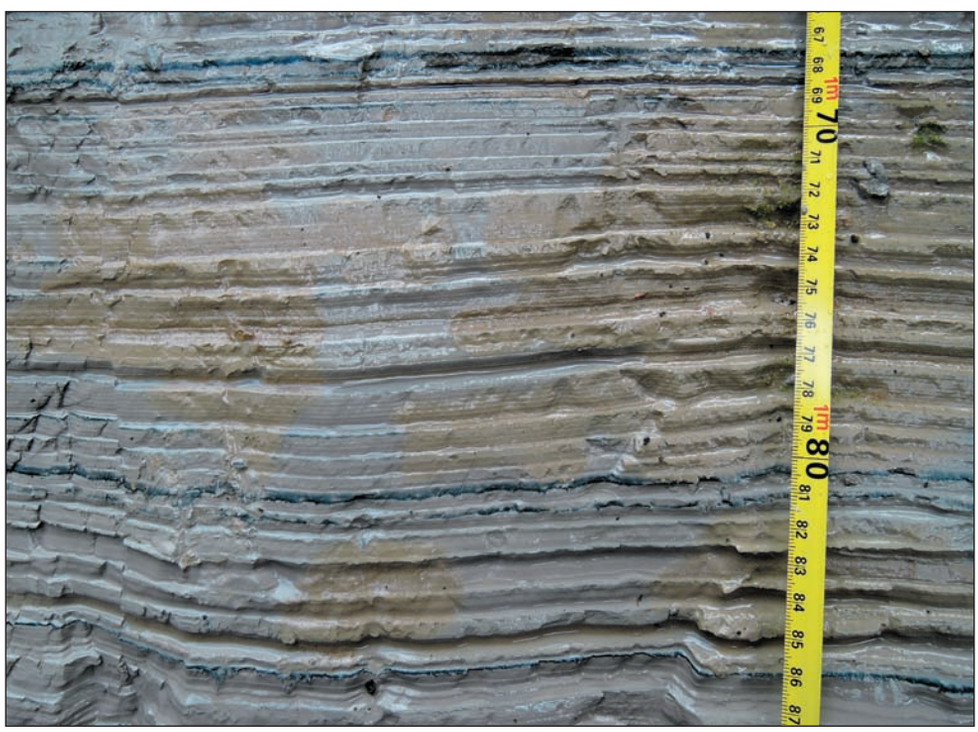

Fig. 9: Close-up of regularly bedded and possibly varved lake sediments in Karlgraben. Note conspicuously black layers e.g. at 67.5 and 80.5 cm.

Abb. 9: Detailaufnahme der regelmäßig geschichteten und möglicherweise warvierten Seesedimente im Karlgraben. Beachte die auffallenden schwarzen Lagen, zB bei 67,5 und 80,5 cm.

embedded in the distal gravel beds of the foreset (Fig. 8).

If our depositional model is correct, the topset of the delta is not preserved in this outcrop; hence we lack a marker for the palaeo-lake level. Bottomset layers outcropping further upstream in Rissbach Valley, provided that they belong to the same lake phase, delineate a minimum lake level of ca. 1100 m a.s.l., i.e. ca. 260 m above the elevation of the Rissbach at Oswaldhütte.

Stop 4: Karlgraben

Located opposite of Laliderer Valley, Karlgraben is one of several steep ravines on the northeastern flank of the central Riss Valley (Fig. 1, inset). The graben can be accessed from Karlsteg, a bridge across Rissbach (where the road to Karlalm starts), by traversing on the orographically right side of the stream until reaching the mouth of Karlgraben[2]. This graben exposes one of the longest, albeit not fully continuous, sediment successions reaching up to ca. 1140 m a.s.l. and documenting that the central Riss Valley was once filled by up to ca. 120 m of clastic sediments.

The lowermost sediments outcropping along Rissbach between Kleiner Bockgraben and Karlgraben (Fig. 1, inset) are crudely bedded, matrix-rich gravels forming indistinct and locally over-steepened foreset of a deltaic facies. These gravels interfinger with thin and discontinuous, diamictic bottomset sediments. Given that the stream erodes bedrock at Karlsteg, the base of these gravels is probably already present a few metres below today's riverbed at the junction

[2] There is some discrepancy between the Austrian map (ÖK) and the Alpenverein map about the labelling of some ravines near Karlalm. We follow the former here.

Fig. 10: Dm-thick sand alternating with thin silt layers in the fining-upward sequence exposed in Karlgraben. Inset shows close-up of sand-silt couplets. Pen for scale.

Abb. 10: Dm-mächiger Sand wechsellagernd mit dünnen Schlufflagen in der oben-fein-Abfolge im Karlgraben. Detailbild zeigt diese Sand-Schluff-Couplets näher. Stift als Maßstab.

of Karlgraben. The foreset is at least some 20 m thick in the nearby Kleiner Bockgraben (not well exposed in Karlgraben) and is overlain by bottomset sediments. The boundary is very sharp, occurs at an elevation of 1075 m a.s.l. and documents a sudden drowning of the delta. The bottomset is at least 3.5 m thick and consists of planar bedded, clay-rich silt showing regular bedding and an individual layer thickness between 0.5 and 1.0 cm. Upon cleaning of the outcrop conspicuously black layers can be seen (Fig. 9). This dark colour is not related to a higher organic carbon content, as these layers have similarly low C_{org} values of 0.1 wt.% as the light coloured background sediment. The dark colour disappears within a few hours when exposed to the atmosphere suggesting that it is likely caused by reduced manganese being oxidised upon contact with the atmosphere. These dark layers therefore likely record episodes of reduced redox potential in the pore water at the time of deposition, possibly related to stagnant bottom-water conditions (years with extensive winter lake ice cover?). If these layers are indeed annual in origin, i.e. varves, they would provide constraints on the absolute duration of the highstand phase of this palaeolake. We counted some 46 layers in a package of 68 cm. Extrapolating this first-order assessment to the entire 3.5 m of exposed bottomset suggest slightly over 200 years for the deposition of these fine-grained lake sediments.

Following a gap in the outcrop a succession of sand follows which is inclined and shows abundant sedimentary structures, including draped lamination, dewatering structures, rip-up clasts, channel structures and graded and convolute bedding (Fig. 10). The succession consists of couplets of several centimetre-thick turbiditic sands topped by thin and commonly laminated silt. This sandy interval becomes increasingly coarse grained up section and grades into gravel composed of rather well-rounded Hauptdolomit components. This coarsening-upward trend is interrupted at ca. 1105 m a.s.l. by a silt layer ca. 0.5 m thick containing abundant slump structures (Fig. 11), which records a last, short-lived lake-level highstand. This silt layer is overlain

Fig. 11: A bottomset layer (at the knees of the person) occurs near the base of the horizontally stratified gravel in the upper reaches of Karlgraben.

Abb. 11: Eine Bank des Bottomsets (bei den Knien der Person) tritt an der Basis des horizontal geschichteten Kieses im oberen Teil des Karlgrabens auf.

by horizontally bedded gravel of fluvioglacial origin which shows incipient cementation giving rise to conglomerate cliffs. Above ca. 1120 m a.s.l. very angular blocks of up to several m^3 in size occur either isolated or as clast-supported mass within the gravel. Sorting is extremely poor and most blocks are composed of Middle Triassic limestones, probably transported to this site during a series of rockfall events from the cliffs of the Falken or Gamsjoch Group, 1 and 2 km to the South and Southwest, respectively.

To summarise, the Karlgraben exposes a lower delta complex topped by a bottomset, followed to a coarsening-upward sequence terminating with rockfall deposits. The entire succession is overconsolidated which again hints towards a pre- to early-LGM age.

Stop 5: Overview 800 m S Hagelhütte

The character of the valley changes profoundly once Hagelhütte (1077 m a.s.l.), a group of wooden houses, is passed. Two large alluvial fans, both inactive today, mark the en-

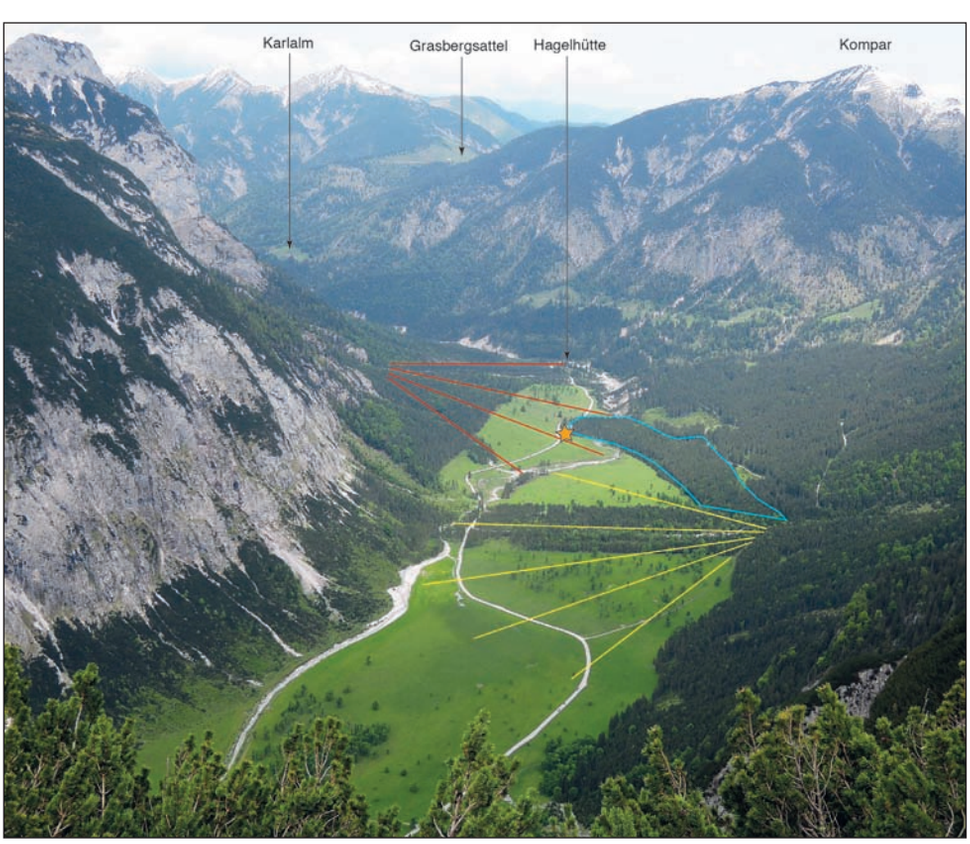

Fig. 12: The valley just north of Großer Ahornboden, view towards the North. The Late Glacial moraine ridge complex (blue framed) dammed a lake basin which was subsequently constricted by alluvial fans from Gramai Graben (yellow) and Großer Totengraben (red). Location of field trip stop 5 is marked by the orange asterisk.

Abb. 12: Das Risstal knapp nördlich des Großen Ahornbodens, Blickrichtung Norden. Der spätglaziale Moränenrückenkomplex (blau eingerahmt) dämmte das Seebecken, welches nachfolgend von den Schwemmfächern aus dem Gramaigraben (gelb) und dem Großen Totengraben (rot) eingeschnürt wurde. Der Exkursionspunkt 5 ist durch einen orangen Stern markiert.

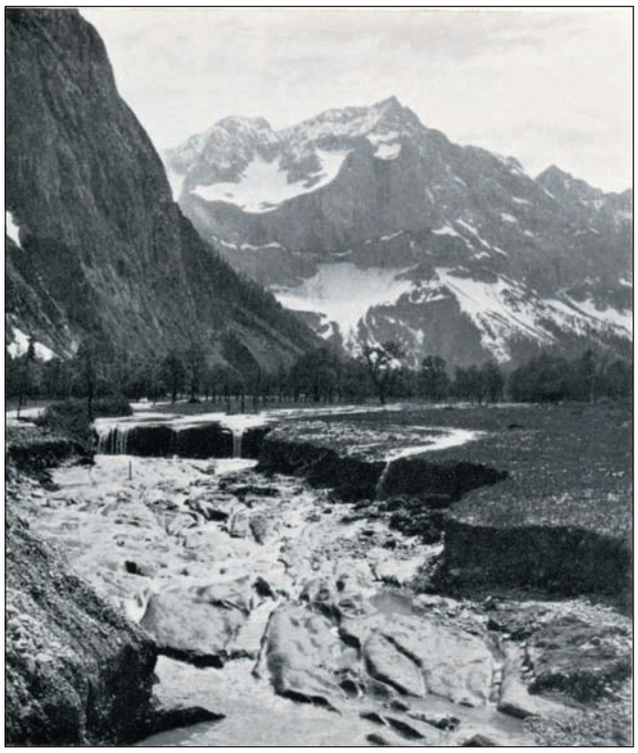

Fig. 13: Historical photograph of the top of the lacustrine sediments exposed beneath ca. 2 m-thick gravel in the northeastern part of the Großer Ahornboden as a results of the 1965 flooding (from Czell et al. 1966). The wall of Bärenwand is on the left and the summit of Spritzkarspitze (2606 m) is in the centre of the background.

Abb. 13: Historische Aufnahme der Oberkante der Seesedimente, durch Bacherosion 1965 unter ca. 2 m mächtigen Kiesen im nordöstlichen Teil des Großen Ahornbodens freigelegt (Czell et al. 1966). Linker Hand die Bärenwand und im Bildhintergrund die Spritzkarspitze (2606 m).

trance to the innermost valley segment, part of which is occupied by the Großer Ahornboden (Fig. 12). The valley profile shows steep walls and the floor is much wider than in most of the valley downstream.

A right-lateral moraine ridge is preserved on the eastern side of the valley, dissected in the South by the fan emerging from Gramaigraben (Fig. 12). The ridge is distinctly separated from the eastern valley flank and splits into sub-ridges near Stop 5. The terminal moraine is neither preserved (in part possibly buried beneath the fan emerging from the Großer Totengraben – see below) nor is the left-lateral ridge. A few strongly weathered limestone blocks up to a few metres in diameter are present on the ridges. These ridges mark an ice advance during the Lateglacial, attributed to the "Schlußvereisung" by Ampferer (1950) and the "Schlern Stadial" by Sommerhoff (1971). These ridges probably represent an advance coeval to Gschnitz (i.e. ca. 17 ka BP – see excursion H in this volume); no attempts were made to date these features using exposure age dating due to the poor quality of the boulders (H. Kerschner, pers. comm. 2014).

South of the ridge lacustrine sediments are present and best exposed along the river banks of Rissbach just east of Stop 5. The sediments are thin-bedded, show rare gyttja layers (but lack peat layers) and locally contain logs of trees up to ca. 40 cm in diameter. Radiocarbon dates range from ca. 5400 cal BP ca. 1.8 m below the top to ca. 5900 cal BP some 3.5 m deeper. In order to assess the start of the lake phase a core was obtained down to a depth of 9 m using a percussion probe. A wood sample at 8.5 m depth was dated to 9147–9465 cal BP suggesting that the lake existed for most of the early Holocene, most likely dammed by the Lateglacial moraine ridge, only part of which is still preserved today.

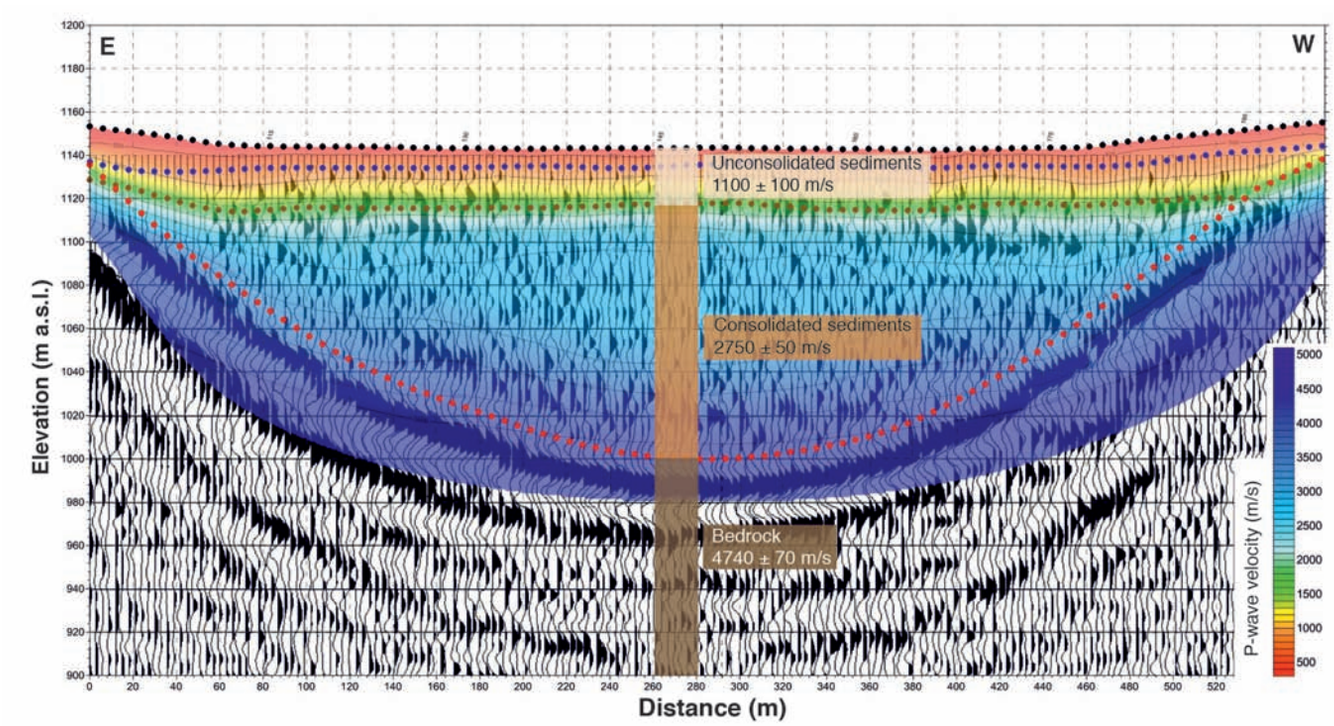

Fig. 14: Seismic section in the northern part of Großer Ahornboden based on data provided by W. Chwatal (pers. comm. 2013). Three main units emerge with different P-wave velocities, representing bedrock, most likely glacially overconsolidated sediments and unconsolidated sediment on the top.

Abb. 14: Seismisches Profil im nördlichen Teil des Großen Ahornbodens basierend auf Daten von W. Chwatal (pers. Mitt. 2013). Drei seismische Einheiten lassen sich anhand der P-Wellengeschwindigkeiten unterscheiden: Felsuntergrund, vermutlich glazial überkonsolidierte Sedimente sowie unkonsolidierte hangende Sedimente.

Fig. 15: Top of lake sediments just north of the Gramaigraben fan sharply overlain by debris-flow gravel. Note rusty-brown stain of the top lake mud (pen) due to oxidation by groundwater.

Abb. 15: Die jüngsten Seesedimente knapp nördlich des Gramaigraben-Fächers sind scharf überlagert von Murschuttsedimenten. Beachte die rostigbraune Färbung der obersten Schluffe (Stift), die auf Oxidation durch Grundwasser zurückzuführen ist.

The areal extent of these lake sediments is not well known but they have been repeatedly encountered at Großer Ahornboden beneath ca. 2 m of gravel (Fig. 13), e.g. during construction at the junction of the small stream coming down from Tränkkarl and Enger-Grund-Bach, i.e. in the west-central part of Großer Ahornboden (K. Höger, pers. comm. 2013). This site (1140 m a.s.l.) is about 20 m higher than the elevation of the northern segment of the ridge (close to Stop 5) that presumably dammed the lake. This calls for a significant lowering of the ridge since the last five thousand years and makes it unlikely that the lake extended further south than the Tränkkarl stream. Had the lake once covered the entire Großer Ahornboden (whose southern end is at an elevation of 1200 m a.s.l.) the dam near Stop 5 would have been at least 80 m higher than today, which appears highly unlikely. Geoelectrical and seismic surveys also suggest that the fine-grained sediments are not present in the southern part of Großer Ahornboden, i.e. south of the fan coming down from Tränkkarl.

Seismic data suggest that the top of the bedrock is located at ca. 1000 m a.s.l. between the Gramai fan and the Tränkkarl fan where the Quaternary sediment-fill is thickest. The elevation of the bedrock top is rather constant in the northern part of the Großer Ahornboden and rises in the southern part (in the area of the Eng Alm) to between 1120 and 1140 m a.s.l. The valley fill is thus ca. 145 m thick in the area south of Stop 5 and the northern part of the Großer Ahornboden, and decreases at Eng Alm to ca. 75 m. These data are consistent with results from geoelectrical surveys. Furthermore, the seismic data provide clear evidence of the U-shaped, glacially formed trough beneath the Großer Ahornboden (Fig. 14).

Two alluvial fans engulf the plain of Großer Ahornboden in the North: the fan emerging from Gramaigraben in the East and the fan from Großer Totengraben in the West. The former shows only outcrops in its most distal part, where debris-flow gravel sharply overlies the clayey-silty lake beds. The top of these latter is marked by a thin (<10 cm thick), brown oxidation zone (Fig. 15). This is consistent with the presence of a series of springs emerging at the top of these impermeable clay-rich sediments. The lake beds can be traced below the fan sediments as shown by both seismic and geoelectric surveys. A wood fragment found 40 cm underneath the top of the lacustrine sediments yielded an age of 5303–5469 cal BP. This is consistent with the dates obtained in the outcrop just east of Stop 5 and constrains the end of the lake to the middle of the 4th millennium BC.

The fan from Großer Totengraben north of the Gramai fan clearly postdates the moraine ridge and pushed the Rissbach all the way to the East (Fig. 12). Subsequently, the stream has eroded the distal portion of the fan exposing its stratigraphy. Blackened wood fragments embedded in silts and clays overlying a weathering horizon yielded ages between 3476 and 3613 cal BP. They are overlain by 9 m of debris flow gravel at this distal section and hence provide an upper age boundary for the onset of debris-flow activity. No organic remains were found in the upper part of this succession. The last accumulation phase on this fan can be constrained to the Little Ice Age based on paleosols containing wood and charcoal pieces exposed along a gully in the southern segment of the fan. The dates cluster around the 16th and 17th century AD. A similar age was reported for the uppermost paleosol near Eng Alm (see Stop 6).

Stop 6: Parking lot at Eng

The final fieldtrip stop is the impressive valley head called Eng 24 km south of Vorderriß where the toll road ends. The rock wall to the South provides impressive insights into the superposition of the Lechtal Nappe by the Inntal Nappe, the latter comprising Middle Triassic platform carbonates including the light-grey Wettersteinkalk. The youngest rocks of the Lechtal Nappe belong to the Schrambach Formation and date the thrusting to the Lower Cretaceous.

The Quaternary sediments and geomorphology has been mapped previously by Ampferer (1950) and Sommerhoff (1971) and are currently being re-mapped for the new map sheets (Büsel, 2013). Moraine ridges are present west and south of Eng Alm and are probably Egesen in age. This alpine pasture has frequently been threatened by gravel deposition by the Engergrundbach and a second, smaller creek draining the cirques east of Spritzkarspitze (2606 m a.s.l.). Sommerhoff (1977) sketched and briefly described a 5 m-high outcrop between Guesthouse Eng and Eng Alm, where three paleosols were exposed, buried beneath gravel. Radiocarbon dates of organic matter provide constraints on the age of these paleosol and the intervening episodes of gravel accumulation (Fig. 16). These dates were published by Som-

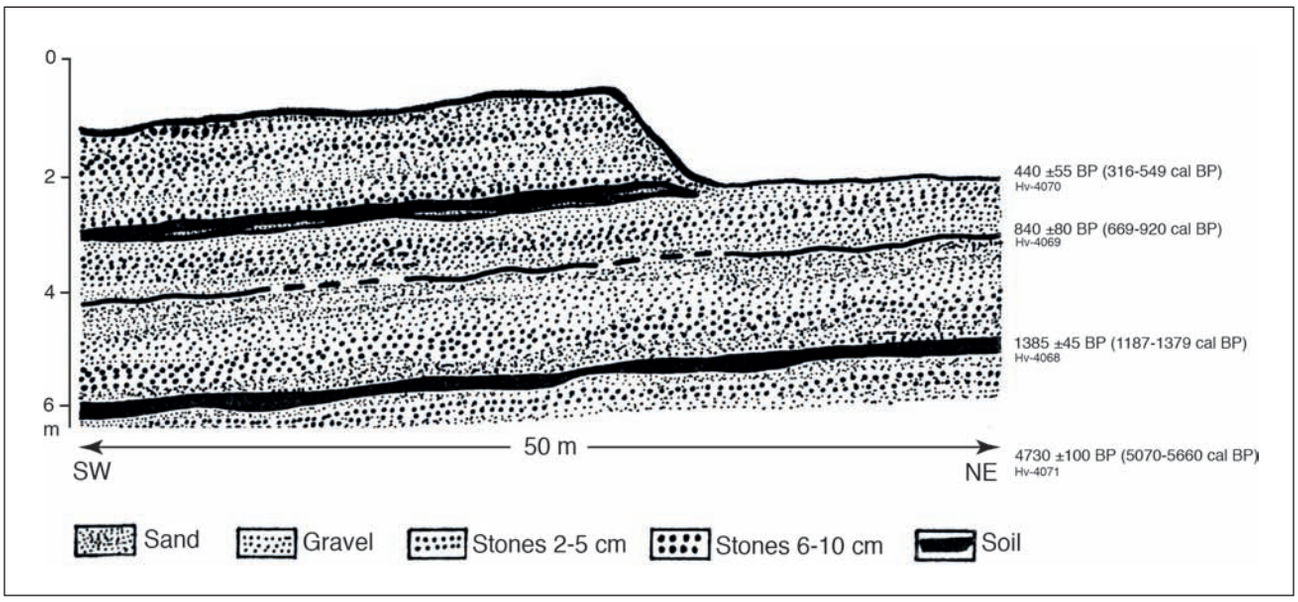

Fig. 16: Former exposure of debris-flow layers interbedded with buried soils near Eng Alm (modified from Sommerhoff 1971). The original radiocarbon values were verified with the laboratory which performed these analyses three decades ago and the calibrated age range (2 σ) is given in brackets (INTCAL13). The laboratory protocol also noted a fourth sample at 7 m depth from the same area (M. Geyh, pers. comm. 2014), which, however, was not published in Sommerhoff (1977). Unfortunately, it could not be reconstructed whether this fourth sample from the 6th millennium BP) was indeed from the same outcrop (G. Sommerhoff, pers. comm. 2014).

Abb. 16: Ehemaliger Aufschluss von Murschuttlagen und zwischengeschalteten Paläoböden nahe der Eng Alm (verändert nach Sommerhoff 1971). Die ursprünglichen Radiokarbondaten wurden nach Rücksprache mit dem Labor, welches diese von drei Jahrzehnten ermittelt hatte, verifiziert und werden hier mit den kalibrierten Werten (2 σ) in Klammer widergegeben (INTCAL13). Das damalige Laborprotokoll vermerkte zudem eine vierte Probe in 7 m Tiefe in diesem Gebiet (M. Geyh, pers. Mitt. 2014), welche jedoch von Sommerhoff (1977) nicht publiziert wurde. Leider konnte nicht mehr eindeutig geklärt werden, ob diese Probe aus dem sechsten Jahrtausend vor heute tatsächlich aus diesem Aufschluss stammt (G. Sommerhoff, pers. Mitt. 2014).

merhoff (1977), albeit lacking further information. We managed to obtain this information from the original laboratory in Hannover (pers. comm. M. Geyh) and calibrated the dates (Fig. 16). The paleosol in 5 m depth dates from early medieval times and the topmost sample buried in 2 m depth yielded a calibrated age of the Little Ice Age, not unlike the dates obtained from the youngest episode of debris accumulation at Großer Totengraben fan (see Stop 5). This underscores the high debris-flow activity in this valley during the Little Ice Age, consistent with historical reports of devastating events during the middle of the 19th century (Czell et al. 1966).

As a final note, in two steep cirques between Spritzkarspitze (2606 m a.s.l.) and Hochglück (2573 m a.s.l.) dwarf glaciers survived at altitudes between 2180 and 2340 m a.s.l. (Fig. 17), i.e. well below the equilibrium line altitude (Kuhn 1993).

Acknowledgements

This article builds on joint field work and interaction with Michael Meyer, Susanne Brandstätter, Katrin Büsel and many Master students of our Quaternary field courses. W.

Fig. 17: View from Großer Ahornboden towards the wall of the main ridge of the Karwendel in the South. The north-facing cirques of Eiskarln and Hochglückkar still host dwarf glaciers, the only ones in this mountain range.

Abb. 17: Blick vom Großen Ahornboden auf die Felswände des Karwendel-Hauptkammes im Süden. Die nordexponierten Kare der Eiskarln und des Hochglückkars enthalten Kleinstgletscher, die einzigen des Karwendels.

Chwatal and R. Scholger provided invaluable support for our geophysical work, M. Geyh and G. Sommerhoff are thanked for useful discussion and H. Sonntag for ongoing support on behalf of Alpenpark Karwendel.

C

References

Ampferer, O. (1903): Geologische Beschreibung des nördlichen Theiles des Karwendelgebirges. – Jahrbuch der Geologischen Reichsanstalt, 53: 169–251.

Ampferer, O. (1950): Geologische Karte des östlichen Karwendel und des Achensee-Gebietes. – M 1:25.000, Innsbruck (Wagner).

Bachmann, G.H. & Müller, M. (1981): Geologie der Tiefbohrung Vorderriß 1 (Kalkalpen, Bayern). – Geologica Bavarica, 81: 17–53.

Bachmann, G.H. & Müller, M. (1982): Exploration in a classic thrust belt and its foreland: Bavarian Alps, Germany. – American Association of Petroleum Geologists Bulletin, 66: 2529–2542.

Bader, K. (1979): Exarationstiefen würmeiszeitlicher und älterer Gletscher in Südbayern. – Eiszeitalter und Gegenwart, 29: 49–61.

Benn, D.I. & Evans, D.J.A. (2010): Glaciers and Glaciation. 2nd ed., 802 p., London (Arnold).

Brandstätter, S. (2006): Quartärgeologische Untersuchungen im nördlichen Rißtal – Karwendel (Bayern-Tirol). – Unpublished Master thesis, University Innsbruck.

Büsel, K. (2013): Bericht 2012 über quartärgeologische Aufnahmen auf Blatt 2223 Innsbruck und auf Blatt 2217 Hinterriß. – Jahrbuch der Geologischen Bundesanstalt 153: 405–411.

Büsel, K. (2008): Untersuchung quartärer Ablagerungen im Tiroler Rißtal. – Unpublished Master thesis, University Innsbruck.

Costantini, D. & Ortner, H. (2014): Klüfte und Deformationsstrukturen in jungpleistozänen Beckensedimenten des Rißtales, Bayern. – GeoAlp, 10: 5–26.

Czell, A., Schiechtl, H.M., Stauder, S.& Stern, R. (1966): Erhaltung des Naturschutgebietes „Großer Ahornboden" durch technische und biologische Maßnahmen. – Jahrbuch des Vereins zum Schutze der Alpenpflanzen und Tiere, 31: 33–56.

Doben, K. (1993): Geologische Karte von Bayern 1:25000, Blatt 8434 Vorderriss und Erläuterungen. – Munich (Bayerisches Geol. Landesamt).

Eisbacher, G.H. & Brandner, R. (1996): Superposed fold-thrust structures and high-angle faults, nortwestern Calcareous Alps, Austria. – Eclogae geologicae Helvetiae, 89: 553–571.

Frank, H. (1979): Glazial übertiefte Täler im Bereich des Isar-Loisach-Gletschers. – Eiszeitalter und Gegenwart, 29: 77–99.

Hillebrandt, V.v., Krystyn, L., Kürschner, W.M., Bonis, N.R., Ruhl, M., Richoz, S., Schobben, M.A.N., Urlichs, M., Bown, P.R., Kmet, K., McRoberts, C.A., Simms, M. & Tomasovych, A. (2013): The Global Stratotype Sections and Point (GSSP) for the base of the Jurassic System at Kuhjoch (Karwendel Mountains, Northern Calcareous Alps, Tyrol, Austria). – Episodes, 36: 162–198.

Kuhn, M. (1993): Zwei Gletscher im Karwendelgebirge. – Zeitschrift für Gletscherkunde und Glazialgeologie, 29: 85–92.

Levy, F. (1920): Diluviale Talgeschichte des Werdenfelser Landes und seiner Nachbargebiete. – Ostalpine Formenstudien, 1, 1–191.

Mair, D. (2014): Quartäre Sedimente des inneren Risstales und im Bereich Großer Ahornboden (Karwendel, Tirol). – Unpublished Master thesis, University Innsbruck.

Mutschlechner, G. (1948): Spuren des Inngletschers im Bereich des Karwendelgebirges. – Jahrbuch der Geologischen Bundesanstalt, 93: 155–206.

Ortner, H., Reiter, F. & Brandner, R. (2006): Kinematics of the Inntal shear zone-sub-Tauern ramp fault system and the interpretation of the TRANSALP seismic section, Eastern Alps, Austria. – Tectonophysics, 414: 241–258.

Ortner, H. & Gruber, A. (2011): 3D-Geometrie der Strukturen zwischen Karwendel-Synklinale und Thierssee-Synklinale. – In: Gruber, A. (ed.): Arbeitstagung 2011 der Geologischen Bundesanstalt Blatt 88 Achenkirch, 51–67, Wien (Geologische Bundesanstalt).

Penck, A. (1922): Die Terrassen des Isartales in den Alpen. – Sitzungsberichte der Preussischen Akademie der Wissenschaften, Sitzung der physikalisch-mathematischen Klasse, 19/20: 182–208.

Sauer, E. (1938): Verbreitung, Zusammensetzung und Entstehung der diluvialen Seeabsätze im oberen Isartal. – Mineralogische Petrographische Mitteilungen, 50: 305–355.

Schmidt-Thomé, P. (1950): Geologie des Isargebietes im Bereich des Rißbach-Stollens und des geplanten Sylvenstein-Staubeckens. — Geologica Bavarica, 4: 1-55.

Sommerhoff, G. (1971): Zum Stand der geomorphologischen Forschung im Karwendel. – Mitteilungen der Geographischen Gesellschaft München, 56: 152–171.

Sommerhoff, G. (1977): Zur spät- und postglazialen Morphodynamik im oberen Rißbachtal, Karwendel. – Mitteilungen der Geographischen Gesellschaft München, 62, 90–103.

van Husen, D. (1987): Die Ostalpen und ihr Vorland in der letzten Eiszeit (Würm). – Map 1:500,000, Vienna (Geologische Bundesanstalt).

Wolf, H.v. (1922): Beiträge zur Kenntnis der eiszeitlichen Vergletscherung des Achenseegebietes in Tirol. – Mitteilungen der Geographischen Gesellschaft München, 15: 147–304.

Wolf, H.v. (1924): Eiszeitstudieen im Risser Gebirge. – Mitteilungen der Geographischen Gesellschaft München, 17: 255–274.

Notes

Glacial dynamics and large pre-LGM rock-slides in the lower Inn Valley and in the Brixen Valley

Gletscherdynamik und große Prä-Würm-Hochglaziale Felsgleitungen im Unterinntal und im Brixental

Jürgen M. Reitner, Alfred Gruber

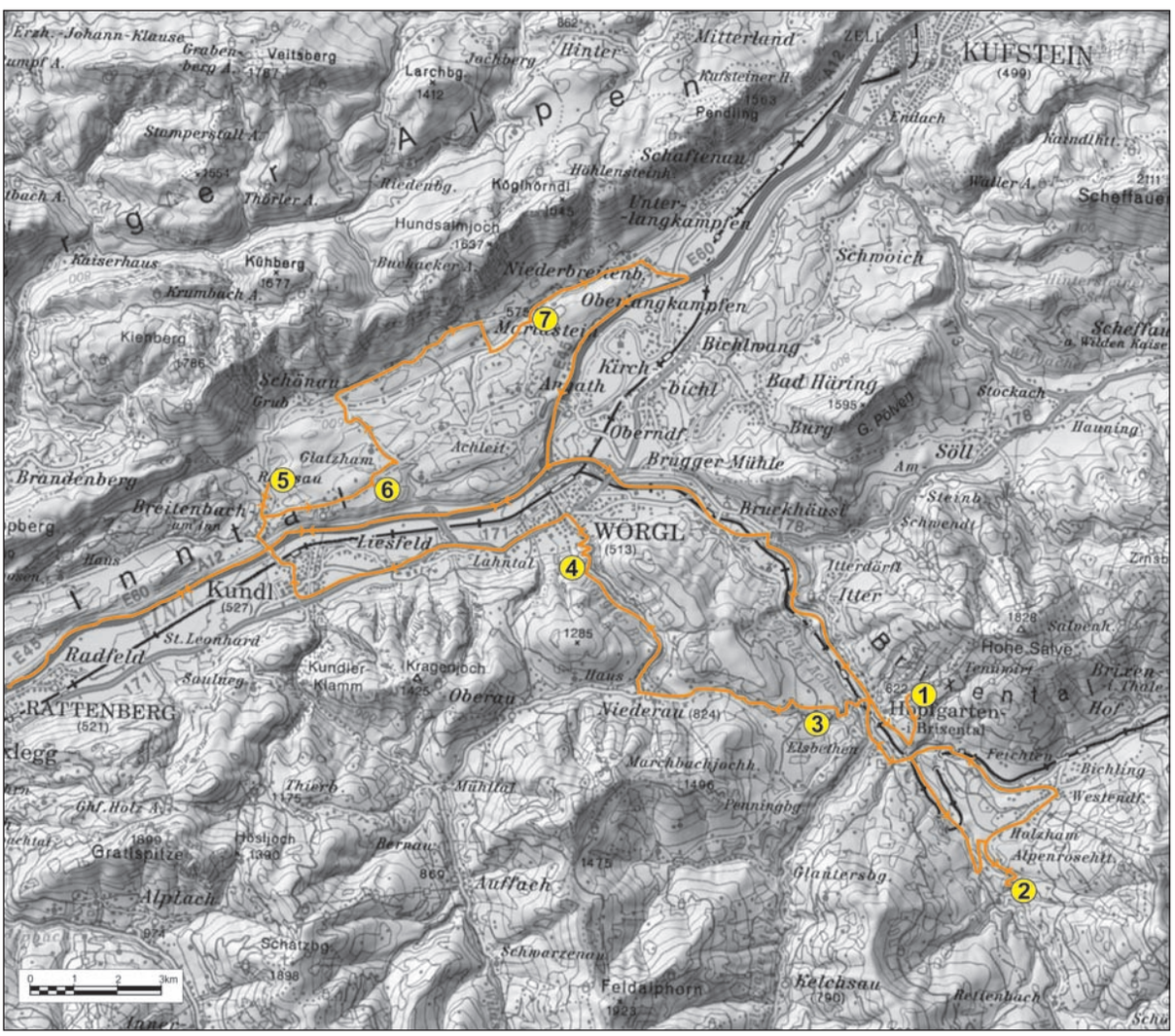

Fig. 1: Excursion route with stops (© BEV topographic map of Austria, scale 1:200,000)

Abb. 1: Exkursionsroute mit den Haltepunkten (Ausschnitt aus BEV – Österreichische Karte 1:200.000).

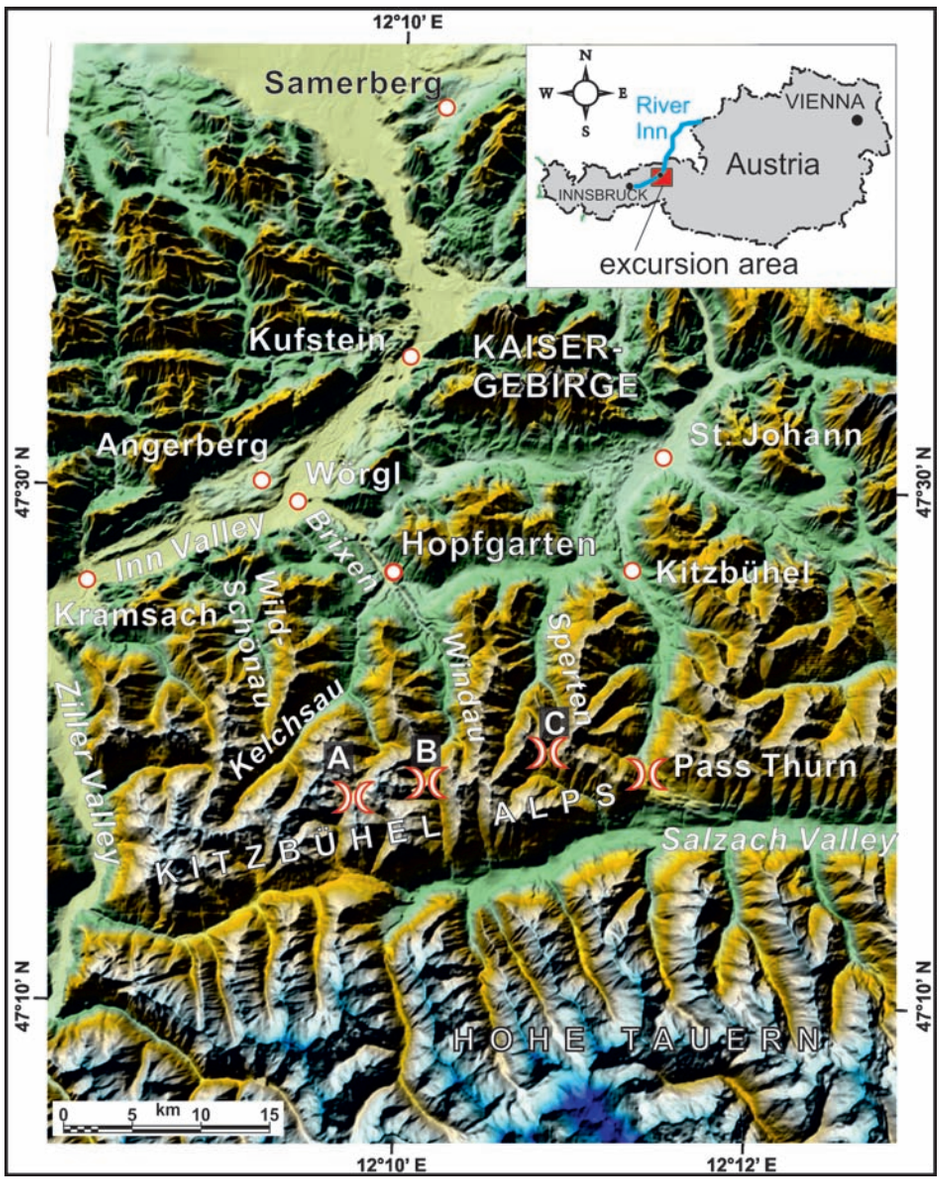

Fig. 2: Digital elevation model showing the location and morphology of the excursion area and its surroundings (modified after Reitner et al. 2010). Bridge symbols indicate cols and former ice transfluences from the Salzach Valley towards the excursion area: A at 1983 m a.s.l. into Kelchsau Valley, B at 1686 m a.s.l. into the Windau Valley and C at 1713 m a.s.l. into the Sperten Valley. The most prominent similar feature is Pass Thurn (1274 m a.s.l.) towards the Kitzbühel area.

Abb. 2: Digitales Höhenmodell (DEM) mit der Lage und Morphologie des Exkursionsgebietes und der weiteren Umgebung (modifiziert nach Reitner et al. 2010). Brückensymbole zeigen die Sättel und ehemaligen Transfluenzrouten vom Salzachtal in das Kelchsautal in 1983 m ü. NN (A), in das Windautal in 1683 m ü. NN (B) und in das Spertental in 1713 m ü. NN (C) an. Der Paß Thurn (1274 m ü. NN) stellt die markanteste derartige Form in Richtung Kitzbüheler Achental dar.

1 Introduction

This excursion examines the landscape evolution of the former Inn Glacier during the last glacial cycle, in particular from the Early Würmian to the Lateglacial. We will visit the lower Inn Valley and Brixen Valley where landforms and deposits document a complex chronology of gravitational, glacial and fluvioglacial processes within a geologically diverse landscape. The route (Fig. 1) includes the type region of the "Early Lateglacial phase of ice decay" (Reitner 2005 & 2007). Hence, the excursion places special emphasis on the ice-flow and glacier dynamics, from the Alpine Last Glacial Maximum (LGM; in the sense of the Würmian Pleniglacial – Chaline & Jerz 1984, van Husen & Reitner 2011), to the collapse of the network of valley glaciers during Termination I.

We present results gained throughout the geological mapping process carried out by the Geological Survey of Austria (Geologische Bundesanstalt) combined with subsurface evidence (e.g. drilling results) provided for infrastructure projects (such as railways) and additional research on sedimentology, geochronology and palynology.

The Inn Valley is the longest longitudinal valley of the Eastern Alps and follows a major strike slip fault, known as the Inntal fault. The Lower Inn Valley (Fig. 2) around the city of Wörgl shows the broadest cross-section of the whole valley consisting of the modern valley floor at around 500 m a.s.l. and a broad terrace-like feature referred to as Unterangerberg terrace with Butterbichl (733 m a.s.l.) as the highest elevation.

Steep rocky cliffs characterise the southern margin of the informal tectonic unit of the Northern Calcareous Alps (NCA) north of the Inn Valley. There, elevations reach up to 1800 m a.s.l. and in the Kaisergebirge Mountains, ENE of Wörgl, peaks rise to 2344 m a.s.l.

In contrast, the Kitzbühel Alps in the South are part of the informal tectonic unit referred to as Greywacke Zone (GWZ) and offer a landscape dominated by meadows with only occasional rocky peaks reaching up to 2400 m a.s.l.. This area is drained by the Brixentaler Ache joining the Inn River at Wörgl, and its tributaries, the Windauer Ache and the Kelchsauer Ache. Hopfgarten (622 m a.s.l.) is the main village of the corresponding Brixen Valley.

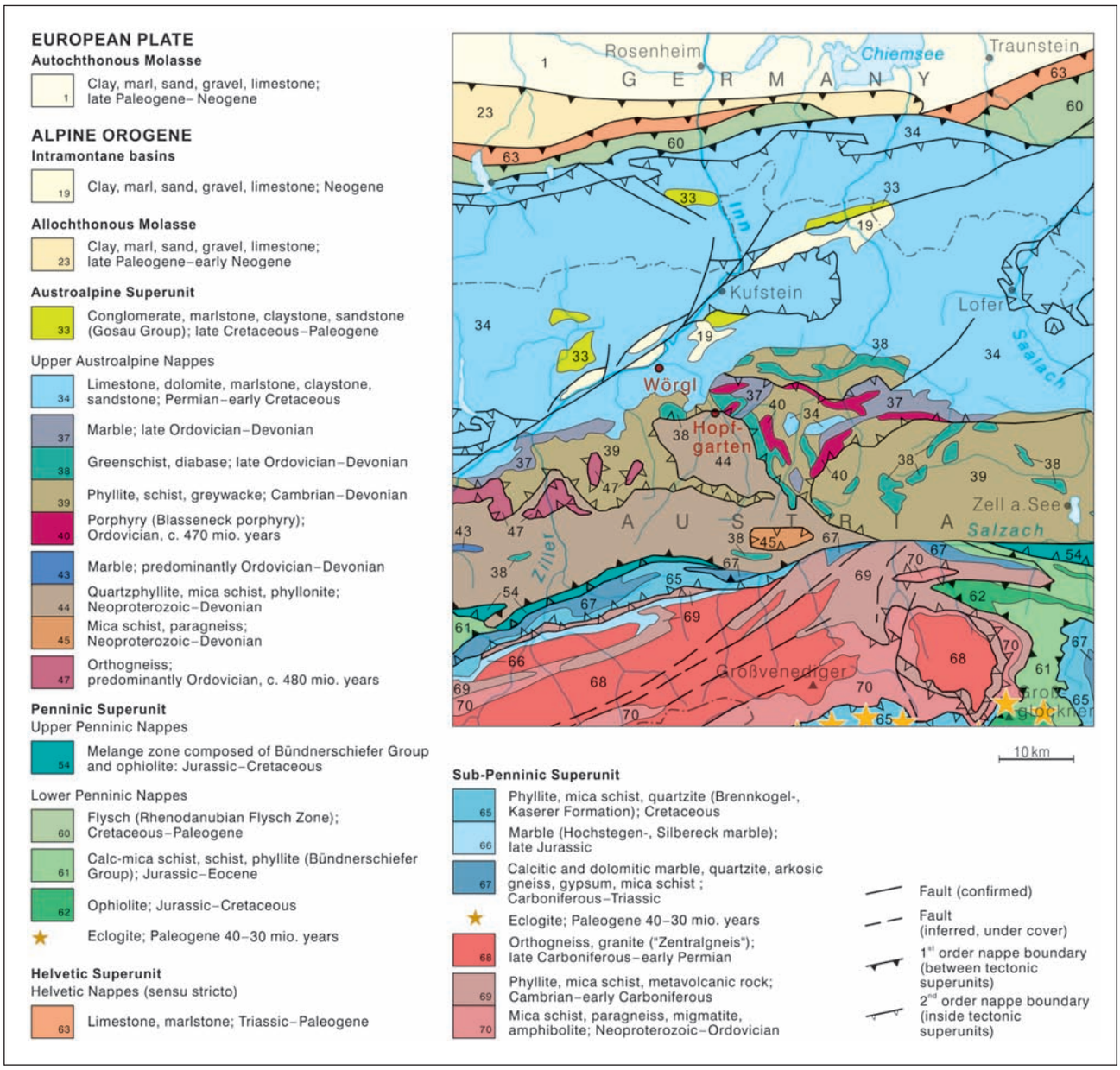

Fig. 3: Geological map of the excursion area (with the location of Wörgl and Hopfgarten indicated in red) and its surrounding (modified after Schuster et al. 2013b).

Abb. 3: Geologische Karte des Exkursionsgebietes (mit den Hauptorten Wörgl und Hopfgarten in rot markiert) und seiner Umgebung (leicht veränderter Ausschnitt aus Schuster et al. 2013b).

2 Geological setting

The excursion area is built up by the Upper Austroalpine tectonic unit (Fig. 3). On one hand, this consists of Palaeozoic meta-sedimentary and meta-volcanic rocks (identical with GWZ), which obtained their weak metamorphic overprint during the Variscan orogeny. On the other hand, this succession is unconformably overlain by a kilometre-thick sequence of terrestrial to marine sedimentary rocks of Permian to Paleogene age (NCA).

According to the new tectonic subdivision of the Eastern Alps (Schmidt et al. 2004, Schuster et al. 2013a, Pestal et al. 2004) the Palaeozoic basement and the sedimentary cover reaching from the Permian to the Oligocene are summarised as the Tirolic-Noric nappe system, which can be subdivided into different nappes. West of the Inntal fault the Tirolic-Noric nappe system is represented by the Inntal nappe overlying the Bajuvaric nappe system which is further to the North (cf. Ortner 2003b, Ortner et al. 2006).

The main deformation overprint occurred in a compressional regime with (mega-)folds, thrusts (nappe-stacking) and strike-slip-faults during the Eoalpine phase (Lower Cretaceous, ~100 Ma) and the Alpine phase (Eocene to Miocene; Ortner 2003b).

The NE-SW striking Inn Valley shear zone constitutes one of the most important strike-slip faults of the Alps with a lateral displacement of tens of kilometres and also vertical offsets. The formation of the lower Inn Valley is directly linked to the activity of this fault beginning with the development of the Tertiary basin of the lower Inn Valley and documenting the oldest deposits of the Palaeo-Inn.

Today's landscape is mainly the legacy of multiple glaciations during the Pleistocene (see ice-extent during the last glaciation in Fig. 4) which re-shaped and modified the tectonically induced drainage system (cf. Frisch et al. 1998).

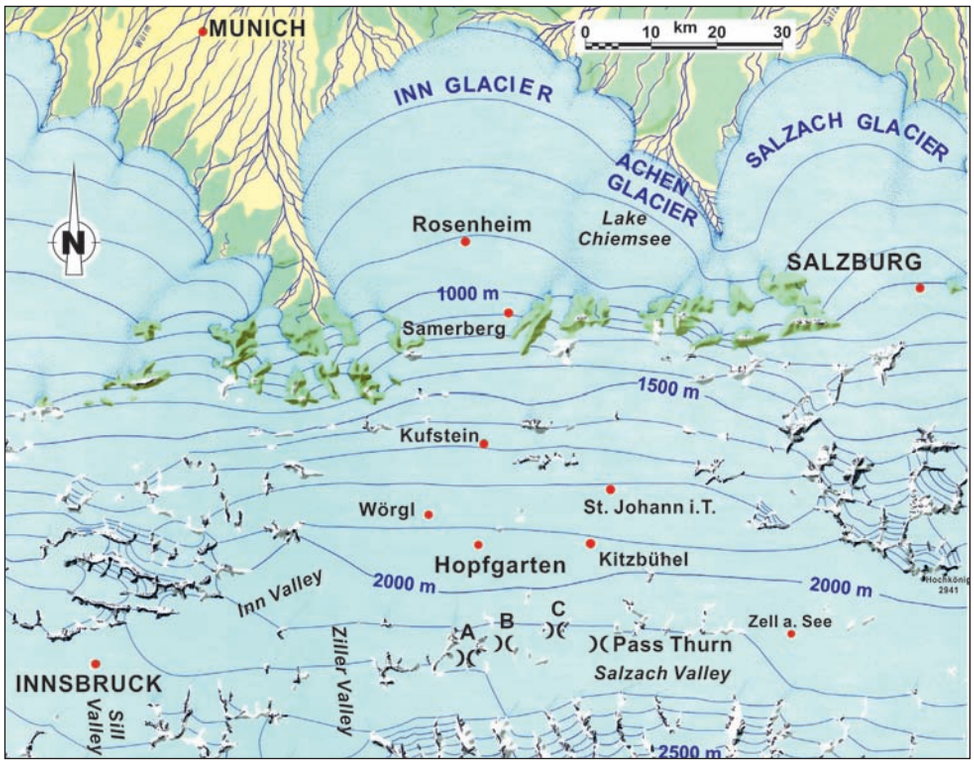

Fig. 4: The network of valley glaciers during the climax of the LGM after VAN HUSEN (1987). Hopfgarten and Wörgl as part of the excursion area and other localities are indicated (for bridge-symbols see Fig. 2).

Abb. 4: Das Eisstromnetz am Höhepunkt des Würm-Hochglazials (LGM) nach VAN HUSEN (1987). Die Lage von Hopfgarten und Wörgl als Teile des Exkursionsgebietes sowie andere wichtige Lokalitäten sind angezeigt (für die Brückensymbole siehe Abb. 2).

3 Excursion part I: Brixen Valley – basin of Hopfgarten

3.1 Stop 1: Southern flank of the Hohe Salve peak

Location: 1.1 km E of Hopfgarten centre at 854 m a.s.l. on the road to the middle station of the cable car
(GPS: WGS84, 47°26'59'' N, 12°10'25.3'' E, 861 m a.s.l.)

Topics: Quaternary geology and morphology, glacier dynamics during the LGM.

This panoramic viewpoint (Fig. 5) provides the opportunity to explain the morphology and Quaternary geology of the basin of Hopfgarten and its hinterland. Looking to the South, the Kitzbühel Alps with the valleys of Windauer Ache and Kelchsauer Ache can be seen. Under good conditions even the peaks of the glaciated Hohen Tauern range, south of the Salzach Valley, are visible. In the foreground thick terraces dominate the scene; whose complex sediment fill is the key for understanding the landscape evolution.

The following description is based on REITNER (2005) and

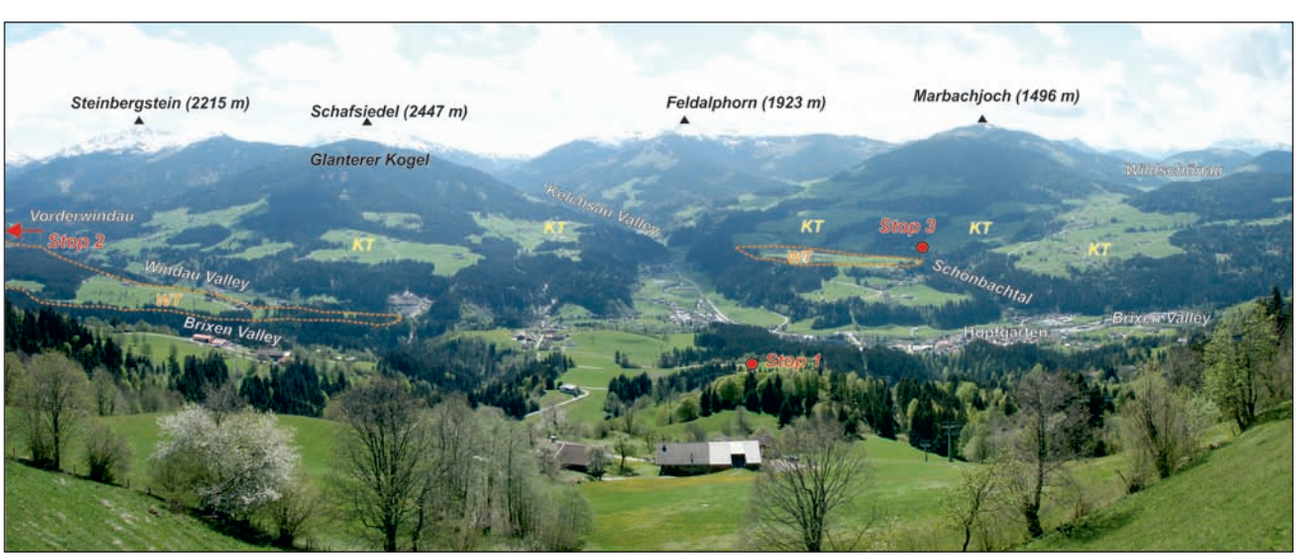

Fig. 5: Overview from the middle station of the cable car at the south-western flank of the Hohe Salve peak (an alternative for Stop 1). The location of the excursion stops 1, 2 and 3 as well as additional topographic locations and terrace systems are indicated. Note the extent and morphology of the Westendorf terrace level (WT, with orange dashed lines) with a slope similar to the modern valleys, compared to various higher kame terraces (KT) with a fan-like morphology and a slope towards the centre of the basin of Hopfgarten.

Abb. 5: Ausblick von der Mittelstation der Seilbahn an der Südwestflanke der Hohen Salve mit der Lage der Exkursionsstopps 1–3 und den topographischen Bezeichnungen und wichtigen quartären Terrassensystemen. Man beachte die Ausdehnung und Morphologie des Westendorfer Terrassenniveaus (WT, orange strichlierte Umrisse) mit einem Gefälle, das ähnlich dem der jetztigen Täler ist. Man vergleiche weiters dieses Terrassenniveau mit den verschiedenen höher gelegenen Kame-Terrassen (KT), die eine fächerartige, ins Zentrum des Hopfgartner Beckens hin abfallende Oberfläche aufweisen.

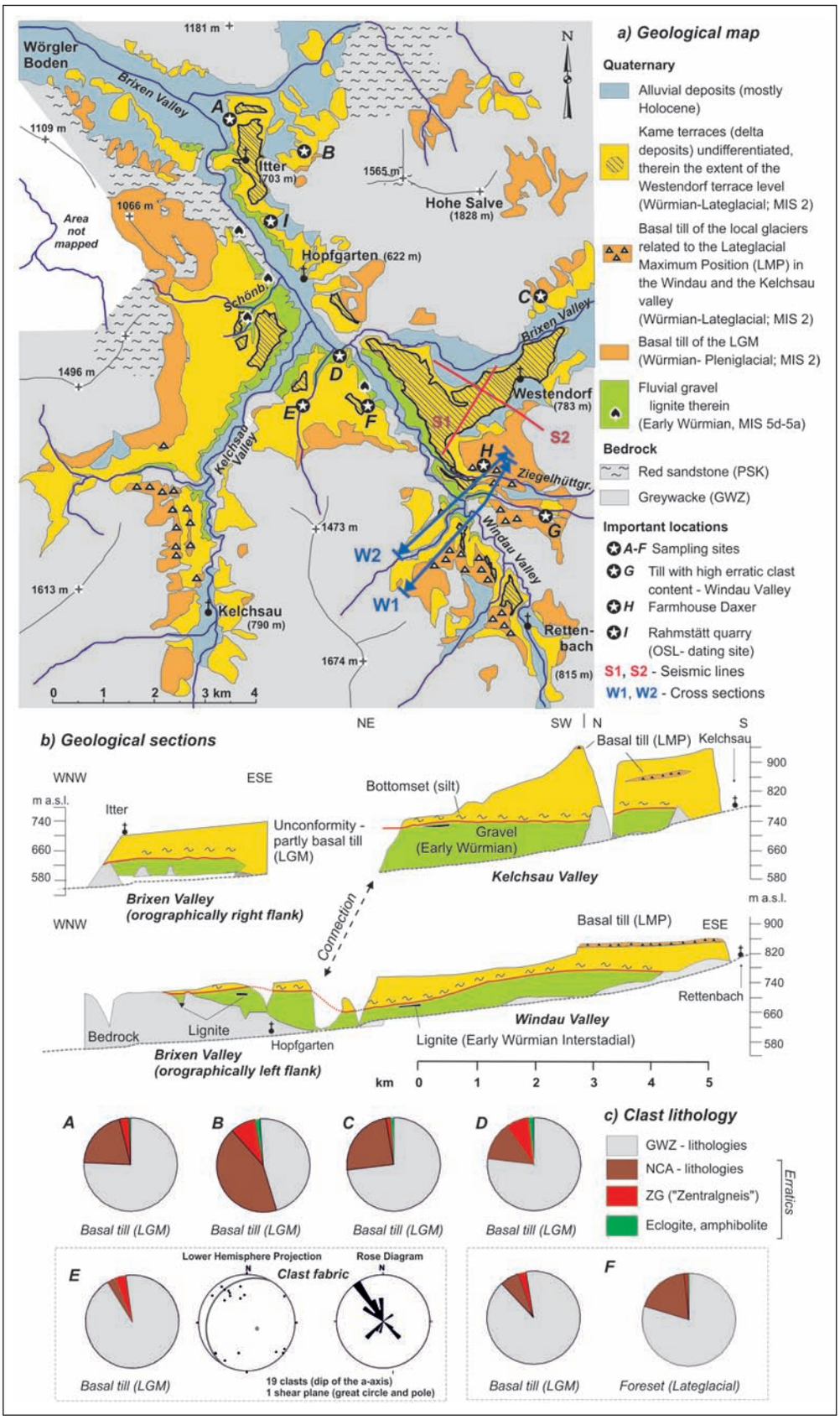

Fig. 6: (a) Simplified geological map of the basin of Hopfgarten after Reitner (2007) with important locations (A to I), position of the seismic lines (S1, S2) and cross sections (W1 & W2). (b) Geological sections along the rivers Brixentaler Ache, Windauer Ache and Kelchsauer Ache. (c) Clast lithology of basal till and delta sediment from selected sample sites (modified after Reitner et al. 2010). GWZ Greywackezone, NCA Northern Calcareous Alps.

Abb. 6: (a) Vereinfachte geologische Karte des Beckens von Hopfgarten nach Reitner (2007), mit wichtigen Lokalitäten (A bis I), Position der Seismiklinien (S1, S2) und geologischen Talquerschnitten (W1 & W2). (b) Geologische Längsschnitte entlang der Brixentaler, Windauer und Kelchsauer Ache. (c) Die Geschiebespektren der Grundmoränen und das Geröllspektrum eines Deltasedimentes von ausgewählten Lokalitäten ist nach Reitner et al. (2010) dokumentiert. GWZ Grauwackenzone, NCA Nördliche Kalkalpen.

Reitner et al. (2010). In the basin of Hopfgarten, terraces up to 150 m high (Figs. 5, 6, 7) are found, which exhibit different levels and extend towards the tributary valleys of the Brixen Valley, the Windau Valley and the Kelchsau Valley. The most prominent terrace and morphostratigraphic reference level is that of Westendorf which can be traced over more than 10 km, extending from its lowest occurrence in Itter upstream, via the village of Westendorf, into the Windau Valley north of Rettenbach. The terrace bodies contain a tripartite sedimentary succession (units A, B and C) which will be characterised in terms of lithofacies, sedimentary processes, palaeoclimatological conditions, chronostratigraphy and palaeogeography.

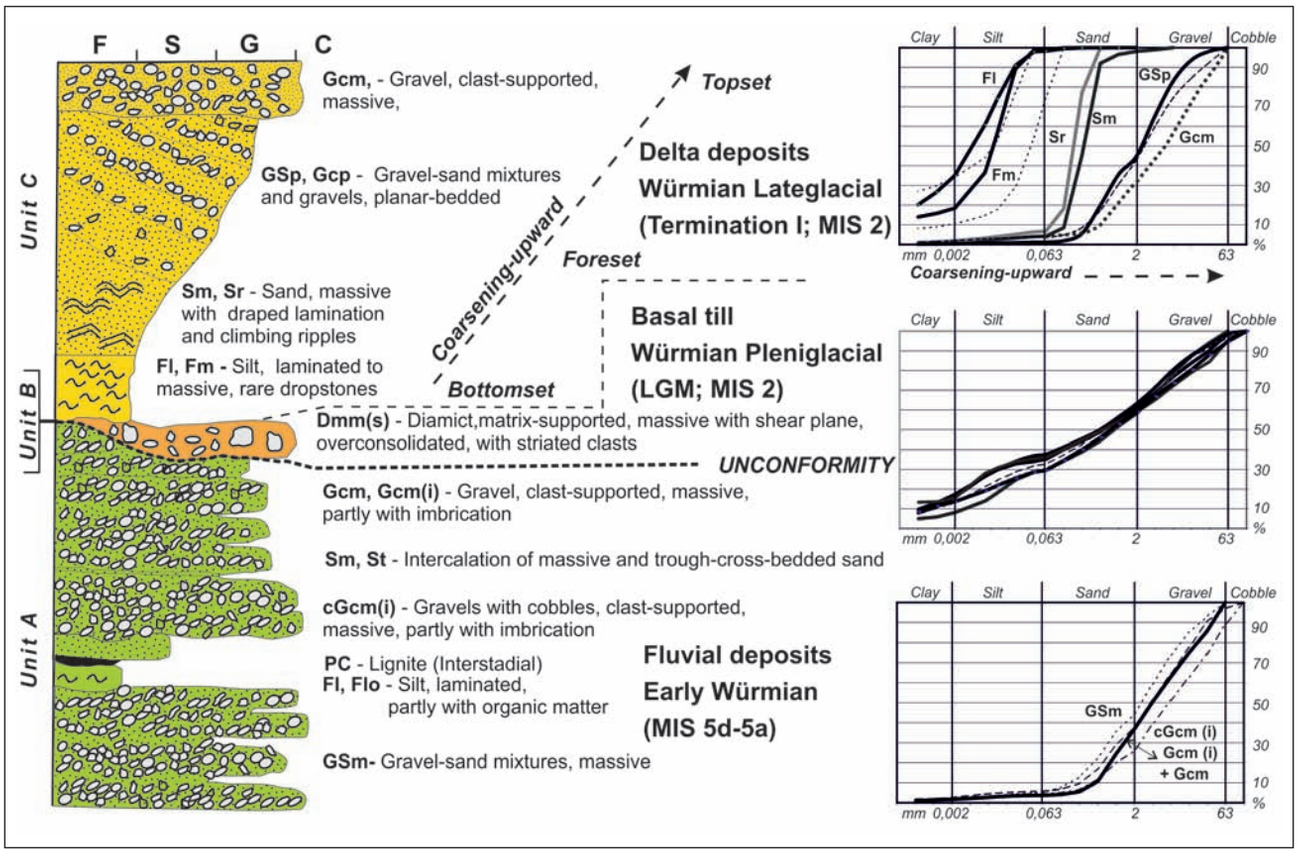

Fig. 7: Idealized lithological column of mapped units in the Hopfgarten area and selected grain-size curves after Reitner et al. (2010). Lithofacies codes are according to Keller (1996) with minor modifications.

Abb. 7: Idealisiertes Säulenprofil der kartierten Sedimenteinheiten im Bereich Hopfgarten mit typischen Kornsummenkurven nach Reitner et al. (2010). Die Lithofazies Codes nach Keller (1996) sind leicht modifiziert.

Predominant fluvial deposits of Early Würmian age (Marine Isotope Stages (MIS) 5d–5a) form the lowest unit A (Fig. 7). The dominant lithofacies of the lowest are horizontally bedded sheets of clast-supported, massive gravels, with clasts up to cobble size and occasionally recognizable imbrication (cGcm (i), for grain size distribution see Fig. 7). Small troughs filled with trough-bedded sand (St) or lenses of massive sand (Sm) are interbedded. These gravel sheets are interpreted as deposits of shallow braided rivers. The only local clast lithologies (GWZ) in combination with their occurrence in the tributary valleys point to a deposition by the precursors of the modern rivers Windauer Ache and Kelchsauer Ache.

At some locations, mostly at the margin of the basin, organic-bearing sediments and lignite are intercalated with the described coarse-grained lithofacies at different altitudes (Zailer 1910, Schulz & Fuchs 1991). This fine-grained subunit, with a thickness of less than 10 m, consists of coal (PC), laminated silts (Fl) and sand (Sm), partly with organic debris (Flo, Sho), and occasionally coarse-grained clast- to matrix-supported diamicts (Dmm, Dcm). This facies association most probably reflects sedimentary conditions of a backswamp area with peat growth and overbank-sedimentation formed upstream of alluvial fans impeding the drainage. Pollen analyses indicate an arboreal environment during the two prominent early Würmian interstadials (MIS 5c and 5a; Reitner & Draxler 2002). Thus, the braided river deposits probably reflect the nonarboreal climatic deterioration of the two early Würmian stadials, MIS 5d and 5b, resulting in considerable fluvial aggradation (Reitner & Draxler 2002). The extent of the Early Würmian gravels show no hint of ice-proximal environments, hence indicating only a small glacier cover in the upper and thus higher valley grounds of the Kitzbühel Alps during the Early Würmian stadials.

Unit A is overlain with an erosive contact by unit B (Figs. 6 & 7), i.e. the basal till of the Würmian pleniglacial (LGM, MIS 2). This subglacial sediment consists of a massive, matrix-supported and over-consolidated diamict (for grain size distribution see Fig. 5) with subangular to subrounded, frequently striated clasts and occasional indications of shear planes (Dmm (s)). In general, the observed thickness of the basal till within the sediment sequence is between 2 and 10 m. Such diamictic sediments with erratic clast lithologies indicate a deposition by a glacier flowing from the Inn Valley into the Hopfgarten Basin, which is commonly referred to as the Inn Glacier.

The clast lithology of the LGM basal till (unit B) changes significantly from the north-westernmost part of the Hopfgarten Basin located closest to the Inn Valley, to its south-eastern part. At the north-westernmost as well as the north-eastern locations (locations A, B and C in Fig. 3) high contents of clasts are ascribed to the Inn Valley drainage system. Limestones from the NCA and dolomite clasts, as well as crystalline rocks, are common. The latter include orthogneiss of the so-called Zentralgneis originating from the Hohen Tauern via the Ziller Valley (see Figs. 2 & 3), eclogite from the Ötz Valley and amphibolites. The content of erratic clasts successively diminishes south of Hopfgarten towards

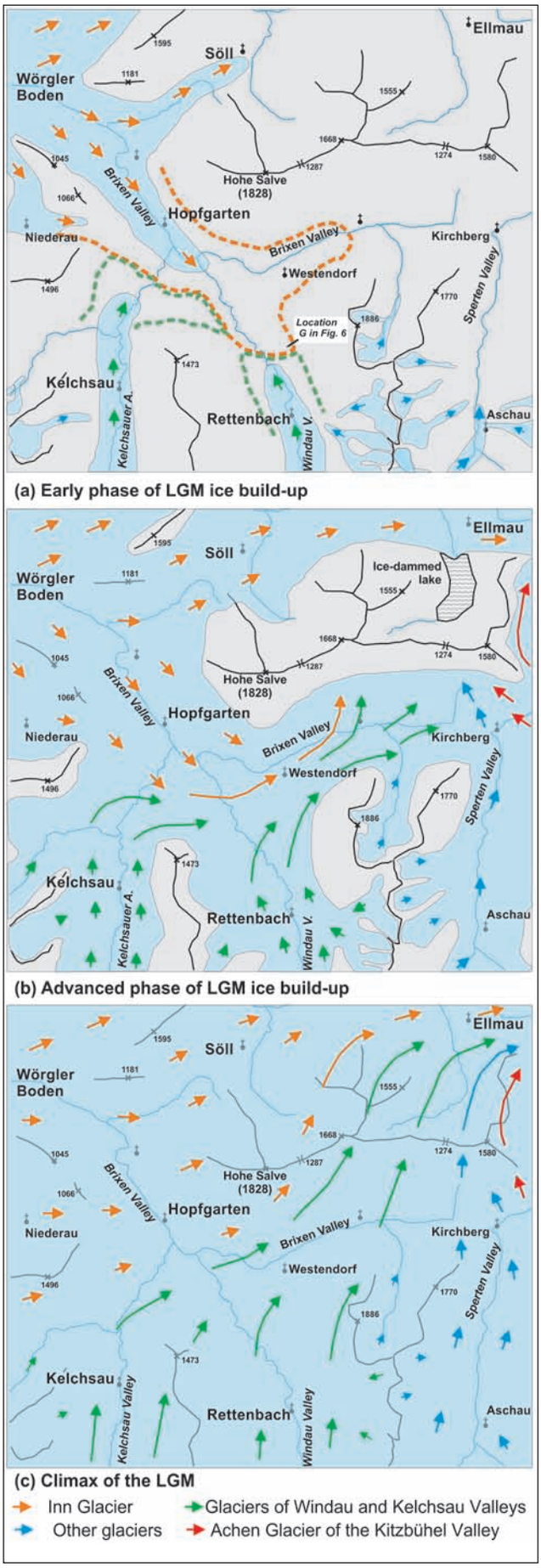

the Windau Valley (trend indicated from location D, to E and F in Fig. 3). There such erratic lithologies, as well as amphibol-bearing micaschists (Hornblendegarbenschiefer from the Ziller Valley), and granite from the Julier region (Engadine), which is the indicator lithology of the Inn Glacier system, from the Julier region (Engadine) can only be found in one location (location G in Fig. 3). This provenance from the Inn Valley is displayed also in the clast fabric of the till at location E (Fig. 3). There a dominant NW-SE trend of the a-axis is present, with a prevailing dip towards NW, also indicated by a shear plane.

The deposits of unit C show in general a tripartite, coarsening-upward delta sequence with a bottomset, foreset and finally a topset typical for Gilbert delta-sequences (Postma 1990). This delta sequence conformably overlies the basal till of unit B and in most cases is directly ontop of the lowest unit A. The latter contact may be classified as a paraconformity, i.e. an obscure or uncertain unconformity in which no erosion surface is discernable and in which the beds and the parts above the break are parallel (definition after Neuendorf et al. 2005).

The bottom set is up to 20 m thick and comprises massive and laminated silts (Fm, Fl) with occasional dropstones. The foreset beds consist of planar-bedded gravel (Gcp) to gravel-sand mixtures (GSp), with intercalated ripple-bedded (including climbing ripples) to massive sands (Sr, Sm) dipping between 10° and 25°.

The occurrence of kettle holes, ice-contact structures as well as the occasional preservation of striae in combination with ripple-drift lamination, indicate rapid sedimentation of ice-contact deltas. These are in some cases of the Hjulström-type (Postma 1990). The final sedimentation in the Hopfgarten Basin and the formation of the prominent Westendorf terrace occurred when the front of the stagnant Inn Glacier blocked the drainage of the whole basin at its north-western margin. All features indicate a formation during the Early Lateglacial phase of ice-decay (Reitner 2007) and thus document the beginning of Termination I. Moreover, this classification is supported by an optically stimulated luminescence (OSL) date (18.7 ± 1.7 kyr BP; Klasen et al. 2007) from the Westendorf terrace west of Hopfgarten (location I – Rahmstätt quarry – in Fig. 6). During this phase local glaciers oscillated towards their Late-

Fig. 8: Ice-flow model from the ice build-up phase to the climax of the LGM. (a) Early ingression of the Inn Glacier into the basin of Hopfgarten and early impediment of Windau and Kelchsau glacier (dashed lines). (b) Advanced phase of ice-build up with the blockage of ice flow towards the East by Achen Glacier. (c) Ice flow during the climax of the LGM, when the ice transfluences (locations A and B in Figs. 2 & 4) from the Salzach Valley to the Windau and Kelchsau Valleys were active. Ice surface around Hopfgarten at 1900 m a.s.l.

Abb. 8: Modell der Gletscherbewegungen von der Vorstoßphase zum Höhepunkt des Würm-Hochglazials (LGM). A) Frühes Eindringen des Inngletschers in das Becken von Hopfgarten und Behinderung des Abflusses von Windau- und Kelchsaugletscher (gestrichelte Linien). B) Fortgeschrittene Phase der Vorstoßphase mit Blockade des Eisflusses gegen Osten durch den (Kitzbüheler) Achengletscher. C) Eisabfluss während des Höhepunktes des LGM, als die Eistransfluenzpässe (Lokalitäten A & B in Abb. 2 und 4) vom Salzachtal in Richtung Windau- und Kelchsautal aktiv waren. Die Eisoberfläche im Raum Hopfgarten lag in 1900 m ü. NN.

glacial maximum positions (LMP). This is indicated by the till of the Lateglacial Windau Glacier on top of the kame terrace in the upper Windau Valley (Figs. 3 and 4). Consequently, the age of the basal till of unit B is regarded as Würmian Pleniglacial because it is conformably superimposed by the delta sequence of Termination I, indicating only a change from a subglacial to glaciolacustrine environment without a major hiatus.

The unconformable contact between the LGM till (unit B) and the fluvial deposits of unit A, in combination with the stratigraphic interpretation of the uppermost peat layer (MIS 5a), indicate that sediments of the Middle Würmian (MIS 4–3) and the advance phase of the LGM (MIS 2) are missing due to glacial erosion. In the Inn Valley (Fliri 1973) and its tributaries such as the neighbouring valley of Wildschönau (e.g. Reitner 2008) such deposits of Middle Würmian age reach a thickness of more than 100 m.

3.2 Ice-flow pattern and glacial erosion during the LGM and previous glaciations

Based upon the distribution of erratics and boulders we conclude that a branch of the Inn Glacier advanced into the Brixen Valley reaching the Hopfgarten Basin earlier than the local glaciers of the Windau and Kelchsau Valleys (Fig. 8a). The dominance of the Inn Glacier can be explained not only by its large and high-elevated accumulation area, but also by ice-dynamics. According to van Husen (2000), the topography of longitudinal valleys (such as the Inn and the Salzach Valleys), especially in their relation to the tributary valleys, had a fundamental impact on the rate of ice build-up as well as on the glacier extent during the major glaciations. In the Inn Valley, the onset of the LGM was characterised by ice congestion in the narrow Inn Valley as a result of a strong inflow of ice, especially from the southern tributaries with large, high-elevation drainage areas (e.g. Ziller Valley, Figs. 2 & 9). As a consequence, the ice surface rose leading to a rapid expansion of the accumulation area, favouring quick ice build-up. Due to this process, the Inn and likewise the Salzach Glacier (Reitner 2005) crossed watersheds to the North before these valleys were filled by local ice.

Clast lithologies in the basal till including Zentralgneis and Hornblendegarbenschiefer support this model, whereby ice from the Ziller Valley, a tributary of the Inn Valley, formed the eastern part of the Inn Glacier system. The same is true for NCA-limestone and red sandstones of Upper Permian to Lower Triassic age (PSK) which crop out between the Ziller Valley and the study area. However, the occurrence of lithologies originating west of Innsbruck (eclogite, Julier granite) cannot be explained solely by transport via laminar ice flow, but require the assumption that there was also a strong ice input from this and other valleys east of Innsbruck. A plausible reason seems to be subglacial erosion of proglacial fluvial gravels ("Vorstoßschotter") deposited in the Inn Valley during the glacier advance at the start of the LGM (van Husen 2000), as well as that of older glacial deposits.

In this early state of ice build-up the Windau and Kelchsau Glaciers were soon blocked in the lower section of their valleys (Fig. 8a). In the Windau Valley the Inn Glacier even reached location G for a short time (Fig 6) as indicated by the erratic-rich till at that location.

In the course of the further advance phase (Fig. 8b) both local glaciers were forced to flow eastwards up the Brixen Valley. Towards the East, Achen Glacier in the Kitzbühel region (also referred to as Chiemsee Glacier) received a strong inflow of ice from the Hohen Tauern via the low transfluence route of Pass Thurn (1274 m a.s.l.). This can be explained by ice dynamical processes in the Salzach Valley similar as those already described for the Inn Valley (see above). As a result, the Achen Glacier obstructed flow east of the Hopfgarten Basin. Thus, the local glaciers of Hopfgarten area were also blocked in Brixen Valley towards the East and were forced to overspill the up to 1200 m-high E-W trending chain E-NE of Hopfgarten towards the N-NE.

This principal pattern of glacier flow was most probably slightly modified in the course of further ice build-up due to the successive onset of ice transfluence (~1700–2000 m a.s.l.; Fig. 2) from the Salzach Valley, and thus from the Hohen Tauern towards the Windau, Kelchsau and other tributary valleys (Fig. 8c). This model of a later increase of the glaciers in the Windau and Kelchsau Valleys implies that the distribution of the erratics within the basal till represents an early phase of ice build-up. The preserved structural elements within the lodgement till at location E (Fig. 6), such as the a-axis of the clasts and shear plains orientations dominantly dipping towards NW, indicate a temperate Inn Glacier which advanced towards SE.

The sedimentary evidence is in general accordance with the reconstruction of the climax of the LGM around 26.5–21 kyr BP (Monegato et al. 2007). At this time, the Inn Glacier, as the biggest glacier in the Eastern Alps, was connected with other Alpine glaciers and formed a network ("Eisstromnetzwerk"; van Husen 1987; Fig. 2) in the sense of transection glaciers (Benn & Evans 1998). The ice surface of this glacier network declined from 2200–2100 m a.s.l. in the Salzach Valley in the South to ~1900 m a.s.l. at Hopfgarten. Hence, an ice flow with a low gradient towards N and NE across the longitudinal and smaller E-W trending valleys (Salzach and Brixen Valleys) was independent from the existing fluvial drainage. During this phase wet-based glacier conditions can generally be assumed on the basis of (i) the occurrence of subglacial traction till (according to Evans et al. 2006) from the valley floors to nearly up to the higher valley flanks, and (ii) the presence of drumlins in the larger valleys (lower Inn Valley, area of Kitzbühel; Reitner 2005; Gruber et al. 2009).

According to this ice-flow model the preservation of pre-LGM sediments well above the modern valley floor throughout the whole Hopfgarten Basin and the lack of glacial overdeepening during the LGM, seems to be the result of a combination of the following factors: mutual blocking of local glaciers between the dominant glaciers, i.e. the Inn Glacier in the West and the Achen Glacier in the East, at the beginning of the LGM, and the effect of an E-W trending basement barrier north to north-east of Hopfgarten during the climax of the LGM.

The results of reflexion seismic surveys close to the village of Westendorf (location indicated in Fig. 6a), however, indicate that there is a considerable overdeepening of 400 to 500 m with a complex sediment fill (see Reitner et al. 2010 for details). These fillings include deltaic sediments from Terminations II (MIS 6) and an older Terminatios as well as

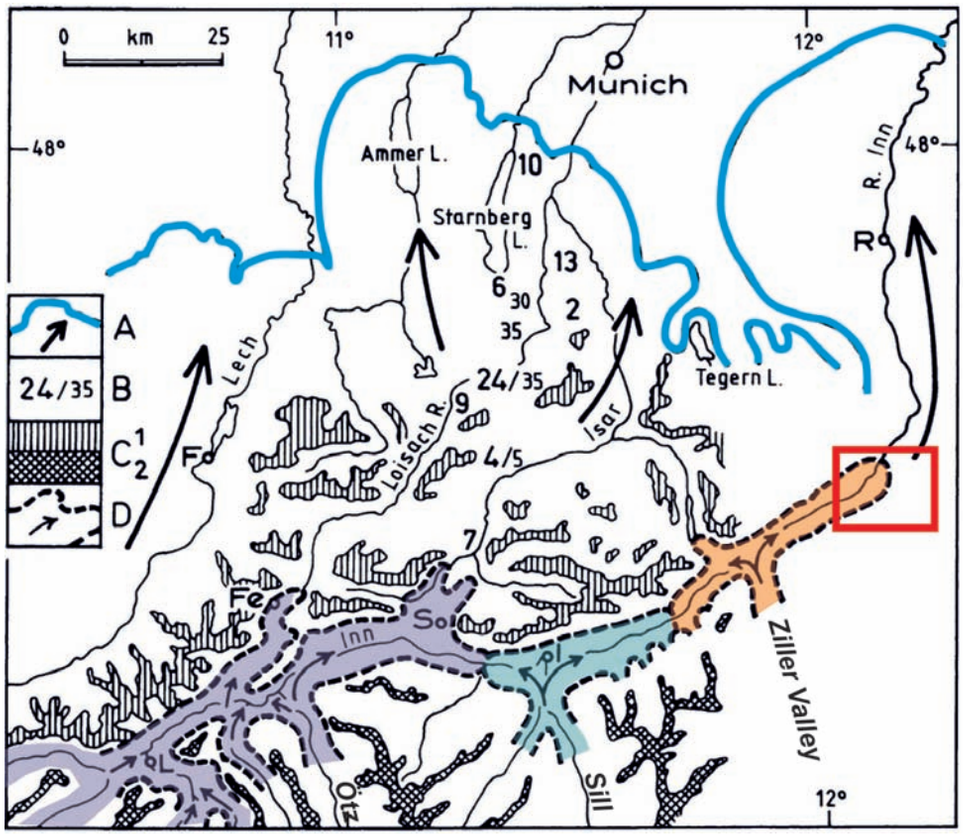

Fig. 9: Sketch modified after VAN HUSEN (2000): Ice streams of the Inn, Lech, Isar and Loisach Valleys. (A) Glacier extent during the Würmian Pleniglacial (LGM, MIS 2). (B) Percentage of crystalline boulders. Small numbers in proglacial sediments. Larger numbers in basal till. (C) Nunataks formed of sedimentary rocks (C1) and crystalline rocks (C2). (D) Probable ice extent in the Inn Valley around the beginning of the final ice build-up during MIS 2 showing a situation with multiple ice congestions. F: Füssen, Fe: Fernpass, I: Innsbruck, L: Landeck, R: Rosenheim, S: Seefeld.

Abb. 9: Skizze aus VAN HUSEN (2000) leicht modifiziert: Die Eisströme des Inn-, Lech-, Isar- und Loisachtales. (A) Gletscherausdehung während des Würm-Hochglazials (LGM, MIS 2). (B) Prozentgehalt von Kristallinklasten. Kleine Zahlen in Vorstoßschotter. Große Zahlen in Grundmoräne. (C) Nunataks bestehend aus Sedimentgestein (C1) und Kristallingestein (C2). (D) Wahrscheinliche Gletscherausdehnung im Inntal am Beginn der finalen Vorstoßphase mit der Darstellung von vielfachen Eisstausituationen. F: Füssen, Fe: Fernpass, I: Innsbruck, L: Landeck, R: Rosenheim, S: Seefeld.

tectonically subsided deposits possibly of Tertiary age. The overdeepening hints towards an ice-flow pattern different from that of the LGM. Based on the model of REITNER et al. (2010) higher elevated ice-transfluence passes existed during older glaciations which were re-activated during the respective phase of ice build-up. Such situations might have enabled a longer phase of unimpeded ice flow along the Brixen Valley and thus more efficient subglacial erosion.

Fig. 10: (a) Up to 10 m high outcrop at Stop 2 at 810 m a.s.l. with horizontally bedded gravel of the topset of a higher kame terrace overlain by a basal till of the Lateglacial glacier advance to the LMP (orange triangles). (b) Outcrop on the orographic left flank of the Ziegelhüttgraben (approximately 250 m NE of Stop 2) at 820 m a.s.l. showing a thick diamict sequence including the basal till of the LMP on top of horizontally stratified topset beds (section SE of Farmhouse Daxer in Fig. 12). Image provided by D. VAN HUSEN.

Abb. 10: (a) Ein bis zu 10 m hoher Aufschluss bei Stopp 2 in 810 m ü. NN zeigt horizontal gelagerte Kiese des Topsets einer höheren Kame-Terrasse, die von der Grundmoräne des spätglazialen Gletschervorstoßes zur spätglazialen Maximalposition (LMP) überlagert sind. (b) Der Aufschluss an der orographisch linken Flanke des Ziegelhüttgrabens (ca. 250 m nordöstlich von Stopp 2) in 820 m ü. NN zeigt eine mächtige Diamikt-Sequenz einschließlich der LMP-Grundmoräne über horizontal geschichteten Topset-Lagen (die Situation entspricht dem Profil südöstlich des Bauernhauses Daxer in Abb. 12). Foto: D. VAN HUSEN.

3.3 Stop 2: Vorderwindau

Location: 2.2 km SSW of the village of Westendorf at 820 m a.s.l. on the road to the hamlet of Rettenbach
(GPS: WGS84, 47°24'46'' N, 12°12'21'' E, 830 m a.s.l)

Topics: kame terrace overlain by local Lateglacial till, glacier dynamics during the phase of ice-decay

The outcrops show basal till on top of the horizontally bedded gravelly topset beds of kame terrace deposits. This terrace can be traced from Rettenbach to Vorderwindau and is

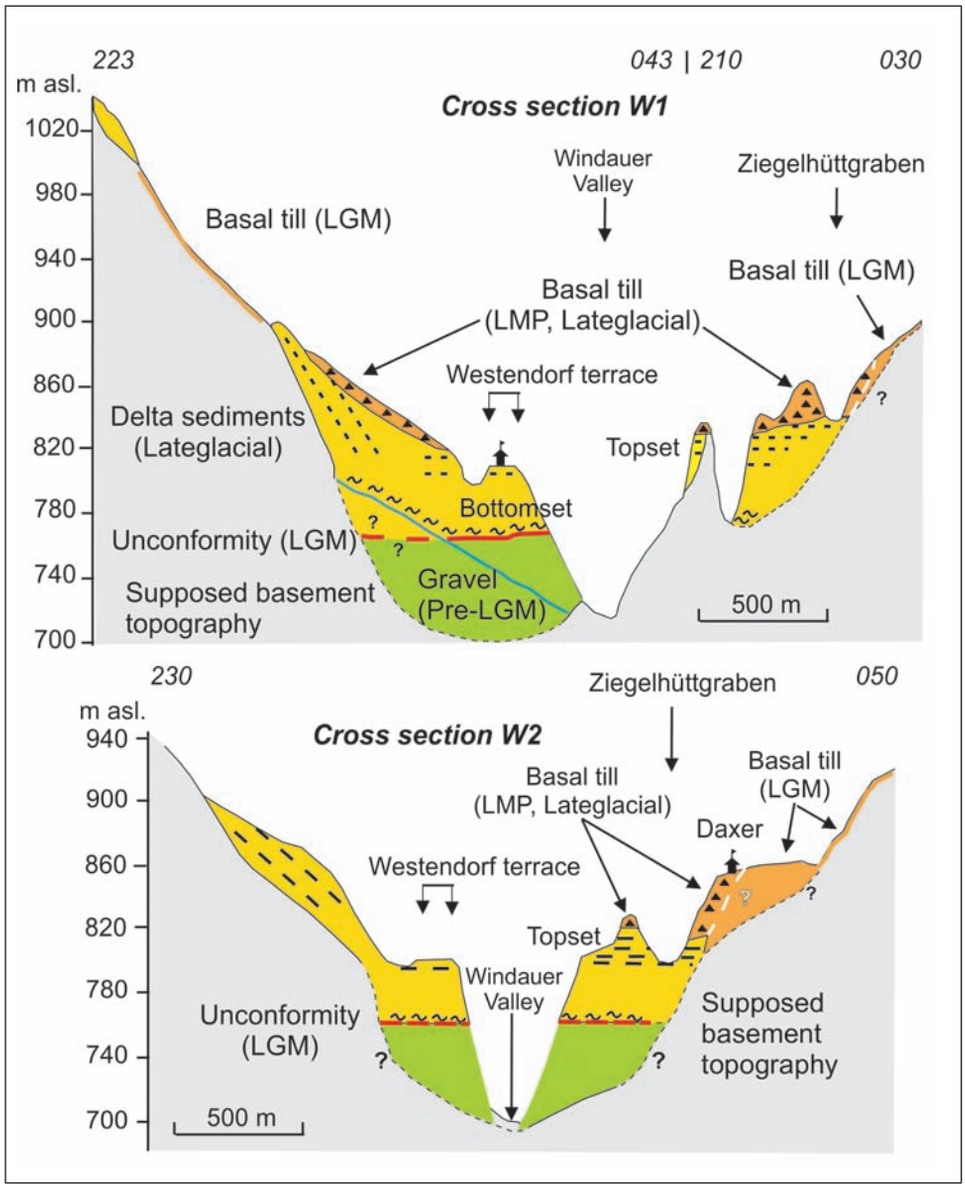

Fig. 11: Geological cross sections W1 and W2 in the Windau Valley (after Reitner 2007, locations see Fig. 6).

Abb. 11: Geologische Querschnitte W1 und W2 im Windautal (aus Reitner 2007, Lage s. Abb. 6).

the most striking feature of the Windau Valley (Fig. 6). The most complete lithostratigraphic section can be found on top of the pre-LGM braided river gravels (unit A) along the Ziegelhüttgraben around Vorderwindau (Figs. 11 & 12) south of the farmhouse Daxer (location H in Fig. 6a). The coarsening-upward sequence is interpreted as a Gilbert-delta succession. It comprises a fine-grained bottomset followed by the foreset indicated by clinoforms and finally by the horizontally-bedded topset. With the exception of very rare but significant occurrences of red sandstone (PSK), all clasts of the described succession are of local origin. Finally, an overconsolidated massive and matrix-supported diamict (Dmm) containing striated clasts, a typical basal till, conformably overlies the coarsening-upward sequence (Fig. 12). This grey-coloured diamict exhibits the same lithological characteristics as the sediments below but also contains rare clasts of "Zentralgneis". This diamict cover, which can be traced from Rettenbach to Vorderwindau (Fig. 6), has an average thickness of around 2 m. However, in the Ziegelhüttgraben SE of Daxer this diamict is 20 m thick and contains shear planes ([Dmm(s)]. This subglacial sediment was deposited by Windau Glacier as can be deduced by the dominance of clasts from the GWZ. Thus, this till indicates during ice decay, a glacial advance of 3 km distance from Rettenbach in the direction of Vorderwindau towards the Lateglacial maximum position (LMP) of Windau Glacier (Fig. 6). In general, evidence which helps to constrain glacier geometry during its LMP is rare. Even at the most terminal position at Ziegelhüttgraben S of Daxer morphological as well as sedimentological evidence of a terminal moraine is missing.

As the Westendorf terrace level, the local morphostratigraphic reference level, is cut into the described delta till sequence (s. Fig 11). The glacier advance towards the LMP occurred before the formation of this terrace level developed.

3.4 Glacial dynamics in the Hopfgarten Basin and stratigraphic implications (after Reitner, 2007)

The highest kame terrace relicts deposited in small ice-marginal niches by local creeks provide the first evidence of ice decay in the Hopfgarten Basin. They indicate the existence of a relict network of valley glaciers in the basin which had lost ~1000 m of ice thickness since the LGM (Fig. 13a). These sediments, which occur at different levels, show that the tongue of the Inn Glacier was stagnant at that time. It is

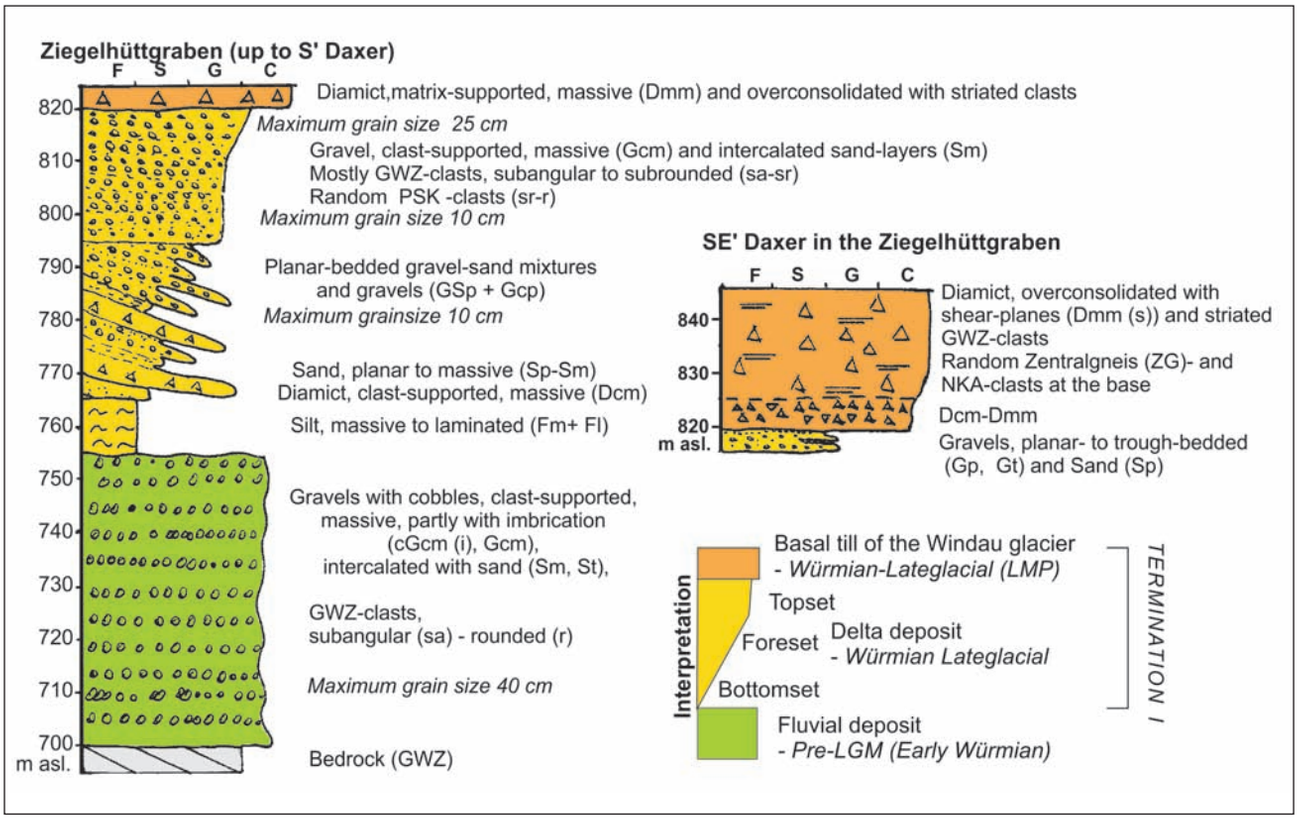

Fig. 12: Sections along and in the Ziegelhüttgraben. The Farmhouse Daxer is location H in Fig. 6a.

Abb. 12: Geologische Profile entlang und im Ziegelhüttgraben. Das Bauernhaus Daxer entspricht der Lokalität H in Abb. 6a.

likely that ice from the Kelchsau and Windau Valleys was still in contact with the stagnant Inn Glacier.

In the course of further ice decay a separation of the local glaciers occurred which finally resulted in a terminus position of Windau Glacier around Rettenbach and that of Kelchsau Glacier in the area of Kelchsau (Fig. 13b). Ice-dammed lakes formed between the two local valley glaciers and the remaining stagnant Inn Glacier in the area of Hopfgarten. It is supposed that the infill of the proglacial water bodies by Gilbert-type deltas took place over a short time period, as there was plenty of erodible material (e.g. till) and abundant meltwater.

The Windau and Kelchsau Glaciers probably advanced for 3 km over their proglacial delta sequences towards their Lateglacial maximum positions (LMP; Fig. 19c) while the proglacial basins were filled up. The missing latero-frontal moraines indicate that the tongues did not reach glaciological equilibrium before they disintegrated following their LMP. At this time the ice transfluences from the Hohe Tauern via the high-elevation cols into the Windau and Kelchsau Valleys ceased. On the base of this general setting a crude calculation of the equilibrium-line altitude (ELA) required for the reconstructed glacier extent of the LMP and its starting position was performed. The results suggest that the ELA during LMP for Kelchsau Glacier was around 1500 m a.s.l. and slightly lower for Windau Glacier. However, their positions prior to the advance at Kelchsau and Rettenbach correspond to ELAs of around 1600 m a.s.l. It has to be stressed that the geometry of the accumulation areas in both valleys was probably determined by the remnants of LGM ice. It has to be considered that "allochthonous" ice (from the Hohe Tauern) was discharged until these transfluences were cut off. Thus, the accumulation area could have been larger and the glacier in general thicker than if only local ice had filled the valley. Such a setting was more sensitive to a small lowering of the ELA. The ELA calculation suggests that an ELA lowering of at least 100 m occurred during ice decay, which resulted in the LMP.

However, the glaciers held their LMP only for a short time period before their fronts retreated up-valley to at least the positions they had before they advanced towards their LMPs (Fig. 19d). This is especially evident for Windau Glacier, as the Westendorf terrace level formed by erosion extends close to Rettenbach. Thus, it is assumed that a rapid collapse of the tongues occurred, since no indications of a stabilisation of an actively receding tongue are found upvalley from the LMP.

This collapse took place while the stagnant Inn Glacier tongue with its ice front in the area west of Itter blocked the meltwater of the entire Brixentaler Ache and its tributaries towards the Inn Valley for the last time. Finally, a lake was filled up in the ice-free area by Gilbert- and Hjulstöm-type deltas, depending on the water depth in the course of delta-front progradation (Postma 1990). Buried dead ice bodies, documented by kettle holes and sediment structures (e.g. climbing ripples) indicate high sediment loads of the rivers and thus a rapid sedimentation process. However, comparing the elevations of the topset at Itter with that of the bottomsets in the upstream areas, the lake level must have dropped during sediment fill as the blocking Inn Glacier melted down to a position west of Itter (702 m a.s.l.; Fig. 19d). The latter indicates a final loss of ice thickness of about 1200 m compared

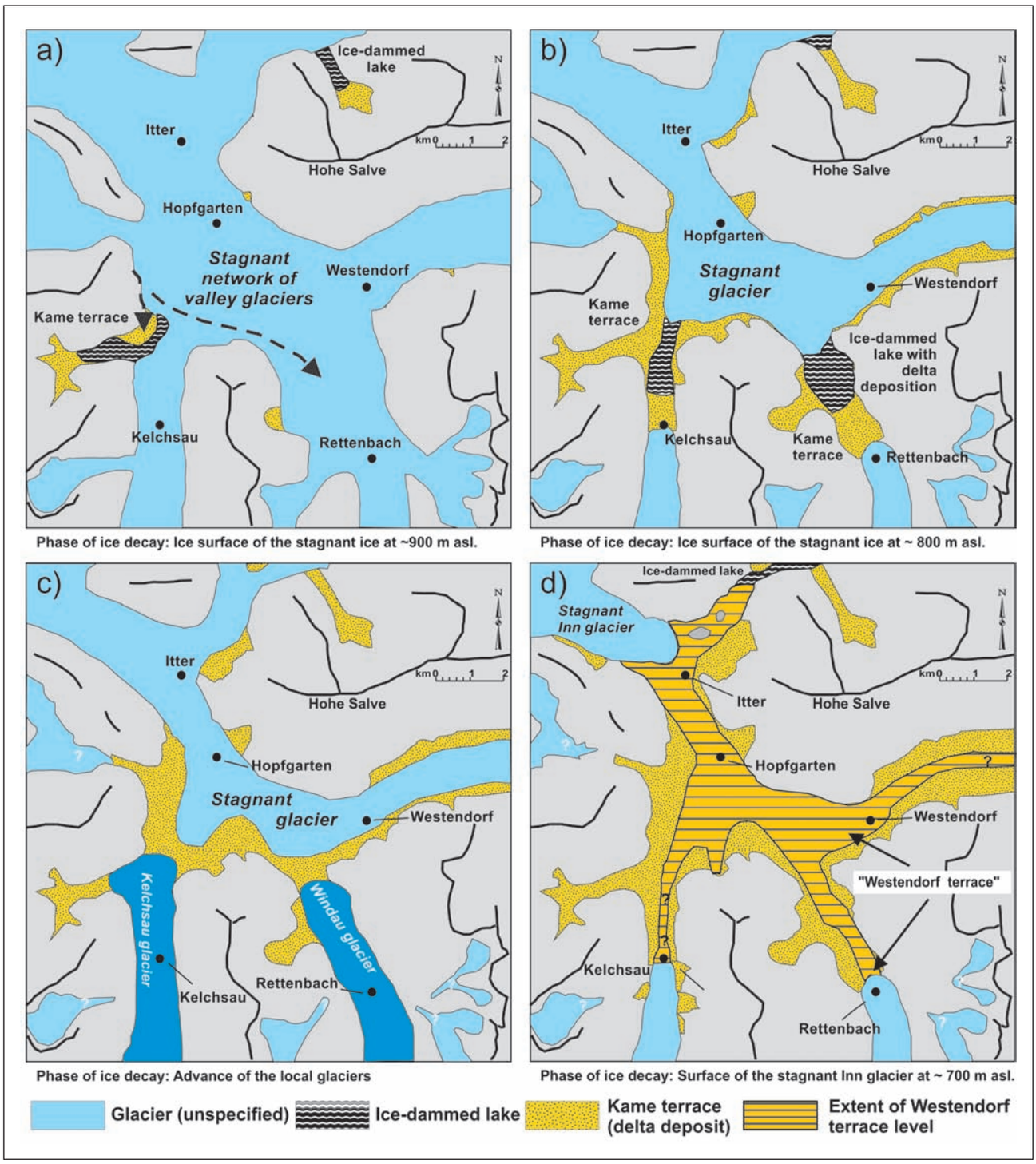

Fig. 13a-d: The reconstructed ice decay and the local glacier oscillations towards the LMP in the basin of Hopfgarten Basin (modified after Reitner 2007).

Abb. 13a-d: Die Rekonstruktion des Eiszerfalls und der Lokalgletscher-Oszillationen zur spätglazialen Maximalposition (LMP) im Becken von Hopfgarten (modifiziert nach Reitner 2007).

to the LGM ice surface (Fig. 5). With the establishment of the Westendorf terrace level between Itter and Rettenbach, as a result of accumulation and erosion, the infill of the deglaciated basin was completed (Fig. 19d). It also shows the setting of the modern drainage system in the Hopfgarten Basin. With continuing down-melting of the ice west of Itter, the base level was lowered resulting in the formation of erosional terraces below the level of the Westendorf terrace. Epigenetic valleys (see cross sections W1 and W2 in Fig. 13b) were formed as the rivers incised into the bedrock below the delta deposits and not into the pre-LGM valley fill. Their formation is regarded as the main reason for the preservation of this unique sedimentary archive.

In summary, the Windau and Kelchsau Glaciers showed an almost synchronous advance within an area which they had occupied during the LGM (Figs. 4 & 8). This advance occurred while the stagnant Inn Glacier experienced continuous down-wasting. The local glacier advances to their LMP during a phase of general ice decay can be regarded as climatically controlled glacier oscillations. Similar to mod-

ern glaciers (e.g. Menzies 1995a, Benn & Evans 1998), a relatively short-lasting climatic deterioration in the sense of lower temperature and/or more precipitation caused an ELA lowering of at least 100 m. The positive glacier mass balance resulted in a probably rapid advance of the small glaciers (e.g. length during LMP: Windau Glacier ~16 km; Kelchsau Glacier ~19 km). This reaction may have been favoured by the presence of former ice remnants within the accumulation areas (see above). In contrast, ice from the various Inn Glacier accumulation areas was supposedly still en route towards its tongue, when the climatic amelioration continued. Based on field evidence even the local glacier tongues did not reach a stable position in the sense of a glaciologically balanced equilibrium, providing a further argument for a short duration of this climatic phase. However, looking at the continuous loss of 200 m of ice thickness of the stagnant Inn ice from the first sedimentary evidence in the Hopfgarten Basin until the formation of the Westendorf terrace, these processes, we conclude, could have taken place within less than 100 years.

In comparison to the ice build-up phase at the beginning of the LGM there was no accelerating effect of ice congestion in the Inn Valley. The bulk of the ice in the Inn Valley was probably inactive and thus unavailable for this kind of ice dynamics, as is evident from the stepped kame terraces in the Inn Valley which appear to indicate a continuous collapse (Bobek 1935).

Based on the re-investigation of the type locality, the term "Bühl stadial", defined as the first halt of the Inn Glacier during its retreat (Penck & Brückner 1909, Mayr & Heuberger 1968), has been abandoned (Reitner 2005 & 2007). The sedimentary and morphological evidence indicates that the Inn Glacier as well as the other Eastern Alpine glaciers became stagnant in the large Alpine valleys followed by massive down-wasting. Hence, this period after the LGM, at the beginning of Termination I, (in other words the Würmian Lateglacial), is best defined as a phase of early Lateglacial ice decay. Only the separated glaciers showed mostly climatically-controlled (e.g. Windau Glacier in the Hopfgarten Basin) but also ice mechanically-induced advances (e.g. Wilder Kaiser) towards their Lateglacial maximum positions (LMP). Furthermore, in most cases no terminal moraines were produced during the LMP that could serve as evidence of glacier tongues in equilibrium with the climate at that time. This is also true for the oscillation of the Gschnitz-(Valley)-Glacier near Steinach am Brenner, which was designated as the "Steinach stadial" (Mayr & Heuberger 1968) and is now also included in the phase of ice-decay (Reitner 2005, & 2006, Ivy-Ochs et al. 2006). Due to the variety of glacial, glaciolacustrine and glaciofluvial processes the term stadial, which was mostly based on the interpretation of morphological features, appears inappropriate for this period of ice decay and the term "phase of ice-decay" ("Eiszerfallsphase" in German) is already applied for such sediments in Austrian geological map sheets (e.g. Lienz ÖK 179, Linner et al. 2013).

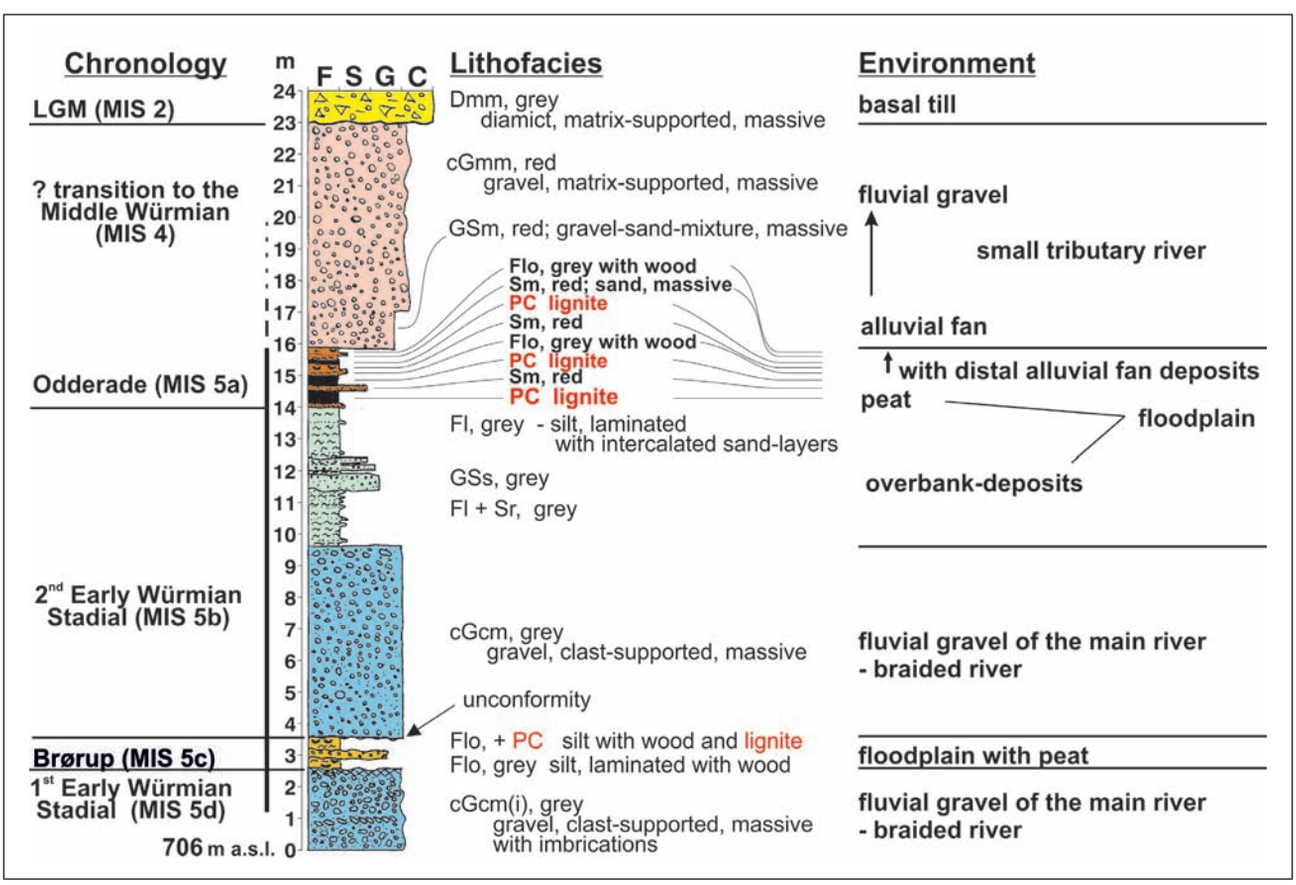

Fig. 14: The sedimentary succession of the profile E Klösterl (Stop 3) in the valley of Schönbach with a chronostratigraphic correlation of the sedimentary units (after Reitner 2005).

Abb. 14: Die sedimentäre Abfolge im Profil östlich von Klösterl (Stop 3) im Tal des Schönbaches mit einer chronostratigraphischen Korrelation der sedimentären Einheiten (nach Reitner 2005).

Fig. 15: Panoramic view from Hennersberg (Stop 4, south of the city of Wörgl) across the Inn Valley towards NW. The Unterangerberg terrace, as well as the steep southern rim of the Northern Calcareous Alps (NCA) with the prominent niches of two rock-slides (Butterbichl and Mariastein) are evident.

Abb. 15: Panoramablick vom Hennersberg (Stopp 4, südlich oberhalb von Wörgl) über das Inntal nach Nordwesten auf die Mittelgebirgs-Terrasse des Unterangerberges. Dahinter sieht man den Steilabfall des Kalkalpen-Südrandes mit den markanten Ausbruchsnischen der beiden Felsgleitungen von Butterbichl und Mariastein.

3.5 Stop 3: Schönbach Valley

Location: creek E of farmhouse Klösterl
(GPS: WGS84, 47°26'30.7'' N, 12°08'35.9'' E, 708 m a.s.l)

Topic: Early Würmian fluvial sediments & lignite

The profile E of Klösterl is the most complete profile below the LGM till (Fig. 14). It shows a depositional environment at the margin of aneinner Alpine alluvial plain formed by a precursor of the river Kelchsau Ache. It is situated in 700 to 730 m a.s.l. and thus 100 to 130 m above the modern valley floor of the Brixentaler Ache. The profile begins with horizontally bedded sandy gravels (Gcm, Gcm (i)) at least 10 m thick and consisting only of local clast lithologies (Fig. 14). This braided-river deposit is overlain by two thin silt layers with wood fragments and compressed peat. The pollen content (Reitner & Draxler 2002) shows a woody vegetation with dominance of spruce (*Picea*) and a high content of fir (*Abies*) as well as a significant presence of beech (*Fagus*). These findings pinpoint the 1st Early Würmian Interstadial (in the sense of the Brørup-Interstadial, MIS 5c). The following 6 m-thick gravels in the same facies as before are superimposed by a grey sand-silt succession which shows a transition to laminated silt. This pollen-free fine-sediment succession is interpreted as overbank sediments. The top of this consists of compressed peat (lignite), partly rich in wood. The vegetation is characterised by a *Picea* and *Pinus* (pine) dominated forest with a low but continuous presence of *Abies*. The sedimentary sequence in combination with the palynological results allows a correlation with the 2nd Early Würmian Interstadial (in the sense of Odderade, MIS 5a). As the peat layer shows increasing amounts of intercalated red sand up section (Fig. 14) a growing influence of a tributary river draining a catchment of red sandstone is documented. This finally led to red gravel-sand mixtures of an alluvial fan and probably marks the transition from the 2nd Early Würmian Interstadial (MIS 5a) to the generally colder Middle Würmian (MIS 4). According to the previous palynostratigraphic correlations, the thick gravel layers below and between the lignites represent the cold 1st and 2nd Würmian Stadials (MIS 5d and 5b). The pollen-free overbank deposits associated with the gravel record a treeless environment during MIS 5b. Thus, the braided-river deposition reflects a climatic deterioration resulting in considerable aggradation, whereas interstadial conditions were characterised by overbank deposition and formation of peat took place in the backwater of partly prograding alluvial fans.

4 Excursion part II: Geological mass movements and the pre-LGM to LGM sedimentary record of the Unterangerberg terrace

4.1 Stop 4: Overview at Hennersberg, Wörgl

(GPS: WGS84, 47°28'32'' N, 12°04'11'' E, 674 m a.s.l.)

This panoramic view point provides an overview of the geology and morphology of the lower Inn Valley.

The most prominent feature is the so-called Unterangerberg terrace on the opposite valley flank of the Inn River reaching up to 230 m above the modern valley floor (Figs. 15 & 16). The smooth surface indicates a subglacial shaping during the LGM, when the ice surface of the Inn Glacier was at approximately 1900 m a.s.l. (van Husen 1987). The same is true for the steep cliffs made up of Triassic carbonate rocks north of this terrace which also show abraded surfaces. In addition, two prominent niches are discernable within these cliffs which are scarps of the rock-slides of Butterbichl in the West and Mariastein in the East. Corresponding to the subglacially shaping the surface terrace consists of the LGM basal till, which shows text-book examples of drumlins (Figs. 16 & 21), corresponds to the overall subglacial overprint of the Unterangerberg terrace.

Geological field evidence (Figs. 18 & 22) shows that the base of the terrace is formed by marine fine-grained sediments (Unterangerberg Formation) but also by conglomerates of fluvial origin (Oberangerberg Formation) of Upper Oligocene age (e.g. Ampferer 1922, Ortner 1996 & 2003a, Ortner & Stingl 2001). They are overlain by Pleistocene sediments first described by Penck & Brückner (1909), and later by Klebelsberg (1935), Heissel (1951, 1955) and Gruber et al. (2009). The pre-LGM Pleistocene sediment sequence comprises two cataclastic rock-slide deposits – Butterbichl and Mariastein –, embedded in the Pleistocene sediments (Figs. 18 & 22). These cataclastic carbonate rock units

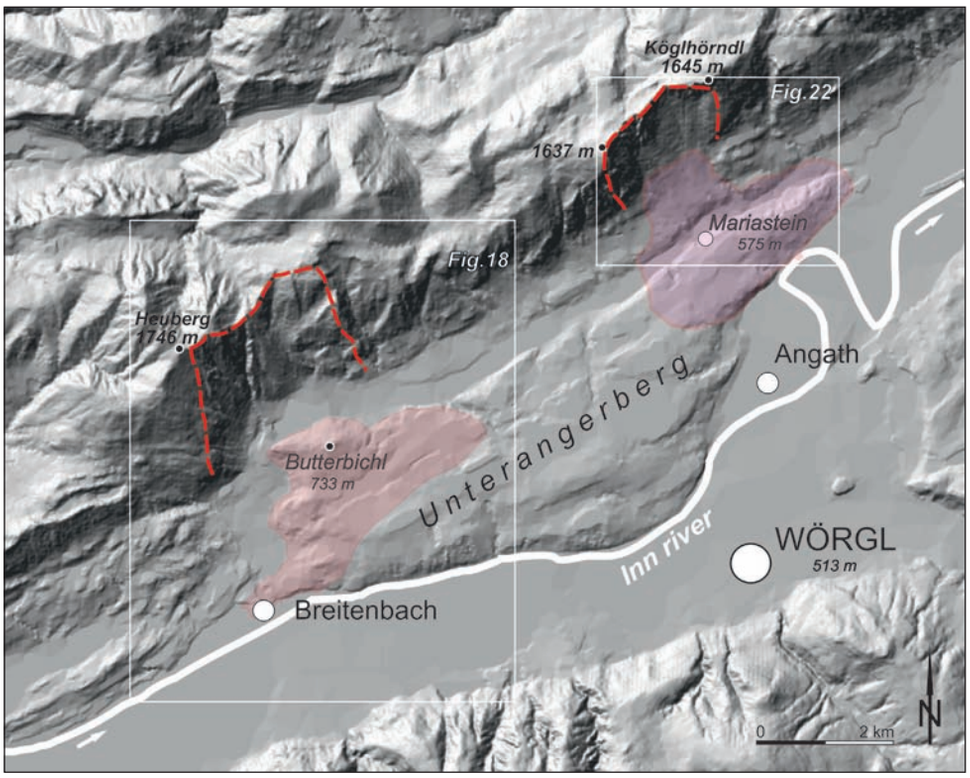

Fig. 16: Digital elevation model of the Unterangerberg terrace and surroundings with the position of the two rock-slide scarps and their rock-slide deposits.

Abb. 16: Das digitale Höhenmodell der Unterangerberg-Terrasse und ihrer Umgebung zeigt die Lage der beiden Felsgleitungen von Butterbichl und Mariastein. Farblich gekennzeichnet sind die Ausbruchsnischen und Ablagerungsbereiche.

were previously interpreted as remnants of tectonic nappes (e.g. Ampferer 1921, & 1922) or as part of the Inn Valley fault shear zone (Ortner 1996, & 2003b). The true nature of these phenomena was first assumed by Penck & Brückner (1909 for Mariastein) and by Heissel (1951, & 1955 for Butterbichl). Between 1995 and 2006, geophysical investigations and numerous drillings (Fig. 22) were performed on the Unterangerberg terrace under the supervision of the "Brenner Eisenbahn Gesellschaft" (BEG) as part of a tunnel prospection campaign (Köhler & Poscher 2007, Poscher et al. 2008, Spitzer 2005). Independently, geological mapping of the Geological Survey of Austria was performed. The combined efforts resulted in a geological model of the Butterbichl rock-slide (Gruber et al. 2009) and a first characterisation of the Mariastein rock-slide (Gruber 2009). Additional geotechnical and mineralogical investigations of the Butterbichl rock-slide were performed by Strauhal (2009). Finally Starnberger et al. (2013) provided a chronological and palaeoenvironmental analysis of the Pleistocene sediments based on ^{14}C and luminescence dating and palynological analyses.

The Riss glaciation (MIS 6) resulted in the formation of two parallel overdeepened troughs separated by a narrow bedrock ridge of Oligocene rocks (Gruber et al. 2009), one located in today's Inn Valley and the other one north of it, just below the cliffs. The latter reaches down to a minimum of 60 m below the modern floor of the Inn Valley as indicated by geophysical data.

Towards the end of the penultimate glaciation (Rissian, MIS 6) this depression was filled by a lake. The corresponding lacustrine sediments were overridden by the rock-slides descending from the mountain flank (Figs. 17 & 18), quasi-synchronously during MIS 5d (Starnberger et al. 2013). These events resulted in a new geometry with a now much smaller lake between these two gravitational deposits. It was separated from the sediment input of the palaeo Inn River due to the above mentioned bedrock ridge. This lake fill started with organic-rich deposits including peat and paleosols of the 2nd Early Würmian Interstadial (MIS 5a) indicating a local vegetation characterised by a boreal forest dominated by spruce (*Picea*), with few thermophilous elements (Starnberger et al. 2013). The subsequent collapse of the vegetation dated to 70–60 ka (i.e. MIS 4) is indicated by very low pollen concentrations which document the potential presence of permafrost. Accordingly, this reduction in vegetation cover is mirrored by a transition from fine-grained lacustrine sediments to diamicts of debris-flow origin. Climatic conditions improved again between 55 and 45 ka (MIS 3) and cold-adapted trees re-appeared during interstadials, forming an open-forest vegetation. MIS 3 stadials were shorter and less severe than the MIS 4 at Unterangerberg, and vegetation during these cold phases was mainly composed of shrubs, herbs and grasses, similar to what is known from today's Alpine timberline. The Unterangerberg lacustrine record ended at ca. 45 ka and, following an erosional unconformity, is topped by coarse-grained fluvial deposits. Their clast lithology documents the re-integration of this small basin into the depositional system of the Inn River due to a strong fluvial aggradation phase in the MIS 3. This is a result of climatic deterioration prior to the onset of the LGM.

4.2 Stop 5: Breitenbach, Moos/Grünbichl

(GPS: WGS84, 47°29'23'' N, 11°58'45'' E, 593 m a.s.l.)

Topic: the Butterbichl rock-slide and its dynamics

The Butterbichl rock-slide deposit covers about 5 km^2 on the sout-western part of the Unterangerberg terrace (Figs.

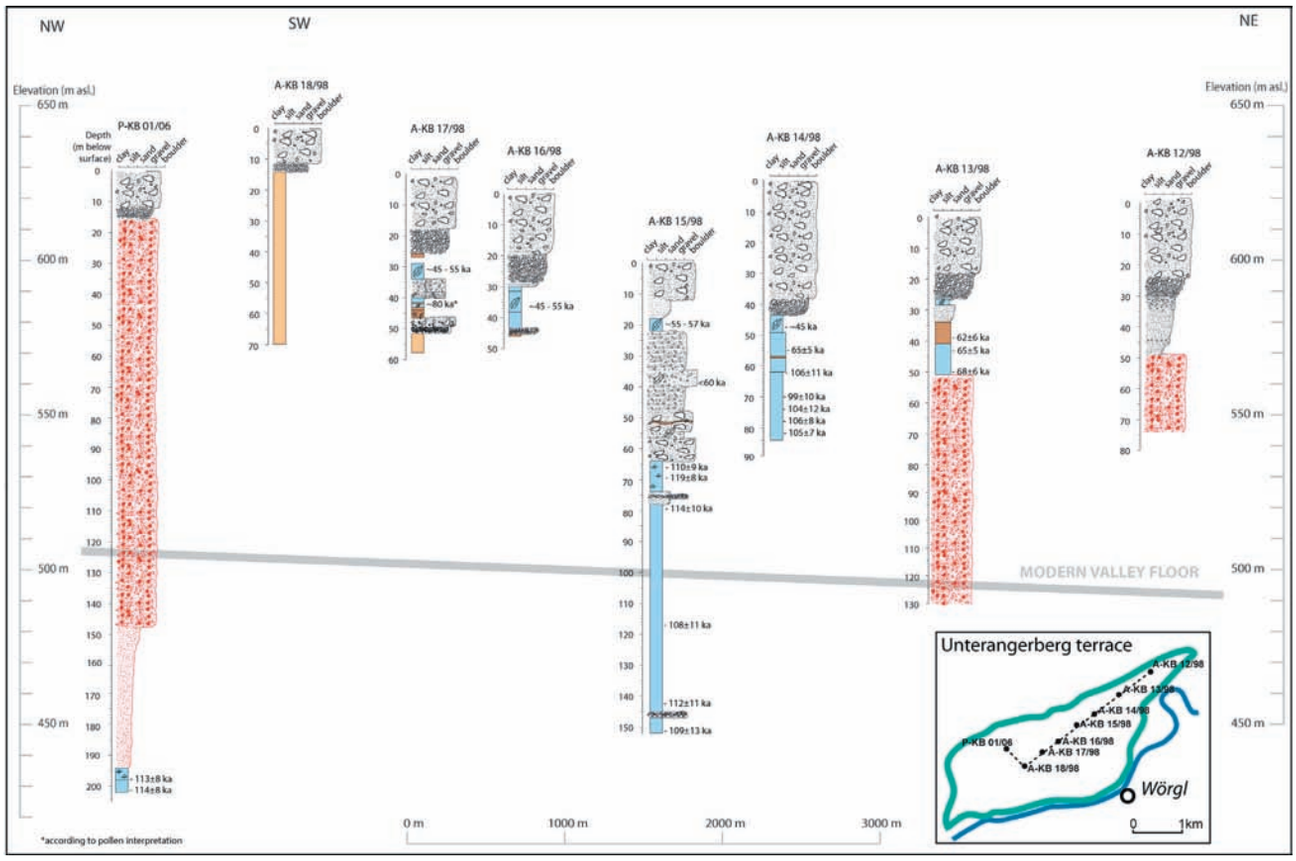

Fig. 17: Schematic overview of drill cores along a NE-SW-NW section across the Unterangerberg terrace, with core lithologies and radiocarbon and luminescence dates (after Starnberger et al. 2013).

Abb. 17: Schematische Darstellung von Bohrprofilen entlang eines Nordost-Südwest-Nordwest Querschnittes über den Unterangerberg. In den Profilen sind die Lithologien und Radiokarbon- und Lumineszenz-Alter ersichtlich (nach Starnberger et al. 2013).

16 & 18a). According to the scarp area, the niche southeast of Heuberg (1746 m a.s.l.), the estimated volume of the collapsed rock mass is ca 300 x 10^6 m^3 (Gruber et al. 2009). The scarp area is made of a stratigraphic succession of Middle and Upper Triassic limestones, dolostones, sandstones and siltstones. This sequence starts with the Wetterstein Fm., dm-bedded, light greyish limestones and dolostones. It is followed by the Raibl Group, a succession of dolostones and fine-grained siliciclastic rocks, which show a transition towards monotonic grey laminated dolostones of the Hauptdolomit. These Triassic strata are overlain unconformably by synorogenic deposits composed of colourful alternating siliciclastic and fossiliferous carbonate rocks, the Gosau Group. This rock sequence was folded during the Alpine orogeny (Lower Cretaceous to Miocene). Especially the dolostones of the Raibl Group were intensively fractured and hence, can be characterised as cataclastic rocks. The main tectonic structure of the cliff is a large anticline (Guffert-Pendling anticline), strongly segmented by SW-NE and S-N trending strike slip faults with sinistral lateral displacement and overthrusts with a movement of the hanging wall towards the North. The scarp evolved in the hinge of this anticline and the slide plain is located on the steep southeast-dipping limb (Figs. 18b & 19). This dip-slip situation enabled a slope failure which can be characterised mainly as a rock-slide. This is shown by the drilling P-KB 01/06 close to the scarp, where the rock succession mirrors the lithology of the source area. However, an analysis of the fragmentation pattern shows differences according to rock mechanic properties, which are especially the brittleness and the inherited tectonic deformation. For example, the limestone and thicker-bedded dolostones are less fragmented, whereas the catalastic rocks of the Raibl Group were fragmented to sand-sized angular grains. This 50 m-thick basal sandy segment of the rock-slide overlies glaciolacustrine sediments dated to 122–105 ka (Starnberger et al. 2013).

The spectacular outcrop of Moos (Fig. 20) provides the opportunity to study not only the grade of fragmentation but also geometricaly aspects of the deformed rock-slide mass. Different categories of rock fragmentation and transitions are evident. The grain sizes of the deposit range from cobble-sized to sand, all showing (very) angular shapes. The alternation of laminated dolostone with thin-layered claystone suggests rocks of the Raibl Group. Occasionally rotated clasts of red silt- to sandstone resemble former infills of fissures during the sedimentation of the Gosau Group. Two kinds of deformation structures are present: present: Overturned shear folds verging towards SW, cuspate-and lobate folds indicating differing mechanical competence.

In contrast to the findings of the drilling P-KB 01/06, where an en-bloc movement is plausible according to the preserved stratigraphy, we suggest that in this more distal part of the rapid mass movement, a higher amount of dynamic fragmentation occurred in the sense of McSaveney & Davies (2006). This process may have resulted in a more sturzstrom (rock avalanche)-like flow. However, we have to

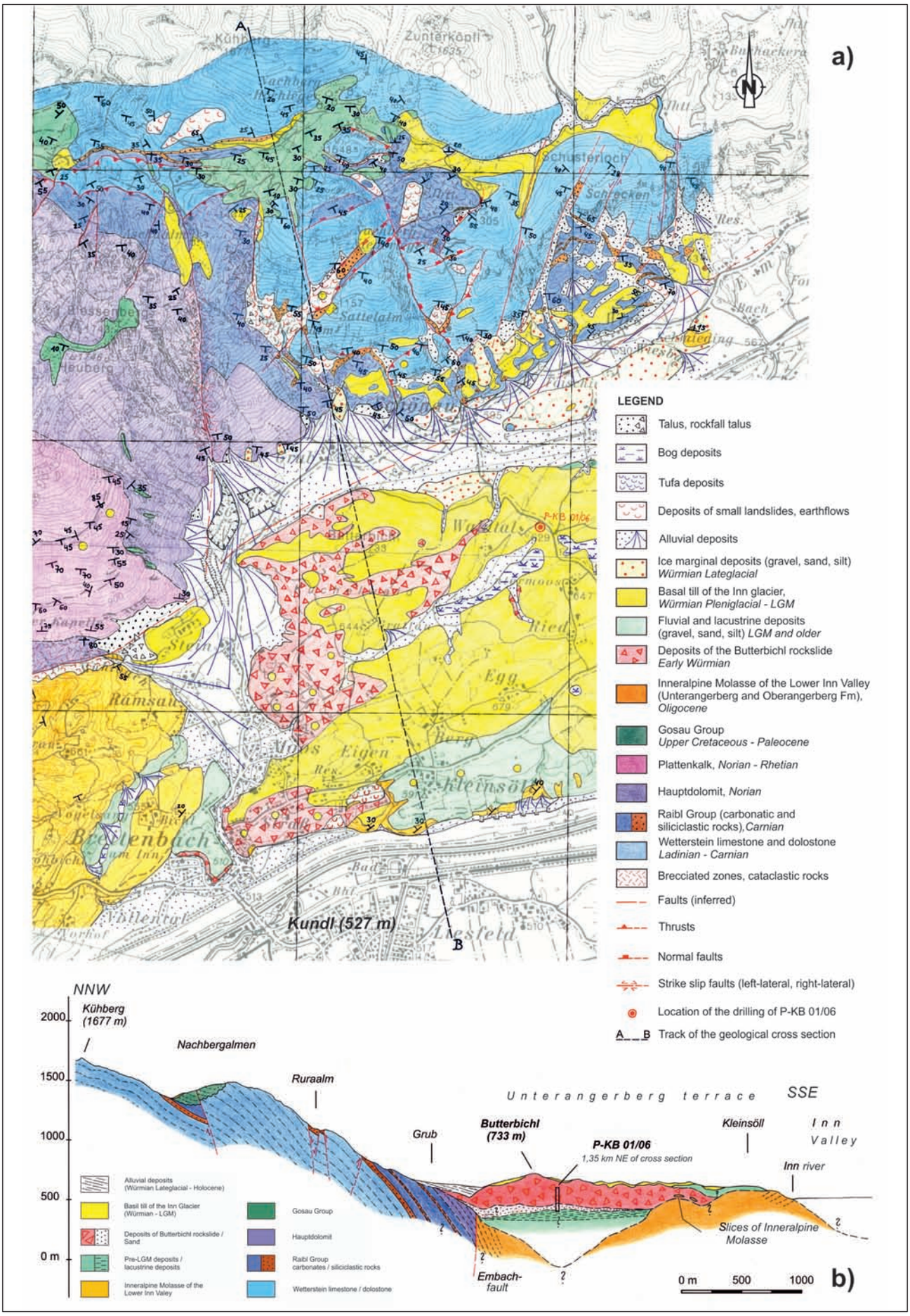

Fig. 18: (a) Geological map of Butterbichl rock-slide area and (b) geological cross section after Gruber et al. (2009).

Abb. 18: (a) Geologische Karte der Butterbichl-Felsgleitung und ihrer näheren Umgebung, mit (b) einem geologischen Profilschnitt, nach Gruber et al. (2009).

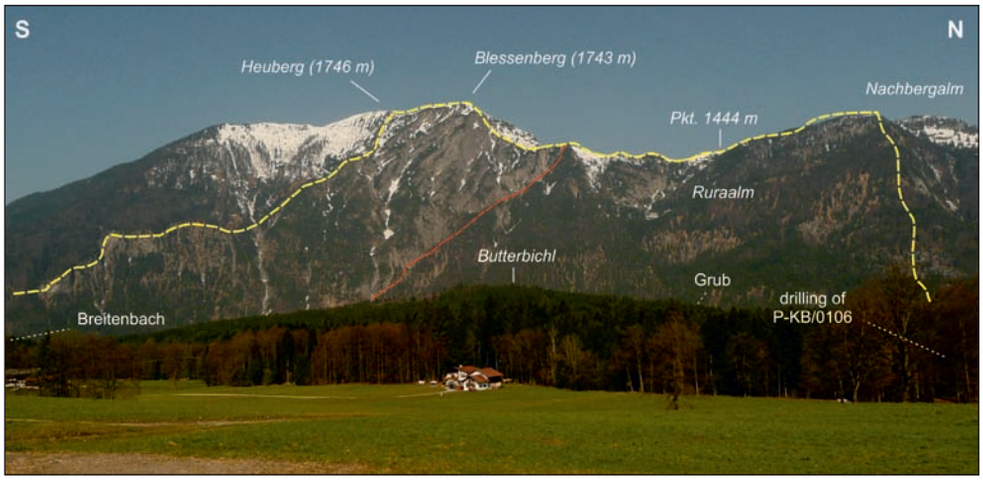

Fig. 19: Reconstructed scarp (yellow dashed lines) of the Butterbichl rock-slide viewed from SE. Note the big N-S-striking E-dipping fault-zone (red dashed lines) in the central part of the image which represents the western scarp of the rock-slide.

Abb. 19: Rekonstruierte Ausbruchsnische (gelb) der Butterbichl-Felsgleitung von Südosten (Egg/Unterangerberg) betrachtet. In der Bildmitte (in Rot) die große N-S-streichende, steil E-fallende Störungszone, die die westliche Abrissfläche der Felsgleitung bildet.

consider that any corresponding palaeo-morphology was abraded by the following glaciation (LGM).

4.3 Stop 6: Egg

(GPS: WGS84, 47°29'21'' N, 12°00'13'' E, 639 m a.s.l.)

The drumlin of Egg (679 m a.s.l.) has the classical appearance of such a landform i.e. a smooth, streamlined hill that resembles an egg half-buried along its major axis with a steeper stoss-side pointing upstream and a more gentle sloping end facing downstream (see Menzies 1979, Clark et al. 2009). The drumlin of Egg (Fig. 21), with a length of around 1 km running WSW–ENE, i.e. parallel to this part of the Lower Inn Valley, is the largest of the drumlin field of the Unterangerberg terrace, which is completely covered by basal till. Drillings performed between the drumlins show that the basal till is underlain by older (glacio-) lacustrine, gravitational and fluvial sediments ranging from the decay of the penultimate glaciation (Termination II) to the LGM. Lateral erosion of the Inn River has made sections through parts of drumlins visible wheren up to 20 m of till can be seen. The drumlin field of the Unterangerberg terrace is consistent with other inner Alpine occurrences in the Eastern Alps in that these subglacial forms occur where valleys broaden with indications of diffluent ice-flow trajectories.

4.4 Stop 7: Mariastein

(GPS: WGS84, 47°31'35'' N, 12°03'09'' E, 557 m a.s.l.)

In analogy to the Butterbichl rock-slide, this second mass movement originated in the southern limb of the E-W-striking Guffert-Pendling anticline. In this case it consists of well bedded lagoonal Wetterstein limestone (Fig. 22). The prominent rock-slide niche (Fig. 23) is located between the peaks of Hundsalmjoch (1637 m a.s.l.) and Köglhörndl (1645 m a.s.l.). The scarp developed approximately in the hinge-zone of the anticline (Fig. 22). As in the case of Butterbichl, the western limit of the niche is defined by a N-S running strike slip fault with sinistral displacement. The 40° southward dipping bedding planes of the Wetterstein limestone conditioned a dip-slope situation which finally generated the sliding plane. Relics of this failure plane are still visible below partly ce-

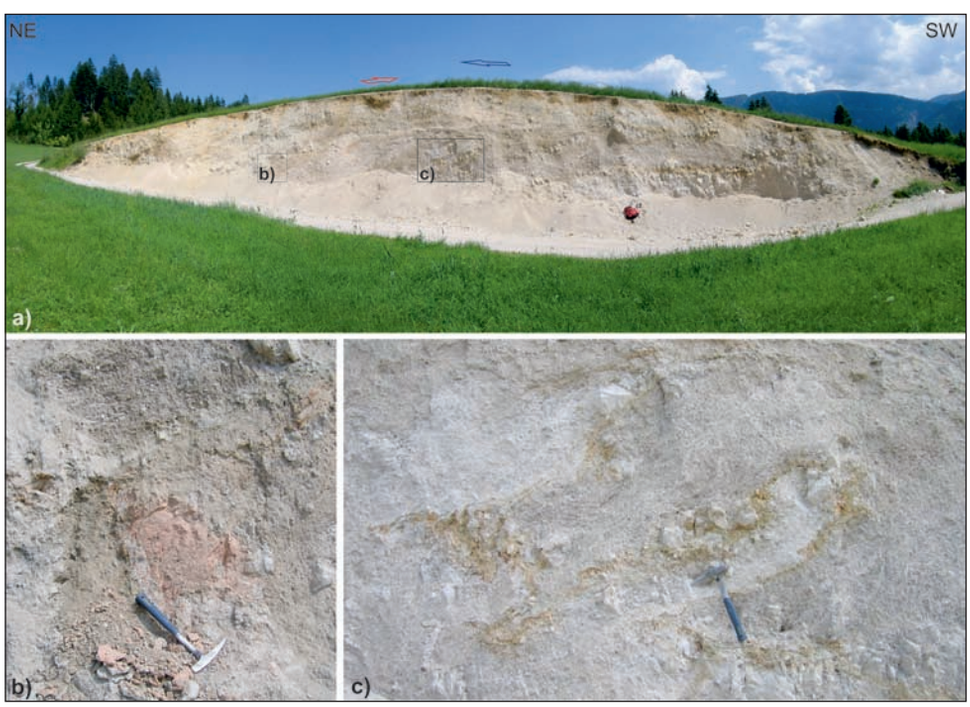

Fig. 20: (a) Outcrop of the Butterbichl rock-slide deposit at Moos (Stop 5). The direction of rock-slide movement (red arrow, S to SSW) and of later ice flow during the LGM (blue arrow, NE) resulted in a smooth topography. (b) Detail of (a) with rotated red clast of the Gosau Group within strongly fragmented carbonate rocks of the Raibl Group. Note the angularity of dolostone clasts. (c) Detail of (a) with shear zones and folds.

Abb. 20: (a) Aufschluss in den Ablagerungen der Butterbichl-Felsgleitung bei Moos (Stop 5). Der rote Pfeil zeigt die Richtung der Massenbewegung (S bis SSW), der blaue Pfeil die nachfolgende glättende Überformung durch den Gletscher während des LGM (NE) an. (b) Detail aus Abb. (a) mit rotiertem roten Klast der Gosau-Sedimente innerhalb der stark fragmentierten Karbonate der Raibler Schichten. Man beachte die Angularität der Dolomitklasten. (c) Detailausschnitt aus (a) mit Scherzonen und Faltenstrukturen.

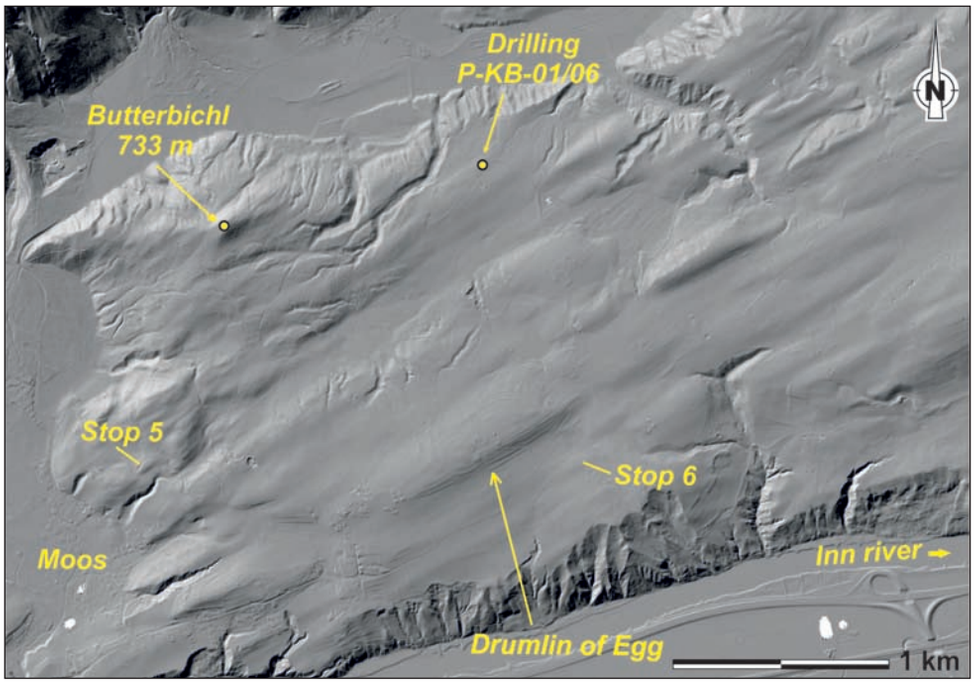

Fig. 21: Digital elevation model of the drumlin field in the southwestern part of Unterangerberg terrace with the most prominent drumlin of Egg (Stop 6) (©DEM: https://portal.tirol.gv.at/LBAWeb/Luftbildübersicht.Show).

Abb. 21: Digitales Höhenmodell des Drumlin-Schwarms im Südwestteil des Unterangerbergs. Der größte Drumlin befindet sich bei der Ortschaft Egg (Stop 6). (©DEM: https://portal.tirol.gv.at/LBAWeb/Luftbildübersicht.Show).

mented slope scree deposits. The entire geometry of the scarp area indicates more precisely the mechanism of the slope failure, i.e. a rock-slide. The deposition area consists largely of decametre-thick, partly cemented blocks made up of Wetterstein limestone and has an estimated extent of ca. 5 km² below the LGM till cover. According to the geometry of the niche the corresponding estimated volume of the rock-slide mass is between 250 and 350 x 10^6 m^3. Close to the Inn River in the vicinity of the motorway station Angath a large rocky cliff of cataclastically deformed greyish dolostones of the Raibl Group represents the most distal part of the rock-slide mass (Fig. 23).

According to the mapping results, the rock-slide deposits of Mariastein rest at the western margin on carbonates of the Raibl Group as well as on Tertiary sedimentary rocks of the Unterangerberg Formation. Apart from this no further outcrops at the base of the rock-slide are available. Even the drillings A-KB 12/98 and A-KB 13/98 terminated within the rock-slide masses (Starnberger et al. 2013). At the south-eastern rim of the rock-slide mass a lense of deformed lacustrine siltstone, free of pollen, was found within the cataclastic deposits. This finding indicates the existence of a lake in the southern forefield of the scarp prior to the slope failure. After the event, the fragmented rock mass was covered by silty lacustrine and later on by gravelly fluvial sediments. The luminescence dating of lacustrine sediments of the drilling A-KB 13/98 provides a minimum age of the rock-slide event of Mariastein (68–62 ka). The sediment cover below the LGM till shows a significant coarsening-upward trend indicating the transition to the LGM.

At the excursion stop Mariastein the huge pillar of quite intact Wetterstein limestone is evident, which provides the foundation of the pilgrimage church of Mariastein.

Acknowledgments

We are grateful to Daniela Lattner (Geologische Bundesanstalt) for calculating the volume of Mariastein rock-slide mass, to Reinhard Starnberger (University of Innsbruck)

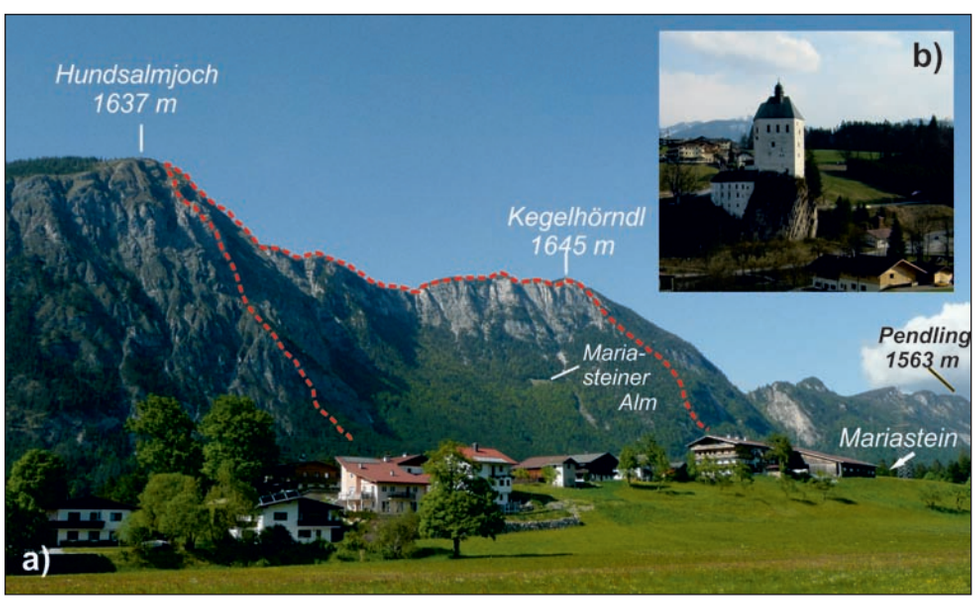

Fig. 22: (a) Scarp area (red dashed lines) of Mariastein rock-slide as viewed from the village of Bichl/Angerberg. (b) Pilgrimage church of Mariastein built on a block of Wetterstein limestone from the rock-slide mass.

Abb. 22: (a) Blick von Süden (Bichl/Angerberg) auf die Ausbruchsnische der Felsgleitung von Mariastein (rot strichliert). (b) Das Innenbild zeigt den mächtigen Block aus Wettersteinkalk, auf dem die Wallfahrtskirche von Mariastein erbaut wurde.

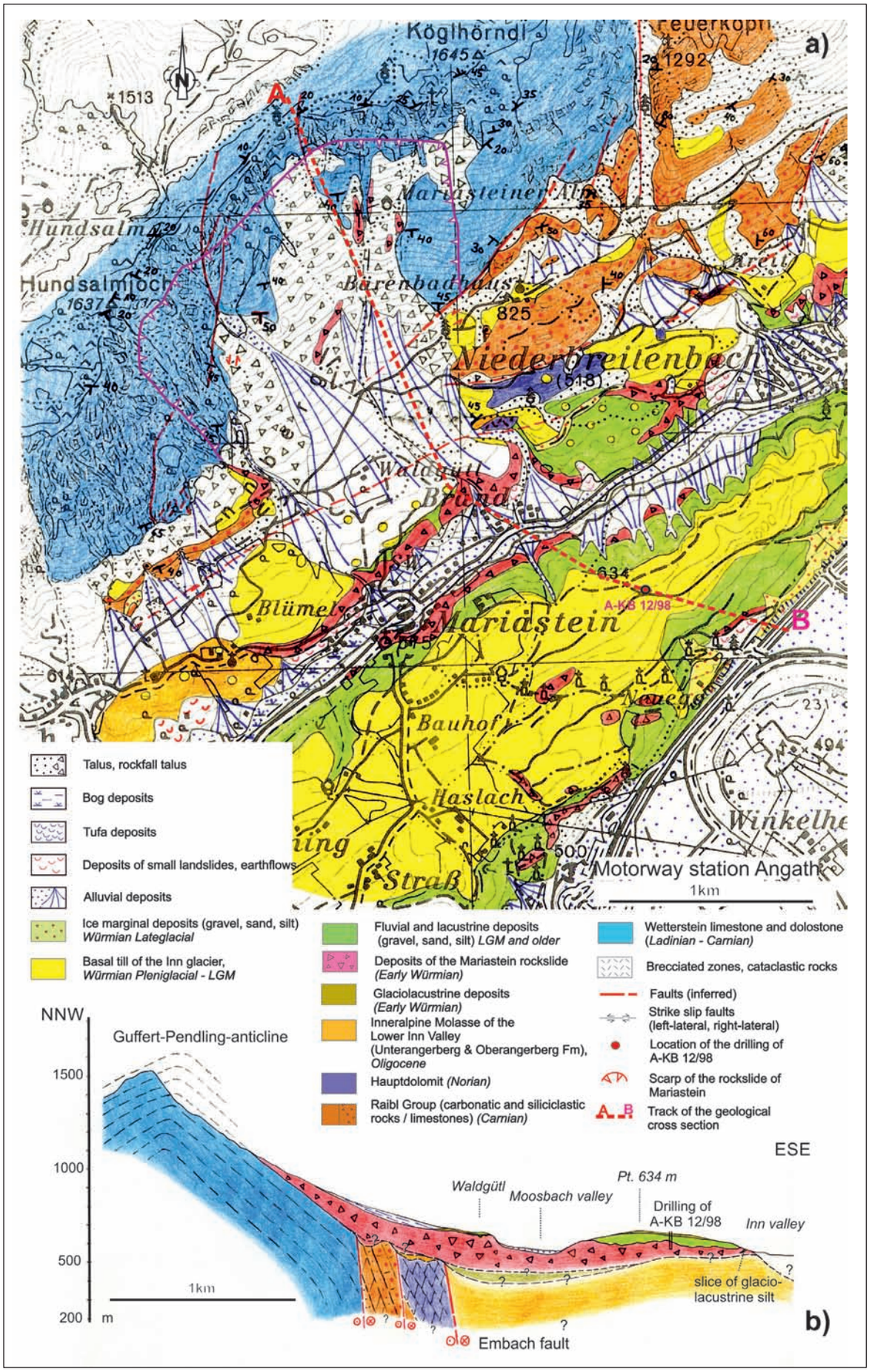

Fig. 23: Geological map of Mariastein rock-slide area (a) and geological cross section (b) compiled from published and unpublished field data of Gruber (2009) and Reitner (unpubl.).

Abb. 23: Geologische Karte der Mariastein-Felsgleitung (a) und ihrer näheren Umgebung, (b) mit einem geologischen Profilschnitt; zusammengestellt aus geologischen Aufnahmen von Gruber (2009) und Reitner (unveröff.).

for providing Fig. 17 and to Monika Brüggemann-Ledolter (Geologische Bundesanstalt) for drawing Fig. 3.

D

References

Ampferer, O. & Ohnesorge, T. (1918): Rattenberg. Geologische Spezialkarte der Österreichisch-Ungarischen Monarchie, 1:75.000, Blatt 5048 – Wien (Geologische Reichsanstalt).

Ampferer, O. (1921): Über die kohleführenden Gosauschichten des Brandenberger und Thierseer Tales in Tirol. – Jahrbuch der Geologischen Staatsanstalt 71: 149–158.

Ampferer, O. (1922): Zur Geologie des Unterinntaler Tertiärs. Mit einem Beitrag von Bruno Sander. – Jahrbuch der Geologischen Bundesanstalt, 72: 105–150.

Bobek, H. (1935): Die jüngere Geschichte der Inntalterrasse und der Rückzug der letzten Vergletscherung im Inntal. – Jahrbuch der Geologischen Bundesanstalt, 85: 135–189.

Benn, D.I. & Evans, D.J.A. 1998: Glaciers and glaciation. – 734 pp.; London (Arnold).

Chaline, J. & Jerz, H. (1984): Arbeitsergebnisse der Subkommission für Europäische Quartärstratigraphie – Stratotypen des Würm-Glazials. – Eiszeitalter und Gegenwart, 35: 185–206.

Clark, C. D., Hughes, A. L., Greenwood, S. L., Spagnolo, M., & Ng, F. S. (2009): Size and shape characteristics of drumlins, derived from a large sample, and associated scaling laws. – Quaternary Science Reviews, 28: 677–692.

Evans, D.J.A., Phillips, E.R., Hiemstra, J.F. & Auton, C.A. (2006): Subglacial till: Formation, sedimentary characteristics and classification. – Earth-Science Reviews, 78: 115–176.

Fliri, F. (1973): Beiträge zur alpinen Würmvereisung: Forschungen am Bänderton von Baumkirchen (Inntal, Nordtirol). – Zeitschrift für Geomorphologie N.F., Supplement 16: 1–14.

Frisch, W., Kuhlemann, J., Dunkl, I. & Brügel, A. (1998): Palinspastic reconstruction and topographic evolution of the Eastern Alps during late Tertiary tectonic extrusion. – Tectonophysics, 297: 1–15.

Gruber, A. (2009): Bericht 2005-2008 über geologische, strukturgeologische und insbesondere quartärgeologische Aufnahmen auf Blatt UTM 3213 Kufstein. – Jahrbuch der Geologischen Bundesanstalt, 149: 550–564.

Gruber, A., Strauhal, T., Prager, C., Reitner, J.M., Brandner, R. & Zangerl, C. (2009): Die „Butterbichl-Gleitmasse“ - eine große fossile Massenbewegung am Südrand der Nördlichen Kalkalpen (Tirol, Österreich). – Swiss Bulletin für angewandte Geologie, 14: 103–134.

Heissel, W. (1951): Beiträge zur Tertiärstratigraphie und Quartärgeologie des Unterinntales. – Jahrbuch der Geologischen Bundesanstalt, 94: 207–222.

Heissel, W. (1955): Zur Geologie des Unterinntaler Tertiärgebietes. – Mitteilungen der Geologischen Gesellschaft, 48: 49–70.

Ivy-Ochs, S., Kerschner, H., Reuther, A., Preusser, F., Heine, K., Maisch, M., Kubik, P.W. & Schlüchter Ch. (2008): Chronology of the last glacial cycle in the Northern European Alps. – Journal of Quaternary Science, 23: 559–573.

Keller, B. (1996): Lithofazies-Codes für die Klassifikation von Lockergesteinen. – Mitteilungen der Schweizerischen Gesellschaft für Boden- und Felsmechanik, 132: 5–10.

Klasen, N., Fiebig, M., Preusser, F., Reitner, J.M. & Radtke, U. (2007): Luminescence dating of sediments from the Tyrolean Alps, Austria, and implications for the reconstruction of ice dynamics during the last glaciation. – Quaternary International, 164–165: 21–32.

Klebelsberg v., R. (1935): Geologie von Tirol. Gebr. Borntträger – 831 pp.; Berlin (Borntraeger).

Köhler, M. & Poscher, G. (2007): Geologische und hydrogeologische Charakteristika der Unterinntaltrasse. – Internationales Symposium Brenner Basistunnel und Zulaufstrecken, 1: 111–117, Innsbruck (Innsbruck University Press).

Linner, M., Reitner, J. M. & Pavlik, W. (2013): Österr. Geologische Karte 1:50.000, Bl. 179 Lienz. Wien (Geologische Bundesanstalt).

Menzies, J. (1979): A review of the literature on the formation and location of drumlins. – Earth Science Reviews, 14: 315–359.

Monegato, G., Ravazzi, C., Donegana, M., Pini, R., Calderoni, G., Wick, L. (2007): Evidence of a two-fold glacial advance during the last glacial maximum in the Tagliamento end moraine system (Eastern Alps). – Quaternary Research, 68: 284–302.

Neuendof, K.K.E., Mehl Jr., J.P. & Jackson, J.A. (Eds.) (2005): Glossary of Geology. 5th Ed. – 779 pp.; Alexandria, Virginia (American Geological Society).

McSaveney, M. J & Davies, T. R. H. (2006): Rapid rock-mass flow with dynamic fragmentation. – In: Evans, S. G., Scarascia-Mugnozza, G., Strom, A. & Hermanns, R. L. (eds.): Advanced Research Workshop: Landslides from massive rock slope failure. NATO Science Series, IV Earth and Environmental Sciences, 49: 285–304 21, Celano, Italy.

Ortner, H. (1996): Deformation und Diagenese im Unterinntaler Tertiär (zwischen Rattenberg und Durchholzen) und seinem Rahmen. – Unpublished PhD thesis, University of Innsbruck, 234 pp.

Ortner, H. (2003a): Cementation and tectonics in the Inneralpine Molasse of the Lower Inn Valley. – Geologisch-Paläontologische Mitteilungen Innsbruck, 26: 71–89.

Ortner, H. (2003b): Local and far-field stress-analysis of brittle deformation in the western part of the Northern Calcareous Alps. – Geologisch-Paläontologische Mitteilungen Mitt. Innsbruck, 26: 109–136.

Ortner, H. & Stingl, V. (2001): Facies and basin development of the Oligocene in the Lower Inn Valley, Tyrol/Bavaria. - In: Piller, W. & Rasser, M. (eds.): Paleogene in Austria. – Schriftenreihe der Erdwissenschaftlichen Kommissionen, 14: 153–196.

Ortner, H., Reiter, F. & Brandner, R. (2006): Kinematics of the Inntal shear zone–sub-Tauern ramp fault system and the interpretation of the TRANSALP seismic section, Eastern Alps, Austria. – Tectonophysics, 414: 241–258.

Pestal, G., Hejl, E., Egger, H., van Husen, D., Linner, M., Mandl, G., Reitner, J., Rupp, C. & Schuster, R.

(2004): Geologische Karte von Salzburg 1:200000. – Wien (Geologische Bundesanstalt).

Poscher, G. & Eder, S., Marschallinger, R. & Sedlacek, C. (2008): Geologie und Geotechnik des Angerbergs, Trassenstudien im Abschnitt Brannenburg – Kundl/Radfeld. – Internationales Symposium Brenner Basistunnel und Zulaufstrecken, 1: 103–114, Innsbruck (Innsbruck University Press).

Postma, G. (1990): Depositional architecture and facies of river and fan deltas: a synthesis. – In: Colella, A. & Prior, D.P. (eds.): Coarse-Grained Deltas. International Association of Sedimentologists, Special Publication, 10: 13–27.

Reitner, J.M. (2005): Quartärgeologie und Landschaftsentwicklung im Raum Kitzbühel – St. Johann i.T. – Hopfgarten (Nordtirol) vom Riss bis in das Würm-Spätglazial (MIS 6-2). – Unpublished PhD thesis, University of Vienna, 190 pp.

Reitner, J.M. (2007): Glacial dynamics at the beginning of Termination I in the Eastern Alps and their stratigraphic implications. – Quaternary International, 164–165: 64–84.

Reitner, J.M., Gruber, W., Römer, A. & Morawetz, R. (2010): Alpine overdeepenings and paleo-ice flow changes: an integrated geophysical-sedimentological case study from Tyrol (Austria). – Swiss Journal of Geoscience, 103: 385–405.

Reitner, J.M. (2008): Bericht 2006/2007 über geologische Aufnahmen im Quartär auf den Blättern 120 Wörgl und 121 Neukirchen am Großvenediger bzw. auf UTM-Blatt 3213 Kufstein. – Jahrbuch der Geologischen Bundesanstalt, 148: 248–254.

Reitner, J.M. & Draxler I. (2002): Die klimatisch-fazielle Entwicklung vor dem Würm – Maximum im Raum Kitzbühel – St.Johann – Hopfgarten (Nordtirol/Österreich). – Terra Nostra, 2002/6: 298–304.

Schmid, M.S., Fügenschuh, B., Kissling, E. & Schuster, R. (2004): Tectonic map and overall architecture of the Alpine orogen. – Eclogae geologicae Helvetiae, 97: 93–117.

Schulz, O. & Fuchs, W. (1991): Kohle in Tirol. – Archiv für Lagerstättenforschung, 13: 123–213.

Schuster, R., Kurz, W., Krenn, K. & Fritz, H. (2013a): Introduction to the Geology of the Eastern Alps. – Berichte der Geologischen Bundesanstalt, 99: 285 pp.

Schuster, R., Egger, H., Krenmayr, H.G., Linner, M., Mandl, G.W., Matura, A., Nowotny, A., Pascher, G., Pestal, G., Pistotnik, J., Rockenschaub, M. & Schnabel, W. (2013b): Geologische Übersichtskarte der Republik Österreich 1:1500000 (ohne Quartär). – Wien (Geologische Bundesanstalt).

Spitzer, R. (2005): Die Angerberg Terrasse: „Vom quartärgeologischen Rahmen zum hydrogeologischen Modell". – Unpublished Diploma thesis, University of Innsbruck, 116 pp.

Strauhal, T. (2009): Mineralogische und geotechnische Eigenschaften von tektonisch- und massenbewegungsbedingten Kakiriten. – Unpublished Diploma thesis,University of Innsbruck, 245 pp.

Starnberger, R., Drescher-Schneider, R., Reitner, J. M., Rodnight, H., Reimer, P. J. & Spötl, C. (2013): Late Pleistocene climate change and landscape dynamics in the Eastern Alps: The inner-alpine Unterangerberg record (Austria). – Quaternary Science Reviews, 68: 17–62.

van Husen, D. (1987): Die Ostalpen in den Eiszeiten. – Veröffentlichung der Geologischen Bundesanstalt, 2: 24 pp.

van Husen, D. (2000): Geological processes during the Quaternary. – Mitteilungen der Österreichischen Geologischen Gesellschaft 92: 135–156.

van Husen, D. & Reitner, J.M. (2011): An outline of the Quaternary stratigraphy of Austria. – E&G Quaternary Science Journal – Eiszeitalter und Gegenwart, 60: 366–387.

Zailer, V. (1910): Die diluvialen Torfkohlenlager von Hopfgarten. – Zeitschrift für Moorkultur und Torfverwertung, 8: 267–281.

The Quaternary of Baumkirchen (central Inn Valley, Tyrol) and its surroundings

Das Quartär von Baumkirchen (mittleres Inntal, Tirol) und seiner Umgebung

Christoph Spötl, Reinhard Starnberger, Samuel Barrett

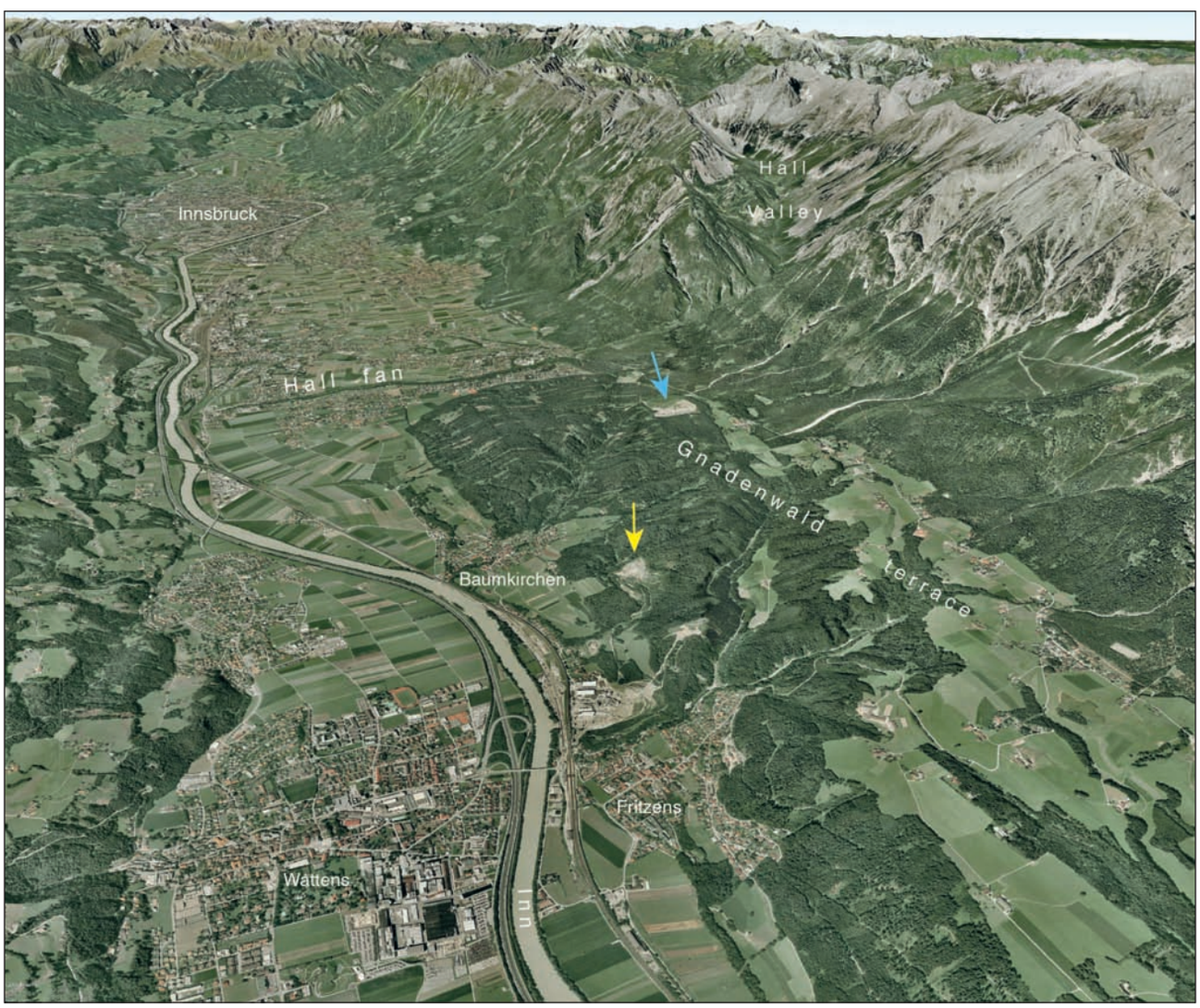

Fig. 1: Oblique aerial view of the central Inn Valley showing the location of the Gnadenwald terrace on the northern side of the valley (view towards WNW; Google Earth Pro image). The two main artificial outcrops, the former clay pit near the village of Baumkirchen and the gravel pit Absam are marked by yellow and blue arrows, respectively. Note the presence of well-developed terraces (so-called "Mittelgebirge") also near Innsbruck on the southern side of the valley.

Abb. 1: Schrägansicht des mittleren Inntales mit dem Gnadenwald-Plateau an der Nordseite des Tales (Blickrichtung WNW; Google Earth Pro Bild). Die beiden künstlichen Aufschlüsse, die ehemalige Tongrube nahe der Ortschaft Baumkirchen und die Schottergrube Absam sind mit einem gelben bzw. blauen Pfeil markiert. Beachte das Vorkommen der klar ausgebildeten Terrassen (Mittelgebirge genannt) auch bei Innsbruck auf der Südseite des Inntales.

1 Introduction

The central Inn Valley in Tyrol has attracted the attention of Quaternary scientists since the second half of the 19th century. The peculiar Hötting Breccia north of Innsbruck, with its famous Pleistocene flora (see excursion F Hötting in this volume), has been one focal point. A second one has been the conspicuous terraces which are present to varying extents between Mötz and Jenbach, straddling the valley flanks for some 70 km. These terraces, referred to as "Mittelgebirge", delineate a previous fluvial accretion level 250–300 m above the Holocene level of the Inn River when the valley floor was about twice as wide as today. A thick succession of fine-grained sediments interfingering with deltaic complexes is overlain by glaciofluvial gravel ("Vorstoßschotter" sensu Penck) and constitutes the sedimentary inventory of these terraces, which are overlain by lodgement till of the Last Glacial Maximum (Hochwürm) ice advance. This coarsening-upwards sequence has been attributed to climate forcing, whereby a drop in temperature and a corresponding lowering of the upper limit of the tree line gave rise to increased sediment input into the rivers and thus strong aggradation. This resulted in the rapid progradation of alluvial fans which blocked the valley's drainage and created accommodation space for lakes to form (van Husen 1983a,b, 2000). Drainage blockage and lake formation may have also occurred as a result of advances of tributary glaciers into the main valleys, either by the ice or, more commonly, by the proglacial sediment wedge.

The best studied and preserved part of the Mittelgebirge is the Gnadenwald plateau on the northern side of the valley some 12 km downstream of Innsbruck (Fig. 1). There, a clay pit near the village of Baumkirchen provided the key chronology, largely thanks to the pioneering efforts of Franz Fliri, which allowed the dating of these sediments to the transition from the Middle to the Upper Würmian (Chaline & Jerz 1984). After almost four decades of dormancy, basic research in this area has recently started again by way of core drilling. This half-day excursion will both review the previous database of the Baumkirchen area and provide insights into the ongoing research activities.

2 A brief history of research

The first Quaternary geology map covering the Gnadenwald terrace was published more than a century ago (Blaas 1890) and already identified basal till capping a succession of "Terrassen Sand und Schotter" (terrace sand and gravel). Blaas mentioned that clay-rich sediments ("blaugrauer Lehm") occur in the deepest outcrops which grade into sand and then gravel, finally overlain by till. His cross section at Baumkirchen (his Fig. 2) does not show these fine-grained sediments nor did he mention a clay pit at this site, which, according to Fliri (1999: 18) was opened around 1880.

"Mittelgebirge" terraces occur also west of Baumkirchen, but are absent east of Jenbach (where the confluence of the Ziller and Inn Valley form a right angle). This led Penck (1890) to propose a palaeolake in the central Inn Valley. He hypothesized that this lake was dammed by the advancing glacier from the Ziller Valley and extended upstream to the western end of the Mieming plateau at Mötz, some 70 km in length (rather than 60 km as stated by Penck 1890).

In their famous monograph Penck & Brückner (1909: 333–335) summarised the field evidence for ice-free, lacustrine conditions in the Inn Valley between Mötz and Jenbach. They coined the (later abandoned) term "Achenschwankung" (Achen oscillation) for this time interval, as they were convinced that the sediment wedge that still dams the Achensee today was formed at the same time (Fig. 2). Penck & Brückner concluded that the palaeolake in the Inn Valley had an average width of 3.5 km and a depth of 200 m. The lake level was placed at 790 m, i.e. 240 m above today´s level of the Inn River at Baumkirchen.

Ampferer (1904, 1908) criticised Penck's model of a large ice-dammed lake in the Inn Valley. He showed that the strong aggradation was not confined to the Inn Valley upstream of Jenbach, but extended into the foreland of the Alps (Ampferer, 1907) and he favoured the model of many small lakes (Ampferer 1908: 111).

Zoeke (1944) studied, but unfortunately never published, heavy-mineral analyses from a series of outcrops of banded clays and silts in northern Tyrol, including one sample from the clay pit of Baumkirchen. She observed an increase in grain size and a decrease in the degree of roundness of the particles downstream hinting towards a dominant sediment source in the eastern part of the palaeolake.

Heissel (1954) studied the Quaternary of the Inn Valley, published a map of the Gnadenwald terrace and the adjacent terrace of the Vomperberg and concluded that "Bänderton und Mehlsand" (banded clay and fine sand) are present near Baumkirchen over an E-W extension of 3 km. Until then, the consensus was that the clastic sediments of the Inn Valley terraces were formed during the Last Interglacial, and this view was based on the observations that the lake sediments preserved rare fossils (e.g., fish and bone remains) and were overlain by basal till of the Last Glacial Maximum. Interestingly, palaeovegetational evidence from pollen was largely ignored, although Sarnthein (1937) had shown already that the pollen concentration and composition in the lacustrine sediments was incompatible with an interglacial vegetation "…in dem keinesfalls Holzgewächse, wohl aber auch kaum mehr als Spuren einer primitiven Vegetation im Inntalraum zu finden waren" (p. 235; note that he did not examine samples from Baumkirchen, but from other lacustrine sediments further west).

Fliri (1964), who mapped the western part of the Gnadenwald plateau with an emphasis on geomorphological features and performed granulometric analyses on gravel samples, also raised doubts and suggested that these sediments were more likely deposited during an interstadial. He also mentioned in passing that occasional remains of fossil fish (10–40 cm in length) and wood were found during mining of the clay pit of Baumkirchen, but none of them were conserved for further study.

At the same time Mayr (1968) studied the Late Pleistocene of the central Inn Valley and in particular the sedimentary succession at the western margin of the Gnadenwald plateau, exposed in the former gravel pit of Mils (which since has been re-filled). He described "Riesen-Eisspaltennetze" (giant ice-wedge networks), up to 40 m in vertical extension, from this gravel pit (see also Fliri, 1971 for a different view on the origin of these fractures).

Things took a major turn when in 1969 the first wood fragments were found in-situ in the banded clays of Baum-

Fig. 2: Partial reproduction of Penck & Brückner's map (1909: their Fig. 60) of the Inn Valley between Imst and Kufstein showing the extent of the dammed lake between Mötz and Jenbach ("Stausee im Innthal" in the original legend) and the supposed front of the Ziller glacier just south of the junction with the Inn Valley ("Gletscherenden der Achenschwankung" in the original legend). The Baumkirchen clay pit is marked by the red dot.

Abb. 2: Teilweise Reproduktion der Karte von Penck & Brückner (1909: ihre Abb. 60) des Inntales zwischen Imst und Kufstein mit der Ausdehnung des Stausees zwischen Mötz und Jenbach („Stausee im Innthal" laut Originallegende), sowie die vermutete Zunge des Ziller-Gletschers knapp südlich der Einmündung in das Inntal („Gletscherenden der Achenschwankung"). Der rote Punkt markiert die Tongrube Baumkirchen.

kirchen (at 681 m a.s.l.) and radiocarbon-dated to about 30 ka (uncalibrated). This jump-started research at this site which was coordinated by F. Fliri, involving an interdisciplinary and international team of scientists. A fleet of articles provides detailed accounts of the sedimentology, plant remains, radiocarbon dates, macro remains, microfossils, etc. of the banded clays (Fliri 1970, 1976; Fliri et al. 1970, 1971, 1972; Felber 1971; Schiegl & Trimborn 1972; Maurer & Nabholz 1972; Resch 1972; Köhler & Resch 1973). This major research phase ended with a pollen study by Bortenschlager & Bortenschlager (1978, and two short reports on palaeomagnetic measurements by Mayr (1976) and by Koci (1981). A useful review was published by Fliri (1975).

In preparation for the planning of a large tunnel system for the high-speed railway in the lower Inn Valley the Gnadenwald plateau was mapped in detail by G. Poscher, who also employed heavy-mineral analyses and suggested the presence of two separate lacustrine sequences (Poscher & Lelkes-Felvári 1999).

Klasen et al. (2007) were the first to apply optically stimulated luminescence dating to inneralpine Pleistocene sediments in Tyrol. They examined samples from the clay pit and obtained dates that were broadly compatible with the radiocarbon chronology.

As part of the current research activities the authors of this article re-sampled all existing wood samples from the clay pit and established a new radiocarbon chronology (Spötl et al. 2013).

3 Setting

The Gnadenwald terrace stretches for 10 km along the northern side of the Inn Valley (Fig. 1). Its average width is 1.5 km (excluding the terrace escarpment), which is only marginally smaller than the width of the Inn Valley proper in this area. The mean elevation of the terrace is slightly over 800 m and reaches up to 879 m at St. Michael. In comparison, the level of the Inn River near Wattens is at 550 m. The terrace is separated from the adjacent terrace of the Vomperberg to the East by the gorge of the Vomperbach and terminates in the West at the large alluvial fan spreading from the Hall Valley (Fig. 1). The counterparts of the Gnadenwald terrace on the southern side of the Inn Valley are much smaller and best preserved on the Weerberg terrace.

The surface of the Gnadenwald terrace is dissected by valleys which join the Inn Valley at a low angle. Although there is active erosion going on in these valleys leading to massive construction efforts to hold back the sediment (e.g., Bärenbach, Larchbach), most of these streams carry lit-

tle perennial water classifying these valleys as dry valleys. Their origin is related to subglacial processes during the Last Glacial Maximum as shown by the presence of overconsolidated basal till covering the valley floor, e.g. in Larch Valley.

The Gnadenwald terrace is composed of a clastic sediment body reaching below today's level of the Inn River and is capped by basal till. The internal structure of the terrace is well known thanks to a number of drill cores and geophysical measurements, which unfortunately, are largely unpublished. These studies were part of the exploration for the railway line in the lower Inn Valley by the Brenner Railway Company. Although the tunnel finally did not penetrate the Gnadenwald plateau exploratory corings up to 329 m deep were made along a SSW-NNE transect across the terrace reaching slightly below the level of the Inn River. Only the northernmost drilling (300 m ESE St. Michael) reached bedrock (Upper Triassic Hauptdolomit) at 619 m and remained therein until the final depth of 541 m. Only a simplified version of a cross section through the eastern part of the terrace has been published so far (Poscher et al. 2002; Köhler et al. 2005) showing sands interfingering with silts and clays, overlain by gravel, and finally till (Fig. 3).

Four open-pit mines provide large-scale access to the sediments on the plateau and its margin: (a) The clay pit of Baumkirchen, whose operation ended in the mid-1990s and which has been partly back-filled since. (b) The former gravel pit Mils located at the western escarpment of the terrace (completely re-filled). (c) The Absamer Grube, formerly known as Pfanzelter gravel pit, on the plateau. (d) The gravel pit Schotterwerk III just east of the clay pit (a). The latter two open-pit mines are currently in operation.

The sediment-fill of the Inn Valley proper, south of the Gnadenwald terrace, has been examined by two reflection seismic lines at Wattens (Weber et al. 1990) and by a 900 m-deep counter-flush-drilling between Wattens and Volders, located 1.5 km SSE of the Baumkirchen clay pit. The drill core did not reach bedrock at 349 m below sea level. A marked increase in seismic velocity ca. 350 m below the level of the Inn valley was attributed to the presence of compact gravel and conglomerate (Weber et al. 1990) which led Preusser et al. (2010) to define this as the base of the Quaternary. Sedimentological and geochemical analyses, as yet unpublished (Steinbrener 2011), add support to this interpretation as does a second deep drilling at Kramsach 27 km downstream of Wattens, which penetrated 372 m of Pleistocene sediments followed by 1028 m of Neogene mudstones, silt- and sandstones, before reaching Triassic limestones 884 m below sea level (Preusser et al. 2010: their Fig. 6).

4 Sediment types

Banded silts and clays

Collectively known as "Baumkirchener Bändertone", these sediments are banded and laminated clayey silts with rare intercalations of fine sand, in particular near their top. Köhler & Resch (1973) reported grain-size analyses of two representative Bänderton samples which contained 8 and 15 % clay fraction, respectively. The dominant grain size is silt and the (fine) sand fraction was less than 5 %. Maurer & Nabholz (1972) reported a significantly higher clay content (55 %) for one sample. The components of the sand fraction are dominantly derived from crystalline rocks. Chlorite and white mica are the most abundant minerals in the 0.063–0.1 mm grain size fraction. The mean carbonate content in the Bänderton is 11.5 wt.% (Köhler & Resch 1973).

The origin of the banding and lamination has puzzled researchers for decades and the consensus is that they do not represent varves, i.e. seasonally deposited layers in annual cycles (Köhler & Resch 1973). These fine layers, however, are very well preserved and the organic content of these silts and clays is low (mostly 0.1–0.3 %; unpublished data) which is consistent with the lack of bioturbation on the lake floor and a presumably high sedimentation rate (cf. pollen results below).

Fliri et al. (1972) reported that the bedding of the Bänder-

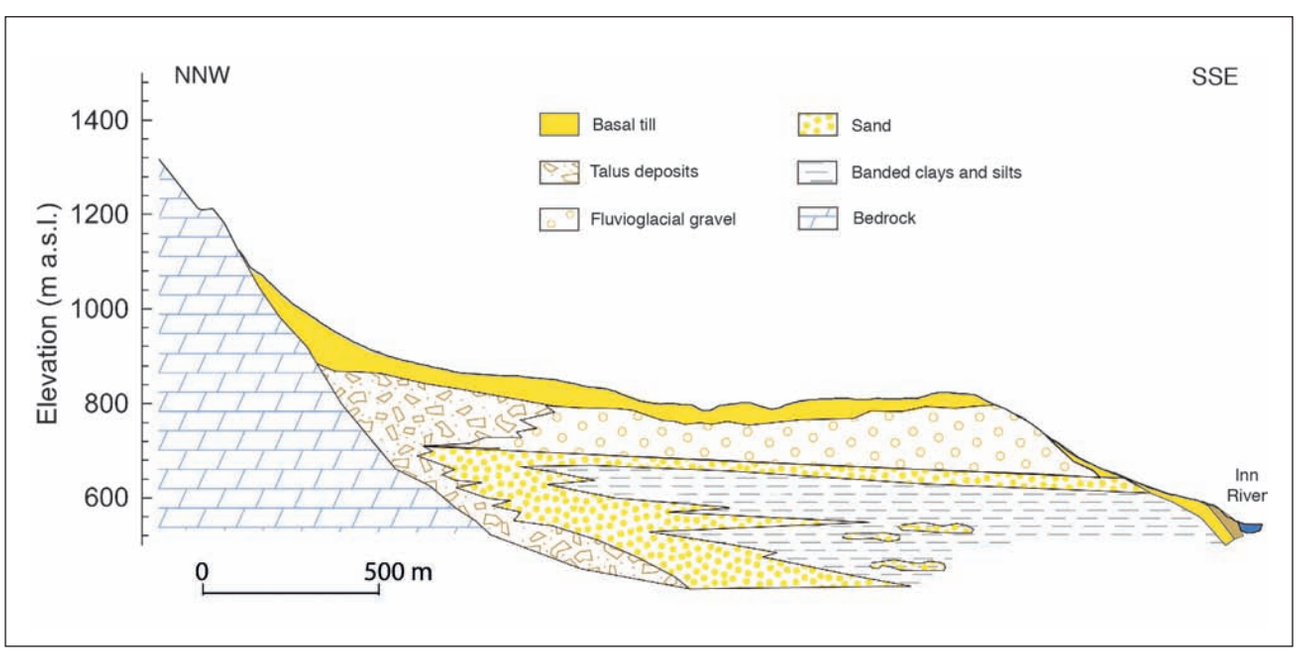

Fig. 3: Simplified and idealised cross-section of the Pleistocene sediment succession of the Gnadenwald terrace (modified after Poscher et al. 2002).

Abb. 3: Vereinfachtes und idealisiertes Profil durch die pleistozäne Sedimentabfolge der Gnadenwald-Terrasse (abgewandelt nach Poscher et al. 2002).

ton dips on average 4° towards SW to WSW. An easterly source of the sediment is also indicated by heavy-mineral analyses (Zoeke, 1944), as well as by slump folds which were present in the former clay pit at 653–655 m a.s.l. and showed a clear west-vergence (Resch 1972: 227).

Dropstones are rare in these silts. Heissel (1954: 296–298) mentioned a conspicuous layer of limestone clasts at approximately 690 m a.s.l. These clasts were poorly rounded and lacked striations. The largest block was 20 x 30 cm in diameter and the embedding clay and silt layers were distorted. The clasts are derived from Triassic Wetterstein Limestone. Heissel hypothesized that these clasts were transported by drifting winter lake ice to the site of deposition rather than by a calving local glacier. The distance to the nearest outcrop of Wetterstein Limestone (at the base of the Hundskopf, 2243 m a.s.l.) is 3.5 km. Mayr (1968: 269) also observed this layer of poorly rounded clasts of limestone in the clay pit. In addition to local limestone (90 %) he also found components composed of Upper Triassic dolomite (Hauptdolomit, 3–5 %) and between 1 and 10 % of gneiss and quartzphyllite. Later, such clasts were also observed in other horizons of the clay pit and proved to be exclusively Wetterstein Limestone (Fliri et al. 1970: 16). These authors also noted the close association of these clasts and the presence of plant remains and suggested avalanches as the process transporting them into the lake.

At the time of clay mining up to 70 m of "Bändertone" were exposed (645–715 m a.s.l) and the top was reported near 750 m a.s.l., delineated by a spring line. An (unpublished) drilling in the clay pit encountered this same sediment type down to 70 m below the base of the clay pit without reaching its base (Patzelt & Resch 1986: 59). This value of 175 m of banded clay was recently revised due to new drillings (see below) resulting in a minimum thickness of 252 m (see Stop 1).

Sands

The "Bänderton" succession grades up section into massive sands which rarely show sedimentary structures and are conspicuously rich in white mica flakes. Preliminary petrographic analyses of two samples from the former gravel pit Mils were published by Ladurner (1955). Based on mapping and drill cores Poscher & Lelkes-Felvári (1999) distinguished two sand facies, an older "Fritzner Sequenz" and a younger "Baumkirchner Sequenz", but no proper description and documentation was provided.

Gravel

Overlying the sands is a thick succession of gravel, known as "Terrassenschotter" since the days of J. Blaas. These sediments show horizontal bedding, shallow channel-fills and occasional sandy intercalations.

Fliri (1971: 11) briefly mentioned "sicher gefroren transportierte Sandgerölle" in sand layers intercalated within the upper part of the fluvioglacial gravel at Absamer Grube (ca. 795 m a.s.l.), i.e. clasts which were transported in a frozen state. Krainer & Poscher (1990) studied these components and noted small-scale subsidence structures above them. They interpreted these clasts as redeposited diamicton and attributed their origin to the erosion of frozen sediment by undercutting of riverbanks during spring peak runoff, clearly pointing towards a very cold climate at that time.

Heissel (1954) reported the finding of bones within the fluvioglacial gravel (*Alces* cf. *alces*) as well as occasional remains of poorly preserved conifer wood. The former bones were recently radiocarbon-dated and currently provide the only direct age control on these coarse-grained deposits (Spötl et al. 2013).

Basal till

The gravel is sharply overlain by till characterised by the lack of bedding, overcompaction, clayey matrix and abundant striated clasts (in particular carbonate components).

Post-LGM alluvial sediments

Locally, younger clastic sediments prograde across the till-capped plateau emerging from steep ravines on the flank of the mountains in the North. One such fan (Urschenbach) has recently been studied in detail (Sanders & Ostermann 2011).

5 Fossil content

Apart from rare bone fragments and remains of wood in the gravel (most of which were lost) only the "Bändertone" yielded a significant number of fossils, largely thanks to the efforts led by F. Fliri who kept an eye on the new exposures in the clay pit and involved various experts. More abundant than fossils are actually trace fossils which were found on many bedding planes. They have been described but not studied by experts and were mostly attributed to fish swimming in close proximity to the muddy lake floor (Fliri et al. 1970, 1971). Most traces are sinusoidal and could be followed for up to a few metres.

Three specimens of fish were found in these sediments and although none of them was preserved completely their original length was probably close to 1 m (Fliri et al. 1970: 15). Unfortunately, also these fish remains have not been studied in detail (nor the older finding of a similarly large specimen in the banded silts of Arzl; Klebelsberg 1932).

Plant remains were found in distinct layers and include fragments of wood (*Pinus mugo, P. silvestris, Alnus viridis, Hippophae rhamnoides*) as well as rare leaves (*Dryas octopetala, Salix,* fern; Fliri et al. 1970: 24–26; 1971: 17; Fliri 1973).

The pollen content of the Bändertone is very low and the state of preservation is poor. Some pollen is clearly reworked and many grains are compressed. The initial pollen studies relied on a total of three samples only (Fliri et al. 1970: 23–24; 1971; 17–18). Later, Bortenschlager & Bortenschlager (1978) analysed in detail 86 cm of typical "Bänderton" subdivided into 117 samples and found rhythmic changes in the abundance of pollen grains. Some layers were extremely poor in pollen (only a few tens of pollen grains per cm^3), while others had high pollen counts (up to 1590 pollen grains per cm^3). In total these authors identified some 17 vegetation periods within 86 cm. The thickness of the individual and presumably annual sediment layers varied between 3 and 8 cm with a mean of 5 cm. No relationship was observed between the grey level of the sediment and the abundance of pollen grains. The average pollen composition comprised 19.9 % trees and shrubs, 78.4 % herbs and 1.7 % spores indicating tundra vegetation. The abundance of the herb *Artemisia* and high percentages of Gramineae, Cyper-

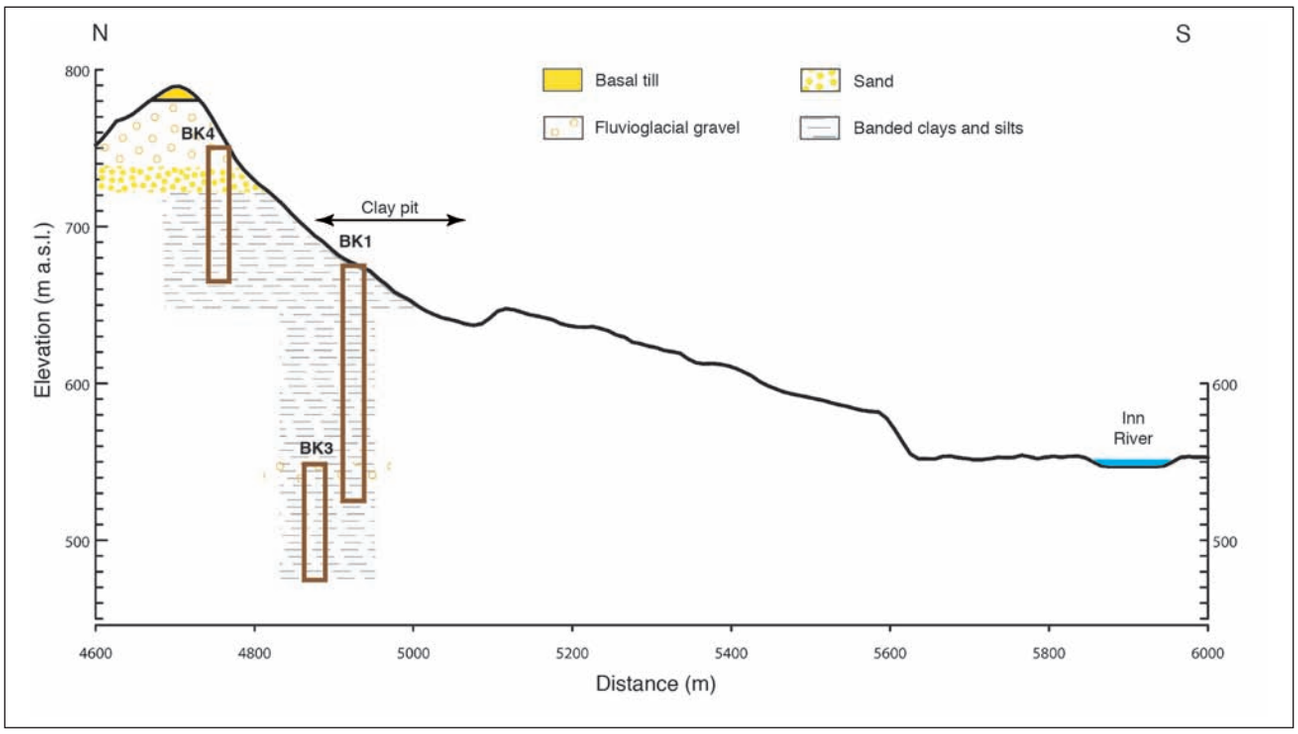

Fig. 4: Simplified cross section of the area of the abandoned clay pit of Baumkirchen showing the location of the recent research drillings. 2x vertically exaggerated.

Abb. 4: Vereinfachtes Profil durch das Gebiet der ehemaligen Tongrube Baumkirchen mit der Lage der jüngst abgeteuften Forschungsbohrungen. 2fache Überhöhung.

aceae and Chenopodiaceae suggest a dry, open, cold steppe (Bortenschlager & Bortenschlager 1978).

Only one study examined other microfossils and found a wide range of remains (Resch 1972). Three samples were examined and the highest abundance of microfossil remains occurred in the 0.315–0.1 mm size fraction. Plant remains included mosses, cuticula, small seeds and fruit remains. Remains of animals included fragments of small gastropod shells, thin-shelled ostracods and insect remains (e.g. head capsules of chironomids). Fish otolithes and characeae were not detected.

6 Chronology

Baumkirchen is well known for its unique and well constrained radiocarbon chronology. Fliri et al. published the initial chronology of wood remains from the clay pit and the most detailed account is given in Fliri et al. (1971: their Table 1). The uncalibrated dates of 13 samples taken over a depth range of 26 m (655 to 681 m) range from 25,500 ± 600 BP to 32,370 ± 600 BP. Later, a piece of *Juniperus* wood was found at 658 m a.s.l. dated at 28,340 ± 630 BP (Patzelt, 1996).

Spötl et al. (2013) recently re-dated all available original specimens and obtained a significantly narrower age range of 30,346 ± 204 to 31,351 ± 303 BP with a mean of 30,790 BP. The calibrated ages (INTCAL13) indicate that the dated interval of the Bänderton succession was deposited between 33.8 and 35.9 cal ka BP (2 sigma range; Spötl et al. 2013). They also reported radiocarbon dates on (elk?) bone fragments reported by Heissel (1954) from the middle part of the gravel in the former Mils gravel pit (27,792 ± 100 and 27,526 ± 107 BP; 31.1-31.9 cal ka BP (2 sigma range), which are currently the only direct dates of the glaciofluvial gravel ("Terrassenschotter") in the central Inn Valley.

Earlier, Klasen et al. (2007) had performed luminescence dating on four samples taken between 660 and 690 m in the clay pit. Infrared-stimulated luminescence yielded mean ages of 37.3 ± 3.5 ka (UV) and 37.8 ± 3.6 ka (post-IR OSL (UV)), whereas infrared-stimulated luminescence (by blue light) gave a higher mean age of 45.0 ± 4.3 ka (all uncertainties of these pooled luminescence ages are quoted at the 1 sigma level). Infrared-stimulated luminescence measurements made on the Baumkirchen sediment in the context of a new drilling project yield slightly younger ages for the radiocarbon-dated part of the section and agree well with the new calibrated radiocarbon ages.

Attempts were also made to date the "Bänderton" succession using palaeomagnetism. Mayr (1976) sampled a 56 m-high section in the clay pit starting at 650 m and performed palaeomagnetic measurements every 50 cm. Unfortunately, only a short preliminary report was published which tentatively concluded that two magnetic anomalies were identified. Koci (1980) re-sampled a 46 m-high profile between 647 and 693 m and found no support of Mayr's magnetic events.

Excursion route

Stop 1: Clay pit Baumkirchen

Clay extraction ceased in the mid-1990s at this important site, which serves as a stratotype for the boundary between the Middle and the Upper Würmian (Chaline & Jerz 1984). Since then, the outcrop quality has gradually deteriorated and presently only the upper levels can be accessed. In order to provide high-quality material for future studies of these

thick lacustrine sediments we obtained a series of drill cores. The initial core (BK1) penetrated 151 m of lake sediments starting from the uppermost still accessible horizon of the clay pit at 676 m a.s.l. (2010). In 2013 we extended this core down to 476 m a.s.l., i.e. 200 m below the clay pit, still remaining in "Bänderton" (core BK3). In addition, we cored the complete transition from the upper part of the "Bänderton" into the sand and finally gravel (core BK4; Fig. 4). Although the base was not reached the cores penetrated a total of 252 m of the lake sediments. Careful inspection of the liner cores shows that the sequence is almost exclusively composed of well laminated silts and clay (Fig. 5). The laminae are entirely clastic and marked by colour and texture changes representing changes in mineralogy, grain size and proportion of matrix and mostly represent single events or sub-seasonal changes in sediment delivery into the lake. Two types of sub-annual layers are easily visible in the clay pit: a matrix/clay-rich material representing quiet conditions in the lake, and coarser layers rich in visible mica flakes which represent high run-off events (e.g. rainfall or snow-melt) when coarser material was transported throughout the lake by over-flows or inter-flows.

While the laminations themselves are not varves, there are regular clay-rich layers, identifiable microscopically, which may be annual markers. These clay-rich layers are thought to have been deposited in very still conditions under a winter ice cover. In some sections, distinct dark coloured layers several millimetres thick are associated with the clay-rich layers and may be roughly considered a representation of years. Although the process by which these dark layers form is not yet understood, they are often associated with thin layers of coarse silt which may represent spring snow melt events. The mineralogy is diverse but varies little overall (Fig. 6).

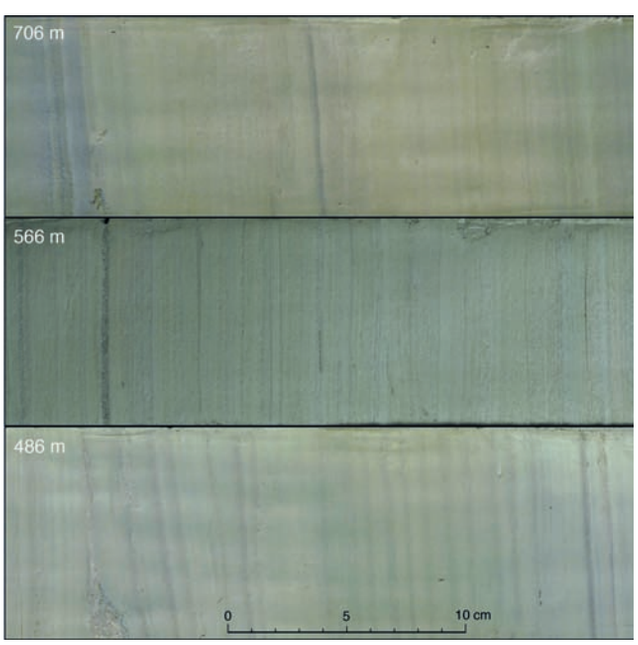

Fig. 5: Core images of Bänderton from three depth intervals: 31 m above, 109 m and 189 m below the upper clay pit horizon, respectively, showing the similarity of the sediment, persistent laminations, and the variation of lamination appearance.

Abb. 5: Bohrkerne des Bändertons aus drei unterschiedlichen Tiefen: 31 m oberhalb, 109 m und 189 m unterhalb des obersten ehemaligen Abbauhorizontes. Die Bilder illustrieren die Ähnlichkeit des Sediments, die persistente Lamination sowie ihre unterschiedliche Detailausprägung.

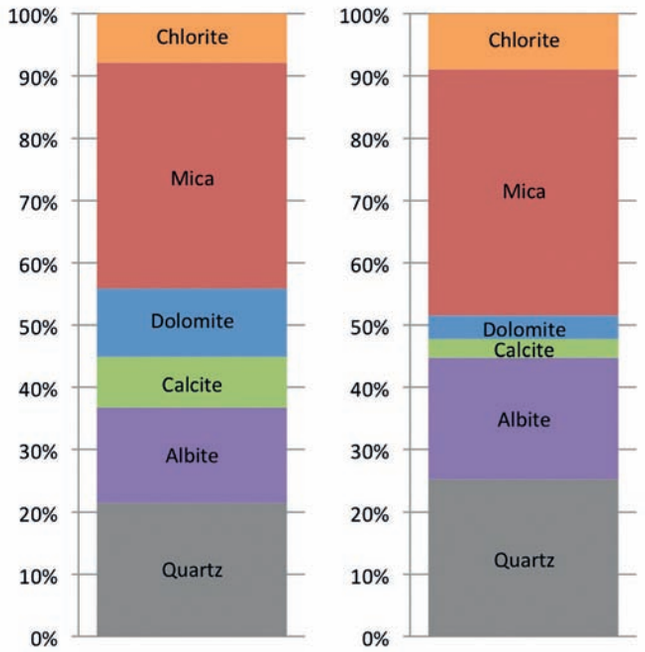

Fig. 6: The mineralogical composition of the "background" sediment of the Baumkirchen palaeolake (left) representing calm lake conditions differs only slightly from that of coarser grained "event layers" (right; X-ray diffraction data, values in weight-%).

Abb. 6: Die mineralogische Zusammensetzung des Hintergrundsediments des Baumkirchener Paläosees (links) reflektiert ruhige Ablagerungsbedingungen und unterscheidet sich nur geringfügig von der der gröberkörnigen Ereignislagen (rechts; Röntgendiffraktometriedaten, Angaben in Gew.-%).

Also visible in the clay pit are turbidites which make up about 1 % of the entire sequence. They are usually coarse silt to fine sand showing a sharp base and upward grading and are also usually rich in mica and quartz and depleted in carbonates. Some of them visible in the clay pit show cross bedding and erosive bases.

The radiocarbon ages, as mentioned above, indicate high sedimentation rates for the upper part of the sequence, which is supported by the palynological analyses. Bortenschlager & Bortenschlager (1978) identified 17 vegetation periods preserved within a sediment column of 86 cm thickness, resulting in an average sedimentation rate of about 5 cm/year. Unpublished luminescence ages from drill cores show that such a high sedimentation rate is common also for the deeper and higher parts of the sequence. The spacing of the microscopic clay-rich layers mentioned above also fits with a sedimentation rate of several centimetres per year.

Stop 2: Gravel pit Absamer Grube

Formerly known as Pfanzelter Grube, this gravel pit offers by far the largest exposure in the central Inn Valley of "Terrassenschotter" and their transition into the LGM basal till (Fig. 7A). Gravel is exposed in the gravel pit between 767 and 830 m a.s.l., i.e. is at least 63 m thick (B. Kempf, Fröschl Bau, pers. comm. 2014). Drillings revealed that the transition to the underlying sands occurs within a few tens of metres below the base of the quarry.

The gravel is crudely stratified and shows shallow cross-bedded channel-fills, imbrication and rare intercalated sand lenses up to about half a metre thick. Flow direction

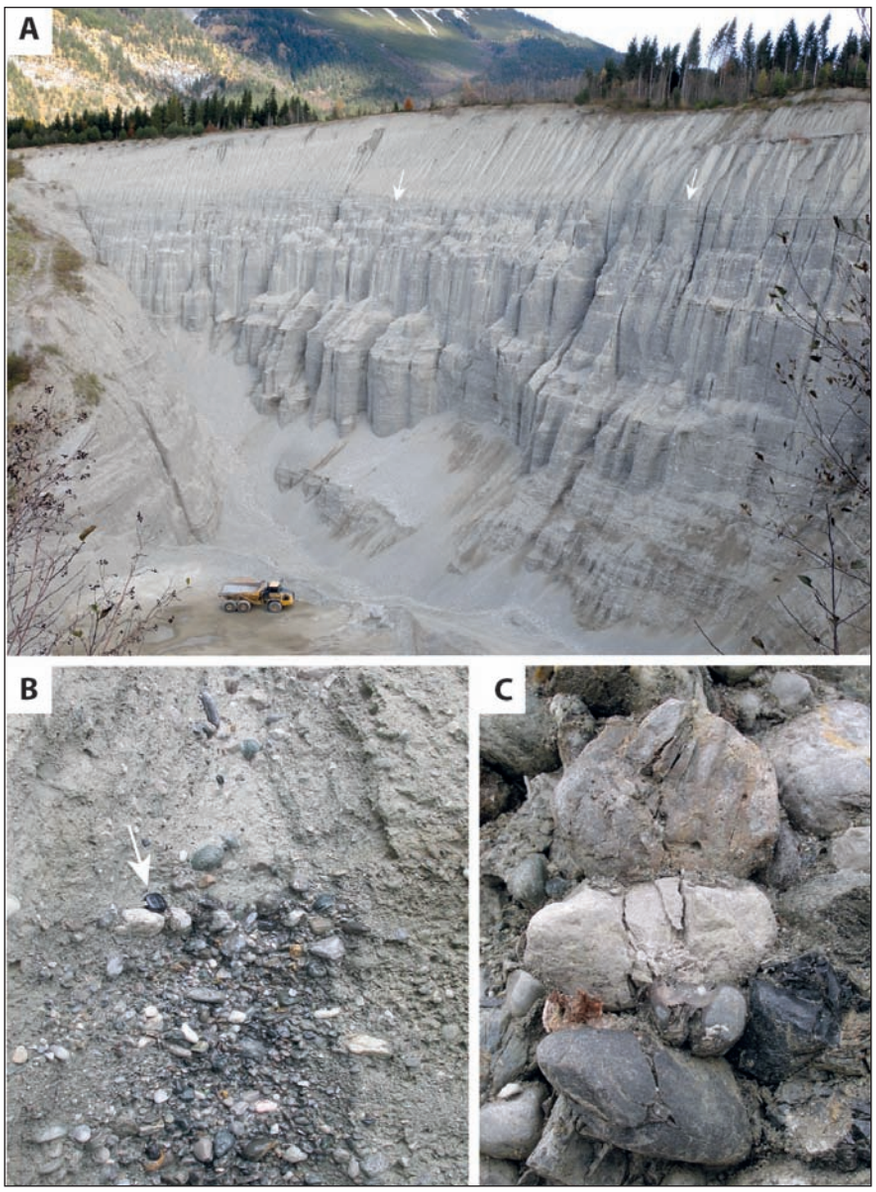

Fig. 7: The Absamer Grube offers the largest exposure of the sediment fill in the Gnadenwald terrace. A: The eastern wall of the pit (view towards NE) exposes ca. 60 m of horizontally stratified gravel ("Terrassenschotter") sharply overlain (arrows) by a very thick basal till. B: Close-up of this sharp boundary marked by a car key (arrow). Note that water washed away the sandy matrix of the underlying gravel in the central part of the picture. Well rounded clasts of gravel are incorporated into the lower part of the till. C: Cracked clasts a few metres beneath the transition to the basal till. Width of image 20 cm.

Abb. 7: Die Absamer Grube bietet den größten Einblick in die Sedimentfüllung der Gnadenwald-Terrasse. A: Die östliche Wand der Schottergrube (Blickrichtung NE) schließt ca. 60 m horizonal geschichtete Kiese („Terrassenschotter") auf, scharf überlagert (Pfeile) von sehr mächtiger Grundmoräne. B: Detail dieses scharfen Kontaktes markiert durch einen Autoschlüssel (Pfeil). Beachte, dass die sandige Grundmasse im zentralen Bereich des Bildes ausgewaschen wurde. Gut gerundete Kiesgerölle wurden in den unteren Teil der Moräne aufgenommen. C: Geknackte Klasten einige Meter unterhalb des Kontaktes zur hangenden Grundmoräne. Bildbreite 20 cm.

according to the cross-bedding was dominantly from West to Southwest (Patzelt & Resch 1986: 54). Outsized blocks of up to several metres in diameter are locally present. Fine-grained sediments and paleosols are completely lacking. Compared to modern Inn sediments these fluvioglacial gravels are texturally less mature (Mangelsdorf 1971). The character of these coarse-grained sediments strongly resembles that of a proglacial outwash fan formed by a braided river network during summer. Clasts composed of sandy matrix have rarely been observed and have been interpreted as clasts which were eroded and transported by the river in a frozen state (see above) pointing towards an Arctic climate. Gravel layers locally show incipient cementation by calcite (locally known as "Sommergfrier").

Patzelt & Resch (1986: 55) summarised the provenance of the gravel clasts and noted a marked abundance of material derived from the Wipp Valley south of Innsbruck, in addition to index clasts such as the granite from the Julier region in the upper Engadin, characterised by greenish feldspar crystals, but also well-rounded fragments of Pleistocene Red Hötting Breccia from the slope north of Innsbruck.

The gravel is sharply overlain by matrix-rich basal till (Fig. 7B) whose first few metres show well-rounded gravel clasts apparently incorporated into the till by erosion of the glacier's gravel substrate. The till is exceptionally thick at this site varying between 10 m and 33 m (B. Kempf, Fröschl Bau, pers. comm. 2014) and has to be removed prior to extraction of the gravel. The greatest thickness is observed on the eastern wall of the quarry and is likely due to drumlinisation. Airborne laserscanning data reveals the presence of WSW-ENE-oriented broad ridges east of the quarry which are regarded as subglacial bedforms. Near the contact to the overlying till cracked pebbles are locally common (Fig. 7C) attesting to over-consolidation caused by ice.

No organic remains have been reported from this outcrop and no chronological information is available. The gravel is clearly younger than the "Baumkirchner Bändertone", and radiocarbon-dated bone fragments found in the former Mils gravel pit 1.2 km to the Southwest suggest an age of 31.1–31.9 cal ka BP (see above), which is currently the best maximum age constraint for the arrival of central Alpine ice in the central Inn Valley (considering that the accumulation rate of these "Vorstoßschotter" was high).

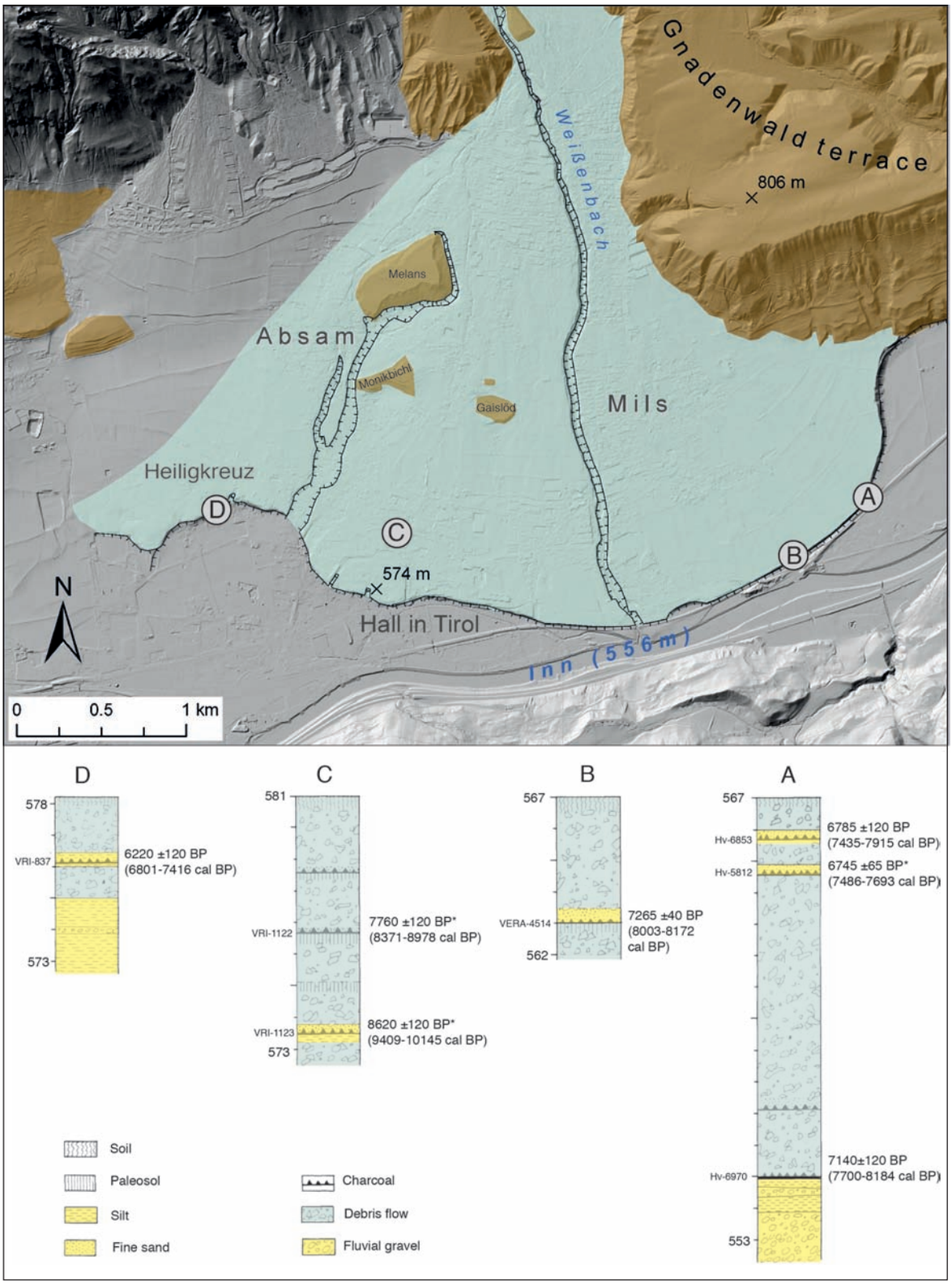

Fig. 8: Map of the alluvial Hall fan modified after Patzelt (2008), superimposed on a digital elevation map (©Land Tirol, tiris, www.tirol.gv.at/tiris). Sediments of the debris-flow fan and those of the Inn River are highlighted by light blue and yellow colours, respectively. Middle to Upper Würmian terrace sediments are shown in brown and form island-like hills inside the fan. Note that the entire southern rim of the fan is an erosive escarpment and streams dissect the fan. Letters A to D refer to sediment sections shown below with radiocarbon-dated organic remains. Ages were calibrated using INTCAL13 and are given in brackets (2-sigma uncertainty range). Data marked by an asterisk were incorrectly printed in Patzelt (2008) and the correct version is given here (G. Patzelt, pers. comm. 2014). Depths in m a.s.l. as well as the radiocarbon lab codes are given on the left side of the columns.

Abb. 8: Karte des Fächers von Hall, modifiziert nach Patzelt (2008), auf der Grundlage eines digitalen Höhenmodells (©Land Tirol, tiris, www.tirol.gv.at/tiris). Die Sedimente des Murschuttfächers und die des Inns sind in Hellblau bzw. Gelb gehalten. Terrassensedimente des Mittleren und Oberen Würm (braun) bilden inselartige Hügel innerhalb des Fächers. Der südliche Rand des Schwemmfächers ist eine erosiv entstandene Böschung und einzelne Bachläufe durchschneiden den Fächer. Die Buchstaben A bis D benennen die unten abgebildeten Profile mit Radiokarbon-datierten organischen Resten. Die Alter wurden mit INTCAL13 kalibriert und sind in Klammer angegeben (2-sigma Unsicherheitsbereich). Werte, die mit einem Sternchen versehen sind, wurden in Patzelt (2008) inkorrekt publiziert und die korrekten Werte sind hier gegeben (G. Patzelt, pers. Mitt. 2014). Die Tiefe in m Seehöhe sowie die Nummern der Radiokarbonlabors sind auf der linken Seite der Profile angegeben.

Stop 3: Overview of Hall fan

The Gnadenwald plateau is terminated in the West by the large alluvial fan emerging from the Hall Valley (Figs. 1, 8A). Its apex is located at ca. 880 m a.s.l. and the distal base is at the Inn River (560 m a.s.l.). This alluvial fan is the largest of its kind in Tyrol (8.6 km^2), except for a few fans in the Vinschgau region of South Tyrol (Klebelsberg 1947; Fischer 1965). As a result of the sediment wedge crossing the Inn Valley, the Inn River was pushed to its southernmost position. By contrast, just 8 km upstream in the city of Innsbruck, the Sill River has forced the Inn to the northernmost rim of the valley where it erodes pre-Quaternary rocks.

The fan from the Hall Valley apparently followed a pre-existing topographic depression carved by the LGM ice into the westernmost extension of today's Gnadenwald terrace. This is shown by the presence of hills made up of fluvioglacial gravel, sand and silt (Heissel 1954: 294) sticking out within the fan (Fig. 8) and the largest of these hills (Melans) is capped by a few metres of till rich in crystalline rock fragments. Its elevation is about 80–90 m lower than the elevation of the base of the till on the western margin of the Gnadenwald terrace. In addition, the flat, till-covered surface of the Melans hill is inclined towards the South, rep-

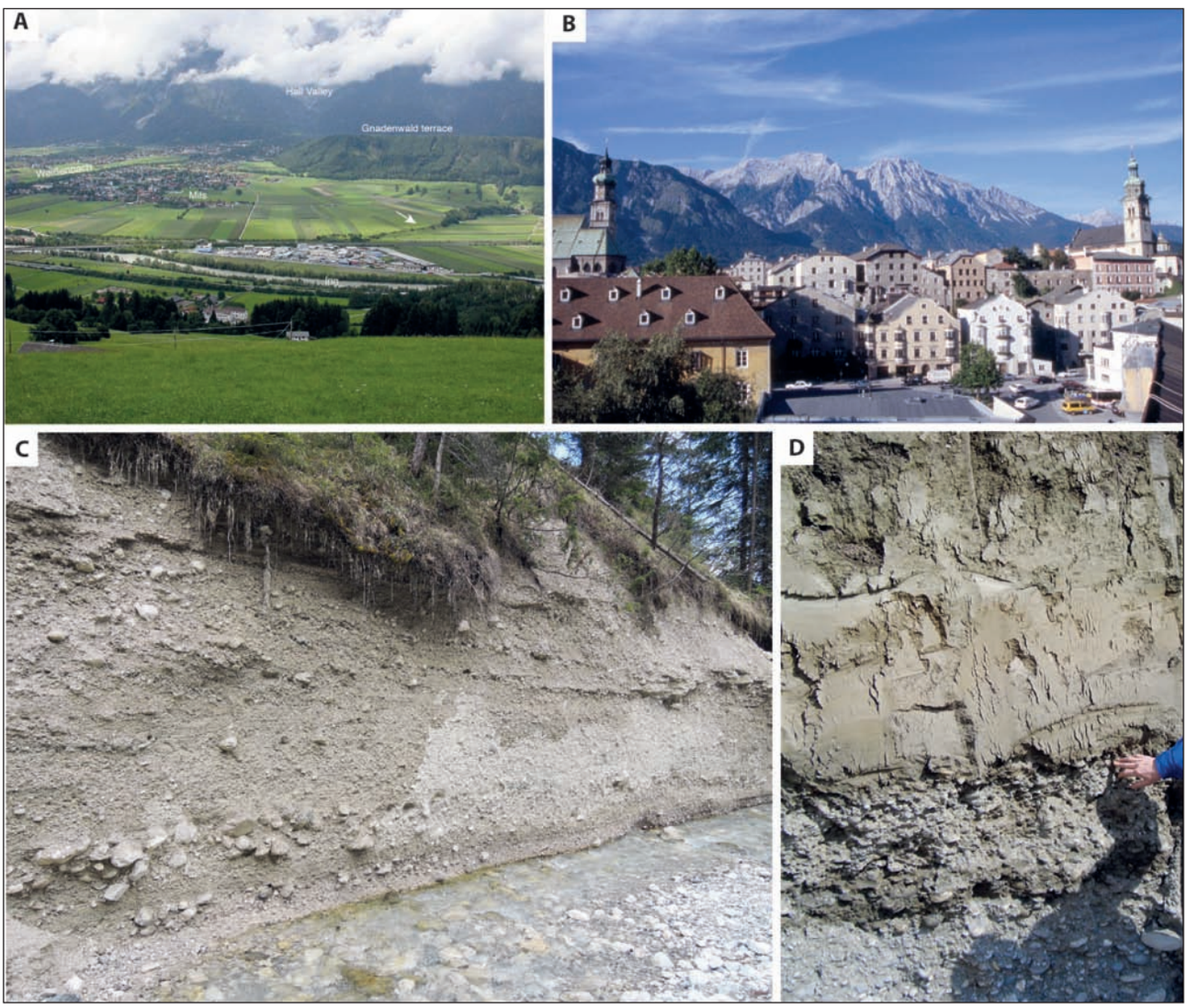

Fig. 9: Images of the Holocene Hall fan. A: Oblique view of the southeastern segment of the fan. The escarpment (white arrow) can be followed all along the southern rim of the fan. B: This escarpment divides the city of Hall in Tirol into a lower level corresponding to the flood plain of the Inn River (houses in the foreground) and a higher level (second row of houses as well as the two churches) which sits on the edge of the fan. View towards NNE. C: Typical character of the texturally immature fan sediment, whereby massive debris-flows alternate with crudely bedded gravel. Some layers near the right margin of the picture show incipient cementation and hence stick out of the wall. Exposure at the Weißenbach near the mouth of the Hall Valley. This outcrop is up to ca. 3.5 m high and overlain by ca. 20 m of debris-flow sediments. D: Brown loamy floodplain sediment sharply overlying partly imbricated fluvial Inn River gravel. These fine-grained sediments were deposited during aggradation of the Hall fan and are also present underneath the city of Innsbruck. Construction site at Südtiroler Straße in the western part of Hall in Tirol.

Abb. 9: Bilder des holozänen Haller Schwemmfächers. A: Schrägansicht des südöstlichen Segmentes des Fächers. Die Böschung (weißer Pfeil) kann den gesamten Südrand des Fächers entlang verfolgt werden. B: Die Böschung teilt die Stadt Hall in Tirol in eine Untere Stadt (Häuser im Vordergrund) und eine Obere Stadt ein (zweite Reihe von Häusern sowie zwei Kirchen), die auf der Kante des Fächers sitzt. Blickrichtung NNE. C: Typischer Charakter des texturell unreifen Fächersedimentes bestehend aus massigen Murschuttablagerungen und damit wechsellagernden, undeutlich geschichteten Kiesen. Einzelne Bänke auf der rechten Bildseite zeigen beginnende Zementation und wittern vor. Aufschluss am Weißenbach am Ausgang des Halltales. Dieser Aufschluss ist etwa 3,5 m hoch und wird von ca. 20 m Murschuttsedimenten überlagert. D: Braunes, lehmiges Überflutungssediment, das mit scharfer Grenze teilweise imbrizierten Kiesen des Inns auflagert. Die feinkörnigen Sedimente wurden während der Aggradation des Haller Schwemmfächers abgelagert und finden sich auch im Untergrund der Stadt Innsbruck. Baugrubenaufschluss Südtiroler Straße im Westteil von Hall in Tirol.

resenting a remnant of the original LGM glacier bed close to the central axis of the Inn Valley (Patzelt 2008).

The fan is clearly inactive and although the Hall Valley is characterised by high relief and abundant sediment supply, even large debris-flow-type events (such as the two events devastating the road into the valley in July 2010 and August 2011) do not get even close to reaching the proximal part of the fan. The only natural stream (Weißenbach) entrenched up to 13 m into the upper part of the fan at Walderbrücke and the entire distal margin of the fan is a steep escarpment up to 15 m high marking the back-cutting of the Inn River since the fan sedimentation has ceased (Figs. 8, 9A). This escarpment gives rise to the characteristic image of the city of Hall in Tirol, where the medieval part of town is located some 14 m above the "Untere Stadt" (Fig. 9B).

The fan sediments are almost exclusively derived from the Hall Valley as shown by the limestone and dolomite clasts and the nearly complete lack of crystalline rocks. Matrix-rich, sandy gravel showing poor bedding and attributed to massive debris flows (Fig. 9C) are rarely interbedded with locally slightly pedogenetically overprinted fine sandy layers. Thin, dark layers containing charcoal pieces have been interpreted as possibly human-induced forest fires (Patzelt 2008).

The 3D geometry of the fan is not known due to the lack of drillings and geophysical measurements, but it is likely that it is considerably thinner than e.g. the Gadria fan in South Tyrol, which formed at about the same time and is about 24 % larger in size (Fischer, 1965, 1990). Air-raid shelters in Hall in Tirol driven into the escarpment of the fan during World War II encountered fluvial sands of the Inn River (i.e. mica-rich fine sands, locally referred to as "Mehlsande"; Heissel 1954: 294) underneath the debris-flow gravel, indicating that the fan at some point in time prograded across the fluvial sediments. This superposition was well exposed along the southeastern escarpment of the Hall fan (Fig. 8A).

Radiocarbon dates of charcoal found in the fan sediments were first reported by Fliri (1977) and subsequently updated by Patzelt (1987 and 2008). They are exclusively from distal portions of the fan (Fig. 8) and indicate that the fan was built during the first half the Holocene. Most dates suggest that the majority of the aggradation occurred during the 9th and 8th millennia BP (Fig. 8) when the fan stretched all the way across the valley and blocked the drainage of the Inn River. As a result, loamy lacustrine and flood-plain sediments were laid down upstream (Fig. 9D). Mined for brick production decades ago west of Heiligkreuz (Blaas 1885: 57) these sediments reach up to an elevation of 576 m a.s.l. on the southwestern corner of the fan (section D in Fig. 8), i.e. 16 m higher than the present-day level of the Inn River flood plain at Hall in Tirol (Patzelt 2008). This shallow lake and its adjacent swampy flood plain extended upstream for up to ca. 9 km into today's centre of Innsbruck, where between 1 and 2 m thick sandy sediments are present beneath the coarse-grained gravel of the Sill fan (Blaas 1896: 183). Drill cores near the old Hungerburg funicular recorded a 2.5 m-thick peat layer which was correlated with this flooding (Patzelt 1987, 2008). Two samples from its base were radiocarbon-dated to 7695 ± 95 BP (8328–8716 cal BP) and 7740 ± 35 BP (8440–8590 cal BP) and a sample near the top of this peat horizon yielded an age of 6260 ± 35 BP (7028-7266 cal BP; INTCAL13 re-calibration, 2-sigma range, original data reported in Patzelt 1987, 2008). These dates are similar to those obtained from the fan itself (Fig. 8) and demonstrate an interval of recurrent high-magnitude debris flows (partly recorded also in nearby fans in the Inn Valley; Patzelt 1987). The palaeoclimatic significance of this strong geomorphological activity – unprecedented in the context of the entire Holocene in the western Austrian Alps – is poorly understood, but a recent comparison with other climate archives points towards a very wet ("pluvial") episode probably in response to a major climate event in the Mediterranean realm between ca. 8200 and 7300 cal BP recorded by the deposition of the youngest of a series of sapropels (Spötl et al. 2010).

References

Ampferer, O. (1904): Studien über die Inntalterrassen. – Jahrbuch der Geologischen Reichsanstalt, 54: 91–160.

Ampferer, O. (1907): Glazialgeologische Beobachtungen im unteren Inntale. – Zeitschrift für Gletscherkunde, 2: 29–54.

Ampferer, O. (1908): Über die Entstehung der Inntal-Terrassen. – Zeitschrift für Gletscherkunde, 3: 111–142.

Blaas, J. (1885): Ueber die Glacialformation im Innthale. – Zeitschrift des Ferdinandeum, 29: 1–120.

Blaas, J. (1890): Erläuterungen zur geologischen Karte der diluvialen Ablagerungen in der Umgebung von Innsbruck. – Jahrbuch der Geologischen Reichsanstalt, 40: 21–49.

Blaas, J. (1896): Der Boden der Stadt Innsbruck. Eine geologische Skizze. – Berichte des naturwissenschaftlich-medizinischen Vereins Innsbruck, 22: 167–192.

Bortenschlager, I. & Bortenschlager, S. (1978): Pollenanalytische Untersuchung am Bänderton von Baumkirchen (Inntal, Tirol). – Zeitschrift für Gletscherkunde und Glazialgeologie, 14: 95–103.

Chaline, J. & Jerz, H. (1984): Arbeitsergebnisse der Subkommission für Europäische Quartärstratigraphie. Stratotypen des Würm-Glazials. – Eiszeitalter und Gegenwart, 35: 185–206.

Felber, H. (1971): Altersbestimmungen nach der Radio-Kohlenstoffmethode an Fossilfunden aus dem Bänderton von Baumkirchen (Inntal, Tirol). – Zeitschrift für Gletscherkunde und Glazialgeologie, 7: 25–29.

Fischer, K. (1965): Murkegel, Schwemmkegel und Kegelsimse in den Alpentälern. – Mitteilungen der Geographischen Gesellschaft München, 50: 127–159.

Fischer, K. (1990): Entwicklungsgeschichte der Murkegel im Vinschgau. – Der Schlern, 64: 93–96.

Fliri, F. (1964): Beiträge zur Morphologie der Gnadenwaldterrasse im mittleren Inntal. – Zeitschrift für Geomorphologie N.F., 8: 232–240.

Fliri, F. (1970): Neue entscheidende Radiokarbondaten zur alpinen Würmvereisung aus den Sedimenten der Inntalterrasse (Nordtirol). – Zeitschrift für Geomorphologie N.F., 14: 520–521.

Fliri, F. (1971): Beiträge zur Stratigraphie und Chronologie der Inntalterrasse im Raum von Innsbruck. – Veröffentlichungen des Museum Ferdinandeum, 51: 5–21.

Fliri, F. (1973): Beiträge zur Geschichte der alpinen Würmvereisung: Forschungen am Bänderton von Baum-

kirchen (Inntal, Nordtirol). – Zeitschrift für Geomorphologie N.F., Suppl., 16: 1–14.

Fliri, F. (1975): Das Inntal-Quartär im Westteil der Gnadenwaldterrasse. – In: Fliri, F. & Leidlmair, A. (eds.): Tirol – Ein geographischer Exkursionsführer. – Innsbrucker Geographische Studien, 2: 79–87.

Fliri, F. (1976): Völs, Hall, Mils, Fritzens, Oelberg and further opportunities for confusing the alpine Würm chronology. – Zeitschrift für Gletscherkunde und Glazialgeologie, 12: 79–84.

Fliri, F. (1977): Neue Beiträge zur Geschichte des Haller Schwemmkegels. – Tiroler Heimatblätter, 1977: 90–93.

Fliri, F. (1999): Baumkirchen. – Heimatkunde eines Dorfes in Tirol. – 512 p., Baumkirchen.

Fliri, F., Bortenschlager, S., Felber, H., Heissel, W., Hilscher, H. & Resch, W. (1970): Der Bänderton von Baumkirchen (Inntal, Tirol). Eine neue Schlüsselstelle zur Kenntnis der Würm-Vereisung der Alpen. – Zeitschrift für Gletscherkunde und Glazialgeologie, 6: 5–35.

Fliri, F., Hilscher, H. & Markgraf, V. (1971): Weitere Untersuchungen zur Chronologie der alpinen Vereisung (Bänderton von Baumkirchen, Inntal, Nordtirol). – Zeitschrift für Gletscherkunde und Glazialgeologie, 7: 5–24.

Fliri, F., Felber, H. & Hilscher, H. (1972): Weitere Ergenbnisse der Forschung am Bänderton von Baumkirchen (Inntal, Tirol). – Zeitschrift für Gletscherkunde und Glazialgeologie, 8: 203–213.

Heissel, W. (1954): Beiträge zur Quartärgeologie des Inntales. – Jahrbuch der Geologischen Bundesanstalt, 98: 252-322.

Klasen, N., Fiebig, M., Preusser, F., Reitner, J.M. & Radtke, U. (2007): Luminescence dating of proglacial sediments from the Eastern Alps. – Quaternary International, 164–165: 21–32.

Klebelsberg, R. v. (1947): Meran-Mais und Hall – von der Geschichte zweier Schuttkegel. – Tiroler Heimat, 11: 13–16.

Klebelsberg, R. v. (1932): Ein Fischfund in den Bändertonen des Inntales (Tirol). – Zeitschrift für Gletscherkunde, 20: 137–138.

Koci, A. (1980): Paleomagnetic research into the laminated silts at the locality of Baumkirchen (Inntal, Tirol). – Zeitschrift für Gletscherkunde und Glazialgeologie, 16: 99–105.

Köhler, M. & Resch, W. (1973): Sedimentologische, geochemische und bodenmechanische Daten zum Bänderton von Baumkirchen (Inntal/Tirol). – Veröffentlichungen der Universität Innsbruck, 86: 181–215.

Köhler, M., Eder, S., Scholz, M. & Poscher, G. (2005): Der Tunnel Vomp-Terfens – Von der Variantenstudie bis zur Bauausführung. – Felsbau, 23: 83–89.

Krainer, K. & Poscher, G. (1990): Ice-rich, redeposited diamicton blocks and associated structures in Quaternary outwash sediments of the Inn Valley near Innsbruck, Austria. – Geografiska Annaler, 72A: 249–254.

Ladurner, J. (1955): Korngrößen und Mineralführung zweier Sande aus der Gnadenwalder Terrasse (Schottergrube Mils bei Hall in Tirol). – Mitteilungen der Geologischen Gesellschaft Wien, 48: 129–137.

Mangelsdorf, J. (1971): Beiträge zur Sedimentologie des Inntalquartärs. – In: Mostler, H. (ed.): Festband des Geologischen Instituts, 300 Jahr-Feier der Universität Innsbruck: 399–440; Innsbruck.

Maurer, H. & Nabholz, W. (1972): Korngrössenuntersuchungen einer Bändertonprobe von Baumkirchen. – Zeitschrift für Gletscherkunde und Glazialgeologie, 8: 235–236.

Mayr, F. (1968): Über den Beginn der Würmeiszeit im Inntal bei Innsbruck. – Zeitschrift für Geomorphologie N.F., 12: 256–295.

Mayr, F. (1976): The Oelberg paleomagnetic events and the problem of radiocarbon dates around 28,000 years B.P. – In: Easterbrook, D.J. & Sibrava, V. (eds.): Project 73-1-24 "Quaternary Glaciations in the Northern Hemisphere", Report no. 3: 208–216; Bellingham (IUGS).

Patzelt, G. (2008): Der Schwemmkegel von Hall. - In: Zanesco, A. & Schmitz-Esser, R. (eds.): Neues zur Geschichte der Stadt, Vol. 2: 12-21; Hall in Tirol (Ablinger Garber).

Patzelt, G. (1996): Jahresbericht 1996 des Instituts für Hochgebirgsforschung, Universität Innsbruck.

Patzelt, G. & Resch, W. (1986): Quartärgeologie des mittleren Tiroler Inntales zwischen Innsbruck und Baumkirchen. – Jahresbericht und Mitteilungen des oberrheinischen geologischen Vereins N.F., 68: 43–66.

Penck, A. (1890): Die Glacialschotter in den Ostalpen. – Mitteilungen des Deutschen und Oesterreichischen Alpenvereins, 23: 289–292.

Penck, A. & Brückner, E. (1909): Die Alpen im Eiszeitalter Vol .1. Die Eiszeiten in den nördlichen Ostalpen. – 393 p., Leipzig (C.H. Tauchnitz).

Poscher, G. & Lelkes-Felvári, G. (1999): Lithofazielle und genetische Aspekte der Schwermineralführung alpiner Lockersedimente (Inntal, Tirol). – Abhandlungen der Geologischen Bundesanstalt, 56: 407–414.

Poscher, G., Fisch, H., Mammel, R. & Sedlacek, C. (2002): Konfliktfeld Untertagebau und alpine Wasserresourcen. – Felsbau, 20: 21–31.

Preusser, F., Reitner, J.M. & Schlüchter, C. (2010): Distribution, geometry, age and origin of overdeepened valleys and basins in the Alps and their foreland. – Swiss Journal of Geosciences, 103: 407–426.

Resch, W. (1972): Mikropaläontologische Untersuchungen im Bänderton von Baumkirchen (Inntal, Tirol). – Zeitschrift für Gletscherkunde und Glazialgeologie, 8: 215–230.

Sanders, D. & Ostermann, M. (2011): Post-last glacial alluvial fan and talus slope associations (Northern Calcareous Alps, Austria): A proxy for Late Pleistocene to Holocene climate change. – Geomorphology, 131: 85–97.

Sarnthein, R. v. (1937): Untersuchungen über den Pollengehalt einiger Moränen und Terrassensedimente des Inntales. – Zeitschrift für Gletscherkunde, 25: 232–236.

Schiegl, W.E. & Trimborn, P. (1972): Die paläoklimatische Bedeutung des Deuteriumgehaltes von fossilen Holzproben aus den Bändertonen von Baumkirchen (Inntal). – Zeitschrift für Gletscherkunde und Glazialgeologie, 8: 231–233.

Spötl, C., Nicolussi, K., Patzelt, G., Boch, R. & Daphne Team (2010): Humid climate during deposition of sapropel 1 in the Mediterranean Sea: Assessing the influence on the Alps. – Global and Planetary Change, 71: 242–248.

Spötl, C., Reimer, P.J., Starnberger, R. & Reimer, R. (2013): A new radiocarbon chronology of Baumkirchen, stratotype for the onset of the Upper Würmian in the Alps. – Journal of Quaternary Sciences, 28: 552–558.

Steinbrener, J. (2011): Sedimentologische und geochemische Untersuchung der Tiefbohrung Wattens I (Tirol). – Unpubl. MS thesis, Univ. Vienna, 151 p.

van Husen, D. (2000): Geological processes during the Quaternary. – Mitteilungen der Österreichischen Geologischen Gesellschaft, 92: 135–156.

van Husen, D. (1983a): A model of valley bottom sedimentation during climatic changes in a humid alpine environment. – In: Evenson, E.B., Schlüchter, C. & Rabassa, J. (eds.): Tills and related deposits: 341–344; Rotterdam (Balkema).

van Husen, D. (1983b): General sediment development in relation to climatic changes during Würm in the eastern Alps. – In: Evenson, E.B., Schlüchter, C. & Rabassa, J. (eds.): Tills and related deposits: 345–349; Rotterdam (Balkema).

Weber, F., Schmid, C. & Figala, G. (1990): Vorläufige Ergebnisse reflexionsseimsischer Messungen im Quartär des Inntales/Tirol. – Zeitschrift für Gletscherkunde und Glazialgeologie, 26, 121–144.

Zoeke, M.E. (1944): Tiroler Bändertone. – Unpubl. PhD thesis, Univ. Göttingen, 50 p.

Notes

The Hötting Breccia – a Pleistocene key site near Innsbruck, Tyrol

Die Höttinger Brekzie – eine Schlüsselstelle des Pleistozäns bei Innsbruck, Tirol

Diethard Sanders, Christoph Spötl

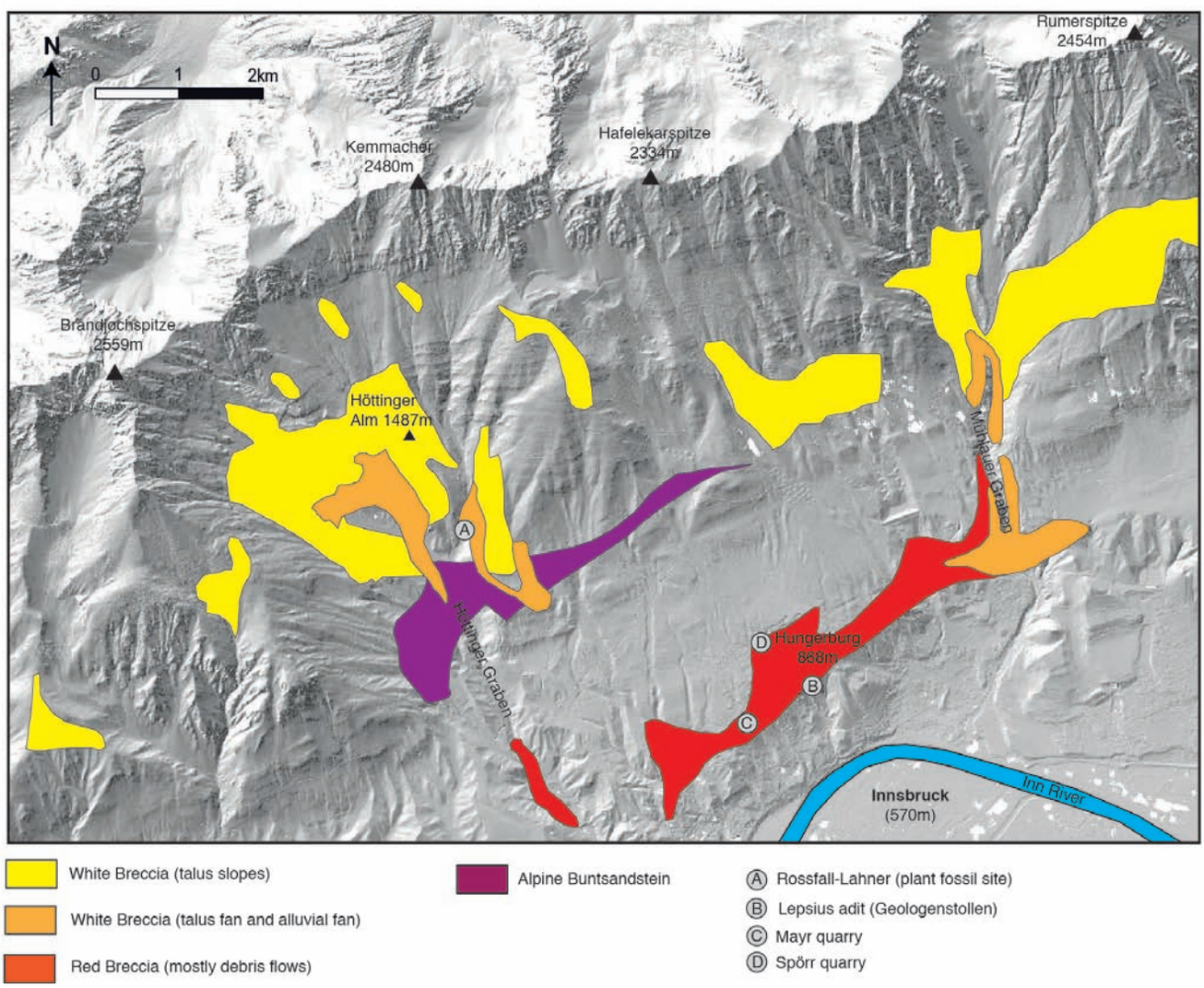

Fig. 1: Laserscan terrain image of the mountain slope north of Innsbruck (© Land Tirol, tiris, www.tirol.gv.at/tiris) showing the areal distribution of Hötting Breccia and the location of sites mentioned in the text.

Abb. 1: Laserscan-Geländemodell der Bergflanke nördlich von Innsbruck (©Land Tirol, tiris, www.tirol.gv.at/tiris) mit den Vorkommen der Höttinger Brekzie und den im Text erwähnten Örtlichkeiten.

1 Introduction

Innsbruck, located in the interior of the Eastern Alps, is not only surrounded by fascinating geology, it also is one of the very few examples worldwide where the historical city centre is built of a Quaternary breccia. Formed as an alluvial-fan and talus deposit the so-called Hötting Breccia ("Höttinger Brekzie", hereafter abbreviated as HB) is a coarse-clastic succession exposed on the mountain slope north of Innsbruck (Fig. 1). Quarried between at least the 14th and the early 20th century, the reddish to light brownish colour of this Pleistocene rock dominates the character of many historical buildings in Innsbruck (Objoes et al. 2012, Siegl & Fahlenbock 2012).

The HB has also been of considerable interest to Earth scientists. Firstly, this can be traced to the fact that this Pleistocene unit is among the only ones in the Alps that contain a flora of interglacial character. Given the stratigraphic setting sandwiched between under- and overlying till the HB provided – historically speaking – the first unequivocal proof of multiple Pleistocene glaciations. Secondly, the breccia outcrops provide a rare example of a well-preserved and well-exposed mountain-flank succession of talus slopes contiguous to alluvial fans.

2 A brief history of research

The HB has attracted the interest of Quaternary geologists since the second half of the 19th century, when plant remains were first discovered at the Rossfall-Lahner site (location A in Fig. 1; see below). Initially considered as Tertiary species (Pichler 1859, Stur 1886) the flora was later identified as a Pleistocene assemblage characterised by the leaves of what is known today as *Rhododendron ponticum* var. *sebinense* (Denk 2006). Wettstein (1892), following up an earlier study by Ettingshausen (1885), provided a monograph of this flora; later palaeobotanical studies by Murr (1926), Gams (1936) and more recently Denk (2006) revealed that some 60 taxa are preserved in fine-grained intervals of the HB.

The HB also played a central role in the historical dispute between those advocating one major glaciation during the Pleistocene versus those arguing in favour of repeated glaciations that had reached the foreland of the Alps. At the core of this debate was an outcrop in the eastern Weiherburggraben north of Innsbruck's zoological garden "Alpenzoo" (location B in Fig. 1). The long-standing question, whether a till cropping out below the Red Breccia is indeed stratigraphically underlying the breccia (as first suggested by Penck 1882) was finally settled in 1913, when a 20 m-long, horizontal adit was excavated along the base of the breccia (plans for this artificial outcrop go back at least a quarter of a century, see Blaas 1889). The construction was initiated by R. Lepsius who also managed to obtain the necessary funds from the Academies in Berlin and Vienna. Known as "Lepsius-" or "Geologenstollen" (location B in Fig. 1) this adit has provided unequivocal evidence that the till is indeed older than the HB (Lepsius 1913, Ampferer 1914). Given the fact that the HB contains plant remains of interglacial character and is, in turn, overlain by younger till, the construction of this adit meant the final defeat of the small group of Quaternary scientists who had negated the possibility of multiple glaciations. A few years later Penck (1921) provided a thorough monograph on the HB.

During road construction between Innsbruck and the Hungerburg plateau ("Höhenstraße") new outcrops in Pleistocene sediments suggested the presence of possibly

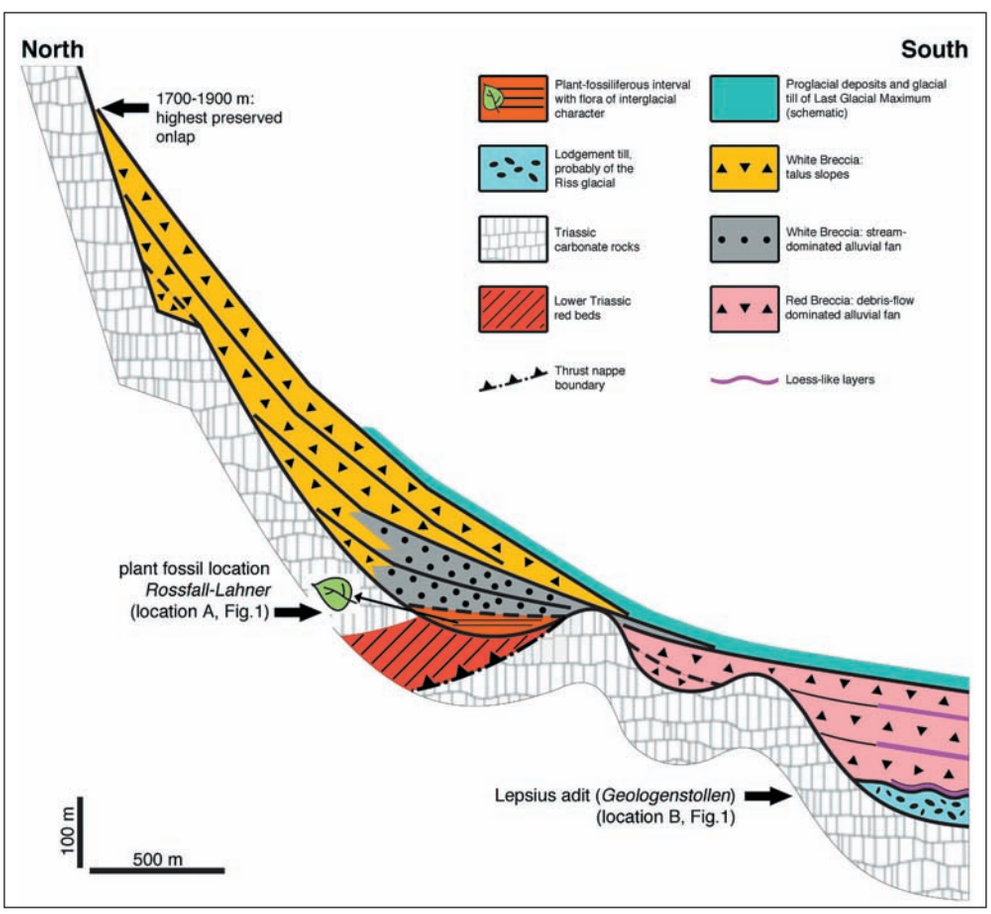

Fig. 2: Schematic cross-section of the mountain slope north of Innsbruck and the internal architecture of the HB (modified from Sanders 2010). Note vertical exaggeration. See text for description and discussion.

Abb. 2: Schematischer vertikal übersteilter Schnitt des Untergrundes und des inneren Aufbaus der Höttinger Brekzie (verändert nach Sanders 2010). Siehe Text für Beschreibung und Erörterung.

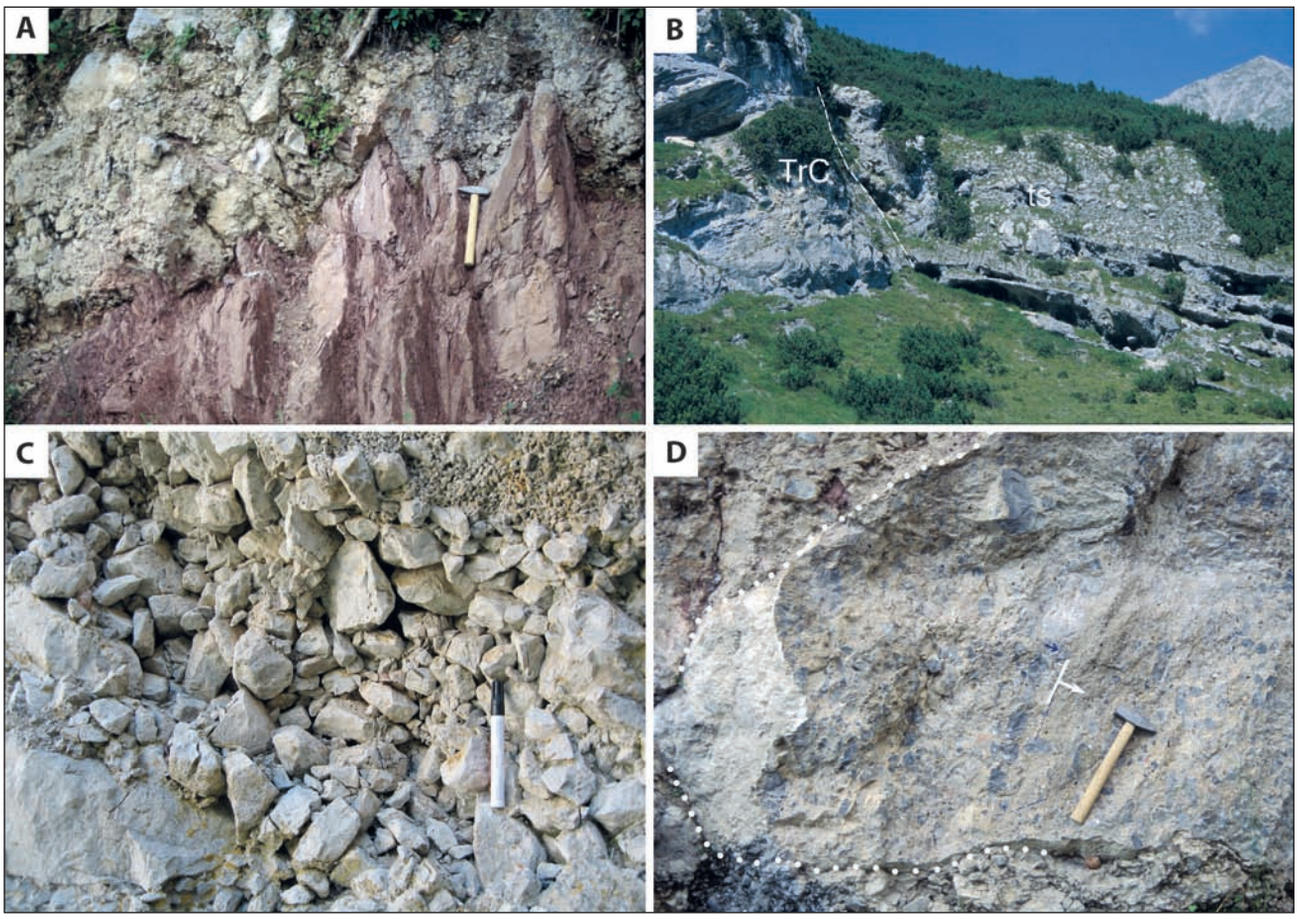

Fig. 3: Field exposures of HB. A. Base of HB at 1110 m a.s.l. along the right flank of the Höttinger Graben ravine. Here, Lower Triassic red beds ("Alpiner Buntsandstein", see Fig. 1) are overlain by the breccia. The red beds supplied lithoclasts and red-coloured matrix to the HB. The hammer is 35 cm in length. B. Onlap of lithified talus-slope succession (ts) onto subvertical cliff of Triassic carbonate rocks (TrC), 1660 m a.s.l. Dashed white line hightlights the onlap surface. Inspection of the contact between the talus and the rock substrate indicated that it is not overprinted by faulting. C. Detail of lithified talus-slope succession in the upper part of the HB, showing a layer with primary openwork clast fabric. The pen is 14 cm in length. D. Intraclast of HB exposed in basal part of HB at 1110 m a.s.l. along the right flank of the Höttinger Graben ravine. In the fully lithified intraclast, stratification (white line with arrow) and tilted geopetal fabrics indicate that it was embedded in an overturned position. White stipples indicate part of the outline of the intraclast. The hammer is 35 cm long.

Abb. 3: Aufschlüsse der Höttinger Brekzie. A. Basis der Höttinger Brekzie auf 1110 m an der rechten Flanke des Höttinger Grabens. Untertriassische Rotsedimente (Alpiner Buntsandstein, vgl. Abb. 1) werden hier von der Brekzie überlagert. Diese Rotsedimente belieferten die Höttinger Brekzie mit Lithoklasten und rötlich gefärbter Matrix. Der Hammer ist 35 cm lang. B. Anlagerung (onlap) einer lithifizierten Talus-Abfolge (ts) auf eine subvertikale Wand aus Karbonatgesteinen der Trias (TrC). Die strichlierte weiße Linie bezeichnet die Anlagerungsfläche. Der Kontakt zwischen der Talus-Abfolge und der Felswand ist nicht durch eine Störung überprägt. C. Ausschnitt einer lithifizierten Talus-Abfolge im oberen Abschnitt der Höttinger Brekzie. Das Bild zeigt eine Kies-Schicht mit einem primär matrixlosen Gefüge. Der Stift ist 14 cm lang. D. Intraklast aus Höttinger Brekzie im basalen Anteil der Abfolge auf 1100 m an der rechten Flanke des Höttinger Grabens. Im Intraklasten zeigen verkippte Geopetal-Gefüge sowie die Stratifikation eine Einbettung in überkippter Lage an. Die weissen Punkte markieren den Umriss des Intraklasten. Der Hammer ist 35 cm lang.

two, stratigraphically distinct till horizons above the HB (Klebelsberg 1929, Katschthaler 1930). Later, Ampferer (1946) studied subsurface exposures excavated during the construction of air-raid shelters in this area and concluded that only one till layer is present above the HB. Paschinger (1950) provided a geomorphological study of the HB. Recent work on the HB focussed on the depositional regimes and facies architecture (Sanders & Ostermann 2006, Sanders 2010) as well as the still unresolved question about its chronological framework (Spötl & Mangini 2006, Gemmell & Spötl 2009) and provided a partial revision of the plant fossils and their palaeoenvironmental significance (Denk 2006).

3 Geological setting

The HB covers the south-facing slope of Nordkette, the southernmost mountain range of the Northern Calcareous Alps built of stacked cover-thrust nappes (Fig. 1). The Nordkette range consists of two superposed thrust nappes (Fig. 2). In the area of interest, the subjacent nappe comprises a Lower to Upper Triassic succession mainly of shallow-marine carbonate rocks and, subordinately, of cellular dolomites and shales. The overlying thrust nappe is mainly composed of Middle to Upper Triassic marine limestones and dolostones; in addition, the basal interval of the higher nappe consists of Lower Triassic red beds (Alpiner Buntsandstein, Werfen beds) exposed between 1040 and 1120 m a.s.l. In the area north of Innsbruck the surface exposure of these red beds narrows from a few hundreds of metres in width in the West to local outcrops only a few metres in extent near the eastern margin (Fig. 1).

The Inn valley follows a sinistral transpressive shear zone at the southern limit of the Northern Calcareous Alps (e.g., Ortner et al. 2006). The area of Innsbruck and the Inn valley fault eastward thereof are among the seismically most

active areas of the Eastern Alps (cf. Reinecker & Lenhardt 1999). The last, slightly damaging quake took place in 1965 (intensity I_o = 6), and more destructive ones of reconstructed I_o ~ 7–8 occurred during the 16th and 17th centuries (Hammerl et al. 2012). In reaction to historical quakes, the walls of city houses were reinforced by pillars made of HB, as well as by iron brackets stabilizing the houses.

3.1 Gross subdivision of the Hötting Breccia

The erosion of the Lower Triassic red beds imparted a characteristic reddish colour on the fine-grained matrix of the HB (Fig. 3A). In addition, erosion of cellular dolomites and limestones stratigraphically above the red beds is responsible for the light brownish colouration of the matrix. As a result, the part of the HB which accumulated downslope and directly on top of the red-bed outcrops has traditionally been termed Red Breccia ("Rote Brekzie") and comprises the major portion of the topographically lower part of the HB (Fig. 1 & 2). The White Breccia ("Weisse Brekzie"), in turn, consists of clasts of carbonate rocks only and contains a light-grey to whitish matrix of lime mudstone. The White Breccia mainly comprises the upper part of the HB.

3.2 Sediments under- and overlying the Hötting Breccia

At most locations, the breccia directly overlies Triassic carbonate rocks. Along its southern margin, however, at Lepsius adit, the breccia is underlain by lodgement till traditionally ascribed to the Riß Glacial (Ampferer 1914, Penck 1921, Patzelt & Resch 1986). Along the base of the HB, a layer of till can be traced for a few hundred metres toward the West. In the outcrop, however, the time-stratigraphic relation between the till and the breccia may appear unclear, because the till may also be an erosional remnant that onlaps the HB; it was this ambiguity that motivated the excavation of the Lepsius adit in 1913 (see above).

The HB is overlain by a clastic succession of complex stratigraphy which, in contrast to the breccia, is largely uncemented. The breccia was lithified before accumulation of these sediments, as indicated by the presence of clasts of HB therein as well as in fluvioglacial gravel ("Terrassenschotter") farther down the Inn Valley. The clastic succession overlying the HB includes also overcompacted lake sediments, which were quarried near Ölberg more than a century ago (Tegelgrube; Stur 1886, Blaas 1889). Cones of *Pinus mugo* var. *pumilio* embedded in these sediments yielded uncalibrated radiocarbon ages close to 50 ka (C. Spötl, unpublished data). This succession is topped by an upper till which formed during the Last Glacial Maximum. Lateglacial gravel deposits were locally deposited on top of this till. During the Holocene the geomorphological activity switched to incision of streams, and the slope of Nordkette became stabilized by vegetation, except for localised erosion areas supplying debris-flow fans (e.g. Rumer Mur). Today, the rock cliffs along the crest of the Nordkette are fringed by scree slopes of low activity. Apart from a glacial cirque (Schneekar) and a nivation kettle (Seegrube) the slope of Nordkette is sculptured by long avalanche ravines.

3.3 Morphology of the substrate of the Hötting Breccia

The truncation surface along the base of the HB shows a differentiated morphology. In the West, near Höttinger Alm (1487 m a.s.l.), the lithified talus slopes onlap very steep palaeo-cliffs that flanked a deep, cirque-like depression filled by diverse breccia deposits (Fig. 3B). Downslope of this depression, field mapping indicates that the HB fills a bedrock-incised ravine approximately 150 m in width (Fig. 1). With respect to their relatively low position on the mountain flank and their scale, the cirque-like depression and the former bedrock ravine are comparable to landforms produced by subsurface evaporite dissolution. In the eastern part of outcrop, the talus successions of the HB locally fill bedrock-incised chutes; farther downslope, the rock substrate shows 'grooves' – roughly parallel to the Inn valley – filled by HB (Fig. 2); these grooves were possibly produced by glacial erosion.

4 Facies and sedimentary succession

Deposits that may be ascribed to the HB are preserved as patches in a 7 km long, SW-NE striking belt. Figure 1 shows that the main outcrops are located in the central and northeastern sector, sheltered from later glacial erosion, whereas more patchy outcrops characterise the southwestern area. Apart from less widespread lithologies briefly characterised farther below, the HB comprises the following major facies types (see Sanders et al. 2009, Sanders 2010, for more detailed descriptions): (i) rockfall-supplied deposits of extremely poorly sorted, clast-supported, disordered breccias of boulders to gravels in unstratified intervals up to a few tens of metres in thickness; (ii) breccias of grain flows of very poorly to well-sorted, gravelly to cobbly openwork clast fabrics building strata typically a few decimetres in thickness and dipping with 25–35° (Fig. 3C); individual strata and stratal packages up to a few metres in thickness of these breccias are widespread in the upper, steep-dipping part of fossil talus slopes of the HB; (iii) breccias to conglomeratic breccias of cohesive debris flows are represented by extremely-poorly (bouldery to gravelly) to moderately sorted (gravelly), typically clast-supported deposits; individual strata are a few centimetres to about one metre thick and do not show a vertical segregation of clast size; large clasts may project from top; amalgamated breccia layers may build intervals a few metres in thickness; in the stratigraphically lower part of the HB, strata of this facies typically dip by a few degrees toward the South (see excursion stop 4 below); in the talus successions in the stratigraphically upper part dip may attain ~35–38°; (iv) water-laid breccias to conglomerates accumulated from ephemeral or strongly fluctuating surface runoff comprise a widely variable suite mainly of torrential channel-fills, sheet-flow deposits accumulated during waning flood stages, and lag deposits formed by slope wash and/or in shallow lateral parts of ephemeral channels; in the lower part of the HB water-laid rudites may comprise a significant to prevalent proportion of a succession; in the talus-fan successions in the stratigraphically upper part of the HB, water-laid deposits also comprise a major part.

Lower part of HB: In the main outcrop area, the stratigraphically lower part of the HB, comprises Red Breccia deposited from alluvial fans (Fig. 1). As mentioned above, the exposure of Lower Triassic red beds in the bedrock narrows from SW to NE. As a result, the overall intensity of red colouration decreases, and intervals of White Breccia become more common toward the Northeast. Along the deeply in-

cised Mühlau gorge, the lower part of the succession consists mainly of White Breccia with a few interfingering intervals of Red Breccia. Erosion of distinct rock types in the substrate gave rise to intervals of the HB which are tinted blackish (due to shales of Partnach Formation and/or Raibl beds) or yellow (matrix derived from erosion of Reichenhall beds). In the alluvial-fan successions, typical depositional geometries are divergent and divergent-oblique sets of beds resulting from prograding and aggrading fan fronts. In the stream-dominated alluvial-fan succession exposed along the Mühlau gorge, cut-and-fill patterns resulting in a complex interfingering of facies are common.

Loess-like layers: In its western outcrop sector, the Red Breccia is intercalated with veneers up to about 20 cm in thickness of polymictic silt to fine sand of probable aeolian origin (Ladurner 1956, Obojes 2003). The veneers of these loess-like deposits are well exposed in the abandoned Mayr quarry (location C in Fig. 1). These distinct layers indicate (a) phases of prolonged halts of deposition at this site, and (b) possibly a dry and cool climate; the latter interpretation is supported by plant fossils (see below). Unfortunately, loess-like deposits in Höttinger Graben reported to contain a 'loess snail' fauna (Penck 1921) are presently not accessible.

Upper part of HB: The upper part of the HB consists of White Breccia accumulated from talus fans that became overlain and downlapped by talus-slope successions (Figs. 3B–C). In the eastern part of the outcrop, the preserved relation between the proximal part of the fan deposits gradually steepening up-section and downlapped by the talus-slope successions indicates that both pertain to the same depositional cycle (Sanders 2010) (Fig. 1 & 2). Upslope from the downlap, the talus slopes of the HB are characterised by a uniform dip in the range of 30–35° (Fig. 3B).

Rossfall-Lahner interval: The famous interglacial flora of the HB is found in the lowermost part of the succession at ~1130–1155 m a.s.l., along the left flank of an avalanche ravine (location A in Fig. 1 & 2). This location was much better exposed in the 19th and early 20th centuries (see photos in Wettstein 1895, and Penck 1921) not the least because of deliberate blasting to exploit the fossiliferous beds (Wettstein 1895, Gams 1936). Chunks of these rocks are still present in a tailing, but are now partly covered by forest. Based on field inspection, sampling of the tailing, examination of fossil collections, and literature data, the original stratigraphy of the "Rossfall Lahner interval" can be reconstructed as follows: (1) a basal interval with torrential conglobreccias to conglomerates, (2) the fossiliferous interval mainly of lithic calcisiltites, parallel-laminated lime mudstones and calcilithic arenites with parallel-horizontal lamination and ripple drift cross-lamination, and (3) an upper interval of conglomerates to breccio-conglomerates with thin, intercalated beds similar to the fossiliferous facies. The main fossiliferous facies probably accumulated in a pond, or ephemeral ponds, influenced by cohesive debris flows and mudflows (Sanders & Ostermann 2006). The fossil flora – a diversified assemblage of trees, shrubs, herbs and grasses – is similar to the flora present at today's site, i.e., clearly of interglacial character (Murr 1926; see below for details). The Rossfall-Lahner interval is overlain by a succession at least 80 m in thickness of alluvial fan- and talus deposits of the HB (Fig. 2). No interval of comparable character to the Rossfall-Lahner interval was found elsewhere along the Nordkette. The nature of the transition from the Rossfall-Lahner interval into the overlying HB remains unclear. If both were part of a genetically-related succession, the vertical transition may indicate a marked climatic cooling from interglacial conditions (fossil flora) into a periglacial setting characterised by accumulation of thick talus slopes. Alternatively, both successions accumulated under contrasting climates and are vertically separated by an unconformity.

Unconformities and intraclasts: In the northeastern part of the outcrop, (i) interfingering of Red and White Breccia in the lower part, (ii) a mappable continuity from the alluvial fan- into the talus slope succession, and (iii) downlap of fossil talus slopes onto underlying talus-fan deposits strongly suggest that they comprise part of the same succession (Sanders 2010). It is unknown, however, how long this depositional phase lasted. In the central and western parts of outcrop, intraclasts up to a few metres in size of HB-type deposits are present within the fan- and talus successions of the HB (Fig. 3D). In addition, intraclasts of, both, White Breccia (talus facies) and Red Breccia (debris-flow facies), are found within the Red Breccia. The intraclasts were fully lithified before redeposition, as indicated by tilted geopetal fabrics of lime mudstone and by rounding of intraclast surfaces. These intraclasts therefore indicate that what has been subsumed as HB in fact consists of several rock units separated by unconformities (Sanders 2010).

5 Fossil flora

The fossils from the HB are generally poorly preserved impressions of deciduous and conifer plants (Fig. 4). Except for the shells of 'loess snails' (Penck 1921), no animal fossils were ever found in the HB. The vast majority of specimens stored in museums and collections across Europe were found in the Rossfall-Lahner interval (see above), where the plant imprints are well preserved, albeit without organic matter (Figs. 4A–E). These specimens classify as an autochthonous flora, which grew next to a shallow pond or ephemeral ponds (Murr 1926, Sanders & Ostermann 2006). In contrast, much fewer and poorer-preserved specimens were reported from finer-grained (sandy-silty) layers locally intercalated in the Red Breccia both in the Mayr quarry as well as in the Spörr quarry (Fig. 4F) (locations C and D in Fig. 1); this latter flora was interpreted as allochthonous (Murr 1926).

A total of 60 taxa were reported from these few sites, and already Wettstein (1895) stated that many of these taxa are living nearby today. Murr (1926) suggested, but not definitely concluded, that the presence of *Rhododendron ponticum* (Fig. 4A) and *Vitis vinifera* subsp. *sylvatica* (common grape vine) might be attributed to a climate with a mean annual air temperature slightly higher than during the last century. Murr (1926) also remarked that the sparse flora preserved in the Red Breccia suggests a cooler climate because it lacks *Rhododendron* and is dominated by genera such as pine (*Pinus sylvestris*), spruce (*Picea abies*) and larch (*Larix decidua*). More recently, Denk (2006) re-evaluated some of the taxa and found no compelling evidence to suggest that the climate at the time of deposition of the Rossfall-Lahner flora was distinctly warmer than today. He also raised serious doubts about the identification of *Vitis vinifera* by Murr (1926), and on the specific determination of *'R. ponticum'*.

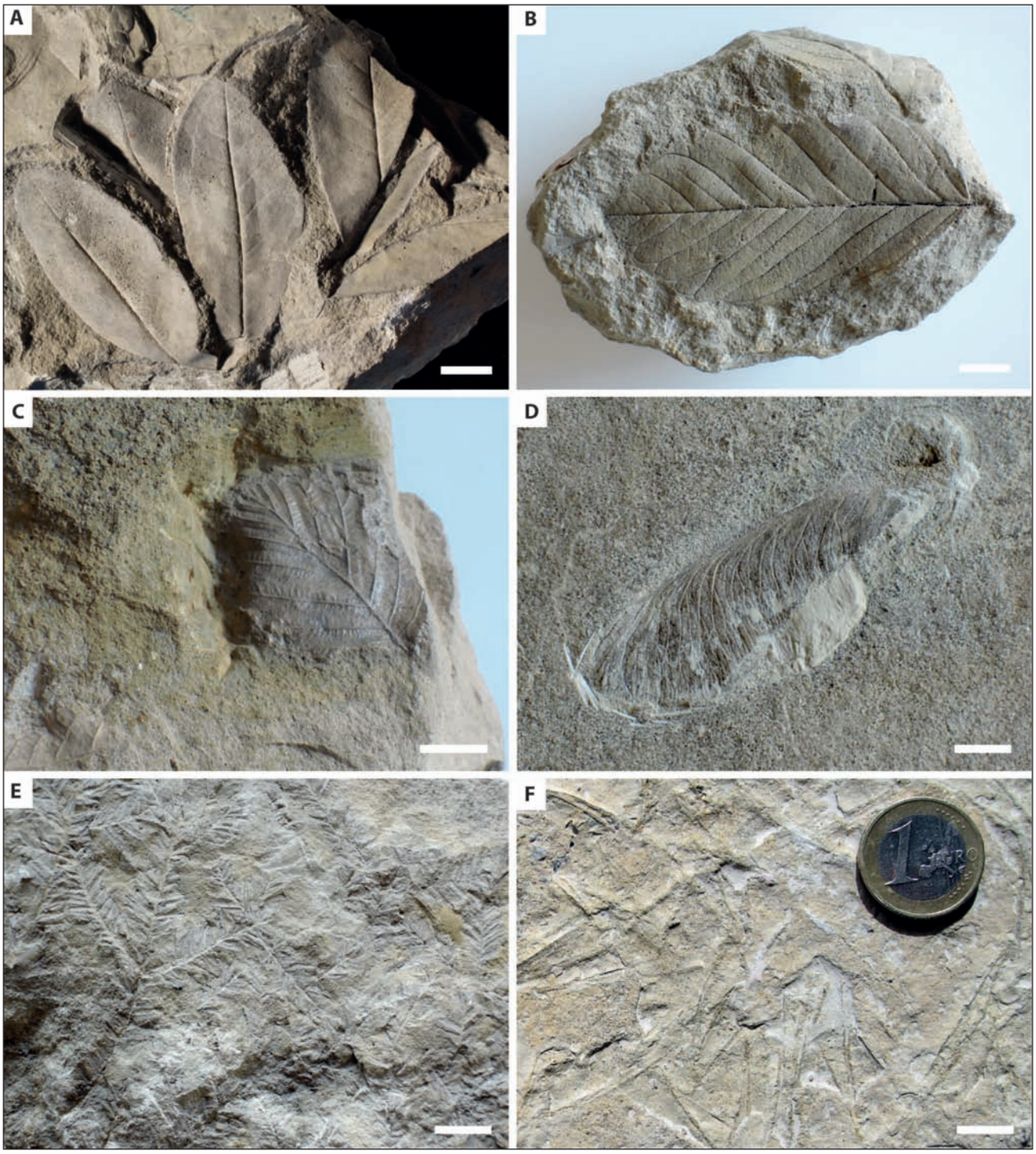

Fig. 4: Plant fossils from the HB. A. Leaves of *Rhododendron ponticum* var. *sebinense*. Rossfall-Lahner. Photo courtesy T. Denk. Scale bar 2 cm. B. *Rhamnus fragula*. Rossfall-Lahner. Scale bar 1 cm. C. *Alnus incana*. Spörr quarry. Scale bar 1 cm. D. Seed of sycamore maple (*Acer pseudoplatanus*). Rossfall-Lahner. Scale bar 1 cm. E. *Taxus hoettingensis*. Rossfall-Lahner. Scale bar 2 cm. F. Needles of *Pinus*. Mayr quarry.

Abb. 4: Pflanzenfossilien aus der Höttinger Brekzie. A. Blätter von Rhododendron ponticum var. sebinense. Rossfall-Lahner. Aus der Photosammlung von T. Denk. Maßstab 2 cm. B. Rhamnus fragula. Rossfall-Lahner. Maßstab 1 cm. C. Alnus incana. Spörr'scher Steinbruch. Maßstab 1 cm. D. Samen des Bergahorns (Acer pseudoplatanus). Rossfall-Lahner. Maßstab 1 cm. E. Taxus hoettingensis. Rossfall-Lahner. Maßstab 2 cm. F. Nadeln von Pinus. Mayr'scher Steinbruch.

The two floras of Rossfall-Lahner and of the Red Breccia do not necessarily reflect different climate regimes (and hence intervals of time), but may simply represent different taphonomic conditions (Murr 1926, Denk 2006).

6 Chronology

Two chronological methods have been applied to provide constraints on the sedimentation age of HB, optically-stimulated luminescence (OSL) and Uranium-Thorium ($^{234}U/^{230}Th$) disequilibrium dating. OSL dating was attempted on samples of two of the lower loess-like silt layers sampled in the abandoned Mayr quarry using horizontal drill cores (Gemmell & Spötl 2009). The single-aliquot regeneration protocol and the post infra-red OSL signal of quartz were used. The ages scatter widely and fading affected the luminescence signals, so that these ages (ranging from 30 ± 13 to 106 ± 15 ka) are

best regarded as significant underestimates of the true deposition age (Gemmell & Spötl 2009).

In order to provide minimum age constraints on the sedimentation of the HB radiometric dating of calcite deposits and cements were performed. Ostermann (2006) attempted to date isopachous calcite spar cements in the White Breccia near Höttinger Alm. These cements range from meniscus to isopachous, and are commonly contaminated with infiltrated, fine-grained detrital material. The latter gives rise to high ^{232}Th contents which render direct cement dating by U-Th methods challenging. For a sample of isopachous cement from talus slopes near Höttinger Alm, Ostermann (2006) applied sequential leaching and obtained an errorchron suggesting a mean cementation age of 109 ± 7 ka (Ostermann 2006). To conclude, U/Th dating of calcite cementing the White Breccia is difficult given its high detrital content (Ostermann 2006). In addition, thin-section observations show that these cements are polyphase and may record several episodes of cementation which might only be potentially resolved by high-resolution sampling.

The most reliable, yet again minimum constraints on the age of breccia sedimentation were obtained from calcite speleothems formed in fractures of the Red Breccia. Two samples from the abandoned Mayr quarry were examined and dated using a series of U/Th dates. A 4 cm-thick crust of mammillary calcite yielded ages between 100.5 ± 1.5 ka at the base and 73.9 ± 1.0 ka at the top (Spötl & Mangini 2006). The ages in between are in correct stratigraphic order (within their analytical uncertainties). A thinner second calcite sample formed between 73.8 ± 1.2 and 70.3 ± 1.8 ka. These dates clearly indicate that the Red Breccia at the Mayr quarry was already lithified and fractured prior to ca. 101 ka allowing seepage water to enter from the soil zone entraining carbon dioxide, dissolving carbonate minerals present in the breccia and re-precipitating calcite further down the flow route as flowstone in the unsaturated zone. Such speleothems have not been observed in other outcrops of the HB, which is likely due to the fact that the studied examples only became accessible due to deep quarrying of the Red Breccia. To summarise, the time span of sedimentation of what is currently subsumed as HB is not known. In view of the substantial thickness of and facies variations within the HB, we may assume that it encompasses a significant amount of time; individual depositional units (e.g., Rossfall-Lahner unit), however, probably accumulated during comparatively short depositional episodes. It seems likely that most time is contained in stratigraphic gaps rather than in the depositional record.

7 Palaeoenvironmental interpretation

A palaeoenvironmental interpretation of the depositional setting of the HB must take into account (i) the overall thickness of the alluvial-fan/talus-slope successions, (ii) the observation that the dip of the Red Breccia suggests a significantly higher elevation of the Inn Valley floor, (iii) the presence of loess-like layers, (iv) the fossiliferous Rossfall-Lahner interval, and (v) potentially large changes in the environmental conditions during the depositional episode of the HB.

(i) Thick successions of alluvial fans and scree slopes are a typical product of physical weathering under periglacial conditions. In mountain ranges undergoing glacial–interglacial cycles, scree production tends to be highest during climatic deterioration preceding glaciations, and shortly after deglaciation. Whereas periglacial scree formation is largely driven by frost shattering, the build-up of talus also is significantly influenced by the extent of vegetation cover of mountain flanks.

(ii) The consistently very low dip of the thick breccia beds in the Mayr quarry high above today's Inn Valley floor suggest that the latter may have been at a higher elevation during deposition of the Red Breccia. This argues in favour of a cold climate when a lowered treeline and more widespread mountain permafrost gave rise to strong fluvial aggradation (cf. van Husen 2000). Alternatively, or in addition, the pinch out of the Red Breccia well above the present valley floor may have resulted from a change in course of the Inn River. The present river takes a wide northward bend at Innsbruck and locally erodes Triassic bedrock along the northern valley flank (being pushed to this side by the alluvial fan of the Sill River; Fig. 1). If the pre-LGM Inn followed a southerly route, the beds of the Red Breccia could have reached down close to the modern level of the valley floor with a similar slope gradient than those of present alluvial fans shedding into the Inn Valley. A corollary of this model is that the Sill River once entered the Inn Valley west of its present course; a hypothesis that is admittedly speculative but not inconsistent with field observations.

(iii) The loess-like layers in the Red Breccia consist of texturally immature aeolian dust whose mineralogical composition is identical to the sediment of today´s Inn River. Their presence demands deflation areas in the adjacent Inn Valley which today is densely covered by vegetation. This argues for a cool and dry climate during deposition of these loess-like layers, which is supported by the palaeobotanical evidence from this quarry (Murr 1926).

(iv) The fossil flora of the Rossfall-Lahner interval is unique and records an interglacial vegetation on the mountain slope not unlike today (Murr 1926). Except for the apical regions of a few, low-active scree slopes high above the Rossfall site, the vegetated mountain flank of Nordkette today is devoid of significant scree production. The flora of Rossfall-Lahner is thus in stark contrast to the thick talus-fan/talus-slope succession of the HB directly overlying these fossiliferous beds.

(v) The contrast between the Rossfall-Lahner palaeoflora and the overlying HB suggests that a warm climatic phase was succeeded by colder conditions that gave rise to scree production and deposition of thick talus. This is essentially the reverse of what is widely seen for Holocene mountain-flank successions in the Alps: rapidly accumulated fan- and talus-slope successions became abandoned and vegetated and, in many cases, subject to erosional incision. A reversal from unconformity cutting to sediment accumulation, in turn, can be accomplished by climatic cooling/drying leading to increased scree production. As mentioned above, the intraclasts within the HB suggest significant episodic erosional downcut.

8 Deformation

Aside of subvertical ruptures the HB shows other types of deformation structures that, however, are difficult to interpret. Much ambiguity results from the fact that the breccia was overridden and partially eroded by a thick, warm-based glacier during the Last Glacial Maximum, such that many brittle deformation features may have resulted from glacial loading. The southern fringe of the HB near Hungerburg is affected by gravitational instability ("Bergzerreißung"), and the key outcrop at Lepsius adit is located in a block that slid downwards (Ampferer 1936). A syncline was described in the Red Breccia that results from an array of subvertical fractures that increasingly open down-section; this structure may reflect glacial loading or gravitational sag due to erosion of sediment below (Ampferer 1936). From an abandoned gravel pit west of the Mayr quarry Ampferer (1936) described two faults in an unlithified, proglacial succession, probably of early Upper Würmian age. The faults stroke SE–NW and showed a very steep dip towards NE. In addition, one of these faults cross-cut a boulder of White Breccia ~ 5 m in size embedded in the gravels. No information of the magnitude of the fault throw was given. Ampferer (1936) interpreted these faults as "Absenkungsklüfte", without specifying a process that caused the fracturation. Unfortunately, this gravel outcrop does not exist anymore. To fracture a boulder of White Breccia embedded in unlithified gravels requires substantial triaxial loading combined with a high differential strain rate. Fault surfaces with kinematic indicators are rare in the HB. On the right flank of the Mühlau gorge, several faults with low-dipping striae were found. A dextral offset is indicated along one of these faults. Another fault found in the basal HB along Rossfall-Lahner shows low-dipping linears indicating a sinistral offset. These faults fit the seismic evidence of active deformation mentioned above.

9 Excursion route (Fig. 5)

Stop 1: Weiherburg: Overview of Quaternary deposits near Innsbruck

This first stop provides an introduction to the topic of this half-day field trip and an overview of the topographic and large-scale geological setting of the central Inn Valley, followed by a concise summary of the Quaternary dynamics (ice advances, glacial overdeepening, terrace formation) giving rise to the landscape around the city of Innsbruck.

Stop 2: Engländergrab: Lateglacial(?) coarse-grained delta

The trail leading from the Alpenzoo towards Hungerburg (Wilhelm Greil Weg) passes outcrops of conglomerate soon after leaving the parking lot. This conglomerate is known in the literature as "Weiherburgdelta" or "Deltaschotter beim Engländergrab", named after the grave of a young Englishman which is located to the West of the trail on top of this small hill.

The conglomerate consists of well-rounded and commonly also well sorted gravel, dominated by metamorphic rocks (Fig. 6A). A few blocks of Red HB up to ca. 1 m in

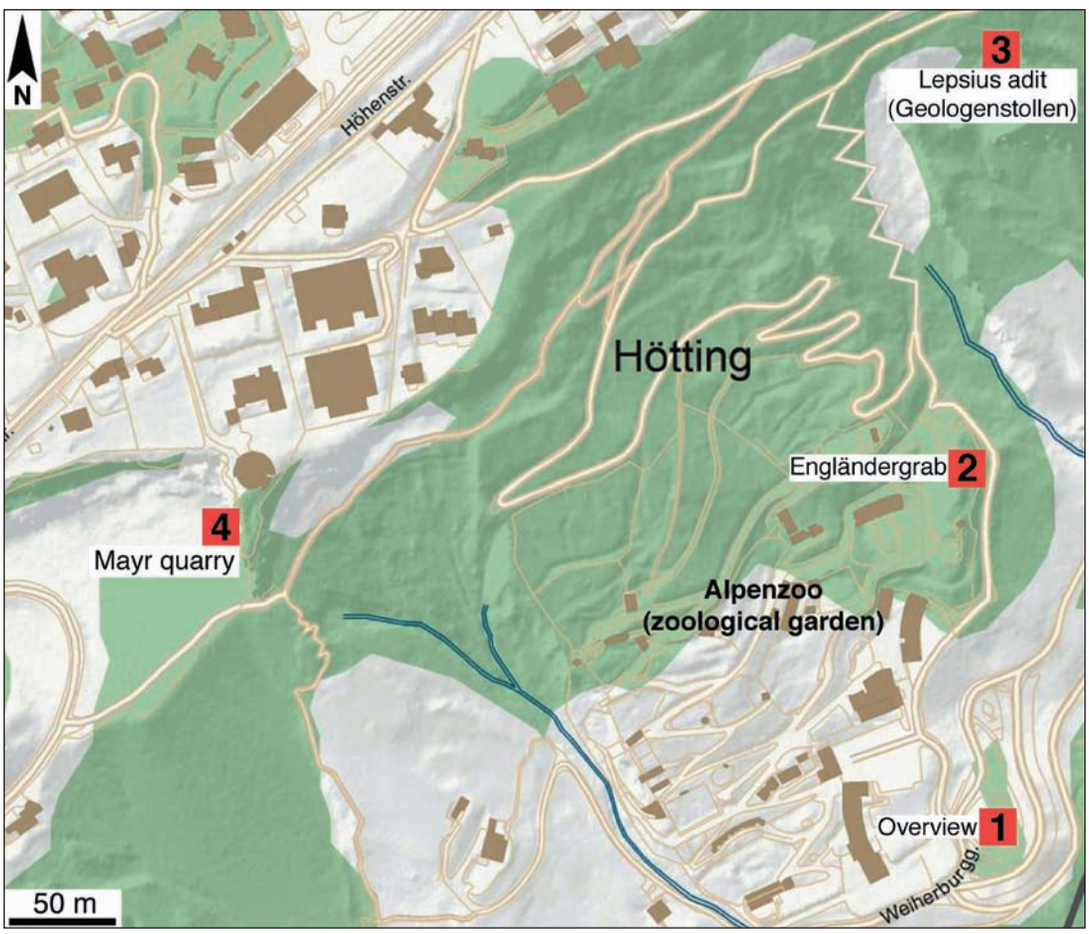

Fig. 5: Excursion route.
Abb. 5: Exkursionsroute.

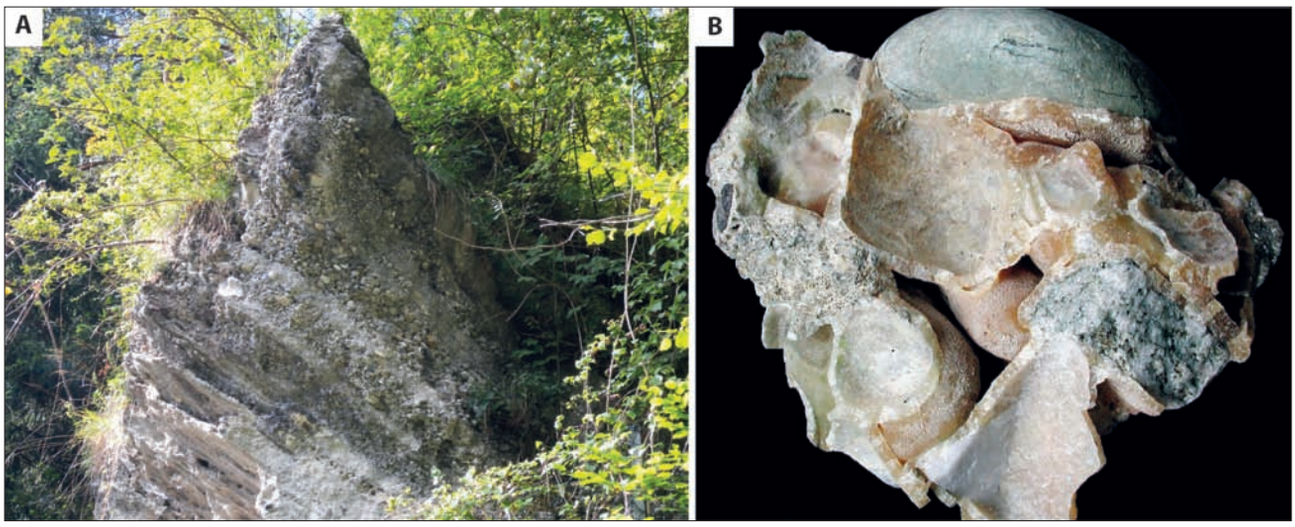

Fig. 6: The conglomerate at Engländergrab. A. Foreset composed of well sorted and rounded gravel. Height of image 3 m. B. Hand specimen of conglomerate showing isopachous calcite cement dated to the early Holocene. Width of specimen 10 cm.

Abb. 6: Das Konglomerat beim Engländergrab. A. Deltaschrägschichtung aus gut sortiertem und gut gerundeten Kies. Höhe des Bildausschnittes 3 m. B. 10 cm breites Handstück des Konglomerats. Zeigt isopachen Kalzitzement, der in das frühe Holozän datiert wurde.

diameter are embedded in the gravel. The degree of cementation varies strongly and well indurated packages (clast-supported fabrics) are interbedded with poorly or even completely uncemented ones. The cements are well developed isopachous rims of calcite (Fig. 6B), commonly showing a yellowish stain. The origin if this phreatic cementation is likely related to the local presence of spring water supersaturated with respect to calcite causing cementation in the shallow subsurface. In fact, tufa is actively forming along the creek discharging the Eastern Weiherburggraben, i.e. immediately east of Engländergrab (Sanders & Rott 2009). This creek is known as Tuffbach (Duftbach in Penck 1921: his plate 2). Fossil tufa likely of Holocene age crops out along the trail just north of Engländergrab demonstrating that the discharge routes have varied over time.

Higher up the gravel beds dip 20–30° which Penck (1921) described as westward. The indurated part of the conglomerate is broken up in individual blocks which show rotations and the dip of the layers therefore varies due to slope movement.

Fig. 7: Original photo of the terrain at Lepsius adit a few years after construction of this artificial tunnel (from Penck 1921: his plate 5). The trail that leads to the adit approximately delineates the boundary between the till and the base of the HB (note: person for scale).

Fig. 7: Das Orginalfoto aus Penck (1921: seine Tafel 5) zeigt den Lepsius-Stollen wenige Jahre nach der Fertigstellung. Der Pfad, der zum Stollen führt (beachte die Person als Maßstab), bezeichnet in etwa die Grenze zwischen der Grundmoräne und der auflagernden Höttinger Brekzie.

Penck (1921) mapped the extent of this conglomerate and reported clay-rich sediments beneath, probably bottomsets. The level of this palaeolake must have been at least at 700 m. No sediments are present stratigraphically above the conglomerate.

Previous workers have made vague and partly conflicting statements about the age of this deposit. Patzelt & Resch (1986) pointed out that dolomite clasts are never decomposed ("verascht"), which implies a rather young age. Samples of calcite cement were dated using U/Th and yielded ages of 7.5 ± 0.2 ka for a sample at Stop 1 and 10.6 ± 0.4 ka for a sample obtained east of Weiherburg (C. Spötl & A. Mangini, unpubl. data). Another sample of this cement yielded an age of 3 ± 0.5 ka, based on an errorchron using four sub-samples (Ostermann 2006). Part or perhaps even most of the localised cementation of the conglomerate was accomplished by calcite-depositing springs along the base of the HB higher upslope (cf. Sanders & Rott 2009). The geological context and the U/Th ages of the cements suggest a deposition of the delta conglomerates prior to the early Holocene. The lack of cracked pebbles in the clast-supported layers argues against ice loading; hence we tentatively attribute the origin of this gravel to the early Lateglacial, i.e. sedimentation in an ice-marginal lake during down-wasting of the Inn glacier.

Stop 3: Lepsius adit: A key location celebrating its 101st year of construction

The area north of Innsbruck has been an ore mining district during past centuries with dozens of adits (Srbik 1913, Heissel & Gstrein 1989). Many more adits and tunnels were since then constructed in search for groundwater (to some extent inside parts of the White Breccia; Heissel 1991), as air-raid shelters during World War II (Ampferer 1946) and for other purposes. One such adit, however, stands out in because it was purely constructed for scientific reasons. Locat-

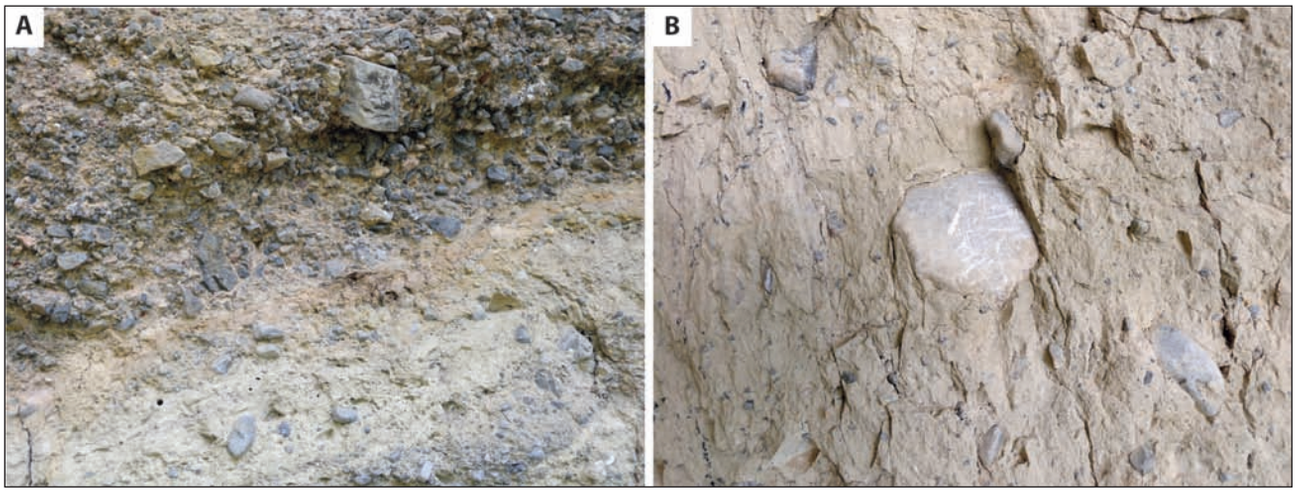

Fig. 8: Details of the till at Lepsius adit. A. Inclined boundary between the till underlying the oldest layers of the Red HB. Note crude stratification in the upper till and medium-brown hue of fine-grained sediment at the boundary which partly stems from a thin layer of loessic material (locally known as Streifenlehm). Width of image 1.5 m. B. Close-up of the till a few metres east of the entrance to the Lepsius adit. Note dominance of limestone and dolomite clasts (partly striated). Width of image 40 cm.

Abb. 8: Details der Moräne beim Lepsius-Stollen. A. Geneigte stratigraphische Grenze zwischen der Moräne und dem untersten Anteil der Roten Brekzie. Beachte die unscharf definierte Schichtung in der Moräne sowie die hellbräunliche, feinkörnige Lage entlang der Grenze; diese Lage stellt wahrscheinlich äolisch antransportiertes Sediment dar (lokal als Streifenlehm bekannt). Bildbreite 1,5 m. B. Detailansicht der Moräne wenige Meter östlich des Eingangs zum Lepsius-Stollen. Beachte die Vorherrschaft von Lithoklasten aus Karbonatgesteinen (Kalke, Dolomite), von denen einige Ritzungen zeigen. Bildbreite 40 cm.

ed in the eastern Weiherburggraben the 20 m-deep horizontal Lepsius adit (also known as "Geologenstollen") was made to settle a long-lasting debate as outlined in the introduction of this article (Fig. 7). The adit is still open after more than a century and convincingly demonstrates that the breccia sealed a pre-existing moraine topography overlain by a thin loessic layer (Fig. 8). Previous workers (e.g. Ampferer 1914, Penk 1921) already reported that the upper part of the till is crudely stratified and rich in local carbonate clasts, whereas the lower part is very matrix-rich.

Two metres east of the entrance of the adit remnants of a 2.5 m-tall tree were found during construction work. This tree was in upright position and apparently rooted in the underlying till. Pieces of this old wood, identified as probably Pinus silvestris (Penck 1921), are still preserved and a radiocarbon analysis yielded an expected infinite age (>50 ka BP; C. Spötl & P.M. Grootes, unpublished data).

During the winter of 2012/13 the forest north of Innsbruck was severely damaged and the trail leading to the Lepsius adit was blocked by fallen trees. In addition, breccia blocks fell onto the trail (and others threaten to become loose soon, e.g. near Lepsius adit) which led to the closure of the trail. At this point it is not clear if and when this trail will be again open to the public.

Stop 4: Mayr quarry: Key outcrop of Red Breccia, and nursery of Innsbruck's rock climbers

This quarry, in operation for several hundreds of years, was abandoned during the early 20th century. Today, only the west-facing quarry cliff approximately 40 m in height still stands free of vegetation (Fig. 9A). Seen from a distance, the cliff shows unbedded intervals up to approximately 10 m in thickness that are vertically separated by back-weathered, intercalated strata (marked by white arrows in Fig. 9A). The thick intervals consist of amalgamated layers of (a) breccias deposited as cohesive debris flows and, mainly in the upper part of the cliff, (b) breccias to conglomeratic breccias accumulated by ephemeral surface runoff (Fig. 9B).

The back-weathered strata are typically up to 20 cm thick and consist of friable, ochre-coloured silt to fine sand with a high porosity of 40–60 %. The sediment consists of a variable mixture of grains composed of quartz, calcite, feldspar, dolomite, micas and clay minerals. Most of the grains are subangular to subrounded. The strata are draped over their substrate (Fig. 9C). Locally, submillimetre lamination parallel to bedding and ripple-drift cross-laminasets are visible. Thicker layers typically are vertically associated with thin sheet-flow deposits of winnowed, parallel-laminated sand to fine-gravelly breccias. The combined characteristics suggest that the back-weathered strata were mainly sourced from aeolian deposition, but they do not show all characteristics of loess (hence referred to as 'loess-like deposits') (Ladurner 1956, Obojes 2003). Plant remnants, such as imprints of pine needles, are typically found along the contact between these layers and overlying breccia beds, and on top of thin sheet-flow layers (Fig. 4F).

Ever since the abandonment of the quarry, its cliffs have been used by Innsbruck-based rock climbers to exercise their skills and as a meeting place. Today, the most difficult ascents reach grade X on the scale proposed by the International Mountaineering and Climbing Federation (UIAA).

References

Ampferer, O. (1914): Aufschließung des Liegenden der Höttinger Breccie im östlichen Weiherburggraben bei Innsbruck. – Anzeiger der Österreichischen Akademie der Wissenschaften, mathematisch-naturwissenschaftliche Klasse, 12.2.1914: 1–5.

Ampferer, O. (1936): Beiträge zur Geologie der Hungerburgterrasse bei Innsbruck. – Jahrbuch der Geologischen Bundesanstalt, 86: 353–358.

Ampferer, O. (1946): Geologische Ergebnisse von Schutzstollenbauten bei Innsbruck. – Sitzungsberichte der

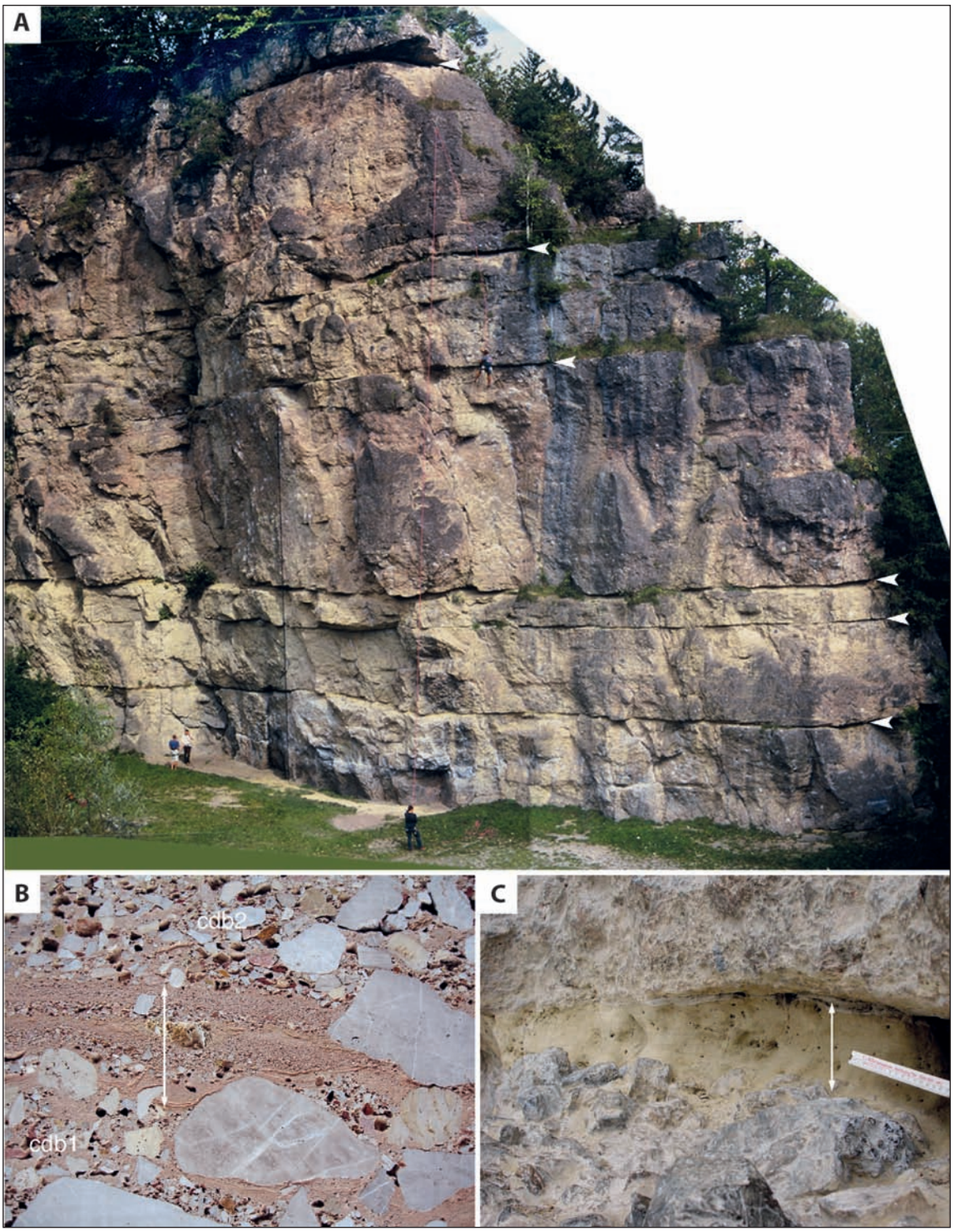

Fig. 9: A. Overview of the west-facing cliff of the former Mayr quarry. The faintly bedded to unbedded intervals up to approximately 10 m in thickness consist of amalgamated debris flows and water-laid breccias. The intercalated, back-weathered strata (marked by white arrows) consist of aeolian-sourced silt to fine sand ('loess-like layers', see text). B. Cut slab of Red Breccia from Mayr quarry. A breccia deposited from a cohesive debris flow (cdb 1) is overlain by an interval (marked with arrow) composed of thin layers of pebbly arenite and pink-coloured, laminated lime mudstone. This interval accumulated during episodes of ephemeral surface runoff. It is sharply overlain by another breccia from a cohesive debris flow (cdb 2). Width of view approximately 25 cm. C. Sharp boundary between a layer of debris-flow breccia with clasts projecting upwards and overlying interval – labelled with arrow – of aeolian-sourced silt to fine sand ('loess-like layer'; see text). The loess-like deposit is sharply overlain by another debris-flow breccia. Scale in centimetres.

Abb. 9: A. Überblick über die westgerichtete Wand des früheren Mayr'schen Steinbruchs. Die bis etwa 10 m dicken, undeutlich gebankten bis ungebankten Intervalle bestehen aus amalgamierten Lagen von kohäsiven Trümmerströmen (Muren) und Ablagerungen von ephemeralem Oberflächenabfluss. Die eingeschalteten, deutlich rückwitternden Lagen (markiert mit weißen Pfeilen) bestehen aus äolisch transportiertem Silt bis Feinsand ('Löss-artige Lagen', siehe Text). B. Geschnittene Platte von Roter Brekzie aus dem Mayr'schen Steinbruch. Eine Brekzienlage eines Murgang-Ereignisses (cdb 1) wird von einem Intervall überlagert (markiert mit weißem Pfeil), das aus dünnen Lagen von kiesführendem Arenit und rosarotem, laminiertem Kalkschlammstein besteht; dieses Intervall bildete sich infolge wiederholtem Oberflächen-Abfluss. Es wird scharf von einer weiteren Murschutt-Brekzie (cdb 2) überlagert. Bildbreite etwa 25 cm. C. Scharfe Grenze zwischen einer Murschutt-Lage mit vorstehenden Klasten am Top und einer hangenden Lage (markiert mit Pfeil) von äolisch antransportiertem Silt bis Feinsand ('Löss-artige Lage'). Die lössartige Lage wird ihrerseits scharf von einer Murschutt-Brekzie überlagert. Maßstab in Zentimetern.

Akademie der Wissenschaften Wien, mathematisch-naturwissenschaftliche Klasse, Abteilung I, 155: 49–62.

Blaas, J. (1889): Die Höttinger Breccie und ihre Beziehung zur Frage nach einer wiederholten Vergletscherung der Alpen. – Berichte des naturwissenschaftlich-medizinischen Vereins Innsbruck, 18: 97–115.

Denk, T. (2006): *Rhododendron ponticum* L. var. *sebinense* (Sordelli) Sordelli in the Late Pleistocene flora of Hötting, Northern Calcareous Alps: witness of a climate warmer than today? – Veröffentlichungen des Tiroler Landesmuseums Ferdinandeum, 86: 43–66.

Ettingshausen, C. v. (1885): Über die fossile Flora der Höttinger Breccie. – Sitzungsberichte der mathematisch-naturwissenschaftlichen Classe der kaiserlichen Akademie der Wissenschaften, I. Abteilung, 90: 260–273.

Gams, H. (1936): Die Flora der Höttinger Breccie. – In: Götzinger, G. (ed.), Führer für die Quartär-Exkursionen in Österreich (III. Intern. Quartär-Konferenz, Wien 1936), 2: 67–72.

Gemmell, A.M.D. & Spötl, C. (2009): Dating the Hötting Breccia near Innsbruck (Austria), a classical Quaternary site in the Alps. – Austrian Journal of Earth Sciences, 102: 50–61.

Gstrein, P. & Heissel, G. (1989): Zur Geschichte und Geologie des Bergbaues am Südabhang der Innsbrucker Nordkette. – Veröffentlichungen des Tiroler Landesmuseums Ferdinandeum, 69: 5–58.

Hammerl, C., Lenhardt, W. A. & Innerkofler, M. (2012): Forschungen zu den stärksten historischen Erdbeben im mittleren Inntal im Rahmen des INTERREG IV-Projektes HAREIA. – In: Zanesco, A. (ed.), Forum Hall in Tirol. Neues zur Geschichte der Stadt, 3: 154–184.

Heissel, G. (1991): Die Abhängigkeit der hydrogeologischen von den geologisch-tektonischen Verhältnissen des Karwendelgebirges, aufgezeigt am Beispiel der Mühlauer Quellen (Tirol, Österreich). – Veröffentlichungen des Tiroler Landesmuseums Ferdinandeum, 71: 17–81.

Katschthaler, H. (1930): Neue Beobachtungen im Gelände der Höttinger Breccie. – Jahrbuch der Geologischen Bundesanstalt, 80: 17–44.

Klebelsberg, R. v. (1929): Neue Aufschlüsse im Gelände der Höttinger Breccie. – Zeitschrift für Gletscherkunde, 17: 319–323.

Lepsius, R. (1913): Die Höttinger Breccie. – Naturwissenschaften, 1: 1122–1127.

Ladurner, J. (1956): Mineralführung und Korngrößen von Sanden (Höttinger Breccie und Umgebung). – Tschermaks Mineralogisch-Petrographische Mitteilungen, 5: 102–109.

Murr, J. (1926): Neue Übersicht über die fossile Flora der Höttinger Breccie. – Jahrbuch der Geologischen Bundesanstalt, 76: 153–170.

Obojes, U. (2003): Quartärgeologische Untersuchungen an den Hängen der Innsbrucker Nordkette (Höttinger Breccie). – Unpublished Diploma thesis, Univ. Innsbruck.

Obojes, U., Unterwurzacher, M. & Spötl, C. (2012): Die Höttinger Brekzie – Entstehung, Eigenschaften und Gewinnung. – In: Siegl, G. & Unterwurzacher, M. (eds.), Die Höttinger Brekzie – ein Tiroler Werkstein. Entstehung, Abbauorte, Geschichte, Verwendung, Erhaltung. Innsbruck University Press: 11–33, Innsbruck (Universität Innsbruck).

Ortner, H., Reiter, F. & Brandner, R. (2006): Kinematics of the Inntal shear zone-sub-Tauern ramp fault system and the interpretation of the TRANSALP seismic section, Eastern Alps, Austria. – Tectonophysics, 414: 241–258.

Ostermann, M. (2006): Thorium-uranium age-dating of "impure" carbonate cements of selected Quaternary depositional systems of western Austria: results, implications, problems. – Unpublished Ph.D. thesis, Univ. Innsbruck, 173 pp.

Paschinger, H. (1950): Morphologische Ergebnisse einer Analyse der Höttinger Breccie bei Innsbruck. – Schlern-Schriften, 75: 1–86.

Patzelt, G. & Resch, W. (1986): Quartärgeologie des mittleren Tiroler Inntales zwischen Innsbruck und Baumkirchen. – Jahresbericht und Mitteilungen des oberrheinischen geologischen Vereins N.F., 68: 43–66.

Penck, A. (1882): Die Vergletscherung der deutschen Alpen, ihre Ursachen, periodische Widerkehr und ihr Einfluss auf die Bodengestaltung. – 483 pp., Leipzig (J.A. Barth).

Penck, A. (1921): Die Höttinger Breccie und die Inntalterrasse nördlich Innsbruck. – Sitzungsberichte der preussischen Akademie der Wissenschaften, physikalisch-mathematische Klasse, 1921: 1–136.

Pichler, A. (1859): Beiträge zur Geognosie Tirols. - Zeitschrift des Museums Ferdinandeum Innsbruck, 3(8): 1–232.

Reinecker, J. & Lenhardt, W.A. (1999): Present-day stress field and deformation in eastern Austria. – International Journal of Earth Sciences, 88: 532–550.

Sanders, D. (2010): Sedimentary facies and progradational style of a Pleistocene talus-slope succession, Northern Calcareous Alps, Austria. – Sedimentary Geology, 228: 271–283.

Sanders, D. & Ostermann, M. (2006): Depositional setting of the sedimentary rocks containing the "warm-interglacial" fossil flora of the Höttinger Brekzie (Pleistocene, Northern Calcareous Alps, Austria): a reconstruction. – Veröffentlichungen des Tiroler Landesmuseums Ferdinandeum, 86: 91–118.

Sanders, D. & Rott, E. (2009): Contrasting styles of calcification by the micro-alga *Oocardium stratum* Naegeli 1849 (Zygnematophyceae) in two limestone-precipitating spring creeks of the Alps. – Austrian Journal of Earth Sciences, 102: 34–49.

Sanders, D., Ostermann, M. & Kramers, J. (2009): Quaternary carbonate-rocky talus slope successions (Eastern Alps, Austria): sedimentary facies and facies architecture. – Facies, 55: 345–373.

Siegl, G. & Fahlenbock, M. (2012): Geschichtliches zur Höttinger Brekzie. – In: Siegl, G. & Unterwurzacher, M. (eds.), Die Höttinger Brekzie - ein Tiroler Werkstein. Entstehung, Abbauorte, Geschichte, Verwendung, Erhaltung. Innsbruck University Press: 35–45, Innsbruck (Universität Innsbruck)

Spötl, C. & Mangini, A. (2006): U/Th age constraints on the absence of ice in the central Inn Valley (Eastern Alps, Austria) during Marine Isotope Stages 5c to 5a. – Quaternary Research , 66: 167–175.

Srbik, R. v. (1913): Überblick des Bergbaues von Tirol und Vorarlberg. – Berichte des naturwissenschaftlich-medizinisches Vereines Innsbruck, 41: 113–279.

Stur, D. (1886): Vorlage der Flora von Hötting im Innthale nördlich bei Innsbruck. – Verhandlungen der Geologischen Reichsanstalt, 1886: 124–125.

van Husen, D. (2000): Geological processes during the Quaternary. – Mitteilungen der Österreichischen Geologischen Gesellschaft, 92: 135–156.

Wettstein, R. v. (1892): Die fossile Flora der Höttinger Breccie. – Denkschriften der kaiserlichen Akademie der Wissenschaften, mathematisch-naturwissenschaftliche Classe, 59: 479–524.

Notes

Holocene glacier and timber line development – the case of Innergschlöss-Schlatenkees, Venediger Range, Hohe Tauern

Holozäne Gletscher- und Waldgrenzentwicklung am Beispiel Innergschlöss-Schlatenkees, Venedigergruppe, Hohe Tauern

Gernot Patzelt

Fig. 1: Schlatenkees in 1857 (from Simony 1865).

Abb. 1: Das Schlatenkees im Jahre 1857 (aus Simony 1865).

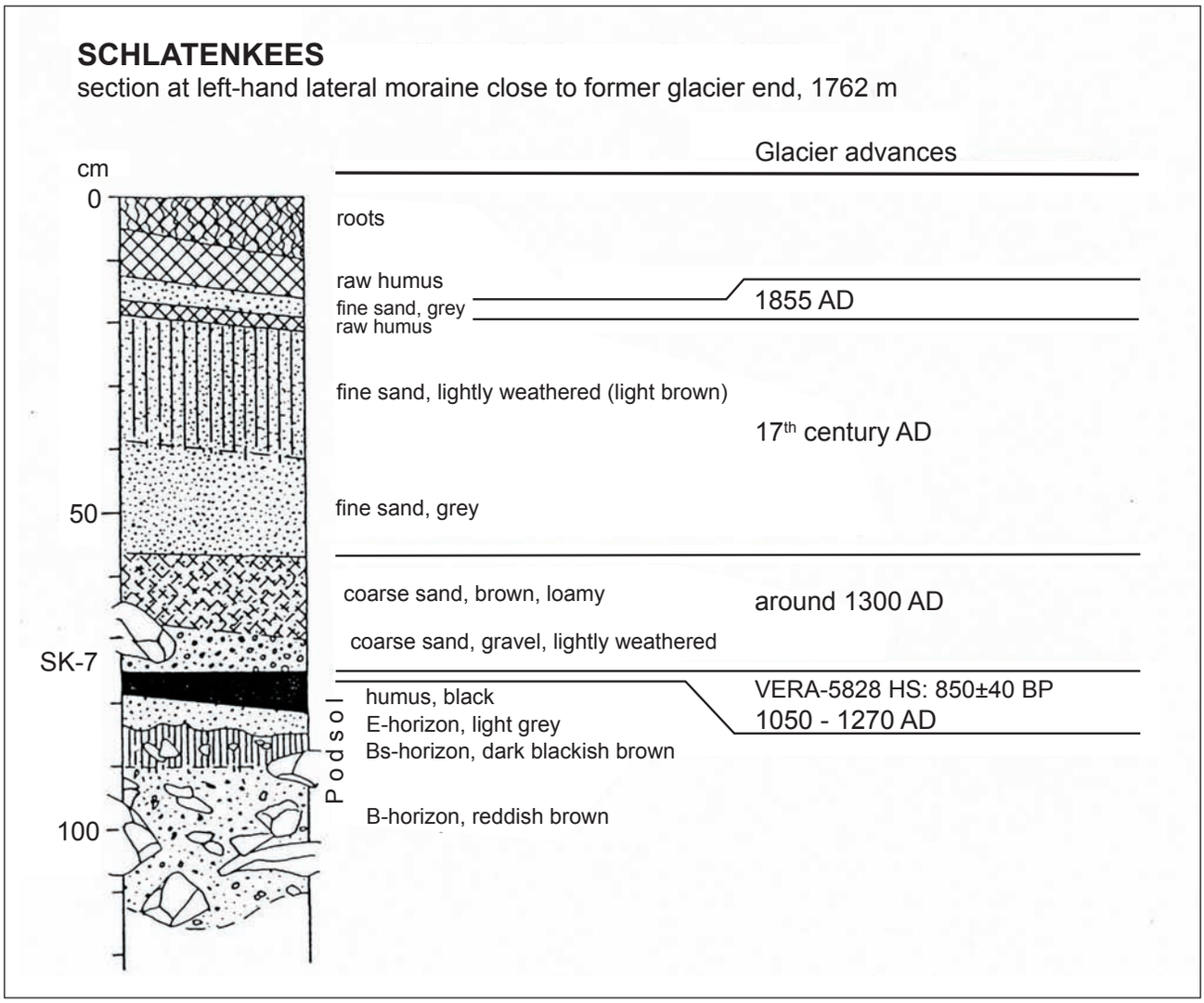

Fig. 2: Sediment profile of the left lateral moraine near the terminal position of the Schlatenkees at Gschlößtalboden (1762 m a.s.l.).
Abb. 2: Sedimentprofil von der endnahen, linken Seitenmoräne des Schlatenkeeses am Gschlößtalboden (1762 m).

1 Preliminary remarks

The postglacial glacier history within the Venediger Range was subject to extensive investigations between 1963 and 1972 (Patzelt & Bortenschlager 1973). Since then significant methodological improvements have occurred, notably dendrochronological analyses by K. Nicolussi (University of Innsbruck) in recent years. These developments have made it necessary to rethink past concepts. The new results will be presented and discussed for the first time during this field trip to the Schlatenkees, which will serve as an example for the reconstruction of glacier history. All radiocarbon ages were calibrated with CALIB 7.0 and the IntCal13 data base (Reimer et al. 2013) and are given as 2σ ranges.

2 The Holocene maximum stages of the Schlatenkees

During the advances of the "Little Ice Age" (LIA), the Schlatenkees transgressed the Gschlößtal valley floor and deposited two distinct end moraine arcs at the opposite side of the valley slope. The younger glacier position was well documented in a painting by Friedrich Simony from 1857 (Fig. 1). Based on the weakly developed soils, the older advance is also assumed to be of modern times, probably from the 17th century AD.

At the steep slope on the right-hand side of the Gschlößbach near the terminal position, an outcrop was dug in the high left lateral moraine. The profile (Fig. 2) shows beneath two fine sand depositions of modern times a layer of stronger weathered coarse sand/gravel above an undisturbed and well developed podzol soil with its corresponding horizons. The upper 2 cm of the 4 to 7 cm thick humus layer that was in contact with the overlying sediments was radiocarbon dated (VERA-5828 HS: 850 ± 40 BP) yielding a calibrated age of 1050–1270 AD. The superimposed glacial sediment must have been deposited shortly after and clearly before the 17th century AD. This date enables a glacier advance to be deduced around 1300 AD. Evidence of further glacier advances around this time period was found at Vernagtferner (Ötztal Mountains; Patzelt 2013) and at Gurgler Ferner (Ötztal Mountains; Patzelt 1994). Tree ring analyses from trees at high altitudes reveal significant cooling in the second half of the 13th century AD (Nicolussi & Patzelt 2001). This temperature decline that led to the glacier advances of the Late Middle Ages and modern times began around 1280 AD and concluded the Medieval Warm Period.

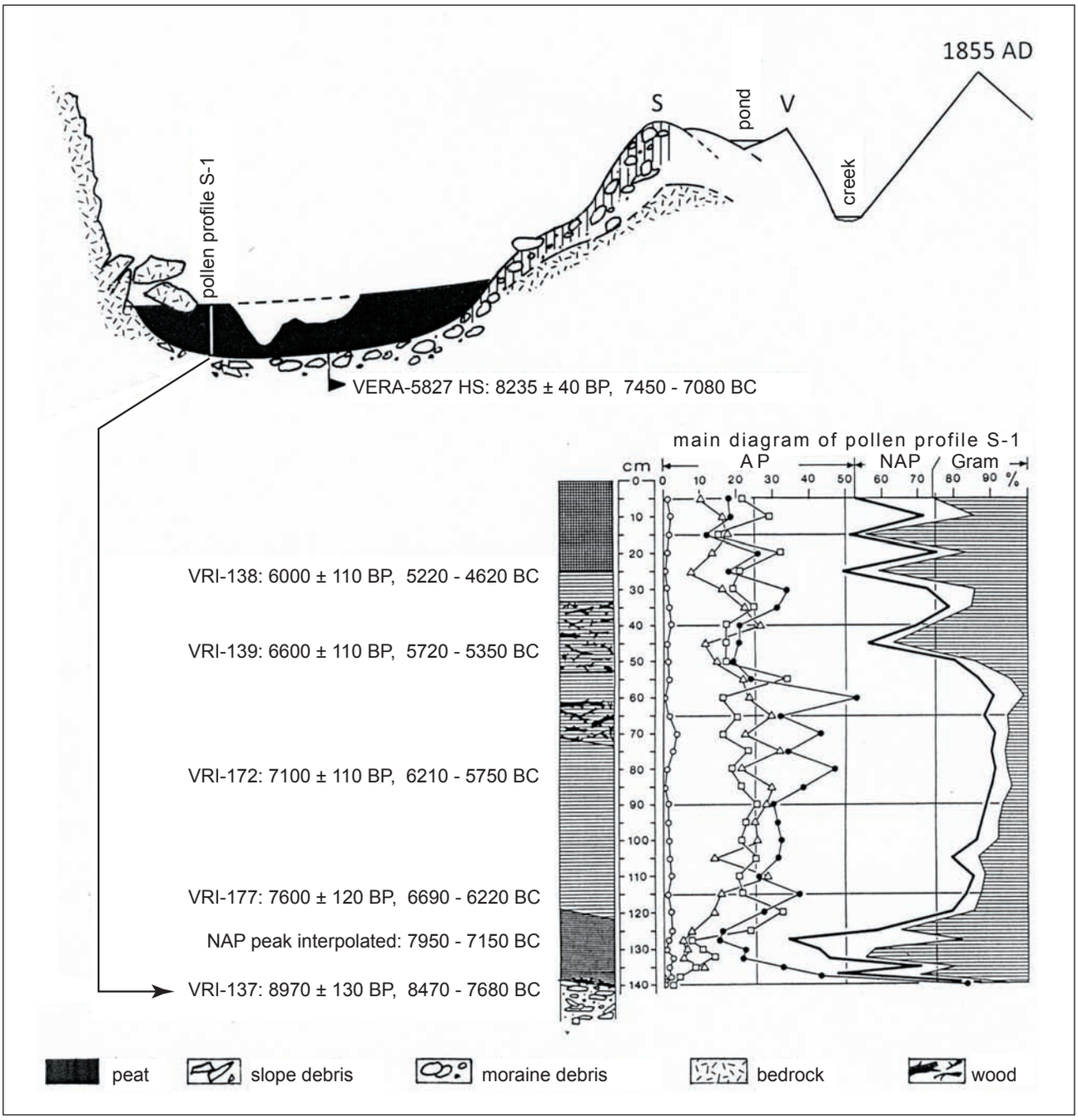

Fig. 3: Cross section of the Schlatenkees moraine complex above Salzboden Lake (2180 m.a.sl.) and main diagram of pollen profile S-1. Analysis by S. Bortenschlager with newly calibrated ^{14}C dates.

Abb. 3: Querprofil durch den Moränenkomplex des Schlatenkeeses oberhalb des Salzbodensees (2180 m) und das Hauptdiagramm des Pollenprofiles S-1. Analyse von S. Bortenschlager mit den entsprechenden, neu kalibrierten ^{14}C-Daten.

3 Postglacial glacier and timber line development

Lateral moraines have been preserved around Salzboden Lake (2137 m a.s.l.). These lie beyond the LIA moraine and represent slightly greater glacier extents. Wood remains from trees were found in the peat bogs in the depressions between the hillslope and distal side of the moraines, which enable to derive a temporal constraint for moraine deposition and the determination of the former forest extent.

In 1972 S. Bortenschlager analysed the pollen profile S-1 (Fig. 3) that originated from a partially eroded peat bog above Salzboden Lake at an altitude of 2180 m a.s.l. He subdivided the profile on the basis of conventional radiocarbon ages.

Recent calibration of the ages at the profile depth of 140 cm yielded a basal age of 8470–7680 BC (VRI-137: 8970 ± 130 BP). This age represents the beginning of peat development. The sample taken from a profile depth of 105 cm shows a calibrated age of 6690–6220 BC (VRI-177: 7600 ± 120 BP). In an intermediate position a distinct non-arboreal pollen peak with a maximum at a profile depth of 127.5 cm can be distinguished for which a time period from 7950–7150 BC was interpolated. In this segment the non-arboreal-pollen content reaches up to 65 % of the total pollen sum, whereby a sharp vegetation response to a congruent temperature decline is demonstrated. However, since corresponding glacial sediments are missing no glacial advance can be allocated to this time period.

Further in-depth investigations offered high minimum ages for moraine "S". A stone pine trunk stemming from the boggy area near the outflow of Salzboden Lake within moraine "S" exhibited 309 tree rings and, according to a radiocarbon age (GrA-52494: 8225 ± 40 BP), grew from 7470–7190 to 7160–6880 BC (calibrated ages for the first and last ring of the tree ring series). A tree trunk in the peat bog located in front of the pollen profile S-1 had 471 tree rings and began to grow in 7348 BC after moraine deposition (analysis: K. Nicolussi). A basal age of the peat bog in the depression on the distal side of the lateral moraine "S" yielded a calibrated age of 7450–7080 BC (VERA-5827 HS: 8235 ± 40 BP). The basal age of the pollen profile (see above) from a location in the peat bog in near proximity to the hillslope is 8470 to 7680 BC (VRI-137, see above) and hence the oldest age of this series. Thereby, the onset of peat formation subsequent to the deposition of moraine "S" is captured, albeit somewhat diffuse.

Another moraine situation well in agreement with these findings was dated to a minimum age of 8420 to 7840 BC (VRI-1887: 9000 ± 80 BC; G. Patzelt, unpublished) and is from Simonykees located near the Rostocker Hütte (2205 m.a.s.l. southern Venediger Range). These two ages suggest the beginning of tree growth within the early Holocene moraines for the time period from 8200 to 8000 BC. It can be presumed that moraine deposition occurred slightly earlier between 8400 and 8200 BC.

The steep moraine slope that delimits Salzboden Lake to the West shows a well-developed podzol soil, which points to an older Holocene age of the moraine. However, hitherto it has not been possible to determine an age for this moraine. It is younger than moraine "S" and may have been deposited in the time period of the non-tree-pollen maximum found in pollen profile S-1. Yet adequate proof for this is still lacking.

There are hardly any other investigations for this early postglacial time period from other Alpine areas. Only the tree ring analyses from around Pasterze Glacier, Großglockner Group (Nicolussi & Patzelt 2001) reach further back in time and allow a short glacier advance around 8200 BC to be deduced. However, according to our current state of knowledge, the Pasterze Glacier did not reach the positions it attained later in modern times. According to the compilations by Joerin et al. (2006, 2008) developments in the Swiss Alps seem to be in agreement with the Eastern Alps from 7800 BC onward. They do not extend back to the time of the glacier advance "S" of the Schlatenkees.

The area called "Salzboden", east of Salzboden Lake rises gently from 2100 to 2200 m a.s.l. and is a glacially overprinted terrace on which several small lakes and peat bogs lie. In the partially eroded bogs remnants of twigs and tree trunks attest to past forest vegetation. Today the area is completely treeless.

After preliminary investigations performed in 2011, K. Nicolussi has now begun the dendrochronological analysis of sample material retrieved in 2012. The project is not yet completed. However, first results are already available. The tree trunk from the bog in front of pollen profile S-1 grew from shortly before 7348 and to at least 6877 BC. The oldest tree so far (SB-8) found directly outside the early Holocene moraine at an altitude of 2192 m a.s.l. had 355 annual rings and grew from shortly before 7637 and to at least 7283 BC. The trunk sample SB-4 at 2170 m a.s.l. yielded a calibrated age of 5010–4800 BC (VERA-5711: 6021 ± 37 BP). The highest location so far for a stone pine sample (SB-7, 2300 m a.s.l.) was dated to 6410–6250 BC (VERA-5871: 7465 ± 30 BP).

The ages of the sampled wood obtained so far lie consistently within the older Holocene. Therefore human influence on forest development during this time can be excluded making these findings suitable for a palaeoclimatic interpretation. It also needs to be emphasized that under present climate conditions no tree growth is possible at the altitude of the Salzboden. The subfossil tree trunks hint at conditions significantly more favourable for forest development than those of today. The time of their growth can be traced back to the Holocene climatic optimum that, in spite of several brief interruptions, was in general clearly warmer than today.

References

Joerin, U.E., Stocker, Th.F. & Schlüchter, Ch. (2006): Multicentury glacier fluctuations in the Swiss Alps during the Holocene. – The Holocene 16: 697–704.

Joerin, U.E., Nicolussi, K., Fischer, A., Stocker, Th.F. & Schlüchter, Ch. (2008): Holocene optimum event inferred from subglacial sediments at Tschierva Glacier, Eastern Swiss Alps. – Quaternary Science Reviews 27: 337–350.

Nicolussi K. & Patzelt, G. (2001): Untersuchungen zur holozänen Gletscherentwicklung von Pasterze und Gepatschferner (Ostalpen). – Zeitschrift für Gletscherkunde und Glazialgeologie 36: 1–87.

Patzelt, G. & Bortenschlager, S. (1973): Die postglazialen Gletscher- und Klimaschwankungen in der Venedigergruppe (Hohe Tauern, Ostalpen). – Zeitschrift für Geomorphologie N.F., Suppl. 16: 25–72.

Patzelt, G. (1994): Former lakes dammed by glaciers and resulting floods in the Ötztal, Tyrol. – Mountain Research and Developement 14: 298–301.

Patzelt, G. (2013): Das Vorfeld des Vernagtferners und seine Umgebung. Begleitworte zur Karte 1:10.000. – Zeitschrift für Gletscherkunde und Glazialgeologie 45/46: 25–39.

Reimer, P.J., Bard, E., Bayliss, A., Beck, J.W., Blackwell, P.G., Bronk Ramsey, C., Buck, C.E., Cheng, H., Edwards, R.L., Friedrich, M., Grootes, P.M., Guilderson, T.P., Haflidason, H., Hajdas, I., Hatté, C., Heaton, T.J., Hogg, A.G., Hughen, K.A., Kaiser, K.F., Kromer, B., Manning, S.W., Niu, M., Reimer, R.W., Richards, D.A., Scott, E.M., Southon, J.R., Turney, C.S.M. & van der Plicht, J. (2013): IntCal13 and MARINE13 radiocarbon age calibration curves 0–50,000 years cal BP. – Radiocarbon 55: 1869–1884.

Simony, F. (1865): Aus der Venedigergruppe. – Jahrbuch des Österreichischen Alpenvereins 1: 1–32.

The moraine at Trins – type locality of the Gschnitz Stadial

Die Trinser Moräne - Typlokalität für das Gschnitzstadium

Hanns Kerschner, Susan Ivy-Ochs, Birgit Terhorst, Bodo Damm, Franz Ottner

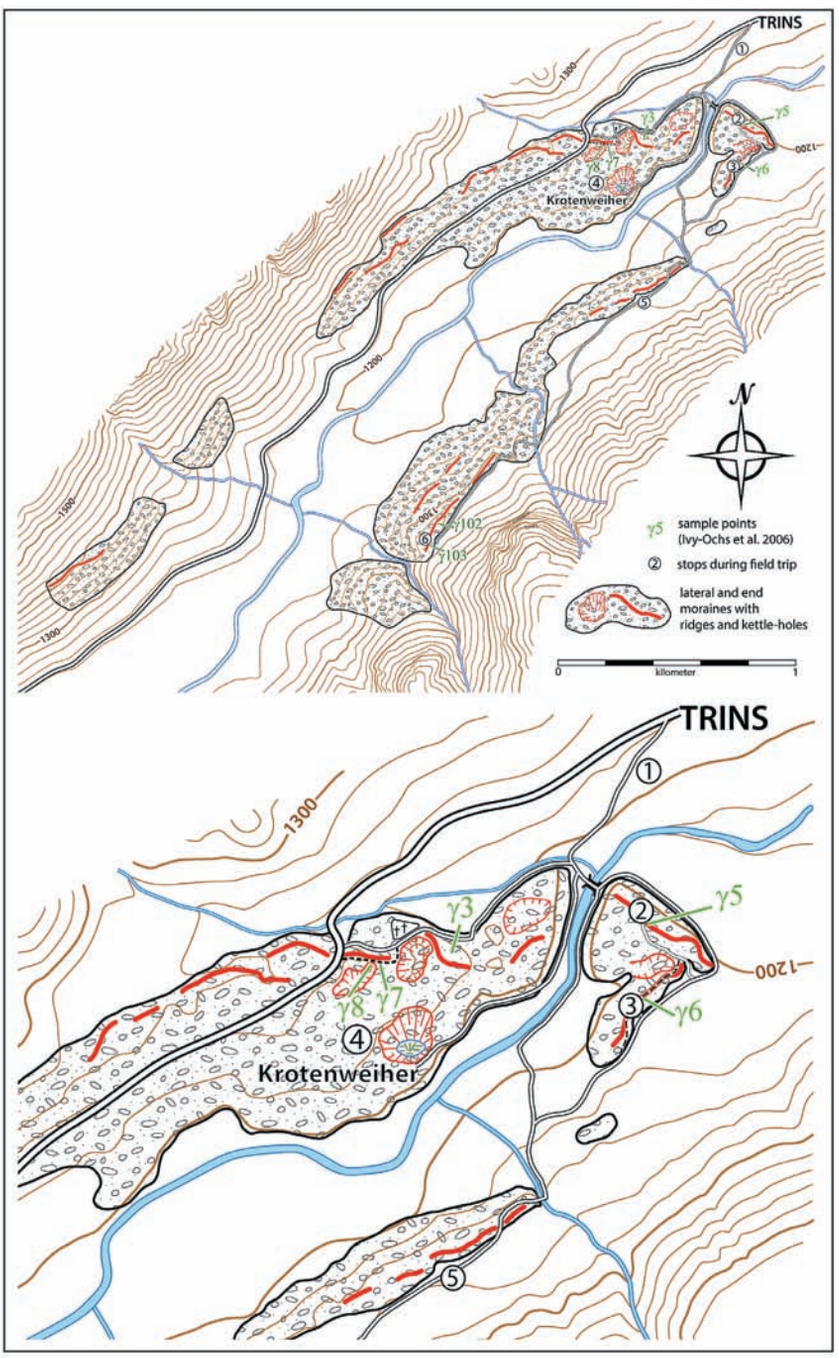

Fig. 1: End moraines and lateral moraines at the village of Trins (Tyrolean Alps) with field trip stops and sample locations.

Abb. 1: Endmoränen und Ufermoränen in der Ortschaft Trins (Tiroler Alpen) mit den Exkursionshalten und den Probestellen.

Fig. 2: End moraine and upper Gschnitztal. The valley is a nicely developed glacial trough. "1": upper end of lateral moraines, Younger Dryas glacier end was roughly at the lower end of clouds to the right of character 1; "2": Stop 2 of the field trip. The outcrop described in the text is to the right of the arrow head.

Abb. 2: Endmoräne und oberes Gschnitztal. Das Tal ist ein schön ausgebildeter glazialer Trog. „1": oberes Ende der Ufermoränen, das Gletscherende der Jüngeren Dryas war etwa beim unteren Ende der Wolken rechts von der Ziffer 1; „2": Halt 2 der Exkursion. Der im Text beschriebene Aufschluss befindet sich rechts der Pfeilspitze.

1 Introduction

In the village of Trins, about 30 km to the south of Innsbruck in the central Alps of Tyrol and 150 km from the end moraines of the LGM, a prominent end moraine traverses the Gschnitz valley (Fig. 1 & Fig. 2). It is so large and well developed that already Pichler (1859) showed it in the first geological map of Tyrol. An extremely detailed map of the moraine was published by Kerner von Marilaun (1890), and finally Penck & Brückner (1901/09) chose it as the type locality for an Alpine-wide glacier advance which they named the "Gschnitz Stadial" (indicated by "γ" on several maps). Penck & Brückner (1901/09) defined the Gschnitz Stadial by the end moraine complex at Trins and by a lowering of the equilibrium line altitude (ELA) of 600 m against "modern", i.e. ca. 1900 AD. This gave rise to considerable confusion later on, as an ELA lowering of 600 m is certainly not enough for the moraine at Trins, while a separate, younger system of moraines exists which requires such a snowline depression (Maisch 1981, Müller 1982, Kerschner 1986). As a consequence, the moraine was attributed to various other "stadials" (glacier advances during the ice recession after the Last Glacial Maximum, LGM) by a number of authors (overview in Kerschner 1986 and Ivy-Ochs et al. 2006). Since the 1960s, it is the type locality for the Gschnitz Stadial again (Mayr & Heuberger 1968). It marks the most prominent Lateglacial glacier advance before the onset of the Lateglacial Interstadial (Bølling / Allerød). An extensive description of the Gschnitz moraine with their implications was given by Ivy-Ochs et al. (2006). It forms the basis for this field guide.

2 Morphology of the moraine system

The moraine at Trins consists of a prominent single ridge on the right-hand side of the modern river (Gschnitzbach) and a set of closely spaced subparallel ridges on the left side with interspersed kettle holes. The large amount of accumulated sediment on the left-hand side of the river suggests that the glacier there was thickly debris-covered with crystalline landslide material from the inner part of the valley for a distance of about 1 km.

The moraine ridge on the right-hand side is about 30 m high and 100 m wide. The distal slope is in the order of 35° and does not show any signs of periglacial reworking. A small outwash terrace stretches down valley for about 500 m. On the proximal side, landslide and moraine deposits of unknown thickness extend about 100–200 m up valley. During the past decades, exposures created during construction work showed that the moraine is composed of predominantly crystalline rock fragments with a considerable number of Mesozoic marbles as smaller clasts.

Large gneiss boulders are almost ubiquitous, and subangular to subrounded boulders can be found all over the surface of the moraine, particularly on the left-hand side of the river. Boulders in the cultivated areas on top of the moraine system, which are shown on the map of Kerner von Marilaun (1890), were removed since then. Lateral moraines and related ice-marginal features are quasi-continuously preserved on both sides of the valley for 3 km reaching to an altitude of 1410 m a.s.l. Together with some remnants above the village of Gschnitz at 1520–1540 m a.s.l. they allow a detailed reconstruction of the glacier tongue for about 6 km. This is rather unique in the Alps and allows a reliable calculation of a number of glaciological parameters (Ivy-Ochs et al. 2006).

3 Glaciological and climatological characteristics

The glacier itself was about 18 km long and had a surface area of 51 km^2. The surface topography was characterised by a long and rather flat tongue, a step up valley from today's Lappones Alm and a wide accumulation basin. The ELA was calculated with an accumulation area ratio (AAR) of 0.63 instead of the standard value of 0.67 (Gross et al. 1977) to account for the debris cover on the lowest part of the tongue. The ELA was at ca. 1930 m a.s.l., about 700 m lower than the average Little Ice Age ELA. Reasonable ELA estimates with other AARs range between 1850 m and less than 2000 m.

Table 1: Glaciological and climatological characteristics of the Gschnitz Stadial glacier at steady state and with 70 % sliding contribution to surface velocity. Data from Ivy-Ochs et al. (2006), data for White Glacier from Cogley et al. (1996).

Tabelle 1: Glaziologische und klimatologische Eigenschaften des Gschnitzgletschers in ausgeglichenem Zustand unter der Annahme von 70 % Gleitanteil an der Oberflächengeschwindigkeit. Die Daten stammen aus Ivy-Ochs et al. (2006), die Daten für den White Glacier aus Cogley et al. (1996).

Basal shear stress	50–75 kPa		ELA / ELA depression for AAR=0.63	1930 m / -700 m
Ablation gradient, lowest 300 m	-2.3 kg $m^{-2}m^{-1}$		ELA / ELA depression for AAR=0.73 (as White Glacier, Canadian Arctic)	1740 m / - 890 m
Volumetric reaction time	260 yr		Annual precipitation at ELA (1930 m) Precipitation change	480 mm a^{-1} -67 %
Temperature Jun–Aug / May–Sep at 1930 m at end moraine at Innsbruck	 -0.7°C / -2.2°C 4.4°C / 2.9°C 8.7°C / 7.3°C		Temperature depression compared to 1931–1960 Jun–Aug May–Sep	 -9.7°C -10.2°C

H

Simple glaciological modelling as described in detail in Ivy-Ochs et al. (2006) shows that the average velocity of the glacier tongue was rather small due to very low basal shear stresses (50–75 kPa). This is typical for glaciers in a dry and cold climate. Accordingly, ablation and accumulation under steady-state conditions were low as well. The ablation gradients of the Gschnitz glacier were rather similar to those from present-day White Glacier on Axel-Heiberg-Island in the Canadian Arctic (Kerschner et al. 1999, Ivy-Ochs et al. 2006). Reasonable quantitative estimates (Table 1) with basal sliding rates of 60–80 % of the surface velocity show that annual precipitation was in the order of 300 to 900 mm a^{-1} or about 20–60 % of present-day amounts at the ELA at 1930 m a.s.l. Summer temperature (June–August) was about 8–10°C lower than today to maintain equilibrium. At the end moraine at Trins, summer temperatures should have been in a range of 4–6°C, and in the Inn valley they were in a range between about 8 and 10°C. Only a scenario with 80 % basal sliding shows positive summer temperatures at the ELA. With all other scenarios the summer temperature at the ELA is negative. This suggests that the glacier was at least partly a cold glacier.

After their deposition, the moraine and its environs were partly reworked by periglacial processes during the Lateglacial. As a consequence, they are overlain by periglacial cover beds (Semmel & Terhorst 2010), which are clearly different from the underlying moraine material under the aspects of soil physics and pedochemistry. Those processes may have played a certain role in boulder instability and possible boulder exhumation on the moraine surface.

4 Age of the Gschnitz Stadial

While earlier authors assumed a Younger Dryas age of the Gschnitz Stadial (summary in Mayr & Heuberger 1968), it became increasingly clear by the early 1970s that the moraine system at Trins predates the Bølling Interstadial (Patzelt 1975). Radiocarbon ages from Krotenweiher peat bog (Fig. 1) fall into the early Preboreal (Bortenschlager 1984, Patzelt & Sarnthein 1995). At other localities, mainly in Switzerland, it can be shown rather unequivocally that higher areas of former Gschnitz glaciers were ice-free at the onset of the Lateglacial Interstadial (summary in Ivy-Ochs et al. 2006). Because of the prominent position of the moraine within the Alpine Lateglacial stratigraphy, it was among the first Lateglacial moraines in the Alps to be chosen for surface exposure dating with terrestrial cosmogenic radionuclides (^{10}Be, ^{26}Al, Ivy-Ochs et al. 2006). Large crystalline boulders with quartz veins and big single quartz crystals are quite frequent on the moraine. The only problem encountered is potential tree growth on top of boulders during the Holocene, possibly even since Allerød times, and subsequent spalling of boulders. Originally, ^{10}Be ages were calculated with a production rate of 5.1 ± 0.3 atoms per gram SiO_2 per year at sea level. This gave an average stabilization age of the moraine of 15.4 ka (Ivy-Ochs et al. 2006). Recalculating the ages with the recently presented global ^{10}Be production rate (Heyman 2014) which is in accordance with the Northeastern North American production rate of Balco et al. (2009) gives a stabilization age of 16.7 ± 1.3 ka, about 1300 years older than previously assumed. This places the Gschnitz Stadial more at the beginning of the Heinrich 1 ice rafting event in the North Atlantic Ocean, implying a rather immediate Alpine glacier response to climatic shifts in the North Atlantic – Western European sector. The sheer size of the moraine and the slow ice velocity near the glacier tongue suggest that the glacier tongue remained close to its terminal position for at least several decades.

5 Field trip localities (Fig. 1)

Here we describe some interesting stops (1–4) during a field trip requiring 2–3 hours of walking. An additional locality (5, 6) requires about an extra one and a half hours of walking. Although the field trip is mainly on well-kept small roads and footpaths, good shoes are necessary. The village of Trins can be conveniently reached by public transport (Postauto bus from the railway station at Steinach, bus stop "Trins Gemeindeamt"). Private cars should be parked at designated parking areas on the proximal side of the moraine.

The field trip described here starts at the village centre of Trins (Gemeindeamt).

Stop 1: Road to the bridge crossing Gschnitzbach

A walk down to the bridge from the Gemeindeamt offers beautiful and instructive views of the end moraine ensemble. It can be clearly seen that the moraine complex is not a single ridge but a massive body of glacigenic sediments.

Stop 2: Top of the moraine ridge

Turning left at the bridge and walking along the outer slope of the moraine leads to a small road leading into the proximal side of the moraine. There, a rather new track leads to the top of the moraine. Before reaching the moraine crest, immediately to the right is boulder Gamma-5 (Ivy-Ochs et al. 2006).

From the moraine crest the steep distal slope can be seen, and it offers also a good impression of the outwash terrace. Farther down valley a bridge of the Brenner Autobahn can be seen. It marks the approximate position of some remnants of lateral moraines, which were deposited during the "Steinach Stadial" (Mayr & Heuberger 1968), which today is interpreted as part of the Lateglacial Ice Decay phase during the earliest part of the Alpine Lateglacial (Reitner 2007). There is also a good view of the inner part of the valley, showing the simple topography of the almost straight valley, the step above Lappones Alm and the remains of the modern glaciers in the background. The glacier end of the Younger Dryas (Egesen Stadial) was near the upper part of the step.

In March 2013 an outcrop at the moraine crest of 50 m in length and 2 m in height was created during construction work. It allowed the detailed sedimentological and pedological analysis of periglacial cover beds and soil development on the moraine. Whereas the lower part of the profile consists of dense moraine material, the upper part of the outcrop is clearly different in the content of coarse-grained (> 2 mm) material, mineralogy and grain size distribution. In the upper part a significantly higher content of silt and coarse silt is present. The lower boundary is undulating and characterised by a clear orientation of rock fragments. The properties of the material indicate an addition of loess-like substance and its transport by solifluction. It forms the parent material for the development of a well-developed and completely preserved brown soil which is about 40 cm thick.

Stop 3: Right-hand part of the end moraine system

A small footpath leads along the crest of the right hand lateral moraine and joins the track near the ski-lift. The distal slope of the moraine seems to have been eroded by a small torrent from the right-hand side of the valley, which formed a cone between the moraine and the hillslope. Boulder Gamma-6 (Ivy-Ochs et al. 2006) sits on the moraine crest. It gave the youngest age, and it cannot be ruled out that it overturned as a consequence of the erosion of the moraine.

Return to the bridge on the road along the river or continue to the right-hand lateral moraine further up (Stops 5 and 6).

Stop 4: Krotenweiher peat bog and left-hand part of terminal moraine

The Krotenweiher ("toad pond") peat bog developed in a kettle hole. Pollen analysis of the peat deposits was made for the first time by R. v. Sarnthein (1936) and later by Bortenschlager (1984). It shows that organic sedimentation started only when forest was already present in the surroundings. The vegetation documented at the base is typical for the Preboreal. This is also supported by the radiocarbon ages from bulk samples (Bortenschlager 1984) and macrofossils (Patzelt & Sarnthein 1995). The 2 sigma errors of the calibrated ages (IntCal13 database: Reimer et al. 2013) cover the period from 10,250 to 11,700 cal BP, which is the entire Preboreal and part of the early Boreal. Unfortunately, the Krotenweiher deposits are not useful for determining a reasonable minimum age of the Gschnitz Stadial.

Walk back to the bridge and turn left, continue alongside the moraine wall and a creek up to the cemetery. At the cemetery to the left (south) we can observe a well-developed kettle hole. Continue upwards on the road to the bridge of the main road. In the forest between the road to the cemetery and the main road, boulders Gamma 7 and 8 (Ivy-Ochs et al. 2006) are hidden.

Alternatively walk on the small road between the kettle hole to the left and the moraine ridge to the right and continue after about 50 m right upwards on an inconspicuous footpath. It leads to boulders Gamma 7 (big boulder immediately at the footpath) and Gamma 8 (to the left below the path in a semicircular depression). Presently (2014) Gamma 8 is partly hidden by a newly built and already derelict shed.

Continue to the main road. To the left at the main road there is a bus stop. Otherwise, continue along the main road back to the centre of Trins.

Stops 5, 6: Right-hand lateral moraine (takes about one and a half more hours)

From the station of the ski-lift (small restaurant and parking area, end of stop 3) continue up valley keeping to the left (wayside signals to Truna Alm) on a small road. After a few hundred metres, the road crosses a small creek and the lateral moraine. Then it runs on slope deposits and small outwash cones between the moraine and the hillslope. Here, the moraine runs parallel to the hillslope at a distance of about 100 m. This is typical for not-so-well nourished, slowly moving glaciers in a dry climate. The lateral component of glacier flow is unable to compensate ablation due to the heat flux from the valley sides.

At a hairpin curve, continue on a track straight ahead. The path crosses a small river (Fallzambach), which formed a cone ending at a 40–60 m high step. It was obviously deposited along the former glacier margin. From there, a road leads along the moraine and ends at Trunabach (Point 6). There the moraine is well preserved with boulders Gamma 102 and 103 from Ivy-Ochs et al. (2006). From the highest point a good view to the opposite side of the valley shows the position of the lateral moraine at Lazaunwald. This is particularly impressive in late autumn, because the hillslope below the moraine has been planted with larch trees.

References

Balco, G., Briner, J., Finkel, R.C., Rayburn, J.A., Ridge, J.C. & Schaefer, J.M. (2009): Regional beryllium-10 production rate calibration for northeastern North America. – Quaternary Geochronology, 4: 93–107.

Bortenschlager, S. (1984): Beiträge zur Vegetationsgeschichte Tirols I. Inneres Ötztal und unteres Inntal. – Berichte des Naturwissenschaftlich-Medizinischen Vereins in Innsbruck, 71: 19–56.

Cogley, J.G., Adams, W.P., Ecclestone, M.A., Jung-Rothenhäusler, F. & Omanney, C.S.L. (1996): Mass balance of White Glacier, Axel Heiberg Island, N.W.T., Canada, 1960–91. – Journal of Glaciology, 42(142): 548–563.

Gross, G., Kerschner, H. & Patzelt, G. (1977): Methodische Untersuchungen über die Schneegrenze in alpinen Gletschergebieten. – Zeitschrift für Gletscherkunde und Glazialgeologie, 12(2): 223–251.

Ivy-Ochs, S., Kerschner, H., Kubik, P.W. & Schlüchter, Ch. (2006): Glacier response in the European Alps to Heinrich event 1 cooling: the Gschnitz Stadial. – Journal of Quaternary Science, 21(2): 115–130.

Heyman, J. (2014): Paleoglaciation of the Tibetan Plateau and surrounding mountains based on exposure ages and ELA depression estimates. – Quaternary Science Reviews, 91: 30–41.

Kerner von Marilaun, F. (1890): Die letzte Vergletscherung der Central-Alpen im Norden des Brenner. – Mittheilungen der kaiserlich-königlichen Geographischen Gesellschaft in Wien, 33: 307–332.

Kerschner, H. (1986): Zum Sendersstadium im Spätglazial der nördlichen Stubaier Alpen, Tirol. – Zeitschrift für Geomorphologie N.F., Suppl. 61: 65–76.

Kerschner, H., Ivy-Ochs, S. & Schlüchter C. (1999): Paleoclimatic interpretation of the early late-glacial glacier in the Gschnitz valley, Central Alps, Austria. – Annals of Glaciology, 28: 135–140.

Maisch M. (1981): Glazialmorphologische und gletschergeschichtliche Untersuchungen im Gebiet zwischen Landwasser- und Albulatal (Kt. Graubünden, Schweiz). – Physische Geographie, 3: 215 pp.

Mayr, F. & Heuberger, H. (1968): Type areas of Lateglacial and Postglacial deposits in Tyrol, Eastern Alps. – In: Richmond, G.M. (ed.): Glaciations of the Alps. – Series in Earth Sciences no. 7, University of Colorado: Boulder: 143–165.

Müller, H.N. (1982): Zum alpinen Spätglazial: Das Zwischbergenstadium. – Zeitschrift für Gletscherkunde und Glazialgeologie, 17(2): 135–142.

Patzelt G. (1975): Unterinntal–Zillertal–Pinzgau–Kitzbühel. Spät- und postglaziale Landschaftsentwicklung. – In: Fliri, F. & Leidlmair, A. (ed.): Tirol – ein geographischer Exkursionsführer. – Innsbrucker Geographische Studien, 2: 309–329.

Patzelt, G. & Sarnthein, M. (1995): Late Glacial morainal arc at Trins in the Gschnitz valley/Tyrol–'Krotenweiher' peat bog; M. Maisch (ed).: 12. Alpine Traverse. – In: W. Schirmer (ed.): Quaternary Field Trips in Central Europe, vol. 2: 669–670; München (Pfeil).

Penck, A. & Brückner, E. (1901/1909): Die Alpen im Eiszeitalter. – 1199 p.; Leipzig (Tauchnitz).

Pichler, A. (1859): Beiträge zur Geognosie Tirols. – Zeitschrift des Museums Ferdinandeum Innsbruck, 3(8), 1–232.

Reitner, J. M. (2007): Glacial dynamics at the beginning of Termination I in the Eastern Alps and their stratigraphic implications. – Quaternary International, 164–165: 64–84.

Reimer, P.J., Bard, E., Bayliss, A., Beck, J.W., Blackwell, P.G., Bronk Ramsey, C., Buck, C.E., Cheng, H., Edwards, R.L., Friedrich, M., Grootes, P.M., Guilderson, T.P., Haflidason, H., Hajdas, I., Hatté, C., Heaton, T.J., Hogg, A.G., Hughen, K.A., Kaiser, K.F., Kromer, B., Manning, S.W., Niu, M., Reimer, R.W., Richards, D.A., Scott, E.M., Southon, J.R., Turney, C.S.M. & van der Plicht, J. (2013): IntCal13 and MARINE13 radiocarbon age calibration curves 0-50,000 years cal BP. – Radiocarbon, 55(4): 1869–1884.

Sarnthein, R.v. (1936): Moor- und Seeablagerungen aus den Tiroler Alpen in ihrer waldgeschichtlichen Bedeutung. I. Teil: Brennergegend und Eisacktal. – Beihefte zum Botanischen Centralblatt, LV: 544–631.

Semmel, A. & Terhorst, B. (2010): The concept of the Pleistocene periglacial cover beds in Central Europe – A review. – Quaternary International, 222: 120–128.

Notes

Landscape archaeological results and discussion of Mesolithic research in the Fotsch valley (Tyrol)

Landschaftsarchäologische Ergebnisse und Diskussion der Mesolithikum-Forschung im Fotschertal (Tirol)

Clemens Geitner, Dieter Schäfer, Stefano Bertola, Sixten Bussemer, Kati Heinrich, Jaroslaw Waroszewski

Fig. 1: Geographical overview of the Stubai Alps and the position of the archaeological site Ullafelsen in the Fotsch valley southwest of Innsbruck (modified after Tirol-Atlas 1995).

Abb. 1: Geographischer Überblick der Stubaier Alpen mit der Position der archäologischen Grabung Ullafelsen im Fotschertal südwestlich von Innsbruck (verändert nach Tirol-Atlas 1995).

Fig. 2: View from the inner Fotsch valley to the north to the Karwendel mountain range of the Northern Calcareous Alps: on the right, in the foreground, the Ullafelsen with its flat top stands out clearly as a roche moutonnée (the white tent is pitched near the archaeological excavation) (photograph: D. Schäfer, 2004).

Abb. 2: Blick vom inneren Fotschertal nach Norden bis zum Karwendelgebirge der Nördlichen Kalkalpen: Rechts im Vordergrund tritt der Ullafelsen mit seiner flachen Kuppe als Härtling deutlich hervor (das weiße Zelt steht nahe der archäologischen Grabung) (Foto: D. Schäfer, 2004).

1 Study area and field trip sites

Our field trip takes us to the key location of Mesolithic research in Tyrol. The archaeological open-air site Ullafelsen is situated at 1860 m a.s.l. in the Fotsch valley of the northern Stubai Alps, around 20 km southwest of Innsbruck (Fig. 1). The catchment reaches from around 900 to 3000 m a.s.l. and is geologically part of the Ötztal-Stubai crystalline complex, i.e. mainly built up of metamorphic rocks (para- and orthogneiss and amphibolite) (Nittel 2011). In terms of climate, the area lies in the transition zone between Northern and Central Alps, so that neither precipitation nor temperature present extreme values (Schlosser 2011). Due to former and recent geomorphological processes, such as glacial sediment accumulation, debris flows and rockfall, both the valley and the slopes are covered by unconsolidated sediments and bedrock is only exposed on steep slopes and on the highest summits.

The vertical sequence of the vegetation units in the Fotsch catchment is typical for the Central Alps with spruce (*Picea abies*) dominating in the montane and Arolla pine (*Pinus cembra*) in the subalpine belt. The timber line has been lowered for centuries by human impact and nowadays reaches elevations of 1800 to 2000 m a.s.l. Nevertheless, the potential timber line reaches at least 2200 m a.s.l. The vegetation pattern above the timber line is composed of dwarf-shrub communities and alpine grasslands (Kemmer 2011).

Human activity and environmental impact are associated with clearing the natural forests, cattle grazing and tourism, mainly in the form of mountain hiking. The Potsdamer Hütte, a mountain hut of the German Alpine Club, is located at the rear of the valley at about 2000 m a.s.l.

Our field trip will take us to three sites, the most significant being the Ullafelsen (1860 m a.s.l.). At the top of this site, we will see some typical profiles of the archaeological excavation, which we can compare to a typical podzol near-

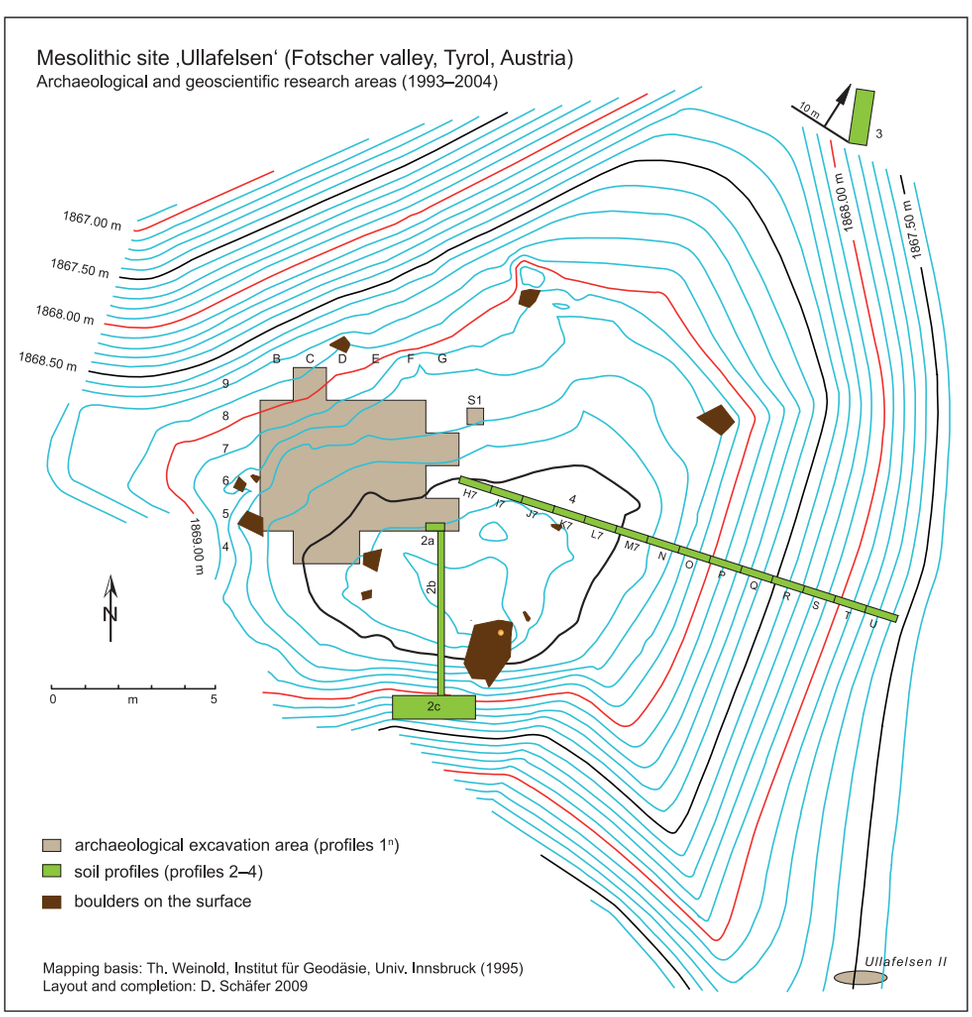

Fig. 3: Detailed plan of the archaeological excavation site and the profile positions 2 to 4 at the top of the Ullafelsen (illustration: D. Schäfer) (Geitner et al. 2011: 119).

Abb. 3: Detailplan der archäologischen Ausgrabung und der Lage der Profile 2 bis 4 auf dem Ullafelsen (Graphik: D. Schäfer) (Geitner et al. 2011: 119).

by. Additionally, we can visit the Kaseralmschrofen (1755 m a.s.l.), another archaeological site, to discuss aspects of the temporal development of settlement and their respective site elevations in the early Holocene. At the third site, near Potsdamer Hütte 2000 m a.s.l.) we will see the dimension of Lateglacial moraines of the Egesen Stadial and we can also discuss Holocene sediment profiles, which show some similarities to those of the Ullafelsen.

2 The archaeological site Ullafelsen

Motivated by the recovery of the 'ice man' at the Tisenjoch, South Tyrol (Italy) in 1991, the University of Innsbruck established a comparative Alpine archaeology. A few years later a systematic search for Mesolithic sites in the alpine and subalpine zone in the Tyrolean Alps began. For the Mesolithic people the tree-line ecotone provided a larger population of game for hunting and offered a diversified repertory for gathering. The alpine zone was also relevant for prospecting and extracting lithic raw materials.

In this context the Ullafelsen site (locally named "Riegelschrofen") was found in 1994 and systematic excavation started in 1995. Since then a total of 12 excavation months (1994–2004) have been invested in this site and some 10 researchers have attended the field campaigns. The main excavation (25 m^2) is situated on the top of Ullafelsen (Fig. 2 and 3), which can be described as a resistant rock area (roche moutonnée) at the lower eastern slope. Since 1999, stratigraphic and soil-scientific investigations were included to better understand how and when the manifold excavation profiles developed (Geitner 2010, Geitner & Schäfer 2010, Geitner et al. 2011).

Judging from geomorphological investigations, Ullafelsen probably became ice-free at the transition from the Older Dryas to Bølling (Kerschner 2011) and was initially covered with unconsolidated glacial and glaciofluvial deposits of an average thickness of 0.5 m. In recent years grass, herbs and dwarf shrubs have grown on top of Ullafelsen, and young Arolla pines have sprung up on the surrounding slopes.

In order to better understand both the natural conditions for the prehistoric land use and the early impact of humans, we have included several aspects of geology, geomorphology, meteorology, glacier history, and soil and vegetation sciences in these studies. A comprehensive overview of the interdisciplinary approach and the results was published by Schäfer (2011a).

Fig. 4: The position of the Ullafelsen (U) southwest of Innsbruck and evidence of the lithic raw material groups used at this site: Q (local quartz); BK (mountain crystal); SA (south alpine silex); NK (silex of the Northern Calcareous Alps); FA (silex of the Franconian Alb). (illustration: D. Schäfer).

Abb. 4: Die Position des Ullafelsens (U) südwestlich von Innsbruck und der Nachweis der Gesteinsrohmaterialien, welche an diesem Fundplatz genutzt wurden: Q (lokaler Quarz); BK (Bergkristall); SA (südalpiner Silex); NK (Silex der Nördlichen Kalkalpen); FA (Silex der Fränkischen Alb) (Graphik: D. Schäfer).

Fig. 5: Section of the archaeological excavation Ullafelsen, square C9, east profile (cf. Fig. 3). Typical features of LL and typical position of charcoal bands at the top of it (photograph: D. Schäfer, 2003).

Abb. 5: Profil der archäologischen Ausgrabung auf dem Ullafelsen, Quadrat C9, Ostprofil (vgl. Abb. 3). Typische Eigenschaften des LL sowie der Position von Holzkohlebändchen direkt oberhalb der LL (Foto: D. Schäfer, 2003).

I

3 Archaeological highlights

In total, 7931 artefacts were found in the main excavation area. Two thirds of them have a length of 1 to 6 mm. In addition to yellow and red artefacts, many pieces are grey, black or brownish coloured, i.e. they are quite similar to the soil in which they were discovered. This aspect and the thorough documentation of all findings made the excavation very time-consuming.

Beside the artefacts, we identified and reconstructed at least 14 fireplaces within an excavated area of 25 m^2. More than 20 ^{14}C-AMS analyses of charcoals allowed to date them to between the mid-Preboreal and the mid-Boreal (9200–7600 cal BC), with a maximum in the second half of the Preboreal. Charcoal wood analysis is in line with the site elevation in this early period of the Holocene (Oeggl & Schoch 2011).

A special highlight is the first successful correlation of the following features with the Alpine Mesolithic, at least for open-air sites (Schäfer 1998, 2011b):

In some parts of the excavation site we observed a relative stratigraphic sequence of specific artefact raw materials (e.g. the secondary use of fireplace 5 to deposit lithic waste from southern Franconian Alb chert ("Fränkischer Hornstein"), from Bavaria, around 200 km northeast of Ullafelsen, see Fig. 4).

For the first time in the Alpine Mesolithic, organic tar remains were found on the surface of many of our stone artefacts. With the help of close stratigraphic documentation and soil sampling in the vicinity of fireplace 3, we found

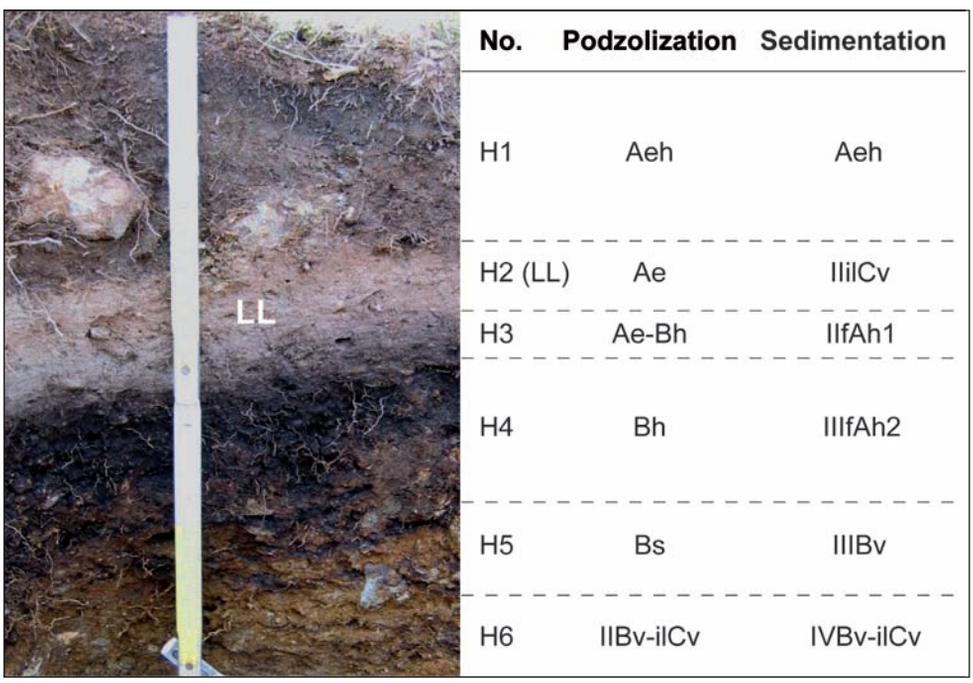

Fig. 6: Profile 3 shows the typical sequence of the sampled mineral soil horizons (H1–H6). The naming of the horizons varies considerably, depending on the interpretation of the profile, whether podzolization or sedimentation was the dominant process (cf. Ad-hoc Arbeitsgruppe Boden 2005) (photograph: C. Geitner, 2004)

Abb. 6: Profil 3 zeigt die typische Abfolge der beprobten Mineralboden-Horizonte (H1–H6). Je nach Interpretation des Profils – Podsolierung oder Sedimentation als dominanter Prozess – weichen die Bezeichnungen der Horizonte deutlich voneinander ab (vgl. Ad-hoc Arbeitsgruppe Boden 2005) (Foto: C. Geitner, 2004).

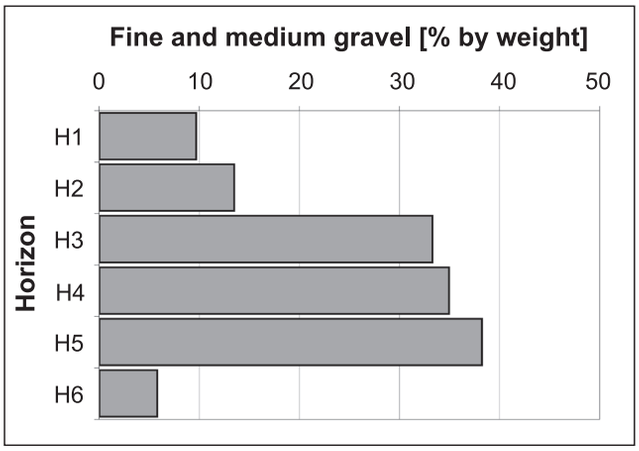

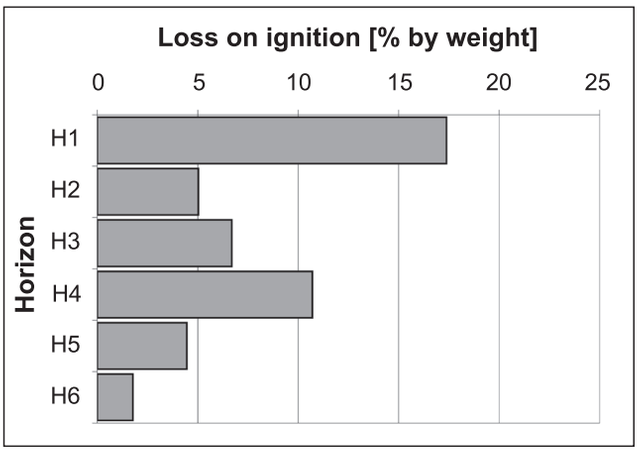

Fig. 7a+b: Amount of fine and medium-size gravel and loss on ignition of fine soil of profile 3 (differentiation of the horizons as in Fig. 6). The strongly varying proportions of gravel are an indication of a multi-layer unconsolidated deposit (Geitner et al. 2011: 127).

Abb. 7a+b: Anteile an Fein- und Mittelkies und Glühverluste der Feinerde des Profils 3 (Zuordnung der Horizonte vgl. Abb. 6). Die stark variierenden Kiesanteile weisen auf ein mehrschichtiges Lockersubstrat hin (Geitner et al. 2011: 127).

clear evidence for the systematic production of birch tar. The microwear analyses of stone artefacts confirm that many of the artefacts were shafted and fixed with it.

We have indications of intentional manipulation of the surface by the Mesolithic inhabitants (smoothing the living floor and covering parts of a fireplace).

As the stone raw materials could be assigned to sources in northern Italy (Val di Non, Trentino), this inventory seems to be the oldest evidence of people crossing the Alps during the early Holocene (Fig. 4). Together with the chert material from the Franconian Alb, we can hypothesize that the Stubai Alps were in the overlap region of two cultural influences: the Italian Sauveterrian and the South German Beuronian (Figs. 12–16). Apart from the raw materials, there are also typological arguments for this interpretation.

All stone tools, plus several unretouched flakes were analysed for use-wear traces (Pawlik 2011). Nearly half of them corroborate our own story, sometimes connected to a specific maintenance history of repeated use/rejuvenation, etc. Bone or antler, wood, hide and leather could be identified as worked (contact) material. By mapping these results, several of these functions can be correlated with single fireplaces and other features. Combining use-wear traces with those of reshafting, retooling and the occurrence of birch tar helped to reconstruct some tool constructions and provided insights into aspects of that raw material economy.

With the extremely time-consuming method of refitting we could restore more than 20 % of any artefacts larger than 5–6 mm. Based on this we have evidence for several forms of blank production and tool rejuvenation. Mapping these results suggested some functional relationships between several areas of our excavation site. So we can demonstrate that some of the subareas were used by Mesolithic humans at the same time.

Figures 12–16 give an overview of typical raw material groups of the Ullafelsen excavation site.

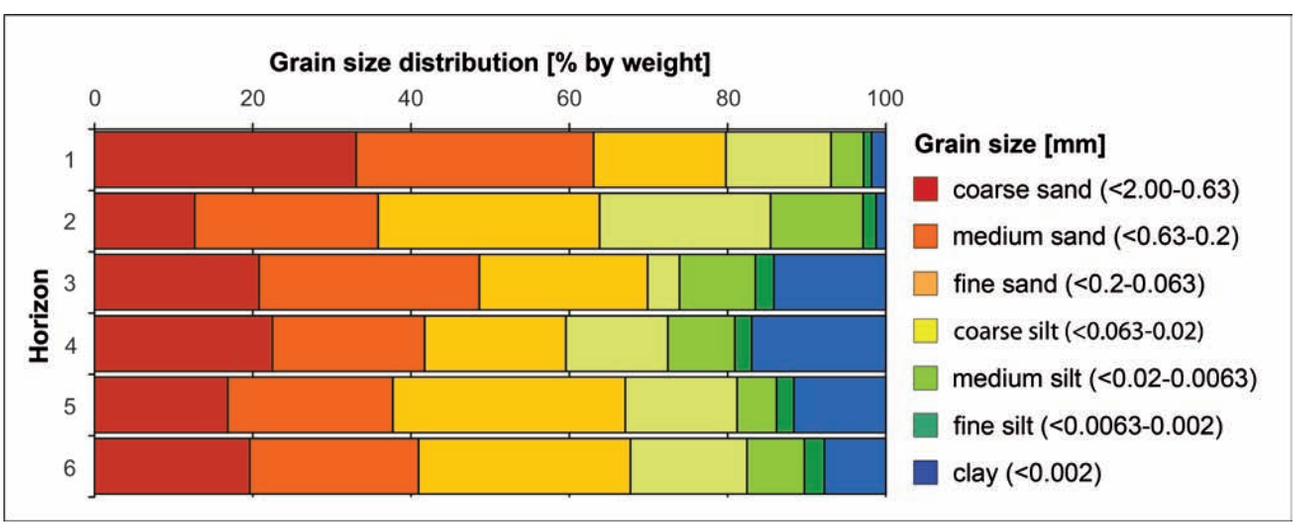

Fig. 8: Grain size distribution of the fine soil for profile 2a (data after Ikinger 2001; differentiation of the horizons as in Fig. 6). The LL (horizon 2) is conspicuous by the high proportion of fine sand, coarse and medium silt (Geitner et al. 2011: 126).

Abb. 8: Korngrößenanteile der Feinerde des Profils 2a (Daten nach Ikinger 2001; Zuordnung der Horizonte vgl. Abb. 6). Die LL (Horizont 2) fällt durch hohe Anteile von Feinsand, Grob- und Mittelschluff auf (Geitner et al. 2011: 126).

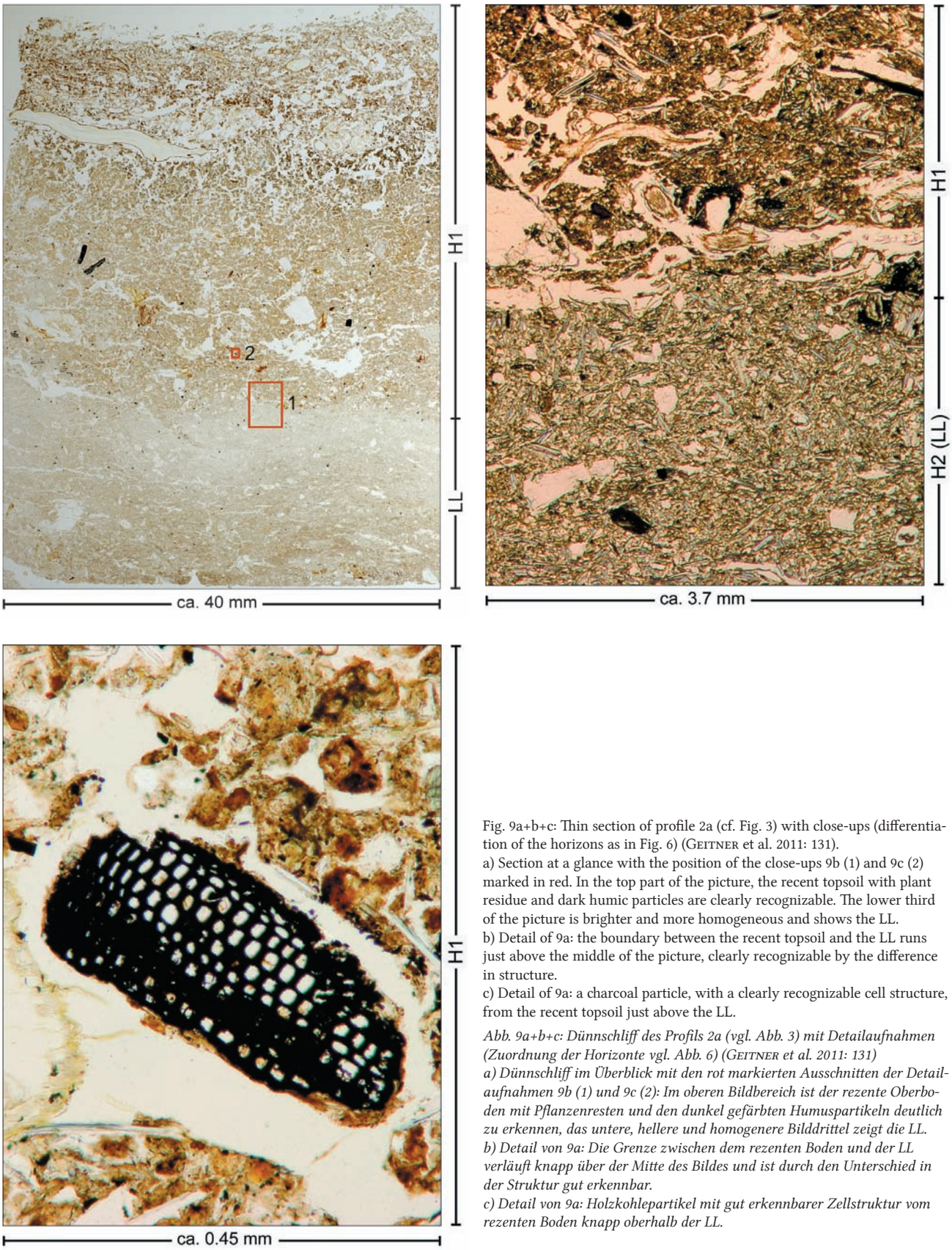

Fig. 9a+b+c: Thin section of profile 2a (cf. Fig. 3) with close-ups (differentiation of the horizons as in Fig. 6) (Geitner et al. 2011: 131).
a) Section at a glance with the position of the close-ups 9b (1) and 9c (2) marked in red. In the top part of the picture, the recent topsoil with plant residue and dark humic particles are clearly recognizable. The lower third of the picture is brighter and more homogeneous and shows the LL.
b) Detail of 9a: the boundary between the recent topsoil and the LL runs just above the middle of the picture, clearly recognizable by the difference in structure.
c) Detail of 9a: a charcoal particle, with a clearly recognizable cell structure, from the recent topsoil just above the LL.

Abb. 9a+b+c: Dünnschliff des Profils 2a (vgl. Abb. 3) mit Detailaufnahmen (Zuordnung der Horizonte vgl. Abb. 6) (Geitner et al. 2011: 131)
a) Dünnschliff im Überblick mit den rot markierten Ausschnitten der Detailaufnahmen 9b (1) und 9c (2): Im oberen Bildbereich ist der rezente Oberboden mit Pflanzenresten und den dunkel gefärbten Humuspartikeln deutlich zu erkennen, das untere, hellere und homogenere Bilddrittel zeigt die LL.
b) Detail von 9a: Die Grenze zwischen dem rezenten Boden und der LL verläuft knapp über der Mitte des Bildes und ist durch den Unterschied in der Struktur gut erkennbar.
c) Detail von 9a: Holzkohlepartikel mit gut erkennbarer Zellstruktur vom rezenten Boden knapp oberhalb der LL.

4 Stratigraphical structure of distinct horizons and the LL (= light layer) phenomenon

Stratigraphic and soil-related research were triggered by an unusual finding in several excavation profiles, i.e. a light-grey layer, referred to as LL (= light layer), which is an important reference (marker) horizon. Figure 5 demonstrates the typical stratigraphic structure of the excavation profiles at the Ullafelsen site. We can clearly recognize a sequence of four layers or soil horizons. This profile structure can also be found in the vicinity of the excavation site (Fig. 6). A light-grey layer (LL) commonly stands out in the central part of the profile sections. It constitutes the lower part of the

predominantly fine-grained top of the unconsolidated sediments, which cover Ullafelsen.

Some characteristics of the LL

The greatly varying proportions of gravel in profile 3 are an indication of these multi-layered unconsolidated deposits (Fig. 7a, LL corresponds to horizon 2). But there are also some differences in the grain sizes of the fine earth (Fig. 8), as the LL includes high amounts of fine sand, coarse and medium silt. Therefore the profile structure also changes from the A horizon to the LL, which can be seen quite clearly in thin sections (Figs. 9a and 9b). Analyses of the mineralogical composition showed the highest proportion of mica (muscovite and biotite) within the LL (Geitner et al. 2011: 128).

As a summary of these features, but also from the macromorphological characteristics of the LL in longer profiles, we assume the typical LL to be the result of aeolian sedimentation. Nevertheless, some LL properties (especially the chemical ones) are quite similar to eluvial horizons of podzols. Last but not least, we found some traces of anthropogenic disturbances within the profiles. That means, we have to consider multiple modes of formation to explain the specific soil features at Ullafelsen.

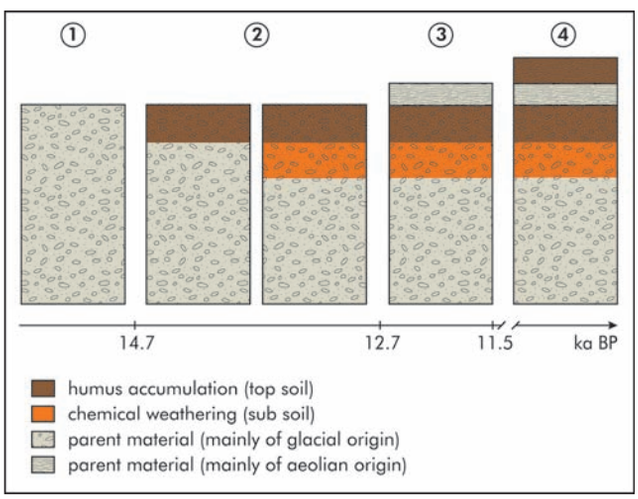

Fig. 10: Hypothetical sequence of four phases of varying dominance of sedimentological and soil-forming processes at the Ullafelsen (time scale after Ivy-Ochs et al. 2009) (Geitner et al. 2011: 139).

Abb. 10: Hypothetische Abfolge von vier Phasen unterschiedlicher Dominanz sedimentologischer und bodengenetischer Prozesse am Ullafelsen (Zeitangaben nach Ivy-Ochs et al. 2009) (Geitner et al. 2011: 139).

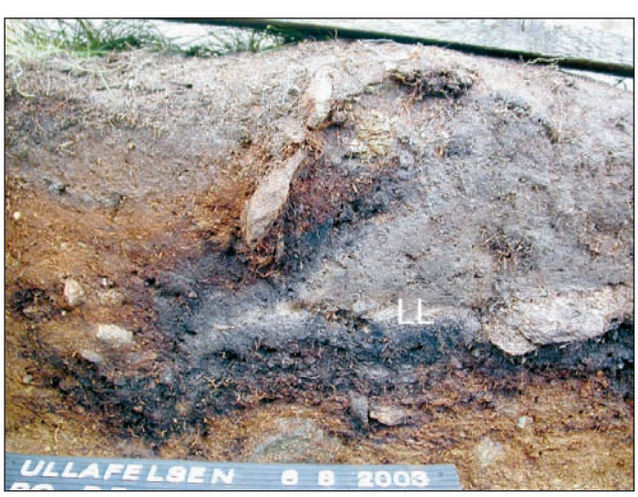

Fig. 11: Section of the archaeological excavation Ullafelsen, square B5, west profile (cf. Fig. 3). Feature of an overturn of LL by the fall of a tree or a bigger shrub (photograph: D. Schäfer, 2003).

Abb. 11: Profil der archäologischen Ausgrabung auf dem Ullafelsen, Quadrat B5, Westprofil (vgl. Abb. 3). Überkippung der LL infolge eines Baum- oder größeren Buschwurfs (Foto: D. Schäfer, 2003).

Vertical distribution of artefacts, charcoal and pollen

The vertical distribution of the artefacts within the excavation profiles shows a distinct pattern that helps us to understand the development of the stratigraphy. Among the ca. 2,500 artefacts recorded in relation to the stratigraphic units, 70 % were found within the LL, on it or slightly above it and 20 % of these ca. 2500 artefacts lay directly upon the LL (Schäfer 2011b). It is therefore obvious that the surface of the LL had once been the living floor. This is also reflected in special structures at the top of the LL (e.g. very distinct delimitations and charcoal bands) (Fig. 5). Most of the charcoal enrichments were also found directly above the LL. Based on the oldest ^{14}C-AMS analysis of five fireplaces positioned directly upon the LL (Schäfer 2011b: 298), a minimum age of 9200–8700 cal BC was determined for the deposition of the LL material.

To validate our stratigraphical interpretation, we conducted pollen analyses of some excavation profiles. The amount and composition of pollen grains within the LL corroborate ideas about both the gradual sedimentation process and the very early Holocene age of LL. The latter is underscored by the high values of *Tilia* (lime) and *Corylus* (hazel) and the lack of pollen from some other species in the LL.

5 Landscape historical aspects

Erosion and sedimentation

As the many artefact and charcoal findings near the surfaces show, soils at the top of the Ullafelsen were quite stable throughout the whole Holocene. Considering its exposed position, this is a truly remarkable result.

The unconsolidated sediments covering the bedrock ridge of the Ullafelsen present a multi-layered structure, which can be traced by the varying stone content. The lower section consists of glacial and in patches fluvioglacial deposits. The upper section starts with the LL and reaches up to the surface. The origin of these younger sediments has not yet been finally clarified. High amounts of silt and fine sand may reflect an aeolian influence. But coarser particles and even larger stones occur within these upper sediments. Due to the isolated location of the Ullafelsen site, this place is well protected against rockfall, debris flows and fluvial dynamics. Therefore we suggest that some of the youngest material was introduced by large avalanches, which reach this site from time to time. Nevertheless, the high content of fine material suggests that aeolian sedimentation has lasted until recent times.

Possible sources of the aeolian sediment

Assuming that the LL is an aeolian layer, we have to discuss where the material came from and when. Judging from the charcoal datings, the LL accumulated at the latest in the very early Holocene (before 9200–8700 cal BC), perhaps even at the end of the Lateglacial. Considering the main wind direction (Northwest), there is a large, mostly flat area at eleva-

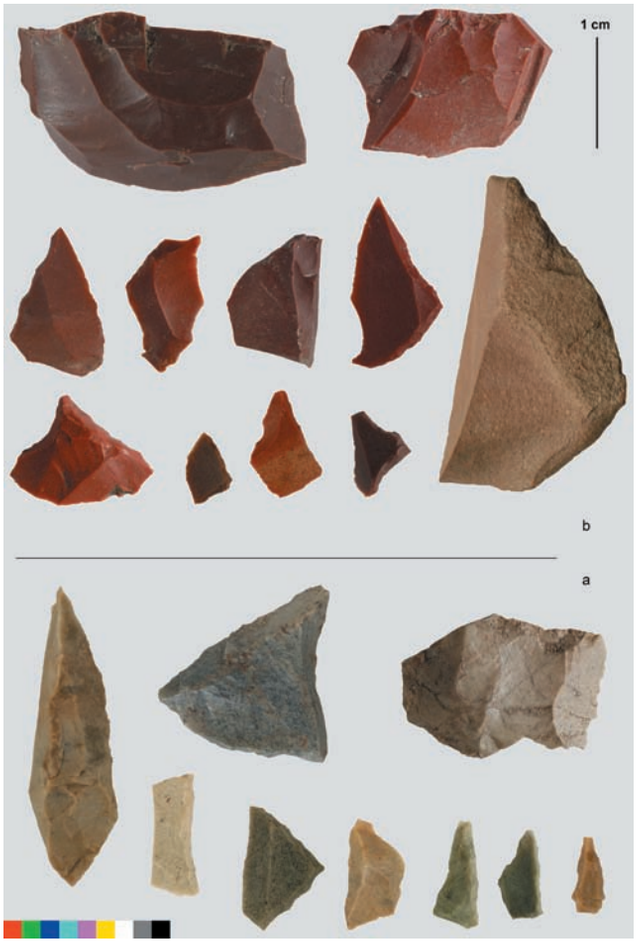

Fig. 12: Ullafelsen, Mesolithic artefacts; raw material: chert of the Northern Calcareous Alps (a: Chiemgau Formation; b: Ruhpolding Formation) [NK in figure 4] (photograph: D. Schäfer, 2014).

Abb. 12: Ullafelsen, Mesolithische Artefakte; Rohmaterialien: Silex der Nördlichen Kalkalpen (a: Chiemgau Formation; b: Ruhpolding Formation) [NK in Abbildung 4] (Foto: D. Schäfer, 2014).

Fig. 13: Ullafelsen, Mesolithic artefacts; raw material: Upper Jurassic chert from the Franconian Alb (Bavaria) [FA in figure 4] (photograph: D. Schäfer, 2014).

Abb. 13: Ullafelsen, Mesolithische Artefakte; Rohmaterialien: Oberjurassischer Silex der Fränkischen Alb (Bayern) [FA in Abbildung 4] (Foto: D. Schäfer, 2014).

Fig. 14: Ullafelsen, Mesolithic artefacts; raw material: southern Alpine chert (Scaglia variegata/Scaglia Rossa from the Valle di Non area (Trentino, Italy) [SA in figure 4] (photograph: D. Schäfer, 2014).
Abb. 14: Ullafelsen, mesolithische Artefakte: Rohmaterial: Südalpiner Silex (Scaglia variegata / Scaglia rossa vom oberen Nonstal (Trentino), SA in Abb. 4) (Foto: D. Schäfer, 2014).

tions between 2300 and 2500 m a.s.l. below the Roter Kogel summit. After the last glacier advances during the Younger Dryas, this area became ice-free and the unconsolidated mica-rich sediments, sparsely covered with pioneer vegetation, facilitated aeolian deflation.

Lateglacial soil development?

If the LL was deposited at the end of the Lateglacial and/or the beginning of the Holocene, the dark and humus-rich horizon below has to be older. Hence this horizon can be interpreted as remains of an older soil formation (fossil Ah and Bv horizons), which probably took place during the Bølling and Allerød, when favourable climate and vegetation conditions prevailed. As far as we know, no comparable results about Lateglacial soil development exist elsewhere in the Alps.

The dark horizon below LL, however, could also be interpreted as the accumulation horizon of a podzol. But this view does not fit with the earlier mentioned properties of the LL that distinguish it clearly from an eluvial horizon.

Synthesis

We identified four phases of soil formation and sediment deposition (Fig. 10): (1) the Ullafelsen probably became ice-free at the transition from the Older Dryas to the Bølling and was buried beneath thin glacial and fluvioglacial sediments. (2) Early deep soil formation took place under a warm climate

Fig. 15: Ullafelsen, Mesolithic artefacts of rough local quartz varieties [Q in figure 4] (photograph: D. Schäfer, 2014).

Abb. 15: Ullafelsen, Mesolithische Artefakte grober lokaler Quarzvarietäten [Q in Abbildung 4] (Foto: D. Schäfer, 2014).

Fig 16: Ullafelsen, Mesolithic artefacts; raw material: mountain crystal [BK in figure 4] (photograph: D. Schäfer, 2014).

Abb. 16: Ullafelsen, Mesolithische Artefakte; Rohmaterialien: Bergkristall [BK in Abbildung 4] (Foto: D. Schäfer, 2014).

during the Bølling and Allerød. (3) The aeolian deposition of sediments rich in mica most probably occurred from the middle to the end of the Younger Dryas, when large deflation areas below the Roter Kogel became ice-free but had not yet been consolidated by vegetation. (4) The youngest cover of the LL indicates that aeolian deposition continued during the Holocene period, albeit at a significantly lower rate.

This hypothesis adds new aspects to the debate about landscape development. Some details of this hypothetical sequence of processes have not been completely resolved yet and investigations on the phenomenon of the LL are continuing. Nevertheless, the importance of aeolian deposits at high elevations in the Alps is also highlighted by other studies (Küfmann 2008a, 2008b). Thus equivalents of the LL might well be present in other parts of the Alps and used as a marker horizon for the boundary between the Lateglacial and the Holocene.

6 Outlook

Some questions related to the LL, and the landscape history associated therewith, are still under discussion. One such aspect is the vegetation history of the Ullafelsen itself, especially the presence or absence of shrubs and trees, since it is surprising that this different layering, including very thin layers, were not disturbed. In fact, it can be assumed that at the latest by the end of the presence of Mesolithic people, a quite dense stand of trees should have been established. But if trees existed there for millennia the manifold stratigraphy would have undoubtedly been destroyed. Is it possible that a site at an elevation of 1860 m a.s.l. had no trees during the entire Holocene? This could only be explained by very special microclimatic conditions. Because of the exposed position of the Ullafelsen, snow cover during the winter is quite thin as snow is typically blown away by the wind. Hence only the lower plants are protected against the very low

winter temperatures. These special microclimatic conditions may have prevented the establishment of trees for millennia. Only in one case did we find a clear disturbance of the LL, which should be connected with the fall of a tree or a larger shrub (Fig. 11). So we can conclude that the structure of the LL also indicates a site-specific vegetation history.

Another point worth further discussion is the effect of anthropogenic disturbances. We could ascertain the LL as a former living floor. The trampling of Mesolithic people likely changed the LL material significantly in terms of density and created an artificial surface. For such a more or less open surface we also expect some local erosion-transport-accumulation processes, which may have affected the grain size distribution of the LL, especially in its upper part. Some of the mentioned differences between LL and eluvial horizons may be explained by these anthropogenic disturbances, thus podzolization influences on the LL cannot be totally excluded.

The horizon above the LL seems to be quite weakly developed. This is probably due to continuous sedimentation but perhaps also to the weak growth of the vegetation. Compared with the lower profile sections, Lateglacial soil development within the glacial deposits was quite strong, which remains to be understood.

7 References

Ad-hoc-Arbeitsgruppe Boden (2005): Bodenkundliche Kartieranleitung. – 5. Auflage; Bundesanstalt für Geowissenschaften und Rohstoffe in Zusammenarbeit mit den Staatlichen Geologischen Diensten (Hannover), 438 pp.; Stuttgart.

Bertola, S. (2011): The flints of Southern Alps (Non Valley, Italy) provenance found in the Mesolithic site of Ullafelsen (Sellrain, Tyrol). – In: Schäfer, D. (ed.): Das Mesolithikum-Projekt Ullafelsen (Teil 1). Mensch und Umwelt im Holozän Tirols 1, 463–505; Innsbruck.

Geitner, C. (2010): Soils as archives of natural and cultural history; examples from the Eastern Alps. – In: Borsdorf, A., Grabherr, G., Heinrich, K., Scott, B. & Stötter, J. (eds.): Challenges for mountain regions – tackling complexity, 68–75; Innsbruck, Wien (Böhlau).

Geitner, C. & Schäfer, D. (2010): Interdisziplinäre Zusammenarbeit an der Schnittstelle von Archäologie und Bodenkunde im Gebirge – Grundsätzliche Überlegungen und Beispiele des Mesolithfundplatzes Ullafelsen (Tirol). – In: Mandl, F. & Stadler, H. (eds.): Archäologie in den Alpen – Alltag und Kult. Forschungsberichte der ANISA 3, 25–42; Haus i. E.

Geitner, C., Bussemer, S., Ehrmann, O., Ikinger, A., Schäfer, D., Traidl, R. & Tscherko, D. (2011): Bodenkundlich-stratigraphische Befunde am Ullafelsen im hinteren Fotschertal sowie ihre landschaftsgeschichtliche Interpretation. – In: Schäfer, D. (ed.): Das Mesolithikum-Projekt Ullafelsen (Teil 1). Mensch und Umwelt im Holozän Tirols 1, 109–151; Innsbruck.

Ivy-Ochs, S., Kerschner, H., Maisch, M., Christl, M., Kubik, P.W. & Schlüchter, C. (2009): Latest Pleistocene and Holocene glacier variations in the European Alps. – Quaternary Science Reviews 28, 2137–2149.

Kemmer, I. (2011): Die rezente Vegetation im inneren Fotschertal / Nördliche Stubaier Alpen. – In: Schäfer, D. (ed.): Das Mesolithikum-Projekt Ullafelsen (Teil 1). Mensch und Umwelt im Holozän Tirols 1, 155–193; Innsbruck.

Kerschner, H. (2011): Spätglaziale Gletschervorstöße im Fotschertal. – In: Schäfer, D. (ed.): Das Mesolithikum-Projekt Ullafelsen (Teil 1). Mensch und Umwelt im Holozän Tirols 1, 97–105; Innsbruck.

Küfmann, C. (2008a): Are cambisols in alpine karst autochtonous or eolian in origin? – Arctic, Antartic, and Alpine Research 40(3), 506–518.

Küfmann, C. (2008b): Flugstaubeintrag und Bodenbildung im Karst der Nördlichen Kalkalpen. – Forschungsberichte Nationalpark Berchtesgaden 54: 1–159.

Nittel, P. (2011): Geologie, Hydrogeologie und Geomorphologie des Fotschertales – Kartierungsergebnisse Projekt „Sellrain" 2006. – In: Schäfer, D. (ed.): Das Mesolithikum-Projekt Ullafelsen (Teil 1). Mensch und Umwelt im Holozän Tirols 1, 61–92; Innsbruck.

Oeggl, K. & Schoch, W. (2011): Holzkohlenanalysen aus Bodenproben des altmesolithischen Fundplatzes auf dem Ullafelsen im Fotschertal. – In: Schäfer, D. (ed.): Das Mesolithikum-Projekt Ullafelsen (Teil 1). Mensch und Umwelt im Holozän Tirols 1, 197–201; Innsbruck.

Pawlik, A.F. (2011): Die funktionale Analyse der Steingeräte und die Rekonstruktion der Aktivitätsbereiche am Ullafelsen. – In: Schäfer, D. (ed.): Das Mesolithikum-Projekt Ullafelsen (Teil 1). Mensch und Umwelt im Holozän Tirols 1, 355–459; Innsbruck.

Schäfer, D. (1998): Zum Untersuchungsstand auf dem altmesolithischen Fundplatz vom Ullafelsen im Fotschertal (Stubaier Alpen, Tirol). – Germania 7: 439–496.

Schäfer, D. (2011a): Das Mesolithikum-Projekt Ullafelsen (Teil 1). Mensch und Umwelt im Holozän Tirols 1, 560 pp.; Innsbruck.

Schäfer, D. (2011b): Das Mesolithikum-Projekt Ullafelsen – Landschaftlicher Rahmen und archäologische Befunde. Arbeitsstand 2009/2010. – In: Schäfer, D. (ed.): Das Mesolithikum-Projekt Ullafelsen (Teil 1). Mensch und Umwelt im Holozän Tirols 1, 245–351; Innsbruck.

Schlosser, E. (2011): Das Fotschertal – regionale Klimatologie und gebirgsmeteorologische Aspekte. – In: Schäfer, D. (ed.): Das Mesolithikum-Projekt Ullafelsen (Teil 1). Mensch und Umwelt im Holozän Tirols 1, 11–16; Innsbruck.

Major Holocene rock slope failures in the Upper Inn- and Ötz valley region (Tyrol, Austria)

Holozäne „Bergstürze“ in der Region Oberinntal-Ötztal (Tirol, Österreich)

Marc Ostermann, Christoph Prager

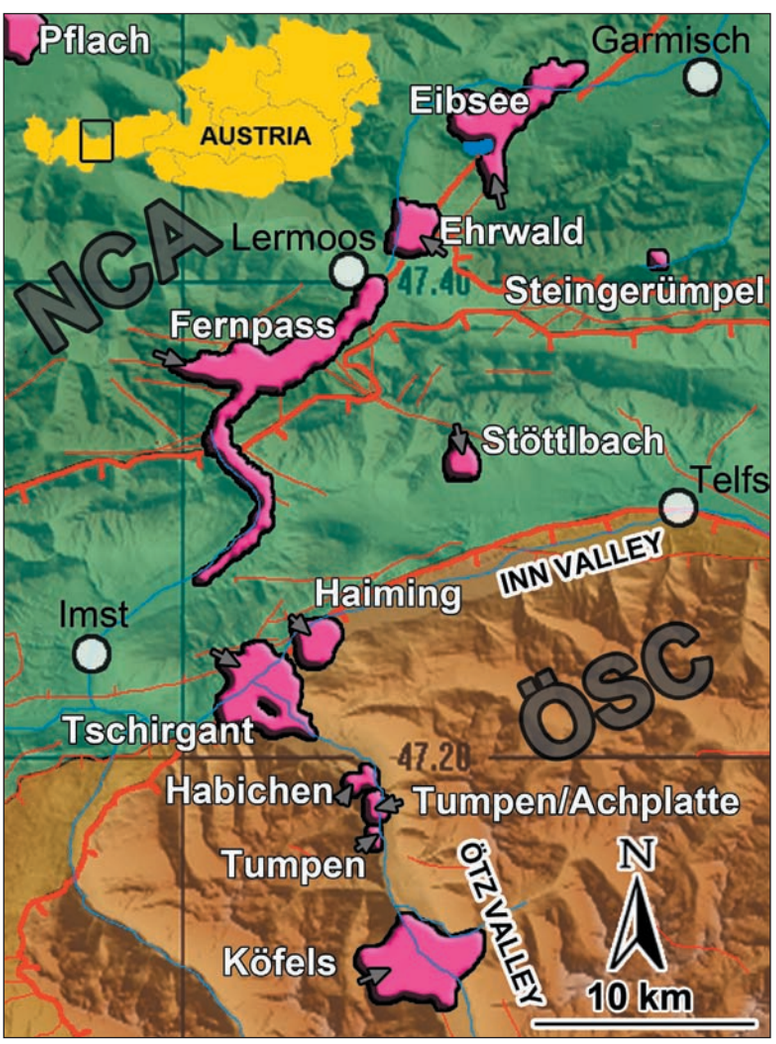

Fig. 1: Overview map of the Fernpass rockslide cluster (pink; Tyrol, Austria). NCA: Northern Calcareous Alps, ÖSC: Ötztal-Stubai-Basement Complex. At least twelve catastrophic rock slope failures are concentrated within an area of about 40 by 20 km.

***Abb. 1**: Übersichtskarte der Bergstürze (in rosa), die zum Fernpass Cluster (Tirol, Österreich) zusammengefasst werden können. NCA: Nördliche Kalkalpen, ÖSC: Ötztal-Stubai-Grundgebirgs-Komplex. Mindestens zwölf Bergstürze sind auf einer Fläche von etwa 40 x 20 km konzentriert.*

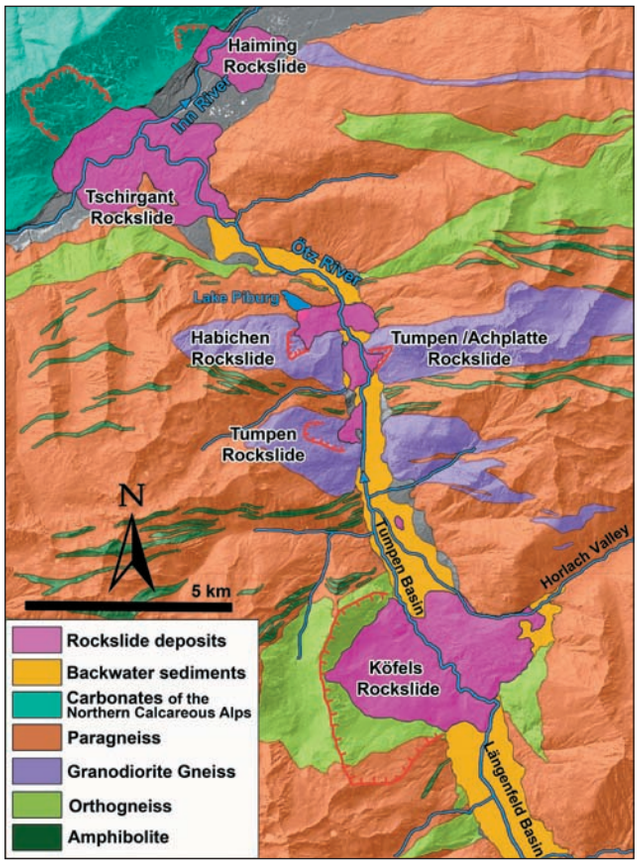

Fig. 2: Simplified geological overview map of the lower Ötz valley with indicated major rock slope failures (pink) and associated backwater sediments (beige).

Abb. 2: *Vereinfachte geologische Übersichtskarte des äußeren Ötztals mit eingezeichneten Bergsturzablagerungen (rosa) und den damit verbundenen Rückstausedimenten (beige).*

1 Introduction

Some of the largest fossil rock slope failures in the Alps are concentrated in the Upper Inn valley and Ötz valley area (Northern Tyrol, Fig. 1). They feature various types of rockslides, rock avalanches and large scale rock falls, with deposition volumes ranging between some 10 to some 100 million m^3 and with run-out distances reaching several kilometres (e.g. Prager et al. 2008). At least 12 major rock slope failures occur within an area of about 40 x 20 km. In this field trip we focus our attention on five major rock slope failures in the lower Ötz valley (Tschirgant, Habichen, Tumpen/Achplatte, Tumpen, Köfels) and provide descriptions and comparisons of these different events. Additionally we address the major causes, the kinematic behaviour and the effects and secondary processes of the catastrophic bedrock failures.

2 Geomorpological and geological setting

The excursion area is dominated by two major alpine valleys, i) the Inn and ii) the Ötz valley (Fig. 2). The Inn valley here follows the NE-striking Upper Inn valley fault zone where polyphase and heteroaxial brittle deformation enabled a substantial fluvio-glacial deepening of the Inn valley between the southernmost margin of the Inn Valley nappe system, as part of the Northern Calcareous Alps (NCA), and the southerly adjacent Ötztal-Stubai-Basement Complex (ÖSC).

The N-trending Ötz valley, one of the main side valleys of the Inn valley, is deeply incised into the metamorphic ÖSC (Fig. 2). The terrain is typically very steep and rugged, with elevations ranging from 678 m at the confluence of the Ötz and Inn river and 3768 m at the highest summit (Wildspitze). The glacially shaped and deepened Ötz valley is filled with various Pleistocene and Holocene sediments (Senarclens-

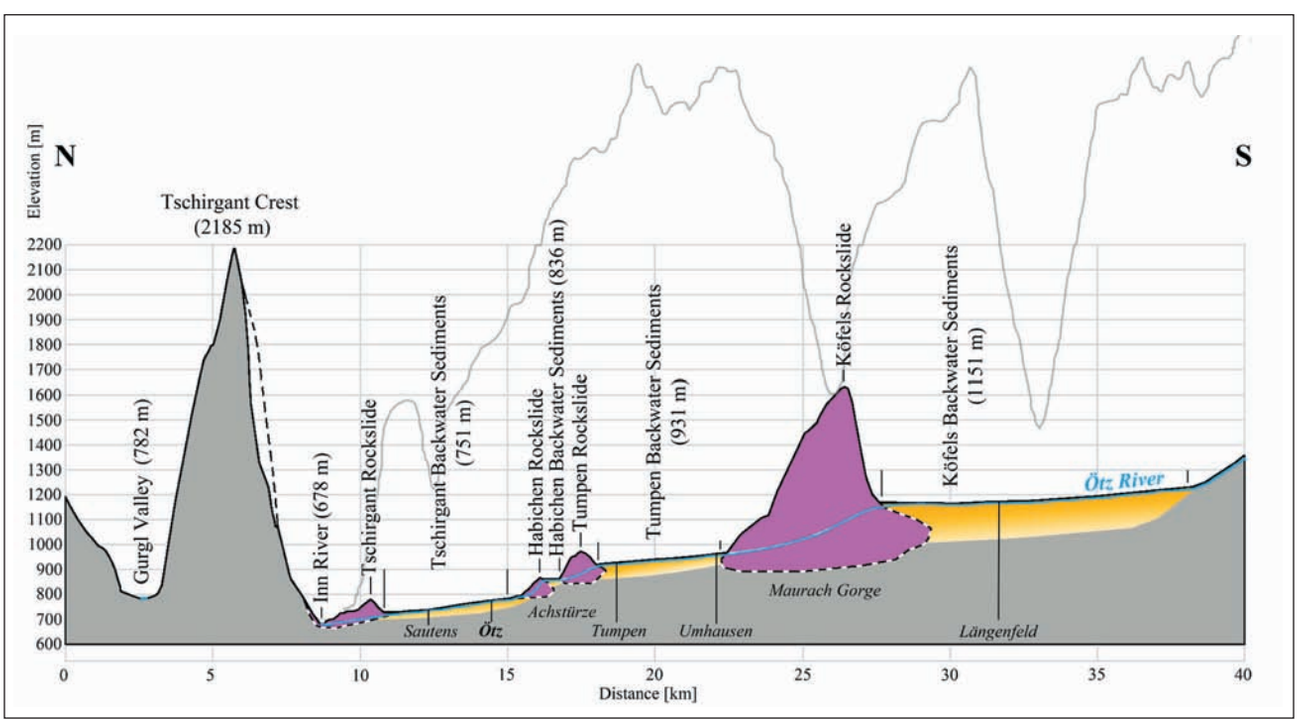

Fig. 3: Schematic river long profile of the lower Ötz river, with indicated major rock slope failures (pink) and corresponding backwater sediments (yellow). The valley is characterised by three valley steps, where the river incised gorges into the rockslide debris.

Abb. 3: *Schematisches Flußlängsprofil entlang dem Unterlauf der Ötz mit eingezeichneten Bergsturzablagerungen (rosa) und den damit verbundenen Rückstausedimenten (gelb-braun). Dieser Talabschnitt ist gekennzeichnet durch drei markante Geländestufen, an denen sich der Fluss schluchtartig durch die Bergsturzablagerungen gegraben hat.*

Grancy 1958). During the Holocene the Ötz valley has been characterised by significant valley steps and flat upstream valley floors, which is attributed to multi-phase landslide events (Fig. 3) and thus to associated backwater sediments (Senarclens-Grancy 1958, Heuberger 1975, including references).

The Tschirgant scarp is situated at the southern margin of the Inntal thrust nappe, here composed of a complex structural succession of Middle to Upper Triassic dolomites, limestones and subordinate evaporites (Fig. 2). The southern margin of the NCA in this area is characterised by polyphase and heteroaxial folding and faulting (Eisbacher & Brandner 1995, Pagliarini 2008).

The Ötztal-Stubai-Basement Complex (ÖSC) consists of polymetamorphic rocks with various protoliths: orthogneisses of plutonic origin, amphibolites of volcanic and plutonic origin, and metapelites and metapsammites of sedimentary origin. Paragneisses (biotite-plagioclase-gneisses) and micaschists prevail and are intercalated with orthogneisses but also amphibolites, eclogites and marbles (Fig. 2). The ÖSC was affected by at least six deformation phases (ductile and brittle), with the northern and central areas being characterised by large-scale, gently E-W-striking, open folds (Hammer 1929, Purtscheller 1978, Oberhauser 1980, Hoinkes & Thöni 1993, Egglseder & Fügenschuh 2013).

Concerning the major Holocene rock slope failures, the rigid rock mass complexes (granodiorite gneisses and orthogneisses) embedded in incompetent paragneiss series failed. Layering and main foliation of all crystalline rock units are generally E-W-trending and thus orientated unfavourably to promote slope failures. Here the rock mass strength and slope deformation behaviour are controlled by the orientation and geomechanical characteristics of different brittle fracture sets.

In the surroundings of the excursion area the NE-trending Inntal and Engadin Line show increased earthquake activity (Drimmel 1980, Reiter et al. 2003). Some strong earthquakes with magnitudes M 5.3 and EMS-98 epicentral intensities I_0 7.5 (MSK) which occurred there are among the most intense ones ever measured in Austria. Some of these seismic events show low magnitudes M=1.2–1.8, but nevertheless pronounced epicentral intensities I_0=3.0–4.0 (MSK) due to shallow-seated focal depths (Prager et al. 2008). Projected into a structural transect (Eisbacher et al. 1990), these earthquakes indicate active tectonics in the thrust sheets of the Northern Calcareous Alps near the base thrust of the Inn Valley nappe.

Active tectonics on the one hand can directly trigger a rock slope failure, but on the other hand also fracture rock masses to high extents. Thus repeated dynamic load-

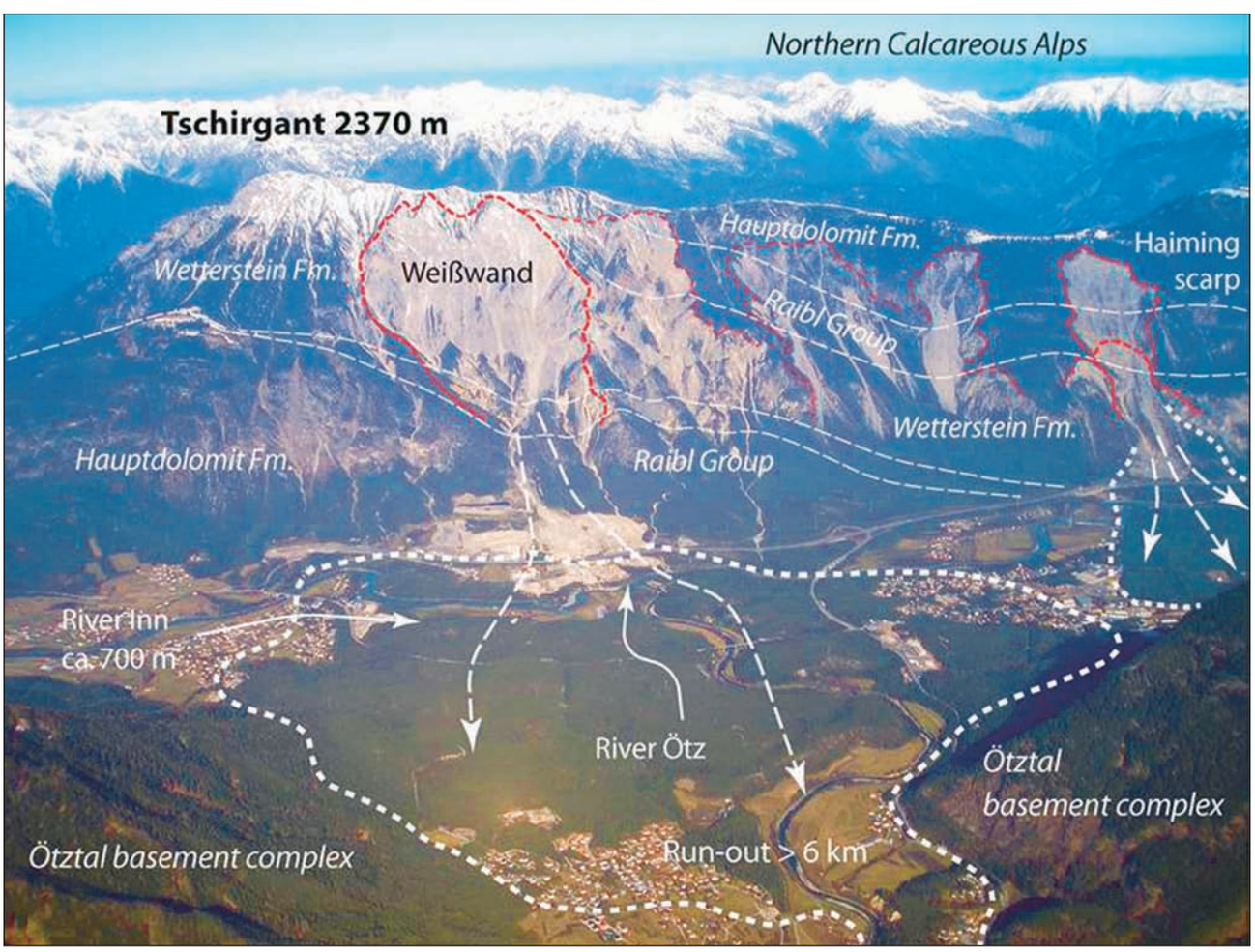

Fig. 4: Overview image of scarp area (Weißwand; red stipped lines) and accumulation areas (white stippled line) of the Tschirgant and Haiming rockslides at the confluence of the Ötz River and the Inn River. View towards the North (from Prager et al. 2008).

Abb. 4: *Übersichtsfoto des Abbruchbereiches (Weißwand; rot strichliert) und des Abblagerungsbereiches (weiß strichliert) des Tschirgant Bergsturzes und des Haiminger Bergsturzes. Blickrichtung Norden (aus Prager et al. 2008).*

ing, even if at subcritical energy levels, can initiate brittle fracture propagation and thus promote progressive failures (rock slope instabilities). Over a longer time period, fracture density and persistence continuously increase in an existing stress field which also determines the size and orientation of fractures (e.g. Einstein & Stephansson 2000). Gravitational creeping and tension fracturing may lead to coalescence of brittle discontinuities, which continuously degrades the slope stability and ends up with shearing along continuous sliding planes when the rock mass strength threshold is exceeded. In view of this and in the long term, deep-seated slope deformations are induced by complex and polyphase interactions of the geological setting (predisposition) with a variety of variable processes (e.g. morphological changes, subcritical fracture propagation, seismic activity and climatically controlled pore pressure changes).

3 Selected rock slope failures

3.1 Tschirgant rockslide

Stop 1

Location: Inn Valley, Tschirgant rockslide accumulation area, Sautener Forchet, South of Area 47, short walk through a typical rockslide hummocky landscape to outcrops where the Ötz River incised into the rockslide deposits
GPS [UTM]: 5232044.12 N, 639845.44 E

Topics: (a) Overview of the scarp area "Weißwand" and general geological situation of the southern margin of the NCA, (b) Bulldozing of fluviatile sediments by the Tschirgant rockslide, (c) Age-dating of the rockslide event, (d) Sedimentology of the rockslide debris

This deep-seated rockslide detached from the location "Weißwand" beneath the summit of the Tschirgant massif (2370 m a.s.l.) in the western part of Northern Calcareous Alps (NCA) (Fig. 4 & 5). The mountain flank with more than 1400 m in vertical height is composed of a tectonically intensely deformed succession of Triassic dolostones, limestones, silt-/sandstones and evaporites. As a result of the polyphase and heteroaxial deformation, the slope failure was controlled by a step-wise coalescence of NE-trending, frequently overturned bedding and fault planes with NW-trending dextral fracture systems. In the scarp area, the competent carbonates of the Wetterstein Formation (Ladinian-Carnian) exhibit bedding planes and several extensive fracture systems, which dip out of the slope and form preferably oriented sliding planes. The slope collapse was furthermore favoured by karst structures in both the Wetterstein Formation and the Rauhwacken of the Raibl Group (Carnian), the latter being encountered with a thickness of several tens of metres at lower sections of the failed slope. Mineralised springs in the Tschirgant area indicate leaching of Ca-sulphate rocks, a process that may have contributed substantially to the time-dependent degradation of rock mass strength and slope stability (Prager et al. 2008). The concave-shaped detachment niche shows intense fracturing and some staggered sliding planes. The geometry of the scarp niche and GIS-based slope analyses indicate a failed rock mass volume of at least 100–125 million m³ (Pagliarini

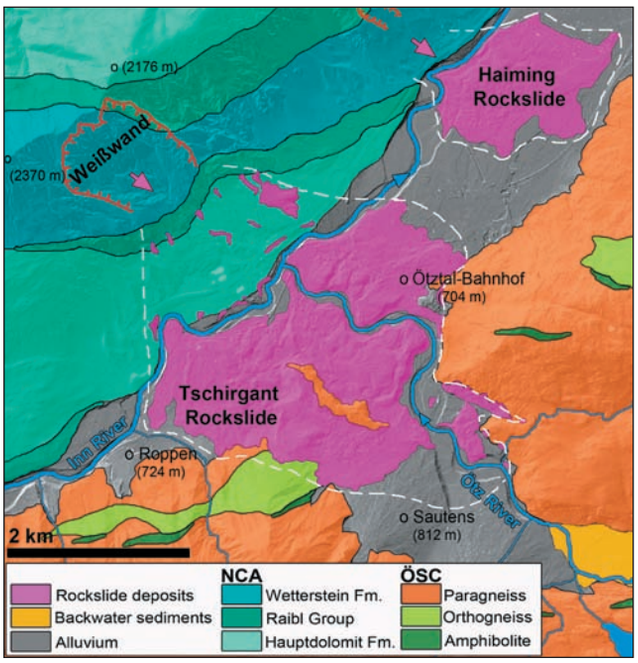

Fig. 5: Geological map of the Tschirgant rockslide area at the confluence of the Inn River and the Ötz River (after Brandner 1980, Patzelt 2012). The dashed white line represents the estimated former extent of the rockslide deposits. The red line indicates the scarps of the catastrophic slope failures.

Abb. 5: *Geologische Karte des Tschirgant Bergsturzgebiets im Bereich der Mündung der Ötz in den Inn (nach Brandner 1980, Patzelt 2012).. Die angenommene ehemalige Ausdehnung der Bergsturzablagerungen ist durch die gestrichelte weiße Linie markiert. Die rote Linie zeigt den oberen Abbruchbereich der Bergstürze an.*

2008). The accumulated Tschirgant rockslide ("Bergsturz") debris spread over an area of at least 9 km², with an estimated volume of about 200–250 million m³ considering spatially varying thicknesses extending up to at least 65 m (based on results from drillings; Patzelt & Poscher 1993). Based on field surveys, the maximum run-out of the rock avalanche ("Sturzstrom") is 6.2 km, and the Fahrböschung is 12° (Patzelt 2012).

Obviously as a result of the dynamic rock mass fragmentation and run-out path characteristics, major areas of the rock avalanche deposits show pronounced geomorphological features including hummocky terrain, transversal and longitudinal ridges as well as funnel- to graben-like depressions. One outstanding feature of the Tschirgant site is that the contact of the basal slide deposits with the valley substrate is locally well exposed. This contact zone displays complex geometries, where in the course of the rockslide event presumably water-saturated valley floor sediments were injected into the rockslide masses filling up steep extension structures (Patzelt & Poscher 1993, Abele 1997, Erismann & Abele 2001) and where diamicts were created by mingling with the rockslide (Prager 2010, Prager et al. 2012). Recently, extensive geological field surveys revealed a "systematic" spatial distribution of both the lithological main units and morphological features. Whereas the grey limestones and dolostones of the Wetterstein Formation dominate the proximal and central accumulation areas, the brown-coloured siliciclastic-carbonate units of the Raibl Group are common at the distal rims, along with some bulldozed ridges made up of displaced valley deposits (Dufresne et al. 2014a, 2014b).

This preserved slope stratigraphy argues against chaotic rock avalanche movements but further indicates laminar slide/flow movements of the rockslide. Further insights in the mechanical behaviour may be obtained from ongoing spatial analyses of morphological terrain features, indicating both compressional and extensional regimes as well as sinkhole-like mass wastes (Dufresne et al. in preparation).

Based on radiocarbon data Patzelt (2012) hypothesized two rockslide events at the Tschirgant site, an older one between 3650 and 3450 cal BP and a younger one between 2950 and 3070 cal BP (2 sigma ranges). In the field there is no evidence for two events. After a critical revision of the numerous ^{14}C dates (Patzelt & Poscher 1993, Patzelt 2012) and the application of two other dating methods (Ostermann, et al., unpublished data) we tend to favour a single event. Meteoric aragonite and calcite cements in the interstitial pore space of post-depositionally lithified rockslide deposits (Prager et al. 2007) yielded U/Th-ages of around 3020 ± 150 BP for the cementation which represent minimum ages for the accumulation (Sanders et al. 2010, Ostermann et al. in preparation). ^{36}Cl-surface exposure ages hint to a mean event age of 2980 ± 500 BP (Ostermann et al. in preparation). Together, the numerical ages deduced by the different methods suggest that mass-wasting took place at ~3–3.3 ka.

J

Stop 2

Location: Ötz Valley, Tschirgant rockslide backwater sediments, beside the road (B 186) just downriver of the village Ötz
GPS [UTM]: 5229888.92 N, 642457.44 E

Topics: (a) Overview of the southern part of the Tschirgant rockslide deposits (b) Fluvio-lacustrine sediments due to the damming of Ötz River by the Tschirgant rockslide (c) Aggradation of alluvial cones on top of backwater sediments.

The Tschirgant rockslide has dammed both the Inn and the Ötz rivers. However both the Inn backwater terraces (Ampferer 1904) and the Ötz backwater sediments are less pronounced, and covered by large alluvial debris cones (e. g. Sautens, Fig. 5) to a great extent.

3.2. Habichen (Piburgersee) rockslide

Stop 3

Location: Ötz Valley, Habichen rockslide accumulation and backwater sedimentation area, Habicher See
GPS [UTM]: 5227594.34 N, 644269.11 E

Topics: (a) Overview of the Habichen rockslide scarp area and accumulation area. (b) Backwater sediments of the Habichen rockslide and the origin of Lake Piburg. (c) Stack effects within coarse grained rockslide deposits (Eiskeller von Habichen).

Deposits of a massive rock slope failure at Habichen have been mentioned by several authors (e.g. Hammer 1929, Klebelsberg 1935, Senarclens-Grancy 1958, Poscher & Patzelt 2000, Prager et al. 2008) but have not been investigated in more detail. The rockslide deposits of Habichen are exposed in the surroundings of Habichen (851 m a.s.l.) close to the distal deposits of the Tschirgant rockslide (Fig. 6).

The rockslide deposits at Habichen cover an area of 0.8 km². In the upper part of the accumulation area the maximal block size reaches about 1 m³, whereas in the lower parts many blocks with a volume of 10–15 m³ occur. The maximum thickness of the rock debris reaches about 30 m near the Ötz river.

The scarp area of the Habichen rockslide is characterised by massive granodiorite gneisses, which occur as approximately 1.5 km-thick lenticular complex, intercalated in mica schists and paragneisses and here crossing the Ötz valley in East-West direction. North of the scarp area and along the banks of Lake Piburg (Piburger See) the dominant rock mass types are biotite-plagioklasgneisses. The biotite-plagioclase-gneisses in the area show a well-developed schistosity and tend to disintegrate into rather small block sizes whereas the massive granodiorite gneisses cause major rock slope failures comprising larger block volumes. The major tectonic lineaments are orientated in three main directions, NE-, NW- and NS-trending, which also has been observed in the joint patterns of the bedrock slopes.

The scarp area shows a well-developed niche between 1180 m and 1850 m a.s.l. and has an areal extent of about 128,000 m² (Fig. 7). The accumulation area starts between 1200 and 1300 m a.s.l. and reaches its lowermost point at

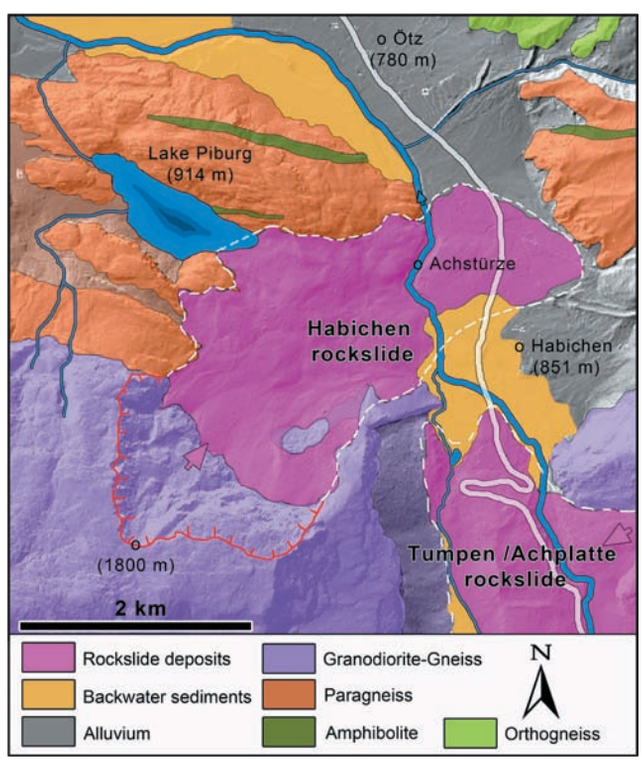

Fig. 6: Geological map of the Habichen rockslide. The dashed white line represents the maximum extent of the rockslide deposits. The red line indicates the scarp of the rock slope failure. Lake Piburg is a backwater lake of the Habichen rockslide. The lake basin has not been silted up because of the low stream power of the inflow. This contrasts to the already silted up lake basin in the main valley.

***Abb. 6**: Geologische Karte des Habichen Bergsturzes. Die angenommene ehemalige Ausdehnung der Bergsturzablagerungen ist durch die gestrichelte weiße Linie markiert. Die rote Linie zeigt den oberen Abbruchbereich der Bergstürze an. Der Piburgersee wurde durch den Habicher Bergsturz aufgestaut und ist im Gegensatz zu dem Rückstau im Haupttal wegen seines wesentlich geringeren Zufluss noch nicht verlandet.*

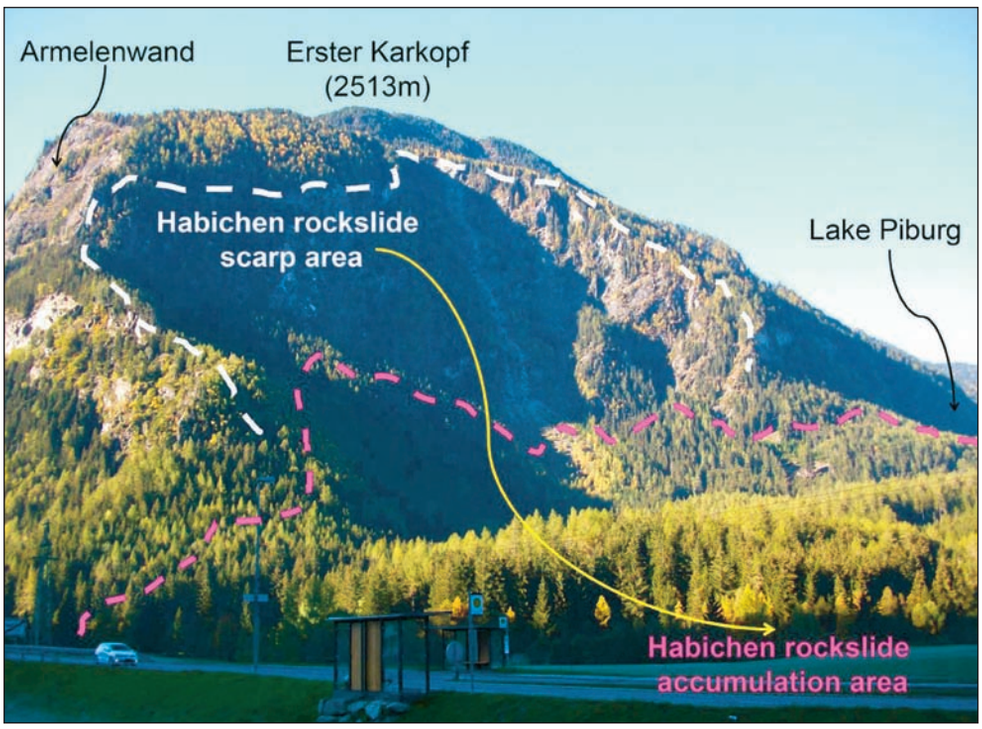

Fig. 7: Well developed detachment niche of the Habichen rockslide, view towards the West. The road in the foreground cuts the backwater sediments, which record the damming of the Ötz river by the rockslide debris.

***Abb. 7:** Abbruchsnische des Habicher Bergsturzes, Blickrichtung Westen. Die Straße im Vordergrund verläuft innerhalb der Rückstausedimente, die durch dem Aufstau der Ötztaler Ache abgelagert wurden.*

the end of the cascades of the Ötz river (Achstürze, approximately 800 m a.s.l.) caused by the Habichen rockslide.

The failing rock masses first propagated in NE-direction towards a bedrock obstacle composed of biotite gneisses, which forced the debris to travel further on towards the East. The rockslide masses dammed the Ötz valley and even ran up the eastern valley flanks for about 100 m. The upper part of the accumulation area is very steep and the thickness of the rock debris low. The basal sliding plane of the rockslide mass is locally exposed showing well-developed lineation. The middle part of the accumulation area is characterised by some ridges and depressions which indicate the change in rock debris propagation from NE to E. Recent slope deformation activity is indicated by toppling features affecting the scarp walls and by fresh rock fall deposits encountered on top of the upper accumulation area.

The Habichen rockslide dammed two surface discharge systems: one at Lake Piburg which has been dammed in the south by the rockslide dam (Fig. 6), and another at Habichen, i.e. backwater sediments of the Ötz river, where the rockslide dam failed and an outburst flood occurred. The deposits cover the Ötz valley floor (Senarclens-Grancy 1958) and feature an impressive cataract (Achstürze) where the Ötz river cut through the damming rockslide barrier. Upstream of the Achstürze lacustrine backwater sediments with well-developed terraces are encountered. Lake Habichen is a tiny remnant of this backwater lake whose maximum extent was about 0.26 km². Lake Piburg lies at 913 m a.s.l. and covers an area of 0.13 km². The rockslide dammed a pre-existing bedrock depression of glacial origin at its southern margin. ^{14}C analyses of lacustrine deposits, obtained from drillings in the central part of the lake, yielded an age of ca. 11500 cal BP (N. Wahlmüller unpubl. data) and indicate a minimum age for the Piburg rockslide barrier.

Along the valley floor the anthropogenic influence is very strong and many blocks have been removed in favour of agriculture.

2.3 Tumpen/Achplatte rockslide

Stop 4

Location: Ötz Valley, Tumpen
GPS [UTM]: 5226529.00 N, 644512.00 E

Topics: (a) Overview of the Tumpen/Achplatte rockslide scarp area and accumulation area (b) Tumpen/Achplatte rockslide deposits and backwater sediments (c) Sink holes, recent rock fall and potential future failures (d) Tumpen rockslide.

A steep mountain ridge on the eastern flank of the Ötz valley starts at the valley bottom (approx. 850 m a.s.l.) and leads up to the summit of the Acherkogel (3007 m a.s.l.). In the lower parts of this granodiorite gneiss unit a rock volume of estimated 35–40 million m³ detached from a niche-shaped scarp area (Fig. 8). The rock debris spread over an area of 0.6 km² with a runout distance of 2.2 km and a Fahrböschung of approx. 24°. The accumulated deposits with a volume of about 60 million m³ consist entirely of granodiorite gneisses showing clast-supported fabrics of cm- to metre-sized clasts and sandy-gravelly matrix. In comparison to the carbonate Tschirgant rockslide, the deposits at Habichen, Tumpen/Achplatte and Tumpen show less amounts of fines (crushed silt-sand-sized rock fragments) and higher porosities.

The Tumpen/Achplatte rockslide caused a total damming of the Ötz river resulting in two separate backwater basins (Senarclens-Grancy 1958). The major one is the Tumpen basin filled by fluvio-lacustrine sediments with a minimum thickness of 60 m up to an elevation of 935 m a.s.l.. Drillings (down to depths of about 845 m a.s.l.) and reflection seismic investigations in the Tumpen basin indicate that the bedrock surface is situated around 200–250 m below ground surface (Poscher & Patzelt 2000). A second, smaller backwater basin (Grube) is developed along the western valley flank at an

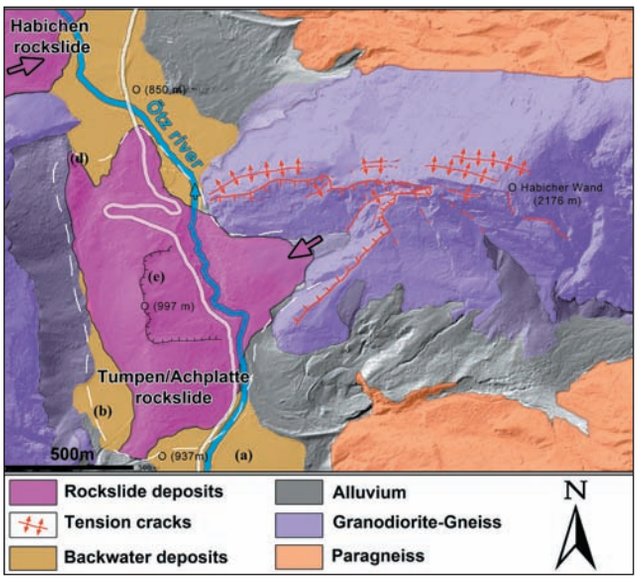

Fig. 8: Simplified geological map of the Tumpen/Achplatte rockslide. The dashed white line represents the assumed former extent of the rockslide debris. a: Tumpen backwater basin, b: Grube backwater basin, c: Habichen backwater basin, d: Eiskeller, e: secondary mass movement within the rockslide debris. The scarp area is characterised by a series of deep tension cracks (see Fig. 9).

***Abb. 8**: Vereinfachte geologische Karte des Tumpen/Achplatte Bergsturzes. Die angenommene ehemalige Ausdehnung der Bergsturzablagerungen ist durch eine gestrichelte weiße Linie markiert. a: Tumpen Rückstaubecken, b: Grube Rückstaubecken, c: Habichen Rückstaubecken, d: Eiskeller, e: sekundäre Massenbewegung innerhalb der Bergsturzablagerungen. Der Abrissbereich des Bergsturzes ist durch eine Reihe von tiefgreifenden Zerrspalten gekennzeichnet (siehe Fig. 9).*

elevation of 910 m a.s.l., i.e. situated about 25 m below the top of the Tumpen backwater plain. Here a small creek was dammed, resulting in a 10–20 m-thick succession of fluvio-lacustrine backwater sediments (Fig. 8).

The Ötz River deeply incised into the Tumpen/Achplatte rockslide mass and cascades down over a vertical distance of 90 m within just about 500 m in horizontal distance. Locally, the accumulated rockslide debris has been affected by fluviatile erosion causing secondary slope instabilities (Fig. 8). Also in the scarp area (Habicher Wand) small- to medium-scale rock fall activities are obvious. Furthermore, some deep-seated tension cracks are encountered in the bedrocks near the scarp area (Figs. 9 & 10).

Concerning the Tumpen basin, some ^{14}C dates of fining-upward fluvio-lacustrine sequences are available from drillings campaign. The younger succession provided an age of about 3380 ± 80 BP (Poscher & Patzelt 2000), i.e. 3840–3440 cal BP (2 sigma range), which is a minimum age for the damming rockslide event. Depth extrapolations of the data suggest that the older sequence and its rockslide barrier may date to about 6000 cal BP (G. Patzelt, personal communication).

At its most distal sections the Tumpen/Achplatte rockslide shows a phenomenon that locally can be observed at very coarse grained to blocky openwork rockslide debris (see also Section 2.5. Köfels rockslide). At the location "Eiskeller" a thermally-induced chimney effect comparable with dynamic ice-caves reduces the temperature of the air circulating within the pore space of the lower parts of blocky rockslide debris to below the outside air temperature (Wakonigg 1996). In winter relatively warm air of the interior part of the blocky rockslide debris exhausts from the upper parts of the deposits; simultaneously in the lower part fresh cold air enters the system and cools down the rocky material to some degrees below the freezing-point. During the snow melting period in spring infiltrating water freezes in the interior of the rockslide deposits as long as the temperature here remains below the freezing-point. This causes a simultaneous release of latent heat warming up the system at least to the freezing-point. In summer the relatively cold air sinks down to the lower sections of the rockslide deposits ("Eiskeller") and displaces the fresh warm air to the upper sections. This airflow loses energy due to the melting of the ice in the interior of the rockslide deposits and thus cools down along its flow path (Wakonigg 1996).

Another geological feature of the Tumpen backwater basin is the occurrence of sinkhole collapses in valley floor sediments, which have been documented repeatedly over the last 300 years (Heuberger 1975, Poscher & Patzelt 2000).

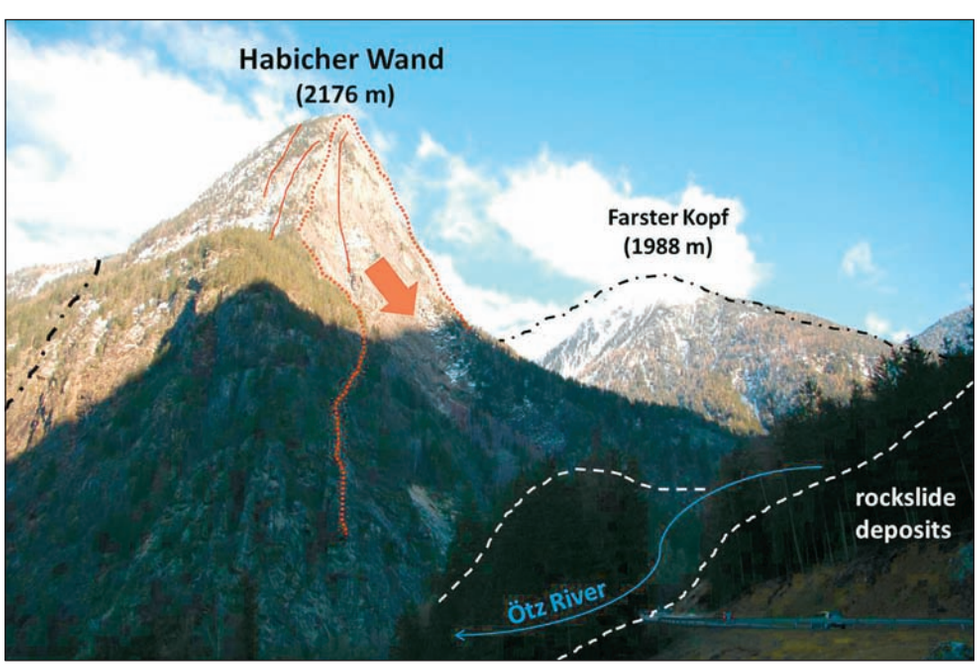

Fig. 9: At the Habicher Wand ongoing small-scale rock fall is common and sometimes even larger rock portions up to some tens of m^3 break off. In the foreground deposits of a large-scale rock failure are present – the Tumpen/Achplatte rockslide. The red lines indicate major tension cracks in the scarp area (see Fig. 8).

***Abb. 9**: Kleine Felsstürze sind an der Habicherwand häufig und manchmal lösen sich auch größere Gesteinsmassen von mehreren Zehner m^3. Der Vordergrund ist von Ablagerungen des Tumpen/Achplatte Bergsturzes gekennzeichnet. Die roten Linien zeichnen den Verlauf großer Zerrklüfte im Abbruchgebiet nach (siehe Abb. 8).*

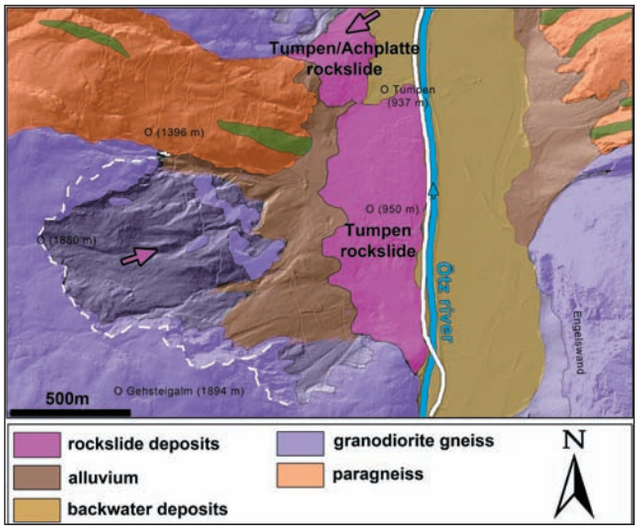

Fig. 10: Simplified geological map of the Tumpen rockslide area. The dashed white line indicates the scarp area within the granodiorite gneiss. Large portions of the rock debris are covered by talus material, alluvial cones and fluvio-lacustrine backwater sediments (the latter affected by several sinkhole collapses within the last 300 years).

Abb. 10: *Vereinfachte geologische Karte des Tumpen Bergsturzgebiets. Die weiße gestrichelte Linie zeigt den Verlauf des Abbruches innerhalb der Granodioritgneise an. Große Anteile der Bergsturzmassen sind mittlerweile durch Hangschuttablagerungen, Murschuttfächer und fluvio-lakustrine Rückstausedimente überlagert (in den letzteren sind in den letzten 300 Jahren mehrmals Erdfälle aufgetreten).*

These events may be attributed to the sedimentological successions encountered, i.e. fine- to medium-grained fluviatile and lacustrine sediments overlying coarse-grained to blocky rockslide debris. Based on geological field surveys and subsurface investigations, these local collapse structures up to several tens of metres in diameter have been attributed to suffusion processes. In general, fine-grained soils can be mobilized by groundwater flow systems and thus be washed into open pore spaces of the underlying rockslide debris. At Tumpen, suffusion may have been favoured by the artificial relocation of the Ötz riverbed in 1691 (due to outburst floods of a glacial lake in 1678 and 1679), whereby the distance between the river and underlying rockslide deposits has been reduced (Poscher & Patzelt 2000).

2.4 Tumpen rockslide complex

In the Tumpen area, at least two further rockslides (Tumpen Dorf, Tumpen Maurach; Poscher & Patzelt 2000) detached from a granodiorite gneiss unit on the western valley flank and left a massive niche-shaped scarp at an elevation of about 1880 m a.s.l. (Fig. 10). Major sets of E-dipping tectonic fractures can be found within the east-facing bedrock slopes. In western sections of the accumulation area the rockslide debris is covered by alluvium to a great extent. In the eastern area the fluvio-lacustrine backwater sediments of the Tumpen/Achplatte rockslide appear to lap onto the sliding masses of Tumpen Dorf.

Subsurface investigations indicate that the accumulated debris extends close to the opposite valley flank (Poscher & Patzelt 2000). Thus a total runout distance of 2000–2200 m and a runout travel angle of 28–30° can be estimated. The age of the event is unknown, but is likely simultaneous or older than the adjacent Tumpen/Achplatte rockslide, because of the on-lapping backwater sediments mentioned above (see also Senarclens-Grancy 1958).

2.5 Köfels rockslide

Stop 5

Location: Ötz valley, Maurach gorge, Köfels rockslide accumulation area
GPS [UTM]: 5220715.00 N, 646426.00 E

Topics: (a) Overview of the Köfels rockslide (b) Characterisation of the rockslide deposits and frictionites ("pumice") (c) Kinematics of major rockslides and rock avalanches (d) Längenfeld backwater basin (d) Emanation of Radon.

The prominent Köfels rockslide (Fig. 11) comprises a volume of about 3.2 km^3 (Brückl et al. 2001) and thus is the largest crystalline rockslide in the Alps. The failing bedrock units, predominantly composed of orthogneisses (granitic augen- and flasergneiss) and some paragneiss, detached from an East-facing slope and buried both the Ötz valley and the opposing mouth of the Horlach valley. Layering and foliation of both the orthogneisses and the surrounding paragneisses are orientated unfavourably to promote slope failures. In fact, this slope collapse was structurally predisposed by fault-related valley-deepening and the coalescence of different brittle fracture systems (Prager et al. 2009).

The rockslide ("Sturzstrom") deposits are laterally and vertically characterised by a high variability in the degree of fragmentation and show different types of fabrics. Domains showing a fault-breccia texture composed of angular fragments within a finer-grained matrix of crushed material are located next to domains showing a high fracture density but without any fine-grained material.

The sliding process was dominated by shearing along distinct high strain zones where the blocks lying in between were deformed by dynamic shattering. These blocks and especially the topmost deposits therefore show a typical, highly permeable openwork fabric, containing crushed rockslide clasts with a jig-saw-fit of corresponding grain boundaries.

The several hundred metre-thick rockslide debris fully blocked the Ötz river and caused the accumulation of up to 100 m-thick fluvio-lacustrine backwater deposits within the Längenfeld basin (Klebelsberg 1951, Senarclens-Grancy 1958, Heuberger 1966, 1975). According to reflection seismic surveys, the top of the bedrock units plunges from approximately 50–80 m below ground in the Längenfeld basin steeply northwards to approximately 400 m below ground at the palaeo-slope toe (Brückl et al. 2001).

Radiocarbon dating of buried wood and surface exposure dating of quartz veins from rockslide boulders indicate that the main slide event occurred around 9800 cal BP and was presumably succeeded by a smaller rockslide event (Ivy-Ochs et al. 1998).

An outstanding feature of the famous Köfels site is the occurrence of frictionites ("pumice"). These fused rocks formed due to the friction heat, which developed on several shear planes during the rapid sliding movement (Preuss 1974, Erismann et al. 1977, Masch et al. 1985, Erismann & Abele 2001).

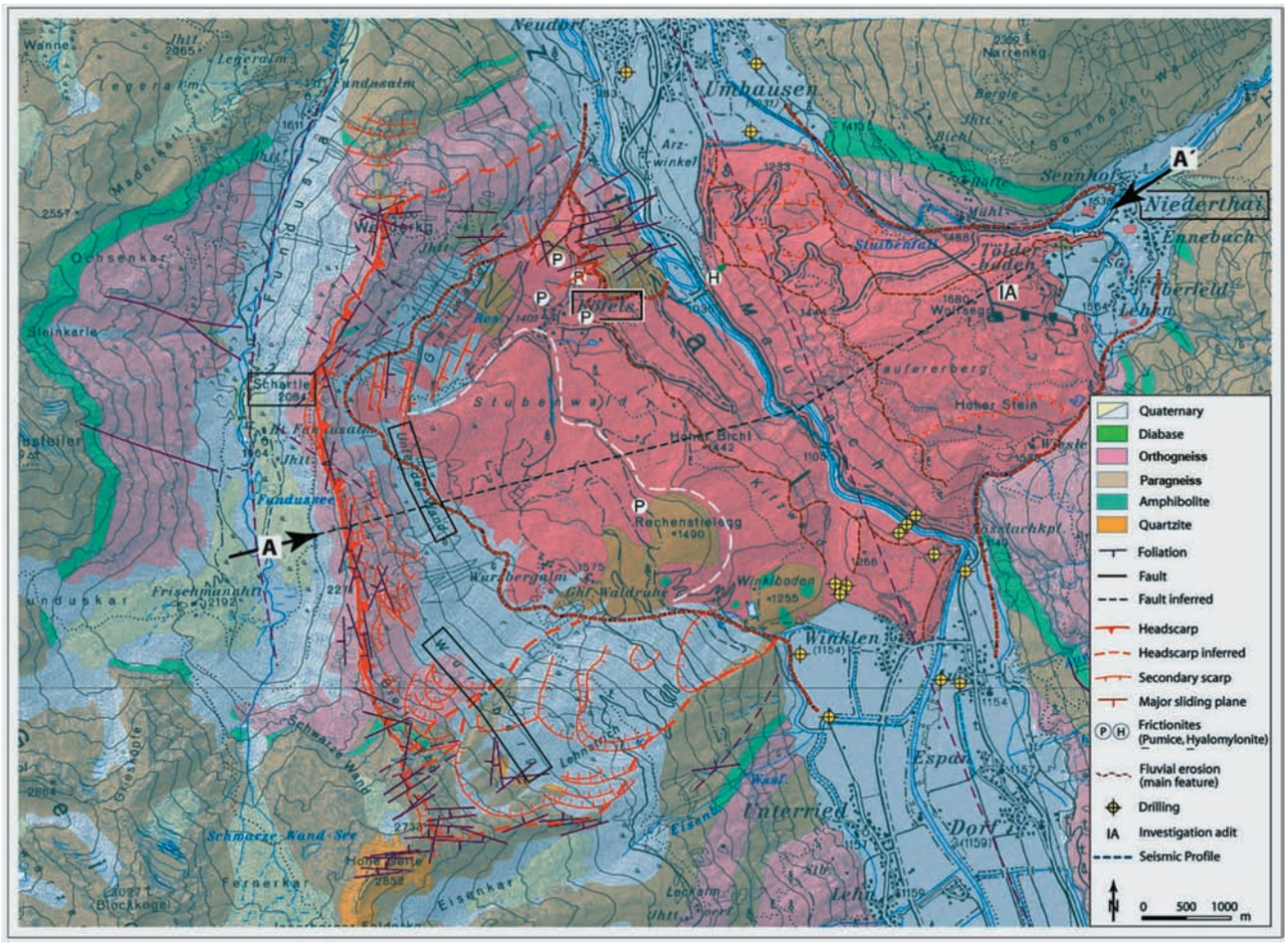

Fig. 11: Geological map of the Köfels rockslide area (from Prager et al. 2009). Displaced rockslide masses enveloped stippled dark red; inferred secondary failure event southwest of Köfels (white stippled).

Abb. 11: *Geologische Karte des Bergsturz von Köfels (aus Prager et al. 2009). Die angenommene ehemalige Ausdehnung der Bergsturzablagerungen ist durch eine gestrichelte rote Linie markiert, der angenommene sekundäre Bergsturz südwestlich von Köfels ist mit einer gestrichelten weißen Linie eingezeichnet.*

Also the extremely high radon concentrations measured in the Umhausen area have been attributed to dynamic rock fragmentation: Purtscheller et al. (1995) showed that the highly crushed orthogneisses of the Köfels rockslide and the thus increased areas of active rock surfaces are the primary source of the radioactive noble gas ^{222}Rn emanations (permeable fabric, see Sect. 2.3 Tumpen rockslide).

Stop 6

Location: Horlach Valley, Niederthai, Köfels rockslide accumulation area
GPS [UTM]: 5220381.00 N, 648696.00 E

Topics: (a) Köfels rockslide deposits and backwater sedimentation (b) Age-dating (c) fluviatile deposits on top of rockslide deposits.

Acknowledgements

The Austrian Science Fund (FWF), ILF Consulting Engineers (Rum/Innsbruck), alpS GmbH (Innsbruck) and the Autonomous Province of Bolzano/Bozen – South Tyrol (Italy) are gratefully acknowledged for supporting this study. Special thanks to Diethard Sanders, Samuel Rothmund (both Univ. Innsbruck) and Anja Dufresne (Univ. Freiburg) for their contributions concerning the Tschirgant and Habichen rockslides.

References

Abele, G. (1974): Bergstürze in den Alpen. Ihre Verbreitung, Morphologie und Folgeerscheinungen. – Wissenschaftliche Alpenvereinshefte, 25: 1–230.

Abele, G. (1997): Influence of glacier and climatic variation on rockslide activity in the Alps. – Paläoklimaforschung, 19: 1–6.

Ampferer, O. (1904): Die Bergstürze am Eingang des Ötztales und am Fernpaß. – Verhandlungen der Geologischen Reichsanstalt, 1904: 73–87.

Brandner, R. (1980): Geologische und tektonische Übersichtskarte von Tirol. – Tirol-Atlas, C1, C3., Innsbruck (Wagner).

Brückl, E., Brückl, J. & Heuberger, H. (2001): Present structure and prefailure topography of the giant rockslide of Köfels. – Zeitschrift für Gletscherkunde und Glazialgeologie, 37: 49–79.

Drimmel, J. (1980): Rezente Seismizität und Seismotektonik des Ostalpenraumes. – In: Oberhauser, R. (ed.), Der geologische Aufbau Österreichs. – 507–527; Wien (Springer).

Dufresne, A., Prager, C. & Clague, J.J. (2014a): Complex

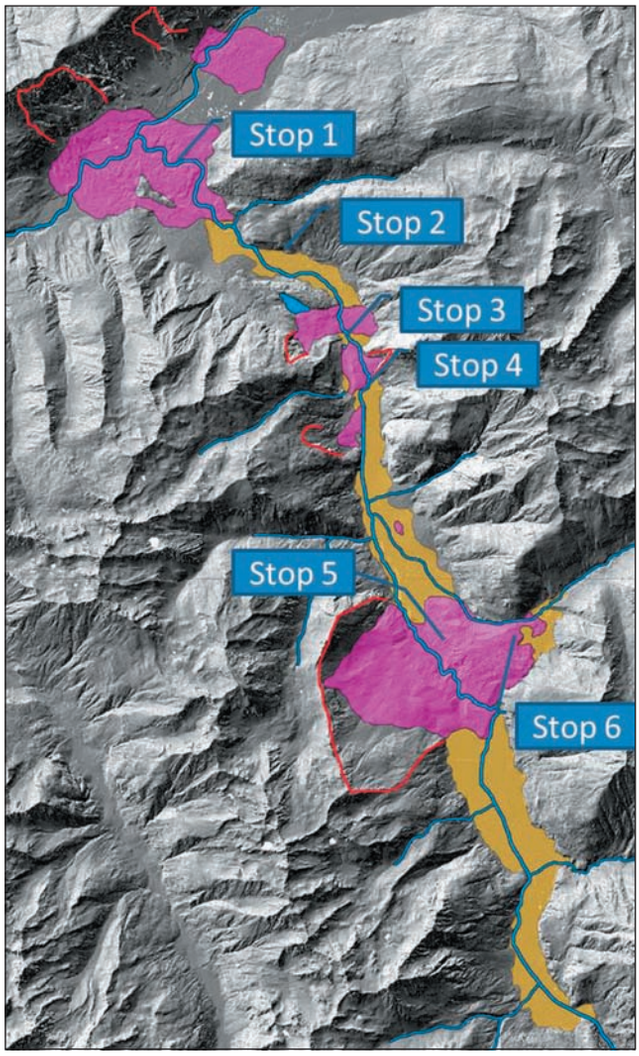

Fig. 12: Excursion map of the lower Ötz valley and surroundings with indicated major rock slope failures (pink) and associated backwater sediments (beige).

Abb. 12: *Exkursionskarte des äusseren Ötztals mit Bergstürzen (rosa) und den damit verbundenen Rückstausedimenten (beige).*

interactions of rock avalanche emplacement with fluvial sediments: field structures at the Tschirgant deposits, Austria. – IAEG XII Congress, Torino 2014.

Dufresne, A., Prager, C. & Bösmeier, A. (2014b): Morphology, lithology, and substrate interactions of the Tschirgant (Tyrol, Austria) rock avalanche deposit: Insights into emplacement processes. – DEUQUA 2014 Abstractband, Innsbruck.

Egglseder, M. & Fügenschuh, B. (2013): Pre-Alpine fold interference patterns in the Northeastern Oetztal-Stubai-Complex (Tyrol, Austria). – Austrian Journal of Earth Sciences, 106: 63–74.

Einstein, H.H. & Stephansson, O. (2000): Fracture systems, fracture propagation and coalescence. – Proceedings GeoEng 2000, Melbourne.

Eisbacher, G. H., Linzer, H.-G., Meier, L., & Polinski, R. (1990): A depth-extrapolated structural transect across the Northern Calcareous Alps of western Tyrol. – Eclogae geologicae Helvetiae, 83: 711–725.

Eisbacher, G.H. & Brandner, R. (1995): Role of high-angle faults during heteroaxial contraction, Inntal Thrust Sheet, Northern Calcareous Alps, Western Austria. – Geologisch-Paläontologische Mitteilungen Innsbruck, 20: 389–406.

Erismann, T.H., Heuberger, H., & Preuss, E. (1977): Der Bimsstein von Köfels (Tirol), ein Bergsturz "Friktionit". – Tschermaks Mineralogisch-Petrographische Mitteilungen, 24: 67–119.

Erismann, T.H. & Abele, G. (2001): Dynamics of rockslides and rockfalls. – Heidelberg (Springer), 316 pp.

Hammer, W. (1929): Geologische Spezialkarte der Republik Österreich 1:75.000, 5146 Ötzthal. – Wien (Geologische Bundesanstalt).

Hammer, W. (1929): Erläuterungen zur Geologischen Spezialkarte der Republik Österreich, Blatt Ötztal. – 58 pp.

Heuberger, H. (1966): Gletschergeschichtliche Untersuchungen in den Zentralalpen zwischen Sellrain- und Ötztal. – Wissenschaftliche Alpenvereinshefte, 20: 1–126.

Heuberger, H. (1975): Das Ötztal. Bergstürze und alte Gletscherstände, kulturgeographische Gliederung. – Innsbrucker Geographische Studien, 2: 213–249.

Hoinkes, G. & Thöni, M. (1993): Evolution of the Ötztal-Stubai, Scarl-Campo and Ulten Basement Units. – In: Raumer, J.F. & Neubauer, F. (eds.), The Pre-Mesozoic Geology in the Alps. – 485–494; Berlin (Springer).

Ivy-Ochs, S., Heuberger, H., Kubik P.W., Kerschner, H., Bonani, G., Frank, M. & Schlüchter, Ch. (1998): The age of the Köfels event. Relative, ^{14}C and cosmogenic isotope dating of an early Holocene landslide in the Central Alps (Tyrol, Austria). – Zeitschrift für Gletscherkunde und Glazialgeologie, 34: 57–68.

Klebelsberg, R.v. (1935): Geologie von Tirol. – Berlin (Borntraeger), 872 pp.

Klebelsberg, R.v. (1951): Das Becken von Längenfeld im Ötztal. – Schlern-Schriften, 77: 399–422.

Masch, L. Wenk, H.R. & Preuss, E. (1985): Electron microscopy study of hyalomylonites - evidence for frictional melting in landslides. – Tectonophysics, 115: 131–160.

Oberhauser, R. (1980): Das Altalpidikum (Die geologische Entwicklung von der mittleren Kreide bis an die Wende Eozän-Oligozän). – In: Oberhauser, R. (ed.): Der Geologische Aufbau Österreichs, 35–48; Wien (Springer).

Pagliarini, L. (2008): Strukturelle Neubearbeitung des Tschirgant und Analyse der lithologisch-strukturell induzierten Massenbewegung (Tschirgant Bergsturz, Nördliche Kalkalpen, Tirol). – Unpublished Diploma thesis, University of Innsbruck, 90 pp.

Patzelt, G. (2012): Die Bergstürze vom Tschirgant und von Haiming, Oberinntal, Tirol – Begleitworte zur Kartenbeilage. – Jahrbuch der Geologischen Bundesanstalt., 152: 13–24.

Patzelt, G. & Poscher, G. (1993): Der Tschirgant-Bergsturz. – Arbeitstagung 1993 der Geologischen Bundesanstalt, Geologie des Oberinntaler Raumes – Schwerpunkt Blatt 144 Landeck, Exkursion D: Bemerkenswerte geologische und quartärgeologische Punkte im Oberinntal und aus dem äußerem Ötztal. – 206–213, Wien (Geologische Bundesanstalt).

Poscher, G. & Patzelt, G. (2000): Sink-hole collapses in soft rocks. – Felsbau, 18: 36–40.

Prager, C. (2010): Geologie, Alter und Struktur des Fernpass

Bergsturzes und tiefgründiger Massenbewegungen in seiner Umgebung (Tirol, Österreich). – Unpublished PhD thesis, University of Innsbruck, 307 pp.

Prager, C., Zangerl, C. & Poscher, G. (2007): Prominent mass movements in the Tyrol (Austria): the deep-seated Tschirgant, Tumpen and Köfels rockslides. – Geo.Alp, 4: 159–162.

Prager, C., Zangerl, C., Patzelt, G. & Brandner, R. (2008): Age distribution of fossil landslides in the Tyrol (Austria) and its surrounding areas. – Natural Hazards and Earth System Sciences, 8: 377–407.

Prager, C., Zangerl, C. & Nagler, T. (2009): Geological controls on slope deformations in the Köfels rockslide area (Tyrol, Austria). – Austrian Journal of Earth Sciences, 102: 4–19.

Prager, C., Zangerl, C. & Kerschner, H. (2012): Sedimentology and mechanics of major rock avalanches: implications from (pre-)historic Sturzstrom deposits (Tyrolean Alps, Austria). – In: Eberhardt, E., Froese, C.R., Turner, A.K. & Leroueil, S. (eds.): Landslides and Engineered Slopes – Protecting Society through Improved Understanding. – Proceedings of the 11th International & 2nd North American Symposium on Landslides: 895–900; London (Taylor & Francis).

Preuss, E. (1974): Der Bimsstein von Köfels/Tirol: die Reibungsschmelze eines Bergsturzes. – Jahrbuch des Vereins zum Schutze der Alpenpflanzen und -tiere, 39: 85–95.

Purtscheller, F. (1978): Ötztaler und Stubaier Alpen. – Sammlung Geologischer Führer, 53: 1–128.

Purtscheller, F., Pirchl, T., Sieder, G., Stingl, V., Tessadri, R., Brunner, P., Ennemoser, O., & Schneider, P. (1995): Radon emanation from giant landslides of Koefels (Tyrol, Austria) and Lang Tang Himal (Nepal). – Environmental Geology, 26: 32–38.

Reiter, F., Ortner, H. & Brandner, R. (2003): Seismically active Inntal fault zone: inverted European rift structures control upper plate deformation. – Memorie della Società Geologica Italiana, 54: 233–234.

Sanders, D., Ostermann, M., Brandner, R. & Prager, C. (2010): Meteoric lithification of catastrophic rockslide deposits: Diagenesis and significance. – Sedimentary Geology 223: 158–161.

Senarclens-Grancy, W. (1958): Zur Glazialgeologie des Oetztales und seiner Umgebung. – Mitteilungen der Geologischen Gesellschaft, 49: 257–314.

Wakonigg, H. (1996): Unterkühlte Schutthalden. – In: Beiträge zur Permafrostforschung in Österreich. – Arbeiten aus dem Institut für Geographie der KFU Graz, 33: 209–223.

Notes

Geomorphology, permafrost and Holocene climate near Obergurgl, Ötztal Alps

Geomorphologie, Permafrost und holozänes Klima in der Umgebung von Obergurgl, Ötztaler Alpen

Karl Krainer

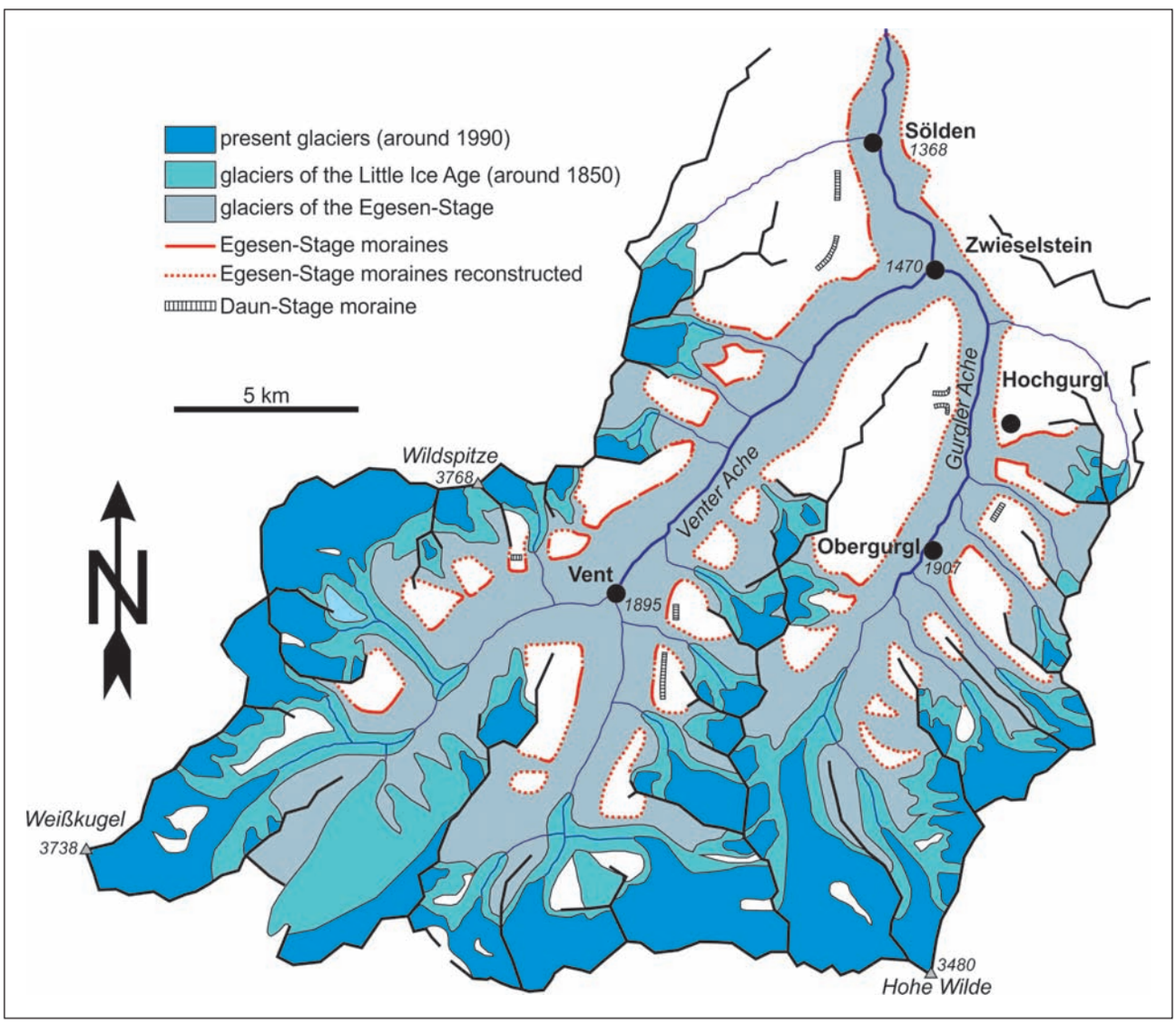

Fig. 1: Reconstruction of the Ötztal Glacier during the Egesen Stage (after Patzelt 1996).

Abb. 1: Rekonstruktion des Ötztalgletschers im Egesen Stadium (nach Patzelt 1996).

1 Introduction and aim of the excursion

Permafrost is widespread in the Alps and includes a large number of rock glaciers, which are the typical and most common permafrost landform.

The rock glacier inventory of the Tyrolean Alps (Austria), which is based on the study of high-quality aerial photographs and laser-scan images, includes 3145 rock glaciers which cover an area of 167.2 km². Of these, 517 (16.4 %) were classified as active, 915 (29.1 %) as inactive, and 1713 (54.5 %) as fossil (Krainer & Ribis 2012).

Tongue-shaped, talus-derived, ice-cemented rock glaciers are the most common type among active and inactive rock glaciers. Glacier-derived rock glaciers containing a massive ice-core are rare.

Most rock glaciers occur in the mountain groups of the Central Alps in which bedrock is composed mainly of metamorphic rocks such as mica schists, paragneiss, orthogneiss and amphibolites ("Altkristallin").

The majority of active and inactive rock glaciers are exposed towards a northern (NW, N and NE) direction. Active and inactive rock glaciers exposed towards S, SE and SW are rare.

The total amount of ice in active and inactive rock glaciers is estimated to be 0.19–0.27 km³ which is small compared to the ice volume contained in the glaciers of the Tyrolean Alps. In Tyrol, glaciers cover an area of 335 km² which is 3 % of the total land area and more than 70 % of the area of all Austrian glaciers (470 km²) (Fischer 2013).

The distribution of active and inactive rock glaciers indicates that the lower limit of discontinuous permafrost in the mountain groups of the central part of the Tyrolean Alps is located at an elevation of approximately 2500 m.

As permafrost temperatures in the Alps are just slightly below zero and the frozen core of rock glaciers is thin, rarely exceeding 25 m, permafrost in the Alps, particularly active and inactive rock glaciers, are very sensitive to climate change. Studies on Alpine permafrost, particularly on active rock glaciers, advanced rapidly during the last two decades (see summary by Haeberli et al. 2006). In the Austrian Alps several rock glaciers have been studied in detail in recent years (e.g. Lieb 1986, 1987, 1991, 1996, Lieb & Slupetzky 1993, Kaufmann 1996a, b, Kaufmann & Ladstätter 2002, 2003, Kellerer-Pirklbauer, Berger et al. 2004, Krainer & Mostler 2000, 2001, 2002, 2004, 2006, Krainer et al. 2002, 2007, Hausmann et al. 2007, 2012).

Hochebenkar rock glacier is one of the largest and most active rock glaciers in the Austrian Alps, which also shows the worldwide longest record of flow velocity measurements.

Pillewizer started to measure flow velocities on this rock glacier in 1938. Since that time, i.e. over a period of more than 70 years, flow velocities on this rock glacier have been measured by terrestrial photogrammetry, since 1951 by terrestrial geodetic methods (theodolite) and since 2008 by differential GPS (Pillewizer 1938, 1957, Vietoris 1958, 1972, Haeberli & Patzelt 1982, Kaufmann 1996, Schneider & Schneider 2001, Kaufmann & Ladstätter 2002, 2003, Ladstätter & Kaufmann 2005). Haeberli & Patzelt (1982) measured the basal temperatures of the winter snow cover in February 1975, 1976 and 1977, and the water temperature of rock glacier springs during summer. They also carried out refraction-seismic measurements along 11 transects on frozen and unfrozen ground. Recently Nickus et al. (2014) presented new data on Hochebenkar rock glacier.

The aim of this excursion is to visit Hochebenkar rock glacier and to present new data on the dynamics of this spectacular active rock glacier. The trail to Hochebenkar provides also a beautiful overview on landforms made by alpine glaciers (glacial trough, hanging trough, glacial striations), an extensive peat occurrence providing data on the climate of the last 8000 years, well-developed earth hummocks and moraines of the Little Ice Age.

2 Geological setting

Bedrock in the drainage area of the Hochebenkar rock glacier is composed of paragneiss and mica schists of the Ötztal-Stubai Complex, a tectonic unit of the Austroalpine nappe system composed mainly of paragneiss and mica schist with intercalations of orthogneiss, amphibolite and locally eclogite (see Hoinkes & Thöni 1993, Konzett et al. 2003, Tropper & Recheis 2003, Thöny et al. 2008). The rocks contain biotite and quartz, subordinately chlorite, muscovite and feldspar in varying amounts. Garnet is present as small phenocrysts. Accessory minerals are apatite, tourmaline and opaque minerals. Fine-crystalline varieties (mica schists) display well developed schistosity, which is less well developed in coarse-crystalline varieties (paragneiss).

Schistosity dips WNW–NW (285–325), locally also towards N and ESE, and dipping angles are mostly 40–45°, and range from 35 to 60°. Small and large-scale folds are observed. At Hochebenkamm the bedrock is cut by steep faults. Along these faults the rock is strongly deformed, jointed and shattered by frost action. Therefore major faults frequently form steep grooves, along which high amounts of debris are produced, particularly during spring and early summer. During this time rock fall produces a thin debris layer on the avalanche snow at the foot of some major faults.

3 Geomorphology

Landforms around Obergurgl (Gurgl Valley, Gaisberg Valley, Rotmoos Valley) are mainly the product of glacial erosion during the Pleistocene glaciations. During the Last Glacial Maximum the Inn Glacier terminated in the Alpine foreland, approximately 40 km north of Rosenheim and the Ötz Glacier was a tributary glacier of this huge glacier. Only the highest peaks stood out from this ice-stream network. During the glacier advance of the Steinach and Gschnitz Stage the Ötz Glacier probably terminated near the confluence of the Ötztaler Ache with the Inn River (Hantke 1983). During the Egesen Stage with its maximum approximately 12,700 years ago the Ötz Glacier ended about 3 km north of Sölden (Fig. 1). Glacier advances during the Little Ice Age with their climax around 1855 are well documented by sharp-crested terminal and lateral moraines, for example in the Gaisberg and Rotmoos valleys near Obergurgl.

The products of glacial erosion such as glacial troughs, cirques, trimlines, roches moutonnées, glacial striations, various till deposits are well preserved around Obergurgl. During the Little Ice Age an ice-dammed glacial lake ("Gurgler Eissee") periodically existed for about 200 years at the confluence of the Langtal and Gurgltal near Langtalereck Hütte southwest of Obergurgl. Terraces composed of fluvial

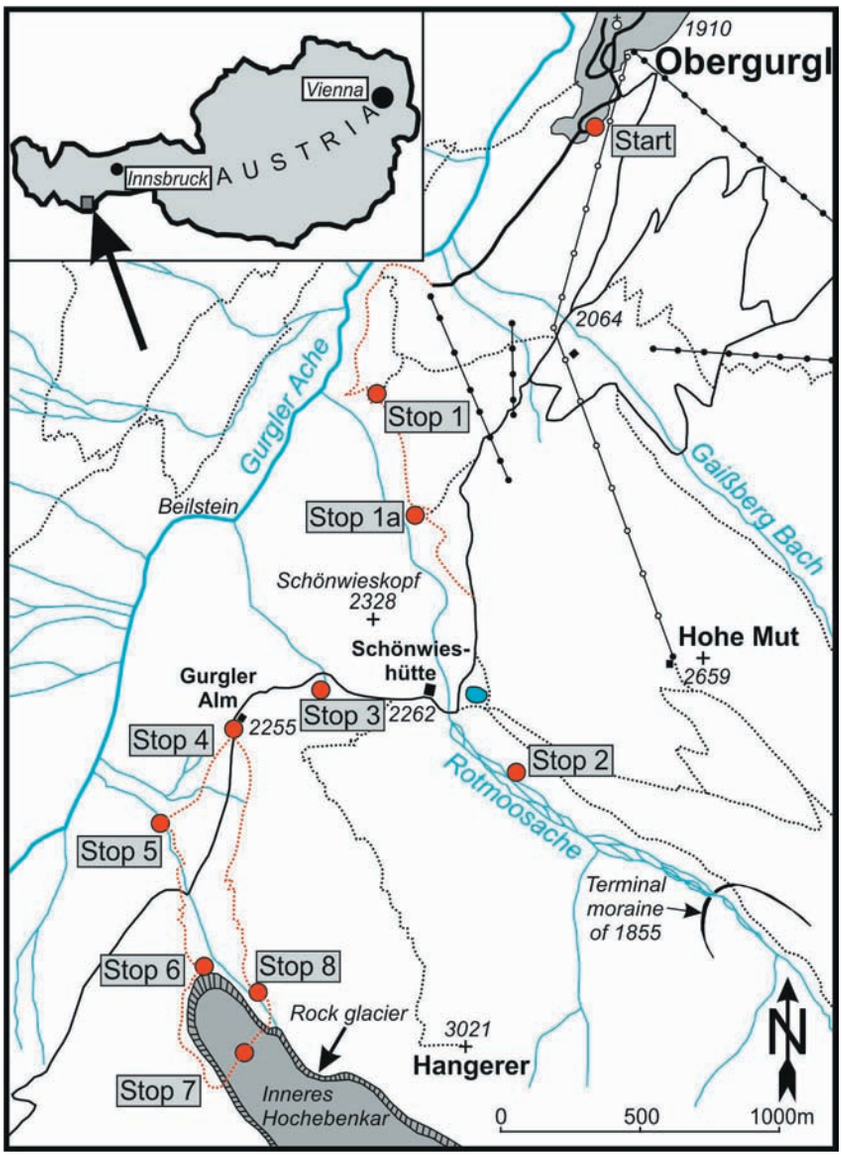

Fig. 2: Map showing excursion route (red line) from Obergurgl to the Hochebenkar rock glacier and stops 1–8 (red circles).

Abb. 2: Karte mit Exkursionsroute von Obergurgl zum Hochebenkar Blockgletscher (rote punktierte Linie) und Haltepunkte 1–8 (rote Kreise).

and lacustrine sediments of this glacial lake are still present south of Langtalereck Hütte (Krainer & Spieler 1999).

4 Permafrost

Permafrost is widespread in the mountain groups of western Austria and is represented by numerous active and inactive rock glaciers. Besides, permafrost occurs in bedrock (fissure ice) and in unconsolidated sediments, particularly in talus and till deposits of north-facing slopes above elevations of 2500 m a.s.l.

Rock glaciers are lobate or tongue-shaped, slowly flowing mixtures of debris and ice with steep sides and a steep front which slowly creep downslope (for a summary see Barsch 1996, Haeberli 1985, Haeberli et al. 2006, Kääb 2007, Vitek & Giardino 1987, Whalley & Martin 1992). Rock glaciers are striking morphological expressions of permafrost creep and belong to the most spectacular and most widespread periglacial phenomenon on earth (Haeberli 1990).

A continuum exists between frozen, ice-rich debris ("ice-cemented rock glaciers") and debris covered glaciers ("ice-cored rock glaciers") as the two end members (Haeberli et al. 2006).

Radiocarbon dating of the frozen core of rock glacier Lazaun (South Tyrol) indicates that the ice of rock glaciers may be up to 10000 years old and that permafrost ice survived even warmer periods during the last 10000 years (Krainer et al. submitted).

Although increased melting of permafrost ice is observed at present, the amount of this additional meltwater is small compared to the total discharge of rock glaciers. The bulk of meltwater is derived from snowmelt and summer precipitation and less than 5 % is derived from the melting of permafrost ice.

The water of some rock glacier springs, particularly in the Ötztal Alps, is highly contaminated by Ni and other heavy metals. Ni is most likely derived from permafrost ice and released by increased melting as indicated by the study of the frozen core of rock glacier Lazaun. Hydrological studies indicate that increased melting of permafrost ice will increase the open pore space and thus the storage capacity for water in unconsolidated sediments. Hydrological simulations indicate that increased melting of permafrost ice will cause a decrease in flood peak discharge and an increase of runoff during recession periods (Rogger et al. in prep.).

In the Ötztal and Stubai Alps 1202 rock glaciers were identified which is more than one third (38 %) of all rock

glaciers in Tyrol. Thus the Ötztal Alps are not only the most glaciated mountain range in Austria, but also have by far the highest density of rock glaciers. These rock glaciers cover a total area of 73.5 km². 352 of these rock glaciers are active, 345 are inactive and 505 are fossil. Within the catchment area of the Ötztal Ache 421 rock glaciers are present (135 active, 142 inactive and 174 fossil) covering an area of 30.5 km² (Krainer & Ribis 2012).

In the catchment area of the Ötztal Ache the following active rock glaciers have been studied in detail: Äußeres Hochebenkar (Haeberli & Patzelt 1982, Kaufmann & Ladstätter 2002, Ladstätter & Kaufmann 2005, Schneider & Schneider 2001, Vietoris 1972), Inneres Hochebenkar (Pillewizer 1957, Vietoris 1972, Haeberli & Patzelt 1982, Kaufmann & Ladstätter 2002), Inneres Reichenkar (Krainer & Mostler 2000a, b, 2002, 2006; Krainer et al. 2002, 2007, Hausmann et al. 2007), Sulzkar (Krainer & Mostler 2004), Rosskar-Schrankar (Figl 2004), Windachtal (Schmidt 2014).

5 Excursion

Introduction

The excursion route from Obergurgl to Äußeres Hochebenkar follows the trail through the "Zirbenwald" (stop 1) to the entrance of the Rotmoos Valley (stop 2). From there the route follows the road to Gurgler Alm (stops 3 and 4) from where we will walk to the gauging station at the front of the rock glacier Äußerers Hochebenkar (stop 5). We will then walk up to the front of the rock glacier (stop 6), and then higher up to an elevation of approximately 2600 m a.s.l. where we will cross the rock glacier (stop 7) and visit a monitoring site at the eastern margin of the rock glacier (stop 8). From there we will walk back to Gurgler Alm and then follow the road back to Obergurgl (see map Fig. 2).

The total length of the trail is approximately 12.5 km, the vertical climb from Obergurgl (University Center, 1940 m a.s.l.), from where the excursion starts, to the highest point at the rock glacier Äußeres Hochebenkar (2600 m a.s.l.) is almost 700 m.

Stop 1: Zirbenwald (*Pinus cembra* forest)

The trail from Obergurgl through the *Pinus cembra* forest (Zirbenwald) to the Rotmoos Valley provides an excellent overview of the landforms produced by the Pleistocene glaciers. During the Last Glacial Maximum (Upper Würm, approximately 25,000 years ago) the glacier at Obergurgl was almost 1000 m thick and the ice surface was at an elevation of approximately 2800 m a.s.l. This valley glacier carved the Gurgl Valley forming a deep, steep-walled glacial trough with a typical U-shaped cross-section.

Rotmoos glacier, which was a small tributary glacier until the Younger Dryas, also carved a U-shaped valley (Fig. 3), but as Rotmoos glacier was much smaller and slower than the glacier in the main valley, glacial erosion was less intensive. The valley floor of the Rotmoos valley remained high above the floor level of the main valley (Gurgl Valley) forming a typical hanging valley. The difference in elevation is approximately 300 m. Rotmoos creek passes down from the lip of the hanging valley to the floor of the main valley by forming steep cascades and a scenic waterfall (Fig. 4).

After the retreat of the glacier the Rotmoos creek quickly cut a small, V-shaped gorge into the bedrock well documenting the difference between glacial and fluvial erosion.

At an elevation of approximately 2200 m a.s.l. glacial striations on the bedrock (paragneiss) are well visible along the trail.

Stop 2: Peat bog

Along the eastern river bank of the Rotmoos Ache a peat deposit is exposed which can be traced laterally over a distance of approximately 800 m (Fig. 5). Peat accumulated in a bog environment where water inhibited decay and oxi-

Fig. 3: Rotmoos Valley, a glacial trough with well-preserved terminal and lateral moraines of the Little Ice Age (1855). View towards the south.

Abb. 3: Das Rotmoostal ist ein glazial geformtes Trogtal mit gut erhaltener Stirn- und Seitenmoräne der Kleinen Eiszeit (1855). Blick Richtung Süden.

Fig. 4: Rotmoos creek passes down from the Rotmoos Valley to the floor of the main valley (Gurgl Valley) forming a waterfall.

Abb. 4: Die Rotmoos Ache überwindet die Steilstufe zwischen dem Rotmoostal und dem Gurgler Tal mit einem Wasserfall.

dation of plant remains. Peat is also present southwest and west of Schönwieshütte and near Gurgler Alm. Due to the high elevation (2260 m a.s.l.) these peat deposits gained attention and have been studied to reconstruct the vegetation history (e.g. fluctuations of the timber line) and climate of the Rotmoos Valley of the last 10 ka (see review by Bortenschlager 2010).

The peat deposit is up to 265 cm thick (Fig. 6). The lower part (265–185 cm) is composed of alternating silt and peat layers. Pollen grains of this part indicate that the timberline was below the elevation of the bog at that time. Radiocarbon ages of the lower part range from 3975 BC at 243 cm to 3000 BC at 183 cm. Patzelt (1973) termed this cool period Rotmoos I and II.

The peat between 180 and 140 cm contains wood fragments which indicate that the forest had reached the elevation of the Rotmoos Valley. Peat at a depth of 136 cm yielded a radiocarbon age of 2680 BC.

Peat accumulation was interrupted by a sandy layer which contains angular clasts up to several dm in diameter at a depth of 135–115 cm. This sediment layer is interpreted to represent deposits of an avalanche from the western flank of the valley. Organic material from a depth of 114 cm yielded an age of 2325 BC. Increasing abundance of non-tree pollen from 85 cm upsection, particularly between 72.5 and 60 cm, indicates cooler climatic conditions and no forest in the Rotmoos valley. Peat at 76 cm yielded an age of 1375 BC, at 55 cm AD, at 51 cm 390 AD. Increasing percentage of non-tree pollen in the uppermost part of the section is interpreted to result from a climate change as well as from human activities (for details see Bortenschlager, 1984, 2010, Gams 1962, Patzelt 1996, Rybnicek & Rybnickova 1977). Peat accumulation at the localities Schönwies I and II is up to 2 m thick and started to form

Fig. 5: Peat exposed along the Rotmoos creek in the Rotmoos Valley south of Schönwieshütte at an elevation of 2260 m a.s.l.

Abb. 5: Torfaufschluss entlang der Rotmoos Ache im Rotmoostal südlich der Schönwieshütte auf einer Seehöhe von 2260 m.

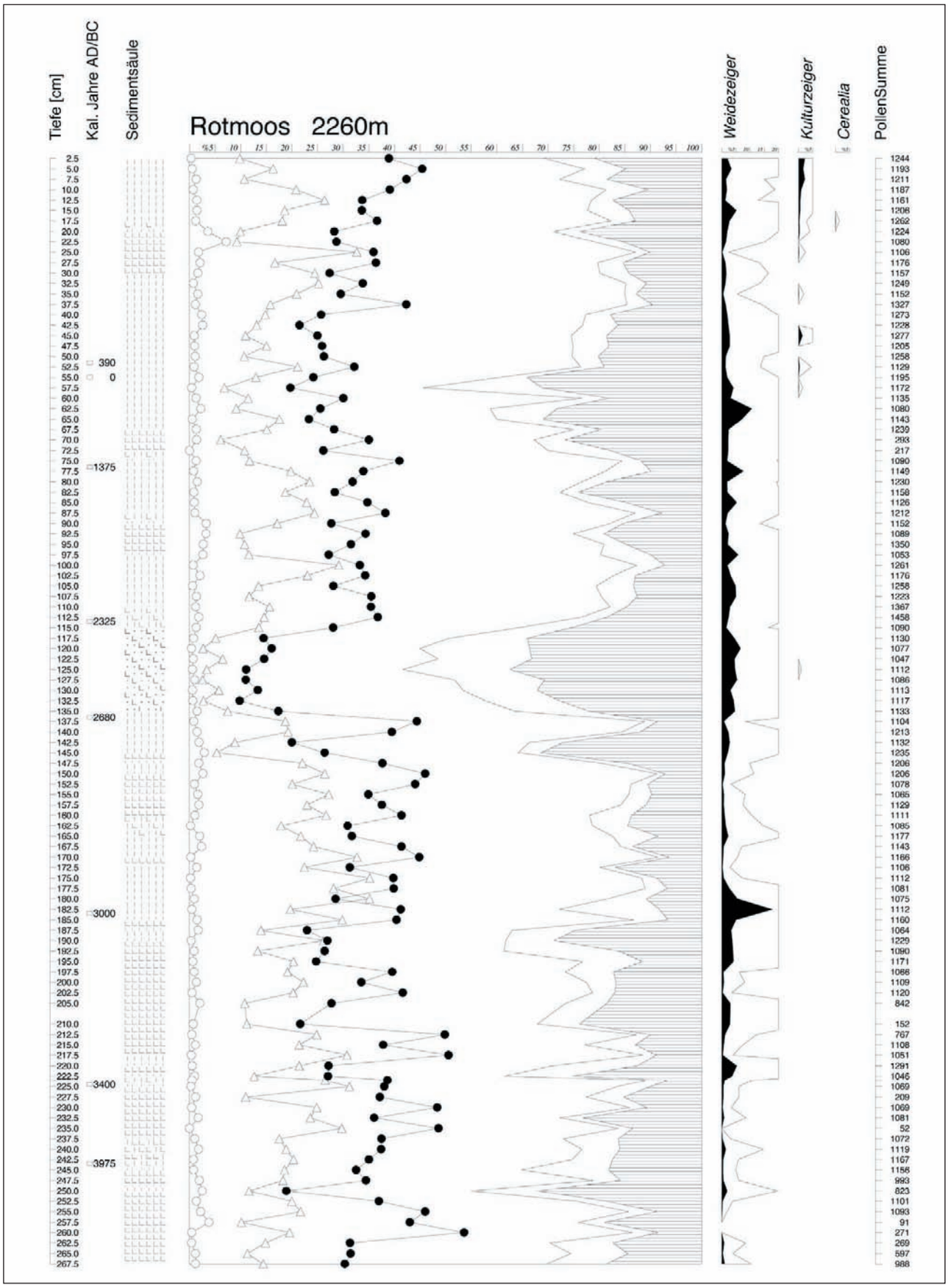

Fig. 6: Simplified pollen diagram of the peat horizon exposed in the Rotmoos Valley (from Bortenschlager 2010).

Abb. 6: Vereinfachtes Pollenprofil des Torfaufschlusses im Rotmoostal (aus Bortenschlager 2010).

8000 BC (Bortenschlager 2010). At Gurgler Alm the peat is up to 140 cm thick and also started to form about 8000 BC. The cool period determined by pollen at the base of the section is ascribed to the Venediger Schwankung of Patzelt (1973) (see Bortenschlager 2010).

According to Patzelt (1996) the Rotmoos valley represents a glacially oversteepened basin which is approximately 40 m deep and at the outlet (near the bridge across the creek south of Schönwieshütte) the Rotmoos creek erosively cut into the bedrock for 6.4 m during the last 4000 years resulting in an erosional rate of 1.6 mm/year. During the last 9000 years the Rotmoos creek cut 14 m into the bedrock (erosion rate of 1.55 mm/year).

Stop 3: Earth hummocks ("Bültenboden")

Earth hummocks are common on the flat to gently sloping alpine pastures around Schönwieshütte (Fig. 7). Earth hummocks are widespread in the Alps above an elevation of 2000 m a.s.l., where the soil is mainly composed of fine-grained sediment (silt to fine-grained sand), where water is present in the soil and the ground is flat or slightly inclined.

Earth hummocks ("Bülten", "thufur") are circular forms of patterned ground ("non-sorted circles"; Washburn 1979) which are commonly 0.5–2 m in diameter and up to 50 cm high. Earth hummocks are most likely the product of cryoturbation and occur in the periglacial environment. They form by lateral and vertical displacement of soil caused by seasonal and/or diurnal freezing and thawing.

In a study of earth hummocks at Peischlachtörl in the northern part of the Schober Mountain Group in East Tyrol (Hohe Tauern Nationalpark) Keuschnig et al. (2007) showed that differences exist in the vegetation between the top of the hummocks and the depressions between the hummocks. The top of the hummocks is characterised by *Caricetum curvulae*-, *Loiseleuria procumbens*-, and *Oreochloa disticha*-type vegetation. The transition zone between the hummocks and the depressions is covered by a *Ligusticum mutellina*-type vegetation and in the depression a *Luzula alpinopilosa*-community including several snowbed species occur.

Earth hummocks in the vicinity of the Schönwieshütte are very similar in shape, composition and vegetation compared to those at Peischlachtörl, but have not been studied in detail.

Frost activity in the earth hummocks depends on the thickness and duration of the snow cover. Thick snow cover prevents infiltration of cold air into the ground and almost no frost activity is observed in the hummocks and in the soil underneath the depressions. When the snowpack is thin, most of the snow is commonly blown into the depressions and cold air infiltrates into the hummocks causing freezing and thawing, whereas underneath the depressions freezing activity is reduced due to the snow insolating effect on the depressions.

Stop 4: Gurgler Alm: overview of the Hochebenkar rock glacier

Hochebenkar rock glacier is located in Äußeres Hochebenkar, a northwest oriented cirque in the southern Ötztal Alps, about 4.3 km SSW of Obergurgl, Ötztal (Tyrol, Austria). This rock glacier is tongue-shaped and extends from an altitude of 2840 m a.s.l. (rooting zone) down to 2360 m a.s.l. (front). The maximum length of this active, NW-facing rock glacier is 1550 m. The width ranges from 160 m near the front to 335 m in the middle part and up to 470 m in the upper part (Figs. 8, 9).

The rock glacier covers an area of 0.4 km² and its the drainage area measures 1 km². The surface layer is coarse-grained with varying grain size and locally well-developed transverse and longitudinal furrows and ridges. A depression is developed in the western part of the rooting zone.

The front is steep and bare of vegetation. The highest peaks surrounding the rock glacier are Hangerer (3021 m) on the eastern side and the Hochebenkamm with its summit at 3149 m a.s.l. on the southern side, separated by the Hochebenscharte (2895 m a.s.l.).

The debris of the rock glacier is derived from the steep walls of the Hochebenkamm. Bedrock in the drainage area of

Fig. 7: Earth hummocks near Schönwieshütte.

Abb. 7: Bülten in der Umgebung der Schönwieshütte.

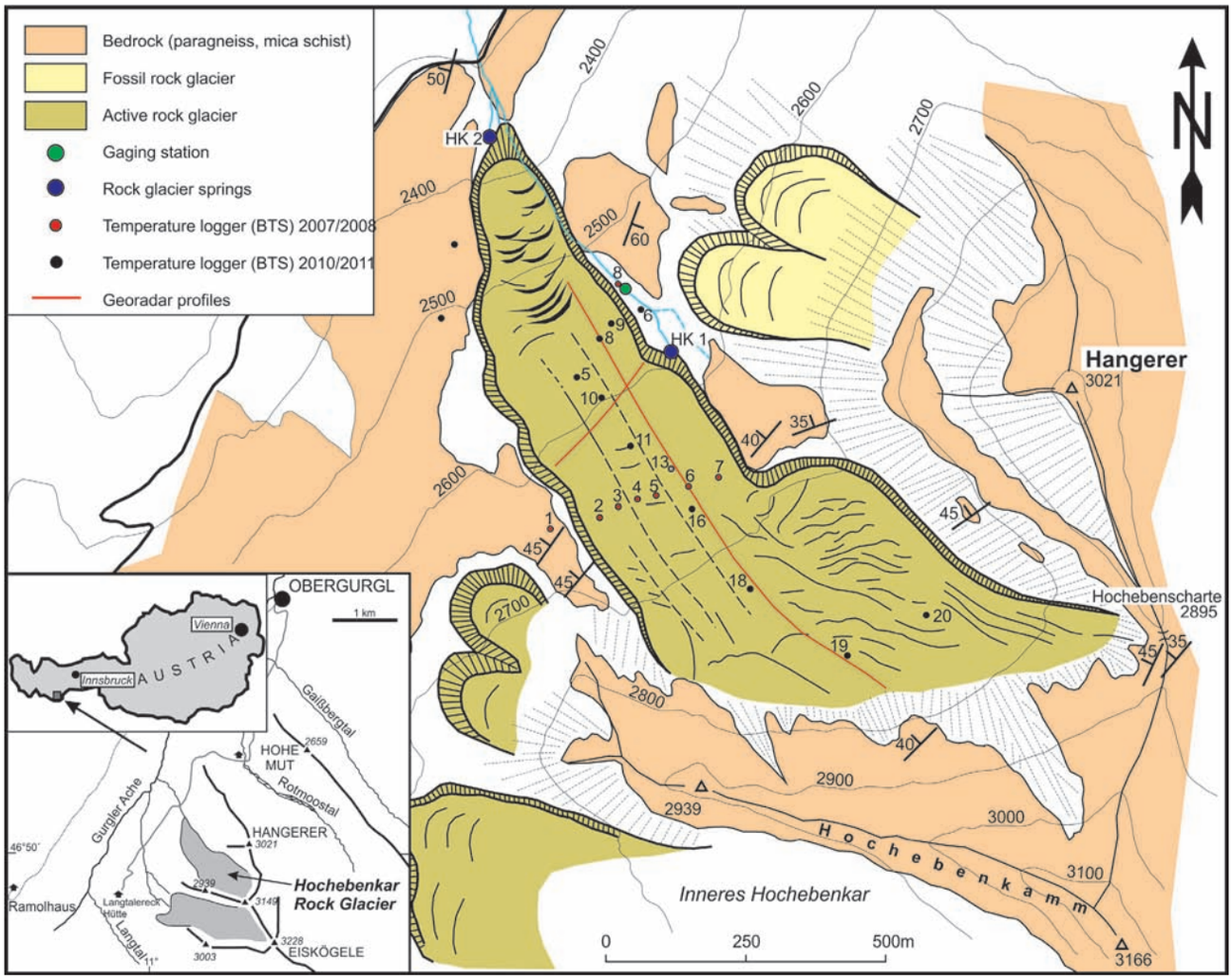

Fig. 8: Geologic-geomorphologic map of the Hochebenkar rock glacier (after Nickus et al. 2014).

Abb. 8: Geologisch-geomorphologische Karte des Hochebenkar Blockgletschers (nach Nickus et al. 2014).

Fig. 9: Hochebekar rock glacier (center), Langtalferner (glacier) on the right, Rotmoos and Gaisberg valleys with small glaciers on the left (photo by Jakob Abermann, September 2009). View towards south.

Abb. 9: Hochebenkar Blockgletscher, rechts Langtal mit Langtalferner, links Rotmoostal und Gaisbergtal mit kleinen Gletschern (Aufnahme von Jakob Abermann, September 2009). Blick Richtung Süden.

the rock glacier is composed of paragneiss and mica schists of the Ötztal-Stubai Complex. At Hochebenkamm the bedrock is cut by numerous steep faults along which high amounts of debris are produced by frost shattering, particularly during spring and early summer.

Stop 5: Gauging station

In September 2008 an automatic gauging station was installed by the Hydrographic Service (Hydrographischer Dienst) of the Federal Government of Tyrol at an elevation of 2220 m a.s.l. to record the total discharge of Hochebenkar rock glacier and its drainage area (Fig. 10).

The discharge of the rock glacier is mainly controlled by water derived from snowmelt, summer thunderstorms and/or snowfall during summer and thus displays pronounced seasonal and diurnal variations in discharge. Runoff starts near the end of April / beginning of May. Maximum flow peaks are caused by fair weather periods with intense melting of snow and ice and by rainfall events during May and June. A rapid decline in discharge is recorded a few hours after the influx of cold air which sometimes is accompanied by snowfall. Short-term floods with peak flows > 300 l/s are triggered by summer thunderstorms with heavy rainfall.

In 2010 discharge increased strongly at the beginning of June with a maximum peak discharge of 620 l/s on June 6, followed by a distinct decrease to a minimum of 24 l/s on June 23 caused by a period of cool weather. Discharge then increased again to a peak discharge of 390 l/s on June 29, followed by continuous decrease to values of 20–30 l/s, interrupted by single peaks up to 276 l/s.

In 2011 the first peak of 211 l/s was recorded on May 13, followed by a strong decrease to 12 l/s on May 17, an increase to 386 l/s on May 27, a decrease to 42 l/s on May 29, followed by a period of high discharge until the end of June with the highest discharge of 427 l/s on June 18. From July 1 onward discharge was mostly < 50 l/s, interrupted by individual peaks up to 318 l/s caused by rainfall events (Fig. 11).

Fig. 10: Automatic gauging station at the meltwater stream of the Hochebenkar rock glacier near Gurgler Alm at an elevation of 2220 m.

Abb. 10: Automatische Pegelstation am Abfluss des Hochebenkar Blockgletschers in der Nähe der Gurgler Alm auf einer Seehöhe von 2220 m.

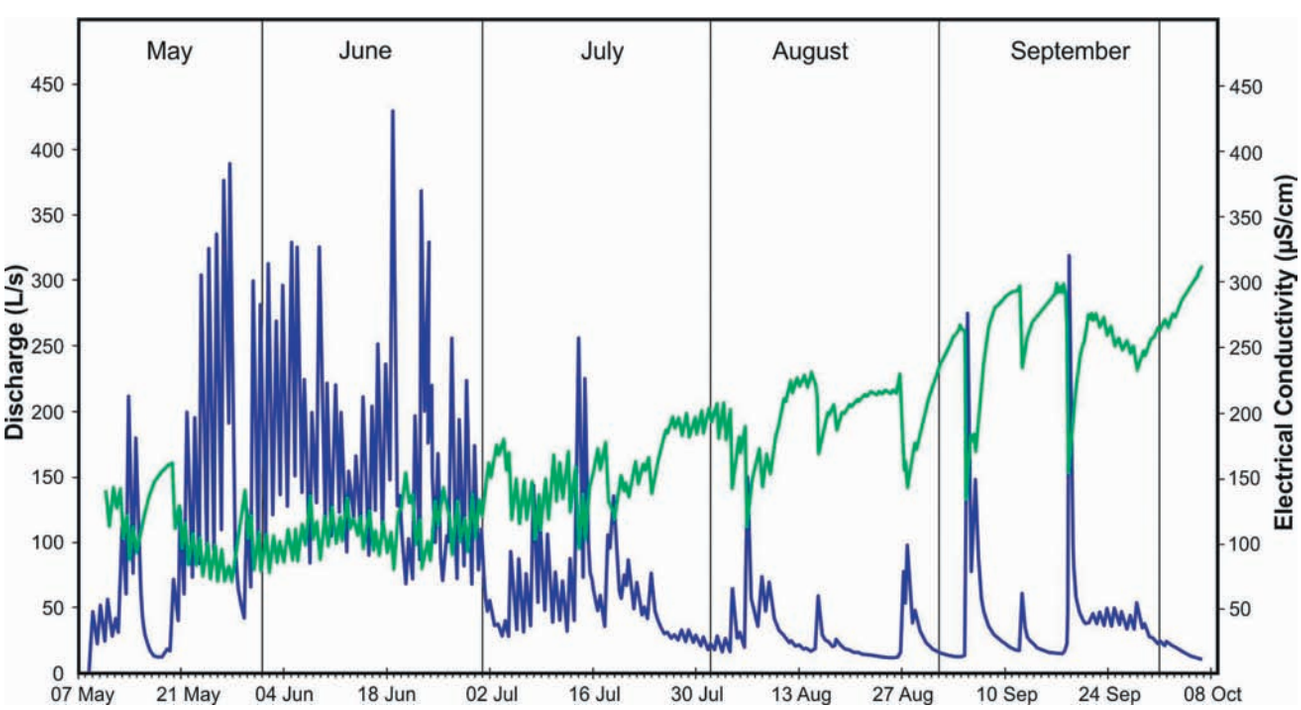

Fig. 11: Hydrograph of the meltwater stream (total discharge) released from the Hochebenkar rock glacier (blue line, scale at left) and electrical conductivity of the meltwater (green line, scale at right) for the period from May until the beginning of October 2011.

Abb. 11: Abflussganglinie des Baches (Gesamtabfluss) des Hochebenkar Blockgletschers (blaue Linie, Skala links) und elektrische Leitfähigkeit des Wassers (grüne Linie, Maßskala rechts) für den Zeitraum Mai bis Anfang Oktober 2011.

In 2012 the first period of high discharge was from June 1 until June 3 with a peak discharge of 400–427 l/s, followed by a marked decrease to 79 l/s on June 5. Discharge increased again to peak discharge of 453 l/s on June 8 and decreased to 63 l/s on June 13. A period of high discharge with pronounced diurnal cycles was recorded from June 15 until July 2. Discharge was mostly between 200 and 400 l/s, and a maximum discharge of 735 l/s was recorded on July 2. The daily range in discharge was mostly > 200 l/s; minimum and maximum discharges occurred in the morning and the evening, respectively.

After July 2 discharge was mostly < 50 l/s, interrupted by single peaks up to 260 l/s.

The values of electrical conductivity vary significantly over the season. At Hochebenkar rock glacier significantly higher values are recorded at the two springs on the eastern side than at the main spring at the front. At the main gauging station electrical conductivity of the total discharge is below 100 µS/cm during spring and increases to values of > 300 µS/cm in October (Figs. 11).

In 2010 electrical conductivity increased from 123 µS/cm on August 26 to 629 µS/cm on October 10. In 2011 a value of 72 µS/cm was recorded on May 25 and increased to 309 µS/cm until October 6. Daily variations of electrical conductivity of 50 to >100 µS/cm are recorded, particularly during the snowmelt period. In general, low values of electrical conductivity are recorded during peak discharge and high values during low discharge.

Stop 6: Front of the rock glacier

At present the front of the rock glacier terminates at an elevation of approximately 2360 m a.s.l. (Fig. 12). The front is steep and bare of vegetation. At the base of the front large blocks of paragneiss cover the ground. The front of the rock glacier is composed of coarse-grained material with high amounts of fine-grained sediment. Several springs emerge at the front. Water temperature of the rock glacier springs remains almost constantly <1.5°C, commonly even <1°C during summer. Even after heavy thunderstorms in summer with rather "warm" rainfall causing peak floods in discharge of the rock glacier the water temperatures does not change. At Hochebenkar rock glacier most of the meltwater is released from springs at the front. A minor amount (ca. 30 %) of meltwater is released from two springs on the eastern side of the rock glacier at an altitude of 2575 m a.s.l.

At springs located at the base of the steep front electrical conductivity is extremely low in May and June (20–30 µS/cm) and increases slightly reaching values of 40 µS/cm by the end of August and 60 µS/cm at the beginning of October. The water temperature at these springs ranges from 0.6 to 1.4°C.

At these springs at the front of the rock glacier the ionic ratio $SO_4^{2-}/(Mg^{2+}+Ca^{2+})$ increases from about 0.6 in June up to 1.2 in late October. In June most of the water released at the springs is derived from the melting of the seasonal snow, whereas towards autumn the amount of snowmelt-derived water decreases and groundwater and meltwater from permafrost ice seem to determine the chemical composition of runoff (Nickus et al. 2014). Generally, the concentrations of sulfate, calcium and magnesium in the rock glacier streams were 2 to 3 orders of magnitude higher compared to average ion concentrations in atmospheric deposition (Nickus et al. 1997) and also exceed values of streams draining catchments without rock glaciers of similar bedrock geology by 1 to 2 orders of magnitude (Thies et al., submitted).

Stop 7: Debris layer, thermal history, flow velocity

The surface debris layer of Hochebenkar rock glacier is coarse-grained with an average grain size of 35 cm on finer grained areas and 58 cm on coarser grained areas in the middle part (Fig. 13). Locally, blocks up to a few metres in diameter occur on the surface. Similar values are recorded from other rock glaciers composed of debris derived from

Fig. 12: View from Gurgler Alm to the steep front of Hochebenkar rock glacier.

Abb. 12: Blick von der Gurgler Alm zur steilen Stirn des Hochebenkar Blockgletschers.

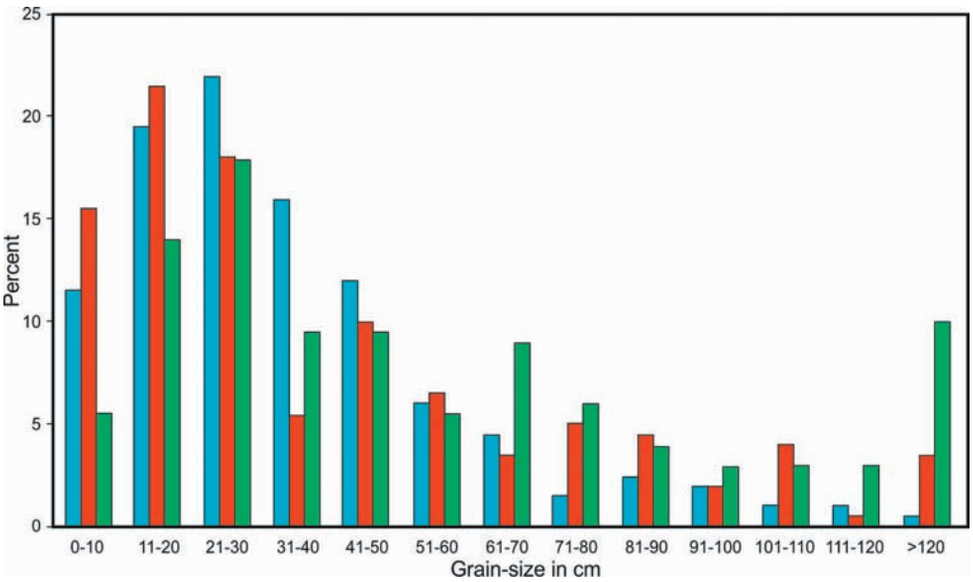

Fig. 13: Grain-size distribution on the surface of the coarse-grained debris layer of Hochebenkar rock glacier at three different sites.

Abb. 13: Korngrößenverteilung auf der Oberfläche der grobblockigen Schuttlage des Hochebenkar Blockgletschers auf drei verschiedenen Stellen.

gneisses and schists (Berger et al. 2004, Krainer & Mostler 2001, 2004).

The coarse-grained debris layer has a maximum thickness of 1.5 m and is underlain by debris containing higher amounts of sand and silt displaying poor to very poor sorting with values of 2.96–3.23 Phi (inclusive graphic standard deviation after Folk & Ward, 1957). Similar values were reported from other rock glaciers (Barsch et al. 1979, Giardino & Vick 1987, Haeberli 1985, Krainer & Mostler 2000, 2004, Berger et al. 2004) and from till (e.g. Menzies & Shilts 1996, Eyles & Eyles 2010).

BTS measurements performed by Haeberli & Patzelt (1982) in February 1975, 1976 and 1977 yielded mean values between -4.8 and -7°C. Similar temperatures were recorded in March 2010.

During winter 2007/2008 eight temperature loggers were installed which recorded the temperature at the base of the snow cover at an interval of two hours (Fig. 14). The temperature at the base of the snow cover on permafrost-free ground near the gauging station remained constantly between 0 and -1°C from November until May. From December until April temperatures varied between -3 and -4°C at the western margin and between -2 and -4°C at the eastern margin of the rock glacier. BTS temperatures were significantly lower in the central part of the rock glacier ranging between -5 and -9.3°C with only minor variations. The lowest tem-

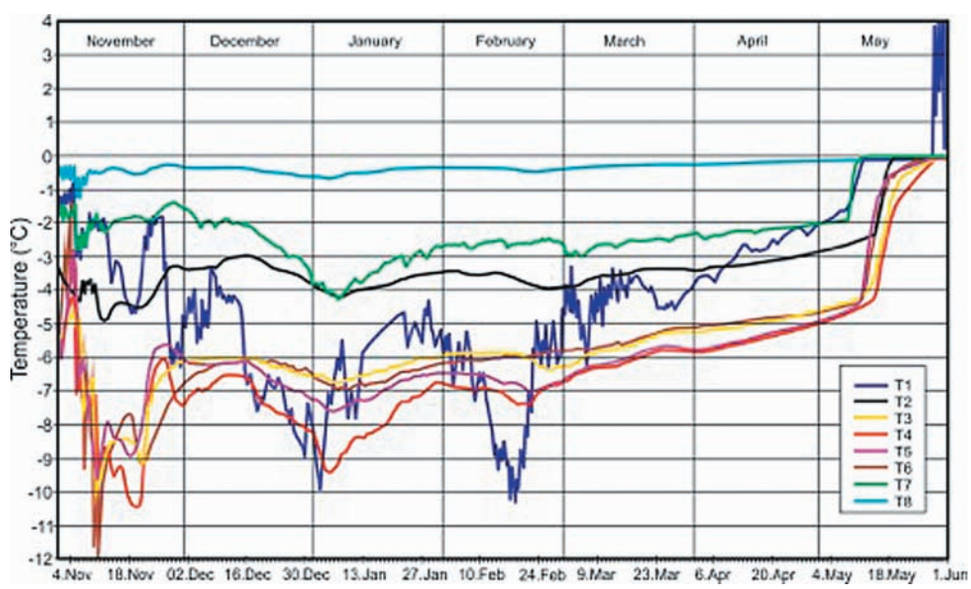

Fig. 14: Temperature at the base of the winter snow cover (BTS) on the rock glacier (T1–T7) and next to the rock glacier (T8) from November 2007 until May 2008. The locations of the temperature loggers T1–T8 are shown in the map (Fig. 8).

Abb. 14: Temperatur an der Basis der winterlichen Schneedecke (BTS) am Blockgletscher (T1–T7) und neben dem Blockgletscher (T8) von November 2007 bis Mai 2008. Die Messpunkte der Temperatursonden T1–T8 sind auf der Karte Fig. 8 dargestellt.

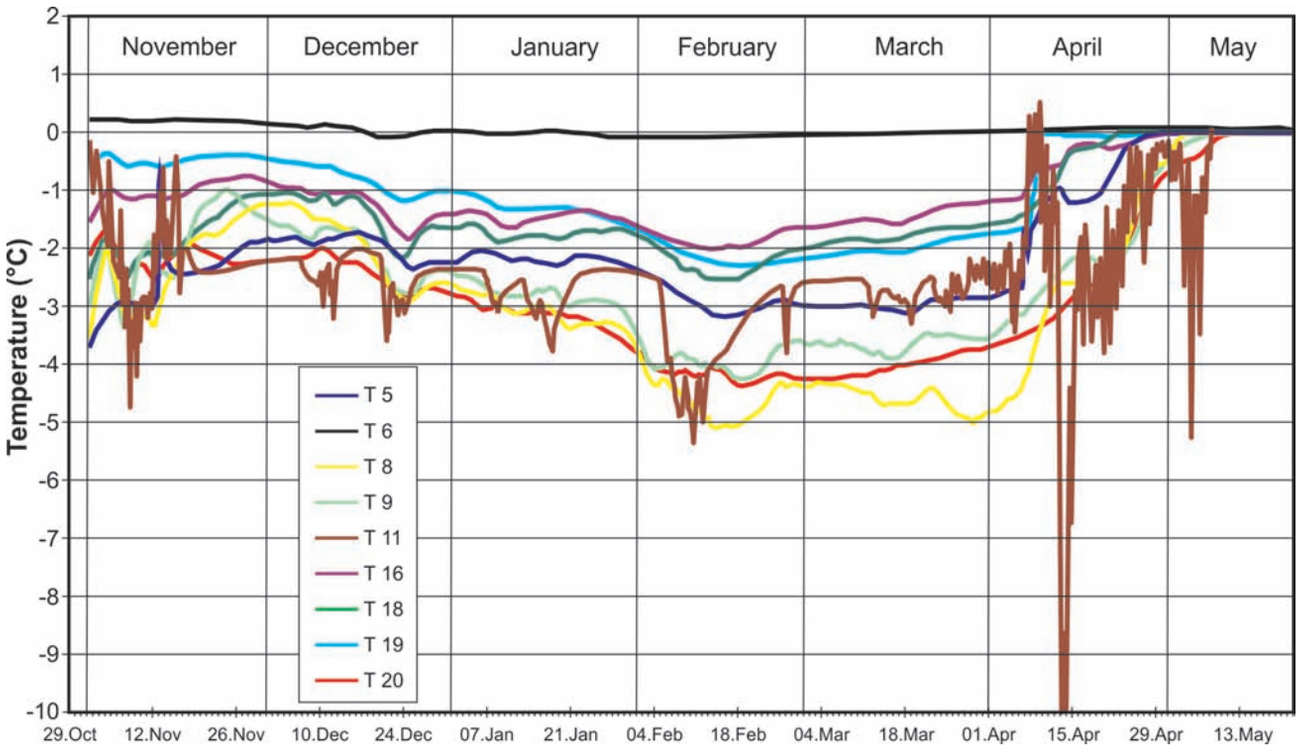

Fig. 15: Temperature at the base of the winter snow cover (BTS) on the rock glacier (T5, T8–T20) and next to the rock glacier (T 6) from November 2010 until May 2011. The location of the temperature loggers is shown in the map (Fig. 8).

Abb. 15: Temperatur an der Basis der winterlichen Schneedecke (BTS) am Blockgletscher (T5, T8–T20) und neben dem Blockgletscher (T6) von November 2010 bis Mai 2011. Die Messpunkte der Temperatursonden sind auf der Karte Fig. 8 dargestellt.

perature (-9.9°C) was observed in early January. Snowmelt started during the first half of May (Fig. 14).

During winter 2010/2011 the BTS temperature adjacent to the rock glacier, on permafrost-free ground (logger 6), was around 0°C during the entire winter (Fig. 15). On the rock glacier one logger recorded large temperature variations during winter indicating that the snow cover at this site was insufficient to prevent the infiltration of air into the debris layer of the rock glacier (Fig. 15). At all other sites no daily temperature cycles were recorded from November until May. BTS temperatures decreased from November until mid-February, when the lowest temperatures were recorded, and increased between March and April (Fig. 15). Minimum temperatures between -2 and -2.5°C were recorded by loggers 16, 18 and 19, and between -3 and -5°C by loggers 5, 8, 9, 10, 11 and 20. Snowmelt started in mid-April (Fig. 15).

Similar BTS temperature patterns were observed on other active rock glaciers in the Ötztal and Stubai Alps (Ölgrube rock glacier – Berger et al. 2004, Reichenkar rock glacier – Krainer & Mostler 2000, Sulzkar rock glacier – Krainer & Mostler 2004) and in the Schober Group (Krainer & Mostler 2001).

For the period 1938–1953 Pillewizer (1957) documented a maximum flow velocity in the upper part (profile B) of the Hochebenkar rock glacier of 75 cm/a, and 85 cm/a during the period 1953–1955. Profile 2 yielded flow velocities of 1.61 m for the period 1951–1952, 1.84 m for the period 1952–1953 and 1.53 m for the period 1953–1955 (Pillewizer 1957, Vietoris 1958).

Significantly higher annual flow velocities (average 3.9 m, maximum 6.6 m) were recorded between 1954 and 1972, whereas between 1973 and 1995 flow velocities were low (average 1.15 m, maximum 2 m). They again increased in 1995 reaching the highest values in 2004 with 1.3 m a at profile 1, then decreased and increased again since 2007 (see Nickus et al. 2014).

From 1936 to 1997 the front of the rock glacier advanced by 165 m (Schneider & Schneider 2001). According to Kaufmann (1996), the front of Hochebenkar rock glacier advanced by 148 m during the last 50 years indicating a mean flow velocity of 3 m/a^{-1} for that period. The lowermost profile 1 yielded the highest flow velocities of 3.57 m/a^{-1} (1953–1955) which increased to 5 m/a^{-1} (Vietoris 1972). Since 1995 a significant decrease in thickness was observed in the lowermost, steep part of the rock glacier.

At Hochebenkar rock glacier, ground penetrating radar measurements were performed along three profiles. The central frequency was 6.4 MHz. The signal quality was high and had a low attenuation, thus indicating that the Hochebenkar rock glacier contains a core of pure ice. The mean thickness of the rock glacier increased from 34 m along profile 1 to 44 m at profile 3 and reached an absolute maximum at profile 3 with 49 m. The shape of the underlying bedrock appeared smooth without ridges or bumps. At the margins of the rock glacier, the reflected GPR signals were affected by the surrounding rock and the thickness close to the margins was probably overestimated, particularly at the margin of profile 2 (Nickus et al. 2014).

Stop 8: Monitoring site (hydrology)

A minor amount (ca. 30 %) of meltwater is released by two springs on the eastern side of the rock glacier at an altitude of 2575 m a.s.l. About 95 m downstream a gauging station

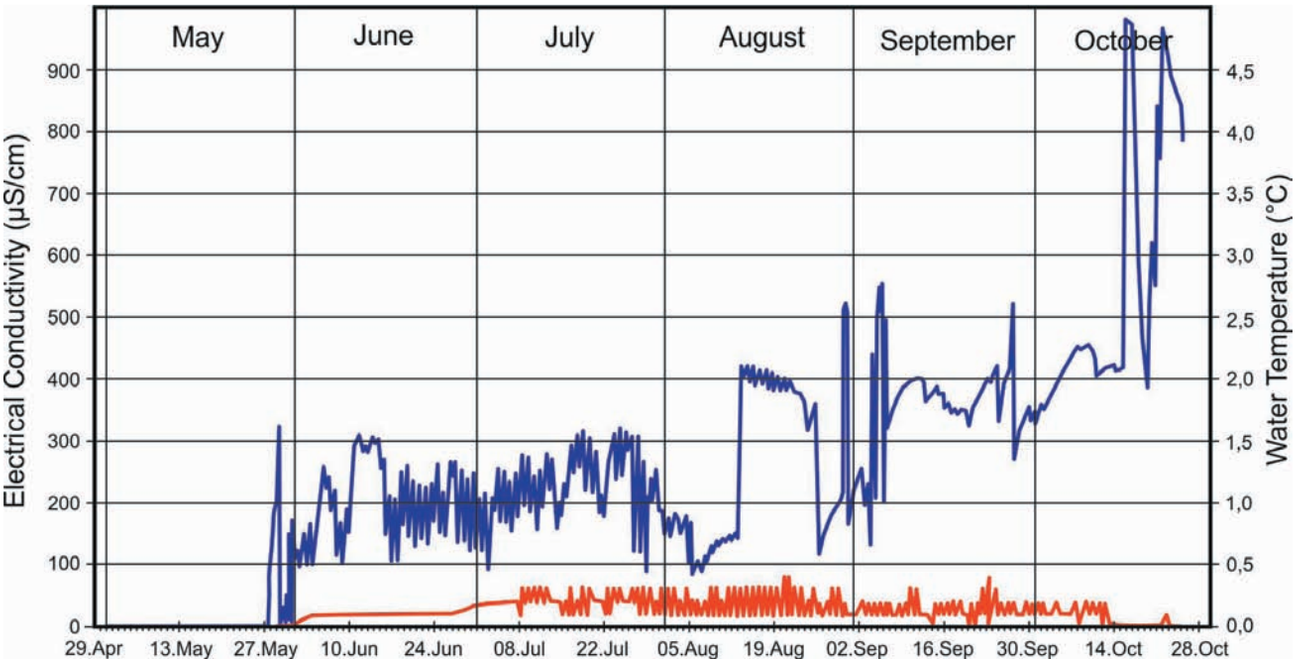

Fig. 16: Water temperature (red line, scale at right) and electrical conductivity (blue line, scale at left) of the spring released from the rock glacier at an elevation of 2575 m.

Abb. 16: Wassertemperatur (rote Linie, Skala rechts) und elektrische Leitfähigkeit (blaue Linie, Skala links) an der Blockgletscherquelle auf 2575 m Seehöhe.

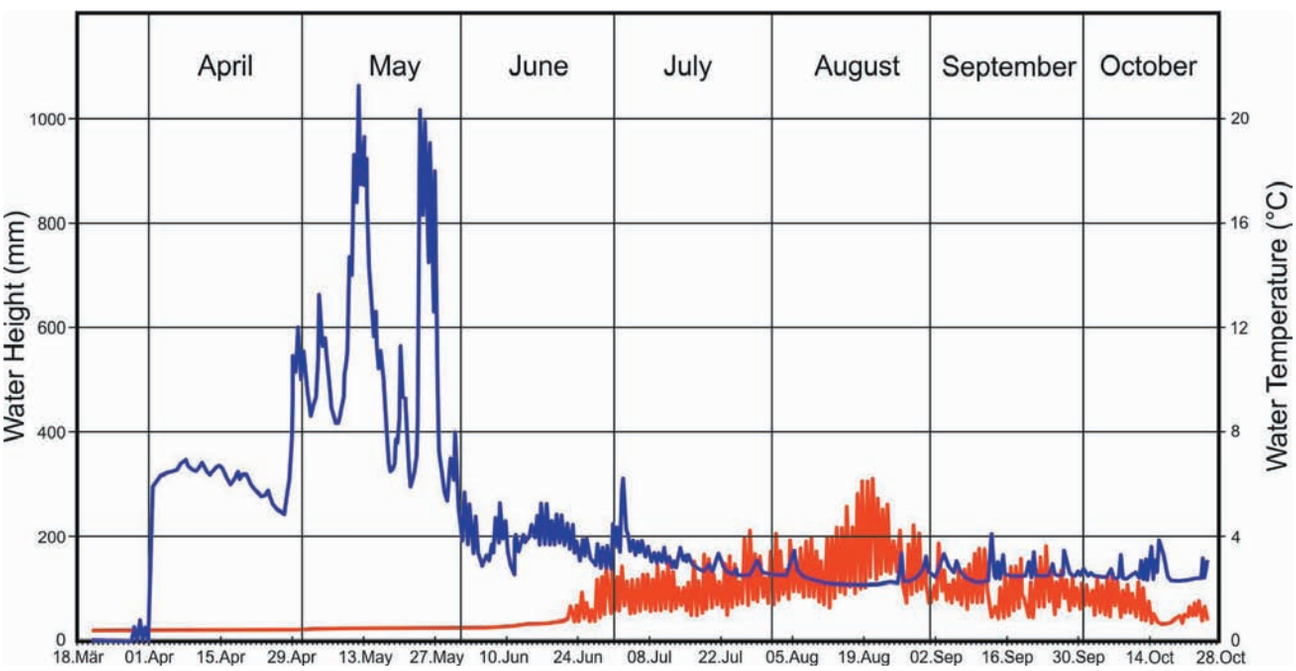

Fig. 17: Hydrograph of the meltwater stream at the gauging station at an elevation of 2555 m (blue line, scale on the left) and water temperature at the gauging station (red line, scale on the right) from April until October 2012.

Abb. 17: Pegelhöhen (blaue Linie, Skala links) und Wassertemperatur (rote Linie, Skala rechts) gemessen an der Pegelstation am Bach neben dem Blockgletscher auf einer Seehöhe von 2555 m von April bis Oktober 2012.

was installed in spring 2007 at an altitude of 2555 m a.s.l. to record the water depth versus time during the melt season. Water depth of the meltwater stream is continuously recorded by a pressure transducer at 1 hour intervals.

At the two springs on the eastern side of the rock glacier the values of electrical conductivity are significantly higher (100–200 µS/cm in June), increasing to 400 µS/cm during August and to 570 µS/cm during September. Water temperature is very low (0.2–0.4°C; Fig. 16).

The seasonal variation in electrical conductivity results from the different mixing ratio of low-mineralized precipitation and higher mineralized groundwater (Krainer & Mostler 2001, 2002, Krainer et al. 2007).

From 2007 until 2013 the monthly means of discharge at the gauging station were highest during June with ~ 100 L/s due to major snowmelt, and decreased towards September (Fig. 17). In 2010, the highest discharge was recorded between June 4 and 16, and daily mean runoff remained well

above 100 L/s during this period. A cold weather period with snow fall down to an elevation of 1900 m caused a strong decrease in discharge down to values of approximately 15 L/s. By the end of June a second snowmelt-induced peak in discharge was recorded. Heavy precipitation between August 2 and 14, with a total amount of 170 mm at the meteorological station Obergurgl, caused a pronounced peak discharge of up to 200 L/s. From mid-August onwards, daily runoff generally remained below 10 L/s interrupted by minor peaks which were caused by rainfall events.

The chemical composition of meltwater released from the Hochebenkar rock glacier has been studied since summer 2007. Electrical conductivity ranges between 100 and 200 µS/cm during major snowmelt in June and increases with decreasing runoff. In autumn, the concentration reaches its maximum, and conductivity is around 500 µS/cm. Heavy summer precipitation events generally cause a dilution of the meltwater, and runoff peaks often coincide with minima of electrical conductivity. The same is observed for sulfate, calcium and magnesium which dominate the ion content of the meltwater released at the spring at an elevation of 2575 m a.s.l and comprise more than 90 % of the ionic balance.

The seasonal course of the solute concentration reflects the varying contributions of snowmelt, precipitation events, groundwater, and melting of permafrost ice to the runoff. This supports the assumption that the high amount of solutes in late summer and fall is released by the melting of the permafrost ice within the active rock glacier. Permafrost ice meltwater seems to be particularly rich in sulfate and the relative contribution of sulfate to the total ion content of the rock glacier runoff generally rises from late spring to fall.

Discussion and conclusion

Morphology and debris properties of the active layer of the Hochebenkar rock glacier are very similar to other rock glaciers composed of debris derived from metamorphic rocks, particularly gneiss and schist (Berger et al. 2004, Krainer & Mostler 2000, 2001, 2004). Based on the grain size of the surface layer this rock glacier is a typical "boulder rock glacier" according to Ikeda & Matsuoka (2006). Temperatures at the base of the winter snowpack (BTS) are typical for active rock glaciers and similar to those recorded from other active rock glaciers in the Austrian Alps (Berger et al. 2004; Krainer & Mostler 2000, 2001, 2004). The pronounced seasonal and diurnal variations in discharge are strongly controlled by the weather conditions. Water released at the rock glacier springs is mainly derived from snowmelt and summer rainfall, and subordinately from melting of permafrost ice and groundwater. Flood peaks are caused by intense snowmelt on warm, sunny days during late spring and early summer, and by rainfall events. The water temperature of the rock glacier springs remains permanently below 1.5°C, mostly below 1°C, and indicates that the water flowing through the rock glacier is in direct contact with permafrost ice (Krainer & Mostler 2002, Krainer et al. 2007). Extremely high values of electrical conductivity at the spring on the eastern side of the rock glacier indicate a much longer residence time of the water compared to the water released at the springs at the steep front which is characterised by very low values indicating that the residence time is short and that the water is derived from melting of ice and snow, and rainfall.

The depression in the rooting zone and the pronounced decrease in thickness in the lowermost part during the last years indicate melting of massive ice and we suggest that Hochebenkar rock glacier has a glacial origin similar to Reichenkar rock glacier (Krainer & Mostler 2000, Krainer et al. 2002, Hausmann et al. 2007, 2012). High ice content is also indicated by annual flow velocities which are significantly higher than those of most other active rock glaciers which show typical values of 0.1–1 m. Schneider & Schneider (2001) showed that flow velocity correlates with mean annual air temperature. Higher flow rates during warmer periods are probably caused by higher amounts of meltwater within the rock glacier and near the base, and probably also by slightly higher ice temperatures.

Hochebenkar rock glacier most likely developed from a debris-covered cirque glacier due to the inefficient sediment transfer from the glacier ice to the meltwater; a model proposed by Shroder et al. (2000) based on studies in the Nanga Parbat Himalaya.

Acknowledgements

I am grateful to the Hydrographic Service (Hydrographischer Dienst) of the Federal Government of Tyrol for providing data from the gauging station near Gurgler Alm and Jakob Abermann (Innsbruck) for providing the photo of Hochebenkar rock glacier (Fig. 9). This excursion guide benefited greatly from the constructive comments and suggestions provided by Christoph Spötl (Innsbruck).

References

Barsch, D. (1996): Rockglaciers: Indicators for the Present and Former Geoecology in High Mountain Environments. – Springer-Verlag, Berlin, 331 p.

Barsch, D., Fierz, H. & Haeberli, W. (1979): Shallow core drilling and borehole measurements in permafrost of an active rock glacier near the Grubengletscher, Wallis, Swiss Alps. – Arctic and Alpine Research, 11: 215–228.

Berger, J., Krainer, K. & Mostler, W. (2004): Dynamics of an active rock glacier (Ötztal Alps, Austria). – Quaternary Research, 62: 233–242.

Bortenschlager, S. (1984): Beiträge zur Vegetationsgeschichte Tirols I. Inneres Ötztal und Unteres Inntal. – Ber. nat.-med. Ver. Innsbruck, 71: 19–56.

Bortenschlager, S. (2010): Vegetationsgeschichte im Bereich des Rotmoostales. – In: Koch, E.M. & Erschbamer, B. (eds), Glaziale und periglaziale Lebensräume im Raum Obergurgl. – Innsbruck University Press, 77–91

Eyles, C.H. & Eyles, N. (2010): Glacial Deposits. – In: James, N.P & Dalrymple, R.W. (eds), Facies Models 4. – Geological Association of Canada, 73–104.

Figl, T. (2004): Die Quartärgeologie des hinteren Sulztales in den westlichen Stubaier Alpen (Tirol) unter besonderer Berücksichtigung der Blockgletscher. – Unpublished Diploma thesis, Univ. Innsbruck.

Fischer, A. (2013): Long term monitoring of glacier mass balance and length changes in Tyrol as a base for glacier foreland succession studies. – Plant Ecology and Diversity, 6, 537–547,

Folk, R.L. & Ward, W.C., (1957): Brazos River Bar: A study in the significance of grain size parameters. – Journal

of Sedimentary Petrology, 27: 3–26.
Gams, H. (1962): Das Gurgler Rotmoos und seine Stellung innerhalb der Gebirgsmoose. – Veröff. Geobot. Inst. E.T.H. Stift. Rübel, Festschr. Franz Firbas. Zürich 37: 74–82.
Giardino, J.R. & Vick, S.G. (1987): Geologic engineering aspects of rock glaciers. – In: Giardino, J.R., Shroder, J.F. & Vick, J.D. (eds), Rock Glaciers. – Allen & Unwin, London, p. 265–287.
Haeberli, W. (1985): Creep of mountain permafrost: Internal structures and flow of alpine rock glaciers. – Mitteilungen der Versuchsanstalt für Wasserbau, Hydrologie und Glaziologie ETH Zürich, 77: 1–142.
Haeberli, W. (1990): Scientific, environmental and climatic significance of rock glaciers. – Memorie della Societá Geologica Italiana, 45: 823–831.
Haeberli, W. & Patzelt, G. (1982): Permafrostkartierung im Gebiet der Hochebenkar-Blockgletscher, Obergurgl, Ötztaler Alpen. – Zeitschrift für Gletscherkunde und Glazialgeologie, 18(2): 127–150.
Haeberli, W., Hallet, B., Arenson, L., Elconin, R., Humlum, O., Kääb, A., Kaufmann, V., Ladanyi, B., Matsuoka, N., Springman, S., & Vonder Mühll, D. (2006): Permafrost Creep and Rock Glacier Dynamics. – Permafrost and Periglacial Processes, 17: 189–214.
Hantke, R. (1983): Eiszeitalter, Band 3: Die jüngste Erdgeschichte der Schweiz und ihrer Nachbargebiete (Westliche Ostalpen mit ihrem bayerischen Vorland bis zum Inn-Durchbruch und Südalpen zwischen Dolomiten und Mont Blanc). – Ott Verlag Thun, 730 p.
Hausmann, H., Krainer, K., Brückl, E. & Mostler, W. (2007): Internal Structure and Ice Content of Reichenkar Rock Glacier (Stubai Alps, Austria) Assessed by Geophysical Investigations. – Permafrost and Periglacial Processes, 18: 351–367.
Hausmann, H., Krainer, K., Brückl, E. & Ullrich, C. (2012): Internal structure, ice content and dynamics of Ölgrube and Kaiserberg rock glaciers (Ötztal Alps, Austria) determined from geophysical surveys. – Austrian Journal of Earth Sciences, 105/2: 12–31.
Hoinkes, G. & Thöni, M. (1993): Evolution of the Ötztal-Stubai, Scarl-Campo and Ulten Basement Units. – In: Raumer, von J.F. & Neubauer, F. (Eds.), Pre-Mesozoic Geology in the Alps. – Springer, Berlin, 485–494.
Ikeda, A. & Matsuoka, N. (2006): Pebbly versus boulder rock glaciers: Morphology, structure and processes. – Geomorphology, 73: 279–296.
Kääb, A. (2007): Rock Glaciers and Protalus Forms. – In: Scott A. Elias (ed.), Encyclopedia of Quaternary Sciences. – Elsevier, p. 2236–2242.
Kaufmann, V. (1996a): Der Dösener Blockgletscher – Studienkarten und Bewegungsmessungen. – Arb. Inst. Geogr. Univ. Graz, 33: 141–162.
Kaufmann, V. (1996b): Geomorphometric monitoring of active rock glaciers in the Austrian Alps. – 4th International Symposium on High Mountain Remote Sensing Cartography. Karlstad – Kiruna – Tromso, August 19–29, 1996: 97–113.
Kaufmann, V. (2012): The evolution of rock glacier monitoring using terrestrial photogrammetry: the example of Äusseres Hochebenkar rock glacier (Austria). – Austrian Journal of Earth Sciences, 105/2: 63–77.
Kaufmann, V. & Ladstätter, R. (2002): Spatio-temporal analysis of the dynamic behaviour of the Hochebenkar rock glaciers (Oetztal Alps, Austria) by means of digital photogrammetric methods. – Grazer Schriften der Geographie und Raumforschung, 37: 119–140.
Kaufmann, V. & Ladstätter, R. (2003): Quantitative analysis of rock glacier creep by means of digital photogrammetry using multi-temporal aerial photographs: two case studies in the Austrian Alps. – In: Phillips, M., Springman, S.M. & Arenson, L.U. (eds), Proceedings of the 8th International Conference on Permafrost, 21–25 July 2003, Zürich, Switzerland, 1: 525–530.
Kellerer-Pirklbauer, A. (2005): Alpine permafrost occurrence at its spatial limits: First results from the eastern margin of the European Alps, Austria. Norsk Geografisk Tidsskrift – Norwegian Journal of Geography, 59: 184–193.
Kellerer-Pirklbauer, A. (2007): Lithology and the distribution of rock glaciers: Niedere Tauern Range, Styria, Austria. – Z. Gemorph. N.F., 51/2, 17–38.
Kellerer-Pirklbauer, A., (2008a): The Schmidt-hammer as a Relative Age Dating Tool for Rock Glacier Surfaces: Examples from Northern and Central Europe. – Proceedings of the Ninth International Conference on Permafrost (NICOP), University of Alaska, Fairbanks, June 29 – July 3, 2008, 913–918.
Kellerer-Pirklbauer, A., (2008b): Surface ice and snow disappearance in alpine cirques and its possible significance for rock glacier formation: some observations from central Austria. – In: Kane, D.L. & Hinkel, K.M. (eds.), Extended Abstracts of the Ninth International Conference on Permafrost (NICOP), University of Alaska, Fairbanks, USA, pp. 129–130.
Kellerer-Pirklbauer A., (2009): Wie alt sind Blockgletscher in den Österreichischen Alpen? Das Beispiel der Blockgletscher im Dösener Tal, Ankogelgruppe, datiert mit Hilfe der Schmidt-Hammer Methode. – In: Schmidt, R., Matulla, C. & Psenner, R. (eds.), Klimawandel in Österreich. Die letzten 20.000 Jahre … und ein Blick voraus. – 65-76, Innsbruck (Innsbruck Univ. Press).
Keuschnig, C., Krainer, K. & Erschbamer, B. (2007): Bodenstruktur, Temperaturen und Vegetation von Bültenböden am Peischlachtörl (nördliche Schobergruppe, Nationalpark Hohe Tauern, Österreich). – Tuexenia, 27: 343–361.
Konzett, J., Hoinkes, G. & Tropper, P. (2003): 5th Workshop of Alpine Geological Studies, Field Trip Guide E4: Alpine metamorphism in the Schneeberg Complex and neighbouring units (immediate vicinity of Obergurgl). – Geologisch-Paläontologische Mitteilungen Innsbruck 26: 21–45.
Krainer, K. & Mostler, W. (2000): Reichenkar Rock Glacier: a Glacier Derived Debris-Ice System in the Western Stubai Alps, Austria. – Permafrost and Periglacial Processes, 11: 267–275.
Krainer, K. & Mostler, W. (2001): Der aktive Blockgletscher im Hinteren Langtal Kar, Gößnitztal (Schobergruppe, Nationalpark Hohe Tauern, Österreich). – Wiss. Mitt. Nationalpark Hohe Tauern, 6: 139–168.
Krainer, K. & Mostler, W. (2002): Hydrology of Active Rock Glaciers: Examples from the Austrian Alps. –

Arctic, Antarctic, and Alpine Research, 34: 142–149.
Krainer, K. & Mostler, W. (2004): Aufbau und Entstehung des aktiven Blockgletschers im Sulzkar, westliche Stubaier Alpen. – Geo.Alp, 1: 37–55.
Krainer, K. & Mostler, W. (2006): Flow Velocities of Active Rock Glaciers in the Austrian Alps. – Geografiska Annaler, 88A: 267–280.
Krainer, K. & Ribis, M. (2012): A Rock Glacier Inventory of the Tyrolean Alps (Austria). – Austrian Journal of Earth Sciences, 105/2: 32–47.
Krainer, K. & Spieler, A. (1999): The sedimentary record of ice-dammed lakes in the Ötztal Alps (Austria). – Zeitschrift für Gletscherkunde und Glazialgeologie, 35(1): 65–86.
Krainer, K., Mostler, W. & Span, N. (2002): A glacier-derived, ice-cored rock glacier in the Western Stubai Alps (Austria): Evidence from ice exposures and ground penetrating radar investigation. – Zeitschrift für Gletscherkunde und Glazialgeologie, 38: 21–34.
Krainer, K., Mostler, W. & Spötl, C. (2007): Discharge from active rock glaciers, Austrian Alps: a stable isotope approach. – Austrian Journal of Earth Sciences, 100: 102–112.
Ladstätter, R. & Kaufmann, V. (2005): Studying the movement of the Outer Hochebenkar rock glacier: Aerial vs. ground-based photogrammetric methods. – 2nd European Conference on Permafrost, Potsdam, Germany, Terra Nostra 2005(2): 97.
Lieb, G.K. (1986): Die Blockgletscher der östlichen Schobergruppe (Hohe Tauern, Kärnten). – Arb. Inst. Geogr. Univ. Graz, 27: 123–132.
Lieb, G.K. (1987): Zur spätglazialen Gletscher- und Blockgletschergeschichte im Vergleich zwischen den Hohen und Niederen Tauern. – Mitt. Österr. Geogr. Ges., 129: 5–27.
Lieb, G.K. (1991): Die horizontale und vertikale Verteilung der Blockgletscher in den Hohen Tauern (Österreich). – Z. Geomorph. N.F., 35: 345–365.
Lieb, G.K. (1996): Permafrost und Blockgletscher in den östlichen österreichischen Alpen. – Arb. Inst. Geogr. Univ. Graz, 33: 9–125.
Lieb, G.K. & Slupetzky, H. (1993): Der Tauernfleck-Blockgletscher im Hollersbachtal (Venedigergruppe, Salzburg, Österreich). – Wiss. Mitt. Nationalpark Hohe Tauern, 1: 138–146.
Menzies, J, & Shilts, W.W. (1996): Subglacial Environments. – In: Menzies, J. (ed.), Past Glacial Environments: Sediments, Formas and Techniques. Butterworth-Heinemann Ltd., Oxford, U.K., p. 15–136.
Nickus, U., Abermann, J., Fischer, A., Krainer, K., Schneider, H., Span, N. & Thies, H. (2014): Rock Glacier Äußeres Hochebenkar (Austria) – Recent results of a monitoring network. – Zeitschrift für Gletscherkunde und Glazialgeologie (in press).
Nickus, U., Kuhn, M., Baltensperger, U., Delmas, R., Gäggeler, H., Kasper, A., Kromp-Kolb, H., Maupetit, F., Novo, A., Pichlmayer, F., Preunkert, S., Puxbaum, H., Rossi, G., Schöner, W., Schwikowski, M., Seibert, P., Staudinger, M., Trockner, V., Wagenbach, D. & Winiwarter, W. 1997: SNOSP: Ion deposition and concentration in high alpine snow packs. – Tellus, 49B(1): 56–71.
Patzelt, G. (1973): Die neuzeitlichen Gletscherschwankungen in der Venedigergruppe (Hohe Tauern, Ostalpen). – Zeitschrift für Gletscherkunde und Glazialgeologie, 9: 5–57.
Patzelt, G. (mit Beiträgen von S. Bortenschlager & G. Poscher) (1996): Exkursion A1 Tirol: Ötztal – Inntal (Exkursionsführer), DEUQUA 1996, Gmunden/Oberösterreich, p. 1–23.
Pillewizer, W. (1938): Photogrammetrische Gletscheruntersuchungen im Sommer 1938. – Zeitschrift der Gesellschaft für Erdkunde, 1938(9/19), 367–372.
Pillewizer, W. (1957): Untersuchungen an Blockströmen der Ötztaler Alpen. – Geomorphologische Abhandlungen des Geographischen Institutes der FU Berlin (Otto-Maull-Festschrift), 5: 37–50.
Rybnicek, K. & Rybnickova, E. (1977): Mooruntersuchungen im Oberen Gurgltal, Ötztalere Alpen. – Folia Geobot. Phytotax., 12: 245–291.
Schneider, B. & Schneider, H. (2001): Zur 60jährigen Messreihe der kurzfristigen Geschwindigkeitsschwankungen am Blockgletscher im Äusseren Hochebenkar, Ötztaler Alpen, Tirol. – Zeitschrift für Gletscherkunde und Glazialgeologie, 37(1): 1–33.
Shroder, J.F., Bishop, M.P., Copland, L. & Sloan, V.F. (2000): Debris-covered glaciers and rock glaciers in the Nanga Parbat Himalaya, Pakistan. – Geografiska Annaler, 82: 17–31.
Thöny, W.E., Tropper, P., Schennach, F., Krenn, E., Finger, F., Kaindl, R., Bernhard, F. & Hoinkes, G. (2008): The metamorphic evolution of migmatites from the Ötztal Complex (Tyrol, Austria) and constraints on the timing of the pre-Variscan high-T event in the Eastern Alps. – Swiss Journal of Geosciences, 101, Supplement 1: 111–126.
Tropper, P. & Recheis, A. (2003): Garnet zoning as a window into the metamorphic evolution of a crystalline complex: the northern and central Austroalpine Ötztal-Complex as a polymorphic example. – Mitteilungen der Österreichischen Geologischen Gesellschaft, 94: 27–53.
Tropper, P., Krenn, K. & Hoinkes, G. (2012): Mineralogie und Petrologie des austroalpinen Kristallins in der südlichen Umgebung von Obergurgl. – In: Koch, E.M. & Erschbamer, B. (eds), An den Grenzen des Waldes und der menschlichen Siedlungen. – Innsbruck University Press, 181–209.
Vietoris, L. (1958): Der Blockgletscher des äußeren Hochebenkares. – Gurgler Berichte, 1: 41–45.
Vietoris, L. (1972): Über die Blockgletscher des Äußeren Hochebenkars. – Zeitschrift für Gletscherkunde und Glazialgeologie, 8: 169–188.
Vitek, J.D. & Giardino, J.R. (1987): Rock glaciers: a review of the knowledge base. – In: Giardino, J.R., Shroder, J.F. & Vitek, J.D. (eds), Rock Glaciers. – p. 1–26, Allen & Unwin, London.
Whalley, W.B. & Martin, H.E. (1992): Rock glaciers: II models and mechanism. – Progress in Physical Geography, 16: 127–186.
Washburn, A.L. (1979): Geocryology. A Survey of Periglacial Processes and Environments. – 406 pp., London, Edward Arnold.

Lateglacial and Holocene advance record of the Gepatschferner, Kaunertal, Tyrol

Spätglaziale und holozäne Vorstöße des Gepatschferners, Kaunertal, Tirol

Kurt Nicolussi, Hanns Kerschner

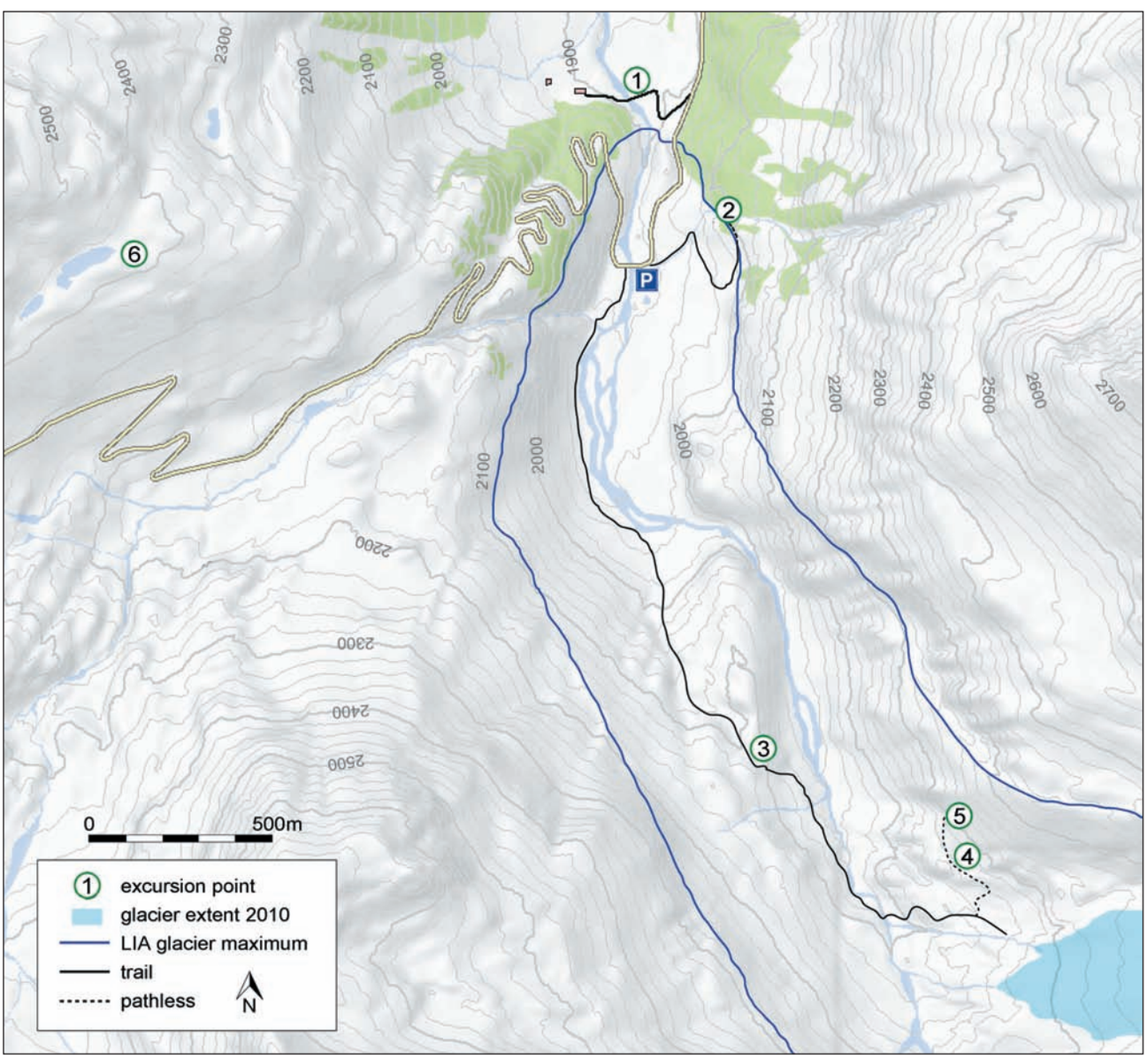

Fig. 1: Overview of route and stops of the excursion. Base map ©Land Tirol – tiris.

Abb. 1: Überblick über Exkursionsroute und Haltepunkte. Grundkarte ©Land Tirol – tiris.

1 Introduction

The Gepatschferner, located just north of the main Alpine ridge in the Kaunertal, is the largest glacier in Tyrol with a length of 7.4 km in the year of 2013 and an area of ca. 16.6 km^2 in the year of 2006 (Hartl 2010). After having reached its last Little Ice Age (LIA) maximum position in 1856 the glacier has been generally retreating. This retreat was interrupted by two minor re-advances around 1920/21 and between 1977 and 1988. During its LIA maximum positions, Gepatschferner terminated near Gepatschalpe at 1890 m a.s.l.

The Lateglacial and most of all the Holocene evolution of this glacier has been in-depth analysed (Kerschner 1979, Nicolussi & Patzelt 2001). The analysis is based on well preserved lateglacial moraines, e.g. on the slopes to the west of Gepatschalpe but most of all on subrecent trees, subfossil logs from the Neoglacial and on a mid-Holocene soil profile. Based on a Holocene tree-ring chronology (Nicolussi et al. 2009) most of the analysed wood samples have been calendarically dated. As a consequence, Gepatschferner's Holocene advance record is one of the most detailed and accurately dated glacier records in the Alps. The route of this excursion leads to several key points contributing to the establishment of the Holocene record, and to a site with well-preserved Lateglacial moraines (Fig. 1).

All radiocarbon dates mentioned in the text were calibrated with OXCAL 3.1 using the IntCal13 calibration data set (Reimer et al. 2013) and a 2 sigma calibration range.

2 Excursion route

Stop 1: Terminal position of Gepatschferner in the mid 19th century

This point is located near a bridge over Falgin Bach and can be reached by leaving the Kaunertal glacier road south of the "Gepatschhaus" and following the gravel road towards "Gepatschalpe" (Fig. 1).

The glacier situation in 1856 at this site is documented by a sketch (Fig. 3) published by Carl Sonklar (1860). It shows the glacier just at its LIA maximum position or at the beginning of the following retreat that continues to last – with two interruptions – until today (Fig. 2). An ongoing advance can be excluded because of the trees visible in the sketch between the main and the tributary terminus of the Gepatschferner: These trees continued to grow even after 1856. The former ice covered area can easily be recognized because of the distinct difference in soil and vegetation cover in the area just south of the bridge. At the left side of the creek an accumulation of blocks indicates the LIA maximum position of the glacier. Lichen measurements at the very end of the glacier forefield prove that the 1855/56 position was indeed the LIA maximum extent of Gepatschferner (Nicolussi & Patzelt 2001).

Stop 2: The 1680 maximum extent of Gepatschferner

This stop can be reached by walking back to the Kaunertal glacier road, following it in southerly direction until a trail leaves the street on the left side. The footpath leads first in southerly direction and then turns to the north. The route follows the trail until it reaches a small LIA lateral moraine and continues pathless to a small group of trees (Fig. 1).

At this site the extent of the LIA glacier forefield is indicated by a double-walled moraine. The inner wall can be assigned to the mid-19th century maximum extent. The outer one dates to the late 17th century: This is, among others, based on a dendrochronological date established for a cembran pine (*Pinus cembra*) log (GP-1996, Fig. 4) which is preserved in the small group of trees at this site. The tree was killed during the late 17th century advance and is part-

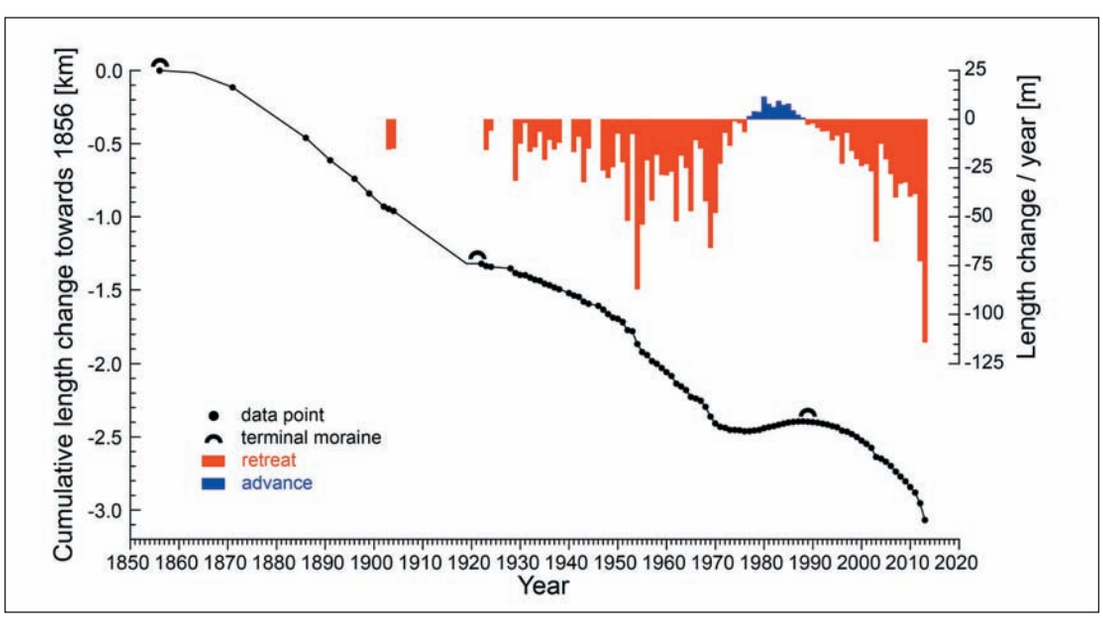

Fig. 2: Cumulated length change of the Gepatschferner terminus between 1856 and 2013 based on moraines, maps and yearly length change measurements. Annually resolved length change data are displayed separately. The cumulated retreat accounts for more than 3 km. It was interrupted by two readvances, ca. 1920/21 and between 1977 and 1988.

Abb. 2: Kumulierte Längenänderung des Gepatschferners zwischen 1856 und 2013 nach Moränenständen, Kartenaufnahmen und Messungen der Längenänderung. Jährlich aufgelöste Längenänderungsdaten sind zusätzlich dargestellt. Der kumulierte Rückzug beträgt mehr als 3 km, er wurde durch zwei Vorstöße um ca. 1920/21 und zwischen 1977 und 1988 unterbrochen.

Fig. 3: "Thor des Gepatschferners im Herbst 1856" / Glacier mouth of Gepatschferner in autumn 1856 (Sonklar 1860). The sketch shows the glacier just reaching or shortly after reaching the LIA maximum extent.

Abb. 3: „Thor des Gepatschferners im Herbst 1856" (Sonklar 1860). Die Skizze zeigt den Gletscher beim oder kurz nach dem Erreichen des Maximalstandes der „Kleinen Eiszeit".

ly covered by the moraine wall. The terminal ring (waney edge with bark) dates the killing of the tree to the summer of 1679. Tree-ring analysis of a further cembran pine log (GP-189, Fig. 4) found nearby on the moraine top yielded a killing date of summer 1680. Further cembran pine remnants found at nearby sections of the moraine wall gave similar or somewhat earlier dates for the outermost rings. However, no waney edges are preserved at these logs (Fig. 4, Nicolussi & Patzelt 2001). With these dendro-dates it can be proven that the LIA maximum extent of Gepatschferner was in 1679/80 as large as or – at some parts of the glacier forefield – slightly larger than the 1855/56 LIA maximum.

Further advances and extents of this glacier, which remained somewhat smaller than the two LIA maxima, can be derived from tree-ring patterns of cembran pines that grew or still grow just outside the glacier forefield. An advancing glacier can damage trees without necessarily killing them and change the climatic site conditions resulting in growth reductions. Such sections of small rings were observed for the years around 1855 where a glacier maximum is proven but also for ca. 1835/40: A glacier advance in these years, that remained somewhat smaller than the following 1855/56 maximum can be assumed to be a consequence of the exceptional climatic conditions in the first decades of the 19th century (Nicolussi & Patzelt 2001). A similar situation – an advance of Gepatschferner to an extent somewhat smaller than the LIA maximum extents – can be assumed for the years around 1630. However, the evidence is less clear and based on few trees. A further LIA advance is evidenced by drawings and aquarelle paintings by Franz Ferdinand Runk, who visited Kaunertal between 1801 and 1805. The pictures show an advancing glacier terminus located ca. 180 m behind the LIA maximum extent. This advance probably stopped soon after Runk's visit (Nicolussi & Patzelt 2001).

Stop 3: Overview of the orographic right lateral moraine of the Gepatschferner

To reach the stop the route guides back to the street, crosses the bridge, turns left and follows the trail into the glacier forefield at the orographic left side of the valley. This trail is first flat and rises afterwards. The stop is at the roches moutonnées just beside the point where the trail starts to lead down to the glacier creek (Falgin Bach).

The eastern side of this section of the glacier forefield is dominated by a huge lateral moraine, which is subdivided by several steep bedrock outcrops (Fig. 5). The moraine was built by several advances of Gepatschferner during the last four millennia, but mainly during the LIA. This can be shown by the analysis of several tree remnants that were embedded into till during these advances and preserved (Nicolussi & Patzelt 2001). Today these tree remnants are uncovered by erosion. The finds are partly in situ, i.e. rooted trunks or tree remnants lying on fossil soils, embedded in till or already repositioned by erosion, i.e. detrital logs.

Findings from the outermost section of the lateral moraine, called profile 1 (Fig. 5), enable the medieval advance history to be reconstructed: the oldest tree remnants, i.e. detrital logs, date back to the early 6th century. However, no clear evidence for the late 6th century AD advance (Holzhauser et al. 2005) is available up to now. In situ tree remnants prove an advance in AD 809 with a glacier surface comparable to the ice level around AD 1920. Further logs date an advance to the mid-12th century and hence into the medieval climate anomaly. The earliest LIA glacier advance is documented by an embedded log with the killing date of AD 1284. The related ice thickness is comparable to the glacier surface level in the late 19th century, ca. 1870. A similar ice thickness was reached by the Gepatschferner during a further advance in or shortly after AD 1462.

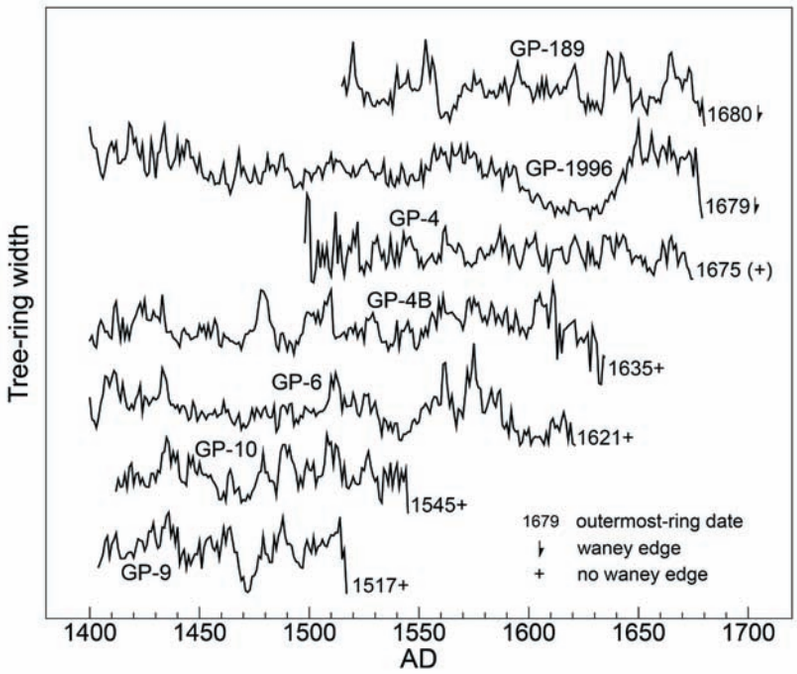

Fig. 4: Standardized tree-ring series of subrecent logs killed during the 17th century advances of the Gepatschferner. Two logs, GP-1996 and GP-189, have preserved waney edges and the dates noted are killing dates. The last-ring date established for the weathered log GP-4 is close to its killing date. These logs prove a LIA maximum extent of the Gepatschferner in 1679/80. The other logs have missing outer parts, therefore the dates presented for the outermost rings are termini post quem for the 17th century glacier advances (Nicolussi & Patzelt 2001, supplemented).

Abb. 4: Standardisierte Jahresringreihen von subrezenten Stämmen, die während der Vorstöße des Gepatscherferners im 17. Jahrhundert überfahren wurden. Bei zwei Hölzern, GP-1996 und GP-189, blieb jeweils die Waldkante erhalten und die angegebenen Jahreszahlen sind die Absterbealter. Diese Stämme belegen einen LIA Maximalstand des Gepatschferners in den Jahren 1679/80. Bei den anderen Stämmen fehlen die äußeren Holzbereiche, daher sind die angeführten Endjahre für die äußersten Jahresringe termini post quem für die Gletschervorstöße des 17. Jahrhunderts (Nicolussi & Patzelt 2001, ergänzt).

Stop 4: Profile 2 – evidence for glacier advances from the 2nd millennium BC to the Roman Period

This excursion point can be accessed by following the trail down to the Falgin Bach, crossing the bridge and walking up to an elevation of ca. 2140 m a.s.l. The route leaves the path, turns towards Northeast and ends at a rocky knoll at ca. 2160 m a.s.l. below the steep lateral moraine.

At this section of the lateral moraine, named profile 2, erosion exposed tree remnants up to an elevation of ca. 2275 m a.s.l. These finds prove several Neoglacial advances from the 17th century BC to the 4th century AD (Nicolussi & Patzelt 2001, Nicolussi 2009). The Löbben advance period (Patzelt & Bortenschlager 1973) is characterised at the Gepatschferner by two advances both dated with in situ or still partly embedded logs (Fig. 6). A first advance reached an ice thickness comparable to the glacier surface height of ca. AD 1930 and culminated just after 1626 BC, a second advance exceeded this glacier level shortly after 1555 BC. The following advance period occurred in the early 12th century (after 1195 BC), however, it is only dated by detrital samples. A first advance during the Göschenen I period occurred around or shortly after 712 BC, a second one is proven for the years around 635 BC. During the latter one the Gepatschferner reached at least an ice thickness comparable to ca. AD 1930. A retreat period in the second half of the Iron Age was followed by another glacier advance that occurred approximately in the first century BC based on ra-

Fig. 5: Overview of the right lateral moraine of Gepatschferner and the 2010 terminus position. The numbers indicate areas (profiles) with finds utilized for the analysis of the Neoglacial advances (profiles 1 and 2: excursion stops 3 and 4) and mid-Holocene variability (profile 3: stop 5) of Gepatschferner (photo K. Nicolussi, 26.8.2010).

Abb. 5: Überblick über die rechte Ufermoräne des Gepatschferners und die Gletscherzunge im Jahr 2010. Die Zahlen bezeichnen die Areale (Profile) mit Funden, die zur Rekonstruktion der neoglazialen Vorstöße (Profile 1 und 2: Exkursionshalte 3 und 4) und der Gletscherschwankungen des Gepatschferners im mittleren Holozän (Profil 3: Exkursionshalt 5) verwendet wurden (Aufnahme K. Nicolussi, 26.8.2010).

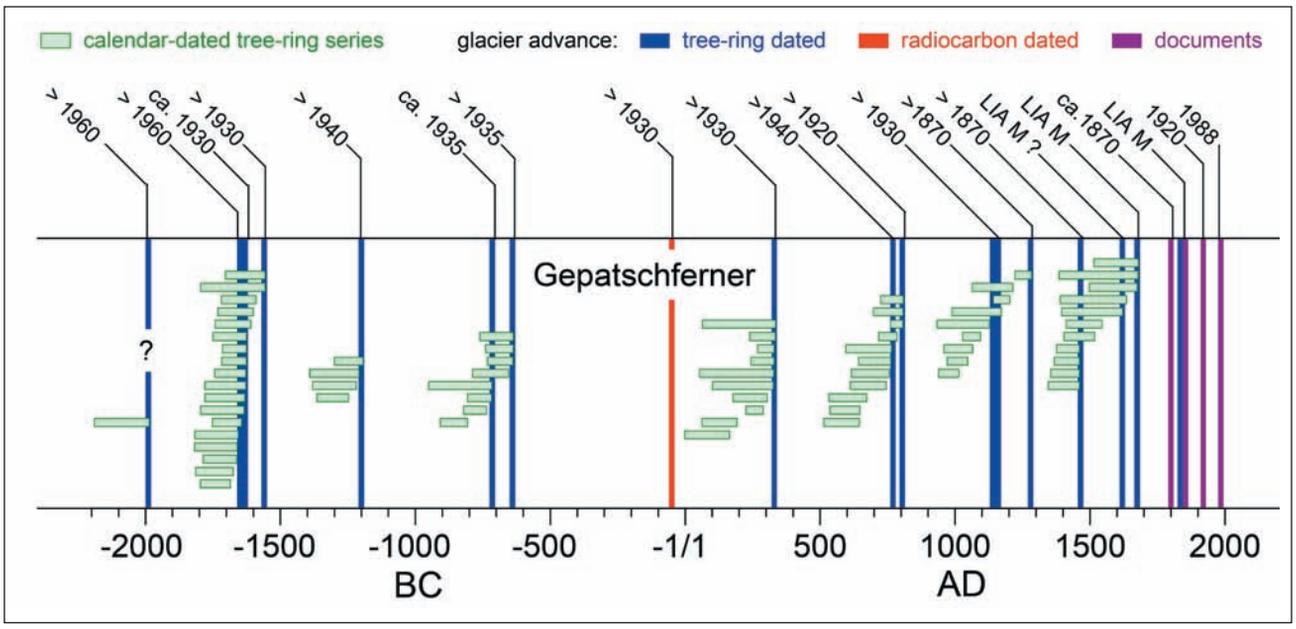

Fig. 6: The Neoglacial advance record of Gepatschferner. The establishment and dating of the advances are based on the different methodical approaches. Extents or minimum extents reached during these advances are indicated in relation to known extents and ice levels during the last ca. 160 years. "LIA M": Little Ice Age maximum extent; ">": advance beyond an extent as it is documented or deduced for the given year (Nicolussi 2009, supplemented).

Abb. 6: Die Vorstöße des Gepatschferners während des Neoglazials. Bestimmung und Datierung der Vorstöße bauen auf verschiedenen methodischen Zugängen auf. Die End- oder Mindestausdehnungen während dieser Vorstöße sind in Bezug auf bekannte Gletscherausdehnungen und Eishöhen während der letzten 160 Jahre angegeben. „LIA M": Maximalstand während der Kleinen Eiszeit; „>": Vorstoß über eine Ausdehnung hinaus, die für das angegebene Jahr dokumentiert oder hergeleitet ist (Nicolussi 2009, ergänzt).

diocarbon dating (Patzelt 1995; sample GP-3, 2020±50 BP, 210 cal BC – 130 cal AD). The last advance period detected at profile 2 can be dated to around AD 335. This advance terminated the several centuries long Roman glacier retreat period. Evidence for this advance is based on several in situ samples indicating that the Gepatschferner reached at least an ice thickness comparable to ca. AD 1930 during this advance. No younger tree remnants have been found at profile 2 so far.

Stop 5: Profile 3 – mid-Holocene glacier situation

The route continues from excursion point 4 for ca. 100–150 m to the Northeast until a steep gully located at the steep scarp is reached.

A sediment complex mainly composed of peat and humus but also containing wood remnants as well as inorganic material and layers was exposed in a gully at ca. 2170 m a.s.l. (Nicolussi & Patzelt 2001). This complex, called profile 3, is about 1.9 m thick and, judging from several radiocarbon and a few dendro-dates, originates from the middle Holocene. Due to the modern retreat of the Gepatschferner the site became free of ice around AD 1950. The organic sedimentation started before ca. 6500 BC (Fig. 7). It was interrupted by the deposition of till before ca. 6050 BC. This inorganic layer can probably be attributed to a glacier advance during the 8.2 ka event (Alley & Ágústsdóttir 2005, Nicolussi & Schlüchter 2012). Disturbances of the organic sedimentation above this till layer and dated into the 6th millennium BC cannot distinctly be related to further glacier advances. An additional clear interruption of the organic sedimentation dates to around 4300 BC. The analysis suggests that this interruption can be attributed to another Gepatschferner advance at the site of profile 3. During the mid-5th millennium BC an advance phase has also been proven for the Tschierva glacier , Engadin (Joerin et al. 2008) and a lowering of the treeline has been suggested in Kaunertal (Nicolussi et al. 2005) both indicating cooler/wetter climate conditions. Moreover, based on tree rings a culmination of relatively cool summers was reconstructed for ca. 4400/4300 BC which also overlaps with this radiocarbon dated advance of the Gepatschferner (Nicolussi et al. 2013). The organic sedimentation at profile 3 after this disturbance lasted at least until ca. 2300 BC without obvious disturbances but possibly until 1659 BC (Nicolussi & Patzelt 2001). However, the top of profile is disturbed due to the Neoglacial advances. An advance of Gepatschferner at ca. 2500 BC is proven by the analysis of twig remains at the top of a fossil soil located at a site that became free of ice in ca. 1960 (profile 4, sample GP-4/1: 4000 ± 50 BP, 2670–2340 cal BC). It did not reach profile 3 and remained therefore smaller than the ice extent of ca. AD 1960 (Nicolussi & Patzelt 2001).

Stop 6: Lateglacial moraines

The route leads back to the parking lot at the bridge of the Kaunertal glacier road over the Falgin Bach. After a short drive to a bus stop and small parking area at 2340 m a.s.l. another good footpath starts at that parking area and leads up to an ensemble of small ponds and lateral moraines at ca. 2400 m a.s.l.

In the vicinity of the LIA Gepatschferner tongue, lateglacial moraines can be found at a number of localities (Kerschner 1979), among them on the southern and eastern flank of Ochsenkopf (Fig. 8; locality "Riffelseite" on the Alpenverein map and in Kerschner 1979). The moraines are easily accessible from the road to the skiing area at Weisseeferner. Viewpoint 6 (Fig. 1) offers an excellent panorama

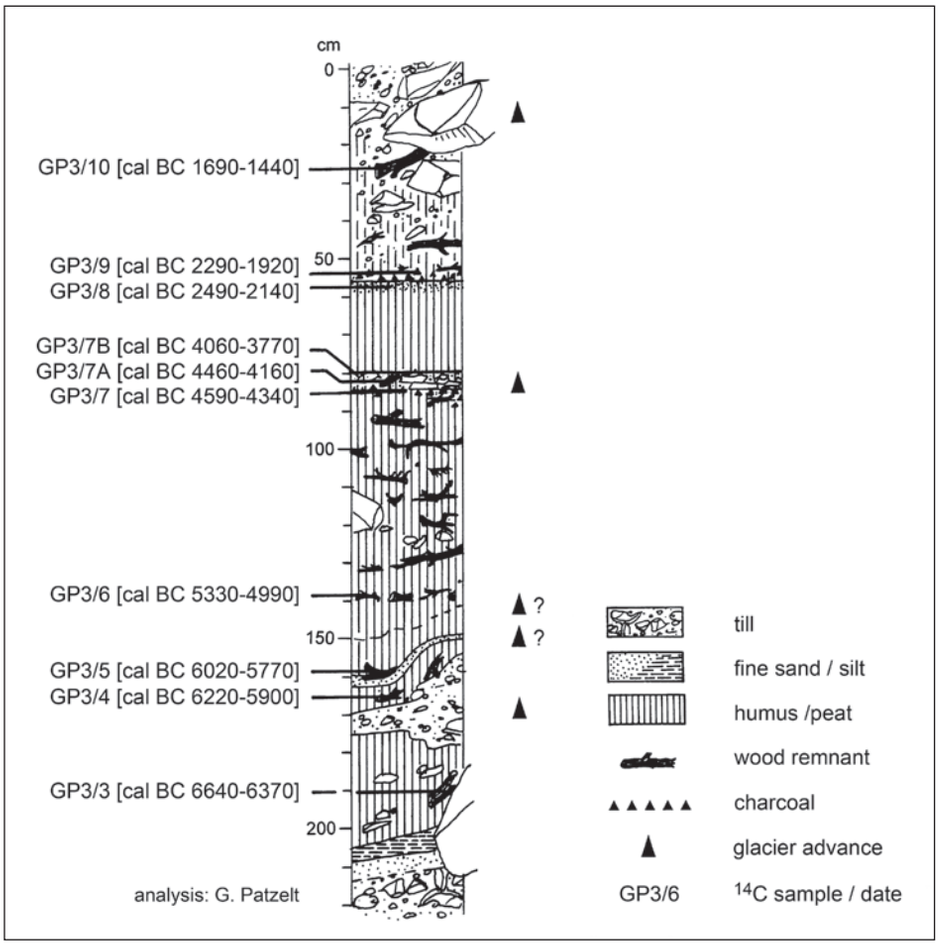

Fig. 7: Analysed mid-Holocene soil and peat profile in the forefield of Gepatschferner (2170 m a.s.l.). The site became free of ice ca. AD 1950. Based on radiocarbon dates and a dendrodate the profile covers the period from the mid-7th millennium BC to ca. 1659 BC. It indicates that the Gepatschferner reached and covered the site only at rare occasions during that time period (Nicolussi & Patzelt 2001, modified).

Abb. 7: Analysiertes mittelholozänes Boden- und Torfprofil im Gepatschfernervorfeld (2170 m). Die Stelle wurde um 1950 eisfrei. Auf der Grundlage von Radiokarbondaten und einem Dendro-Datum deckt das Profil die Zeit vom mittleren 7. Jahrtausend v. Chr. bis ca. 1659 v. Chr. ab. Es zeigt, dass der Gepatschferner während dieser Zeit diese Stelle nur selten erreichte oder überfuhr (Nicolussi & Patzelt 2001, verändert).

of the moraines, of Gepatschferner and of the rock glaciers in Innere Ölgrube (eastern side of Kaunertal).

The well preserved moraines consist mainly of fine material with a number of comparatively small boulders on top. The morphology of the moraines shows some signs of postdepositional overprint, but in general their appearance is comparatively fresh and undisturbed. They can be traced down to another set of lateral moraines on the eastern flank of Ochsenkopf at altitudes between ca. 2300 and 2200 m a.s.l. There, the moraines labelled "b", "c" and "d" in Fig. 8 are well preserved and in places also rather blocky. In particular moraine "c" stands out with steep flanks and the general appearance resembling a railway embankment. Lateral moraines on the right-hand side of Kuhgrube cirque show that a connection between the glaciers existed at least until the deposition of moraine "d". The fresh morphology of the well preserved moraines and their relation to the LIA moraines in the catchment is typical for moraines of the "Egesen Stadial". Together with other moraine assemblages they allow the reconstruction of a glacier tongue with a glacier end just north of the present-day hydropower dam. The accumulation area of the glacier covered the entire basin of the upper Kaunertal and the southernmost independent cirques (Kuhgrube, Innere Ölgrube). Further down valley, most glacier tongues from the cirques and from Kaiserbergtal did not reach the main glacier any more. At the mouth of Wurmetal on the eastern side of the valley, an ice contact with the main glacier cannot be ruled out. However, if so, it was not significant.

While moraines "b" to "d" can be classified as Egesen stadial moraines, the situation is less clear for moraine "a". It runs higher up and is clearly less well preserved than the other moraines. It is also discordantly overlain by the lateral moraines from Kuhgrube cirque. Therefore, moraine "a" is cautiously classified as a Daun stadial moraine and should be of Prebølling age. In this context it should be noted that today more moraines are classified as Egesen stadial at the cost of Daun stadial moraines than in Kerschner (1979). This is due to the experience gained during the past 35 years.

A classification of most of the moraines as Egesen stadial is supported by an ELA lowering of 200 m relative to the LIA mean ELA of the catchment (Kerschner 1979) for the maximum glacier extent (moraine "b"). Up to now the Lateglacial moraines in Kaunertal have not been absolutely dated, but a comparison with dated localities elsewhere suggests a Younger Dryas age (Ivy-Ochs et al. 2009). Radiocarbon ages of 9390 ± 160 BP and 9370 ± 160 BP (VRI-32 and VRI-35; 9170–8300 cal BC and 9160–8290 BC; Felber 1970) from trees, which were overrun by a creeping hillslope in the valley bottom not far south from the present-day dam show that the valley was already tree covered in the early Preboreal.

The comparatively large number of closely spaced lateral moraines on the southern flank of Ochsenkopf shows that the thickness of the glacier tongue fluctuated around a rather constant value for a longer period of time. This may, however, have led to significantly different glacier lengths, as is indicated by the already much larger vertical spacing of the moraines on the eastern side of Ochsenkopf a few hundred metres downstream.

If only the larger moraines are considered, three main

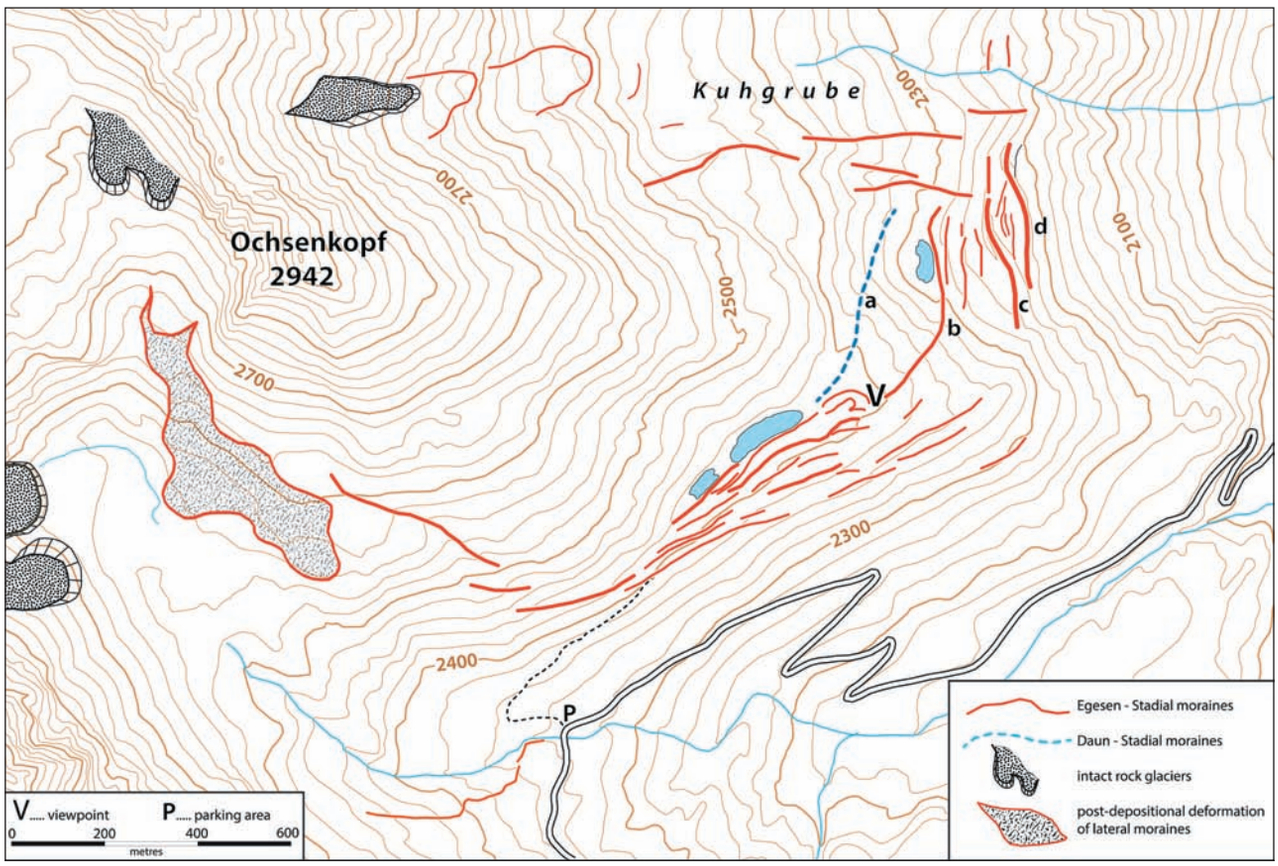

Fig. 8: Lateglacial lateral moraines on the southern and eastern flank of Ochsenkopf. The moraines and contour lines are derived from laserscan hillshades (© Land Tirol – tiris). Hence the map is more detailed and correct than the map of the same site in Kerschner (1979).

Abb. 8: Spätglaziale Ufermoränen an der südlichen und östlichen Flanke des Ochsenkopfs. Der Moränenverlauf und die Höhenlinien sind nach den Laserscan-Hillshades (© Land Tirol – tiris) gezeichnet. Die Karte ist daher detaillierter und genauer als die Kartierung derselben Stelle bei Kerschner (1979).

L

phases of glacier growth can be distinguished. While the largest advance had its terminus just to the North of the dam, a lateral moraine of a smaller advance can be seen on the eastern side of the reservoir, especially if the water level is low. Old air photographs show that no more moraines can be distinguished in the area covered by the lake. More recently, laser scan hillshades allowed the identification of scattered end moraine fragments outside the LIA glacier ends in the upper basin of Kaunertal, which may correlate to similar moraines in the upper reaches of neighbouring Langtaufers and Radurschl valleys.

The locality at Ochsenkopf allows also a very nice view of the active rock glaciers at Innere Ölgrube in the East and some inactive and relict rock glaciers at the foot of Glockturm (3353 m) to the South (Berger et al. 2004).

3 Conclusions

The Lateglacial moraines have not yet been directly dated, however, most of them can be appointed to the Younger Dryas due to their stratigraphic positions and the correlated ELA depressions.

The advance record of Gepatschferner is still among the most important Holocene glacier records in the Alps. On the one hand, it is based on a profile of organic sediments and on the other hand on more than 70 calendar-dated tree remnants. Only few advances beyond an extent comparable to mid-20th century glacier dimensions are recorded between ca. 6500 and ca. 1700 BC. The proven advances during the last approximately 4000 years, the Neoglacial are interrupted by several multi-centennial retreat phases during which Gepatschferner was shorter than during the mid-20th century. The Neoglacial culminated in the late Little Ice Age for which two maximum extents 1679/80 and 1856, with virtually the same extent can be documented.

References

Alley, R.B. & Ágústsdóttir, A.M. (2005): The 8k event: cause and consequences of a major Holocene abrupt climate change. – Quaternary Science Reviews, 24: 1123–1149.

Berger, J., Krainer, K. & Mostler, W. (2004): Dynamics of an active rock glacier (Ötztal Alps, Austria). – Quaternary Research, 62: 233–242.

Felber, H. (1970): Vienna Radium Institute radiocarbon dates I. – Radiocarbon, 12: 298–318.

Hartl, L. (2010): The Gepatschferner from 1850–2006: changes in length, area and volume in relation to climate. – Unpubl. Diploma thesis, University of Innsbruck.

Holzhauser, H., Magny, M. & Zumbühl, H.J. (2005): Glacier and lake-level variations in west-central Europe over the last 3500 years. – The Holocene, 15: 789–801.

Ivy-Ochs, S., Kerschner, H., Maisch, M., Christl, M., Kubik, P.W. & Schlüchter, Ch. (2009): Latest Pleistocene and Holocene glacier variations in the European Alps. – Quaternary Science Reviews, 28: 2137–2149.

Joerin, U.E., Nicolussi, K., Fischer, A., Stocker, T.F. & Schlüchter, C. (2008): Holocene optimum events inferred from subglacial sediments at Tschierva Glacier, Eastern Swiss Alps. – Quaternary Science Reviews, 27: 337–350.

Kerschner, H. (1979): Spätglaziale Gletscherstände im inneren Kaunertal (Ötztaler Alpen). – Innsbrucker Geographische Studien, 6 (Leidlmair – Festschrift II): 235–247.

Nicolussi, K. (2009): Alpine Dendrochronologie – Untersuchungen zur Kenntnis der holozänen Umwelt- und Klimaentwicklung. – In: Schmidt, R, Matulla, C. & Psenner, R. (eds.): Klimawandel in Österreich. (Innsbruck University Press), Alpine Space – man & environment 6: 41–54.

Nicolussi, K. & Patzelt, G. (2001): Untersuchungen zur holozänen Gletscherentwicklung von Pasterze und Gepatschferner (Ostalpen). – Zeitschrift für Gletscherkunde und Glazialgeologie, 36: 1–87.

Nicolussi, K., Kaufmann, M., Patzelt, G., van der Plicht, J. & Thurner A. (2005): Holocene tree-line variability in the Kaunertal, Central Eastern Alps, indicated by dendrochronological analysis of living trees and subfossil logs. – Vegetation History and Archaeobotany, 14: 221–234.

Nicolussi, K., Kaufmann, M., Melvin, T.M., van der Plicht, J., Schiessling, P. & Thurner, A. (2009): A 9111 year long conifer tree-ring chronology for the European Alps – a base for environmental and climatic investigations. – The Holocene, 19: 909–920.

Nicolussi, K., Matuschik, I. & Tegel, W. (2013): Klimavariabilität und Siedlungsdynamik am Beispiel der Feuchtbodensiedlungen im Raum Oberschwaben, Bodensee und Nordostschweiz 4400–3400 BC. – In: Bleicher, N., Schlichtherle, H., Gassmann, P. & Martinelli, N. (ed.): Dendro – Chronologie – Typologie – Ökologie. Festschrift für André Billamboz zum 65. Geburtstag: 61–77; Freiburg i. Br..

Nicolussi, K. & Schlüchter, Ch. (2012): The 8.2 ka event – Calendar-dated glacier response in the Alps. – Geology, 40: 819–822.

Patzelt, G. (1995): Die klimatischen Verhältnisse im südlichen Mitteleuropa zur Römerzeit. In: Bender, H. & Wolff, H. (ed.): Ländliche Besiedlung und Landwirtschaft in den Rhein-Donau-Provinzen in der römischen Kaiserzeit. – Passauer Universitätsschriften zur Archäologie, 2: 7–20.

Patzelt, G. & Bortenschlager, S. (1973): Die postglazialen Gletscher- und Klimaschwankungen in der Venedigergruppe (Hohe Tauern, Ostalpen). – Zeitschrift für Geomorphologie N.F., Suppl. 16: 25–72.

Reimer, P.J., Bard, E., Bayliss, A., Beck, J.W., Blackwell, P.G., Bronk Ramsey, C., Buck, C.E., Cheng, H., Edwards, R.L., Friedrich, M., Grootes, P.M., Guilderson, T.P., Haflidason, H., Hajdas, I., Hatté, C., Heaton, T.J., Hogg, A.G., Hughen, K.A., Kaiser, K.F., Kromer, B., Manning, S.W., Niu, M., Reimer, R.W., Richards, D.A., Scott, E.M., Southon, J.R., Turney, C.S.M. & van der Plicht, J. (2013): IntCal13 and MARINE13 radiocarbon age calibration curves 0–50,000 years cal BP. – Radiocarbon 55(4): 1869–1884.

Sonklar, K. (1860): Die Oetzthaler Gebirgsgruppe. – 292 p., Gotha (J. Perthes).

Notes

List of authors

Samuel Barrett
Institut für Geologie
Universität Innsbruck
Innrain 52
A-6020 Innsbruck
samuel.barrett(a)uibk.ac.at

Stefano Bertola
Institut für Geologie
Universität Innsbruck
Innrain 52
A-6020 Innsbruck
stefano.bertola(a)uibk.ac.at

Sixten Bussemer
Institut für Geographie und Geologie
Universität Greifswald
F.-Ludwig-Jahn-Straße 17a
D-17487 Greifswald
sixten.bussemer(a)uni-greifswald.de

Bodo Damm
Institut für Strukturforschung und Planung
in agrarischen Intensivgebieten
Universität Vechta
Postfach 1553
D-49364 Vechta
bodo.damm(a)uni-vechta.de

Clemens Geitner
Institut für Geographie
Universität Innsbruck
Innrain 52
A-6020 Innsbruck
clemens.geitner(a)uibk.ac.at

Alfred Gruber
Geologische Bundesanstalt
Neulinggasse 38
A-1030 Wien
alfred.gruber(a)geologie.ac.at

Ulrich Haas
Bayerisches Landesamt für Umwelt
Abt. 10: Geologischer Dienst
Referat 102: Geologische Landesaufnahme, Geogefahren
Haunstetterstraße 112
D-86161 Augsburg
ulrich.haas(a)lfu.bayern.de

Kati Heinrich
Institut für Interdisziplinäre Gebirgsforschung
Technikerstraße 21a
A-6020 Innsbruck
kati.heinrich(a)oeaw.ac.at

Martin Herz
Bayerisches Landesamt für Umwelt
Referat 102: Geologische Landesaufnahme, Geogefahren
Dienststelle Hof
Hans-Högn-Str. 12
D-95030 Hof
martin.herz(a)lfu.bayern.de

Thomas Hornung
GWU Geologie-Wasser-Umwelt GmbH
Ingenieurbüro für Geologie,
Kulturtechnik und Wasserwirtschaft
Bayerhamerstraße 57
A-5020 Salzburg
office(at)gwu.at

Susan Ivy-Ochs
Labor für Ionenstrahlphysik
Otto-Stern-Weg 5
CH-8093 Zürich
ivy(a)phys.ethz.ch

Hanns Kerschner
Institut für Geographie
Universität Innsbruck
Innrain 52
A-6020 Innsbruck
hanns.kerschner(a)uibk.ac.at

Maria Knipping
Institut für Botanik (210)
Universität Hohenheim
D-70593 Stuttgart
maria.knipping(a)uni-hohenheim.de

Karl Krainer
Institut für Geologie
Universität Innsbruck
Innrain 52
A-6020 Innsbruck
karl.krainer(a)uibk.ac.at

Ernst Kroemer
Bayerisches Landesamt für Umwelt
Referat 102: Geologische Landesaufnahme, Geogefahren
Dienststelle Hof
Hans-Högn-Str. 12
D-95030 Hof
ernst.kroemer(a)lfu.bayern.de

David Mair
Institut für Geologie
Universität Innsbruck
Innrain 52
A-6020 Innsbruck
david.mair(a)uibk.ac.at

Kurt Nicolussi
Institut für Geographie
Universität Innsbruck
Innrain 52
A-6020 Innsbruck
kurt.nicolussi(a)uibk.ac.at

Marc Ostermann
Institut für Geologie
Universität Innsbruck
Innrain 52
A-6020 Innsbruck
marc.ostermann(a)uibk.ac.at

Franz Ottner
Institut für Angewandte Geologie
Department für Bautechnik und Naturgefahren
Universität für Bodenkultur Wien
Peter Jordan Straße 70
A-1190 Wien
franz.ottner(a)boku.ac.at

Gernot Patzelt
Patscherstraße 20
A-6080 Innsbruck-Igls
gernot.patzelt(a)uibk.ac.at

Christoph Prager
alpS gmbH
Grabenweg 68
A-6020 Innsbruck
prager(a)alps-gmbh.com
ILF Beratende Ingenieure
A-6063 Rum bei Innsbruck
christoph.prager(a)ilf.com

Jürgen Reitner
Geologische Bundesanstalt
Neulinggasse 38
A-1030 Wien
juergen.reitner(a)geologie.ac.at

Diethard Sanders
Institut für Geologie
Universität Innsbruck
Innrain 52
A-6020 Innsbruck
diethard.g.sanders(a)uibk.ac.at

Dieter Schäfer
Institut für Geologie
Universität Innsbruck
Innrain 52
A-6020 Innsbruck
dieter.schaefer(a)uibk.ac.at

Christoph Spötl
Institut für Geologie
Universität Innsbruck
Innrain 52
A-6020 Innsbruck
christoph.spoetl(a)uibk.ac.at

Reinhard Starnberger
Institut für Geologie
Universität Innsbruck
Innrain 52
A-6020 Innsbruck
reinhard.starnberger(a)uibk.ac.at

Birgit Terhorst
Institut für Geographie
Universität Würzburg
Am Hubland
D-97074 Würzburg
birgit.terhorst(a)uni-wuerzburg.de

Jarosław Waroszewski
Institute of Soil Science and Environmental Protection
Wrocław University of Environmental and Life Sciences
ul. Grunwaldzka 53
PL-50-357 Wrocław
jaroslaw.waroszewski(a)up.wroc.pl

DEUQUA EXKURSIONSFÜHRER

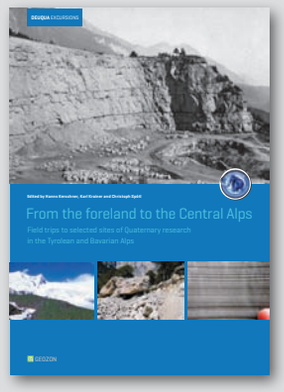

From the foreland to the Central Alps – Field trips to selected sites of Quaternary research in the Tyrolean and Bavarian Alps

ISBN 978-3-941971-10-3

160 pp., A4, 34,– Euro

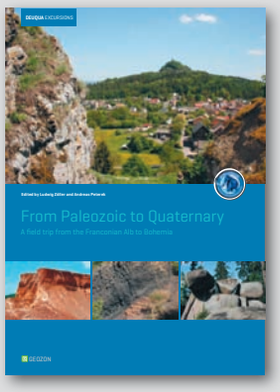

From Paleozoic to Quaternary – A field trip from the Franconian Alb to Bohemia

ISBN 978-3-941971-08-0

120 pp., A4, 34,– Euro

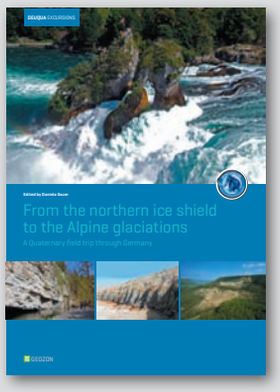

From the northern ice shield to the Alpine glaciations – A Quaternary field trip through Germany

ISBN 978-3-941971-06-6

88 pp., A4, 29,– Euro

Eiszeitlandschaften in Mecklenburg-Vorpommern

ISBN 978-3-941971-05-9

164 pp., A4, 34,– Euro

LANDSCHAFTSGESCHICHTE

Zur jungquartären Landschaftsentwicklung der Mecklenburgischen Kleinseenplatte

ISBN 978-3-941971-09-7

78 pp., A4, 22,– Euro

Zur Landschafts- und Gewässergeschichte der Müritz

ISBN 978-3-941971-00-4

94 pp., A4, 29,– Euro

Neubrandenburger Geologische Beiträge 11

ISSN 1616-959X

88 pp., 17 x 24 cm, 8,50 Euro

Neubrandenburger Geologische Beiträge 12

ISSN 1616-959X

72 pp., 17 x 24 cm, 8,50 Euro

Gerne unterstützen wir auch Sie bei Ihrer wissenschaftlichen Veröffentlichung. Wir publizieren print und digital:

- **Bücher** (Monographien, Reihen, Tagungsbände, Festschriften, Dissertationen etc.)
- **Zeitschriften** (Disziplinäre oder institutionelle Journals, Neugründung, Archivierung etc.)
- **Dokumente** (Artikel, Diskussionspapiere, Berichte, Protokolle, Karten, Daten etc.)

OPEN ACCESS eBOOKS

GEOZON

Geozon Science Media
Pettenkoferstr. 16–18
D-10247 Berlin
Germany

Tel. 030-20 23 83 19-0
Fax 030-20 23 83 19-9
E-Mail: info@geozon.net
Online: www.geozon.net

E&G – QUATERNARY SCIENCE JOURNAL

Vol. 63 No 1

104 pp., A4, 27,– Euro

Vol. 62 No 2: Environment – Man – Geohazards in the Quaternary

100 pp., A4, 27,– Euro

Vol. 62 No 1: Middle to Upper Pleistocene paleosols in Austria

80 pp., A4, 27,– Euro

Vol. 61 No 2

92 pp., A4, 27,– Euro

Vol. 61 No 1

100 pp., A4, 27,– Euro

Vol. 60 No 4: Quaternary landscape evolution in the Peribaltic region

104 pp., A4, 27,– Euro

Vol. 60 No 2–3: Glaciations and periglacial features in Central Europe

188 pp., 17 x 24 cm, 54,00 Euro

Vol. 60 No 1: Loess in Europe

208 pp., 17 x 24 cm, 27,00 Euro

Vol. 59 No 1–2

176 pp., A4, 54,– Euro

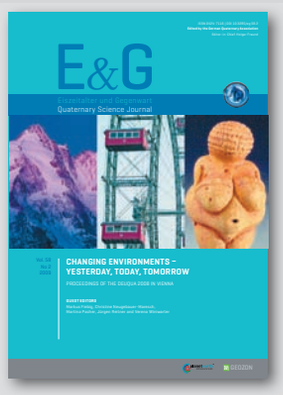

Vol. 58 No 2: Changing Environments – Yesterday, today, tomorrow

60 pp., A4, 27,– Euro

Seit 1951 bietet „Eiszeitalter und Gegenwart" (heute: E&G – Quaternary Science Journal) ein Publikationsforum für die Quartärsforschung. Es erscheinen ausschließlich begutachtete Original-Artikel und Tagungsbeiträge.

Das Journal erscheint 2x jährlich als gedruckte und digitale Ausgabe. Im Rahmen des wissenschaftlichen Open Access stehen alle Nummern kostenlos zur Ansicht und zum Download im Internet bereit.

Für die Einreichung von Artikeln nutzen Sie bitte unser Online-Submission-System unter:

www.quaternary-science.net

CALL FOR PAPERS

GEOZON

Geozon Science Media
Pettenkoferstr. 16–18
D-10247 Berlin
Germany

Tel. 030-20 23 83 19-0
Fax 030-20 23 83 19-9
E-Mail: info@geozon.net
Online: www.geozon.net

EDITOR
DEUQUA
Deutsche Quartärvereinigung e.V.
Office
Stilleweg 2
D-30655 Hannover
GERMANY
Tel: +49(0)511-643-36 13
info@deuqua.de
www.deuqua.de

MANAGING EDITORS
Hanns Kerschner,
Karl Krainer,
Christoph Spötl

PUBLISHING HOUSE
Geozon Science Media
Pettenkoferstr. 16-18
10247 Berlin
GERMANY
Tel. +49(0)30-20 23 83 19-0
info@geozon.net
www.geozon.net

DESIGN
Sascha Fricke

COVER PICTURES
Top photo:
For centuries the Hötting Breccia, a famous Pleistocene slope deposit containing a diverse flora, was mined at Mayr quarry north of Innsbruck. Photo Raimund v. Klebelsberg, probably from early 20th century.
Small photos (from left to right):
Little Ice Age moraine ridge on the right side of Schlatenkees, Eastern Tyrol. Photo Karl Krainer.
Rockslide Tschirgant. Photo Marc Ostermann.
Fine-scale, rhythmic bedding of clayey silt of the Middle Würmian palaeolake Baumkirchen. Photo Christoph Spötl.

PAPER
Printed on 100% recycled paper
Climate neutral production

PRINT
ISBN 978-3-941971-10-3

ONLINE
DOI 10.3285/g.00011
Free download: www.geozon.net

The Deutsche Nationalbibliothek lists this publication in the Deutsche Nationalbibliografie; detailed bibliographic data are available in the Internet at http://dnb.d-nb.de

DOI 10.3285/g.00011
ISBN 978-3-941971-10-3
www.geozon.net